Determination of accelerated ageing in critical illness

Jack Alexander Sullivan



A thesis submitted to the University of Birmingham for the degree of
DOCTOR OF PHILOSOPHY

Supervisors: Prof. Janet M. Lord & Dr Leda Mirbahai

Institute of Inflammation and Ageing
College of Medical and Dental Sciences
University of Birmingham
30th June 2022

UNIVERSITY OF
BIRMINGHAM

University of Birmingham Research Archive

e-theses repository

This unpublished thesis/dissertation is copyright of the author and/or third parties. The intellectual property rights of the author or third parties in respect of this work are as defined by The Copyright Designs and Patents Act 1988 or as modified by any successor legislation.

Any use made of information contained in this thesis/dissertation must be in accordance with that legislation and must be properly acknowledged. Further distribution or reproduction in any format is prohibited without the permission of the copyright holder.

Abstract

Aims:

The primary aim of this research was to test the hypothesis that injury or critical illness is sufficient to cause an acceleration of the ageing process. This hypothesis is to be tested by quantifying the immune, cellular, and epigenetic changes which occur following injury, such as a severe burn or following illness such as COVID-19 or sepsis. A secondary aim was to see if cellular senescence could be reversed.

Methods:

Absolute telomere length was measured via qPCR in PBMCs taken from burns patients following admission and again at 6 months post injury (n = 33) and compared with the telomere length of healthy controls (n=28). Flow cytometry was used to profile the immune system of burn patients 6 months post injury (n = 31) and healthy controls (n = 27) to look for signs of immunosenescence. Immunohistochemistry was used to see how the percentage of $p16^{INK4A}$+ senescent cells changed in injured and non-injured skin taken from burns patients over a long period (n = 7). A compound library was used in 48-hour exposures in an x-ray induced senescence hTert-BJ fibroblast model, as well as in non-senescent hTert-BJ control fibroblasts to identify compounds with a senescence modulating ability. Changes in cell viability and SA-βGal activity were measured. Patients had their methylomes profiled using either the illumina 450k or EPIC array. Burns patients were profiled following admission (n = 53) and again 6 months post injury (n = 34) as were a cohort of septic (n = 66) and non-septic (n = 68) ICU patients and patients with severe (n = 38) or moderate (n = 25) COVID-19 infections. Their epigenetic ages were calculated using the Horvath, Hannum and DNAm PhenoAge clocks. Differential methylation gene and pathways analysis was also performed.

Total RNA sequencing was performed on RNA isolated from the PBMCs of burn injury patients who survived “unsurvivable” burn injury and patients who died following severe burn injury. The sequencing platform was the illumina HiSeq Xten.

Results:

There was no significant difference between the mean absolute telomere length of PMBCs of burns patients taken at admission to hospital or 6 months post injury ($p = 0.35$). There was also no significant difference between the patient's absolute telomere lengths at admission ($p = 0.85$) or 6 months post ($p = 0.35$) injury when compared to healthy controls. Signs of immune ageing were observed in burn injury survivors 6 months post injury in comparison to a healthy control population. Burn patients showed a lower proportion of naïve CD4+ T cells ($p = 5.6e\text{-}07$) and recent thymic emigrants ($p = 0.00024$) as well as a greater proportion of total CD4+ memory cells ($p = 1.1e\text{-}07$) than the control cohort. Immune remodelling was also observed in CD8 T cell and B cell sub-populations. Epigenetic clocks showed mixed results, with burns and COVID-19 patients only showing epigenetic age acceleration according to the Horvath clock, and septic and non-septic ICU patients showing significant epigenetic age acceleration according to the Hannum and DNAm PhenoAge clocks. Burns patients had significantly greater epigenetic ages following admission compared with 6 months post injury according to all clocks. ICU patients who died had significantly greater epigenetic age acceleration than those who survived, with septic patients having the greatest epigenetic age acceleration. Patients with severe COVID-19 had significantly greater epigenetic age residuals than those with moderate infections. Multiple pathways which relate to long term patient outcomes such as cell cycle and signalling, chromatin remodelling, metabolic pathways, and pathways regulating cell death and apoptosis were significantly differentially methylated between groups. No significant differences were observed in the RNA expression profiles of patients who survived severe burn injuries considered "unsurvivable" compared with patients who died.

Conclusion:

Not all, but most areas examined showed evidence that suggests injury and severe infection are associated with accelerated ageing.

Acknowledgements

Funding:

- This project was funded by the NIHR SRMRC. The views expressed are those of the author and not necessarily those of the NIHR, the Department of Health and Social Care or the Ministry of Defence.

Data:

- I would like to thank Dr Niharika Duggal for contributing healthy control flow cytometry data for comparison.
- I would also like to thank Dr Claudia dos Santo and Dr Alexandra Binnie for access to septic and non-septic ICU patient DNA methylation data.
- I would like to thank the organising clinicians who gave me access to samples collected as part of the PHOSP-Covid study for use in the DNA methylation analysis portion of this thesis.
- I would like to thank Dr Jon Hazeldine for contributing cytokine and neutrophil data.

Thanks:

- The first person I would like to thank, and the person without whom, none of this would have been possible is my primary supervisor Prof Janet Lord. I would like to say thank you for the huge amount of advice, guidance and support you have given me over the past few years which have helped me develop as a researcher, and I hope, prepared me for the road ahead.
- I would like to thank Dr Leda Mirbahai, my PhD co-supervisor and MRes supervisor. I'll always be grateful that you took a chance taking me on for a research masters and helped me get to where I am today.
- I would like to thank Dr Jon Hazeldine and Dr Kirsty McGee. I'd like to thank Jon for his invaluable advice on pretty much every aspect of the research process from how to do a

particular experiment to where the PBS is kept. I would like to thank Kirsty for teaching me about the wonderful world of flow cytometry, for helping me in a pinch and for seeming to be the person who keeps the lab actually functioning! I'd also like to thank them both for all the jokes along the way.

- I'd like to thank Dr Yung-Yi Chen for her company during the many hours of tissue staining but most importantly I'd like to say thank you for taking me under your wing and showing me IHC, microscopy and cell culture inside and out.
- I would like to thank the entire IIA lab 1 group for their day-to-day advice, help and good company during my time studying.
- I would like to thank all members of the SIFTI team, those who developed the study long before I arrived, the team members who helped store down samples in the past, and who are still doing it now, and the whole support team of clinicians and nurses who help the study to function.
- I would like to thank all the participants and their families who donated their time and samples to this study out of a desire to help others.

Friends and Family:

- I would like to thank my friends for being there for me and checking in when I've been busy writing and working.
- I'd like to thank my family, for being there for me from the beginning. I can't sum up all of the things you've done for me, so I'll just say - thank you.
- Finally, I would like to thank my partner, Meg. You have been there for me and supported me during my masters and throughout my PhD, during the good and the bad for which I'll always be grateful. I've only been able to do this because you were there.

Contents

Abstract.....
Acknowledgements.....
Contents.....
1. Introduction 1
1.1 General introduction to ageing 1
1.1.1 Ageing as a malleable process 3
1.1.2 Impact of major trauma on morbidity and mortality 6
1.2 How might trauma impact the ageing processes? 8
1.2.1 The inflammatory response to trauma 8
1.2.2 Telomere attrition and trauma 11
1.2.3 Cellular senescence and trauma 13
1.2.3.1 Measuring cellular senescence 16
1.2.3.1.1 $p21^{WAF1/CIP1}$ and $p16^{INK4A}$ 16
1.2.3.1.2 γH2AX 16
1.2.3.1.3 Senescence associated β-Galactosidase (SA-βGal) 17
1.2.4 The impact of cellular senescence 17
1.2.5 Immune senescence 20
1.3 Epigenetics: a way to measure biological ageing 25
1.3.1 The Horvath epigenetic clock 28
1.3.2 The Hannum epigenetic clock 29
1.3.3 The DNAm PhenoAge epigenetic clock 29
1.3.4 The use of epigenetic clocks 30
1.3.4.1 Reversibility of the epigenetic clock 31
1.3.5 What we know so far about the impact of trauma on the epigenetic clock 31
1.4 Trauma and ageing, commonalities, and differences 33
1.5 Conclusions and directions for research 36
1.6 Hypothesis, Aims and Objectives of the thesis 37
2. Methods 38
2.1 Burn study participant recruitment 38
2.1.1 Inclusion criteria 38
2.1.2 Exclusion criteria 38
2.1.3 Consent procedure 38
2.1.4 Sample collection and storage 41
2.1.5 Clinical data collection 41

2.1.6 PBMC Isolation 41
2.2 Sepsis group study 42
2.2.1 Inclusion criteria 42
2.2.2 Exclusion criteria 43
2.2.3 Consent procedure 43
2.2.4 Clinical data collection 43
2.2.5 Sample collection and storage 43
2.2.6 DNA methylation processing 44
2.3 COVID-19 group study 44
2.3.1 Inclusion criteria: 44
2.3.2 Exclusion criteria: 44
2.3.3 Consent procedure 44
2.3.4 Clinical data collection 45
2.3.5 Sample collection and storage 45
2.4 DNA extraction and quality checks 45
2.4.1 DNA Extraction 45
2.4.2 DNA Quality control 45
2.4.2.1 Nanodrop DNA presence and quality checks 45
2.4.2.2 Qubit fluorometer and DNA quantification 46
2.4.2.3 DNA integrity 46
2.5 DNA methylation 47
2.5.1 Illumina 450K array 47
2.5.2 Illumina Infinium EPIC array 48
2.5.3 DNA methylation analysis 48
2.5.3.1 Quality control and processing 48
2.5.3.2 Normalisation and epigenetic age generation 48
2.5.3.3 Pathway enrichment analysis 48
2.6 Absolute Telomere length analysis 49
2.7 RNA Extraction and quality checks 51
2.7.1 RNA extraction 51
2.7.2 RNA Quality control 51
2.7.2.1 Nanodrop RNA presence and quality 51
2.7.2.2 Qubit fluorometer RNA quantification 51
2.7.2.3 RNA integrity 51
2.8 RNA Sequencing 53
2.8.1 Library preparation 53

2.8.2 sequencing platform and data 53
2.8.3 RNA sequencing analysis 53
2.9 Human cell culture and senescence induction 54
2.9.1 Human cell culture 54
2.9.2 Senescence induction using X-ray irradiation 54
2.9.2.1 Senescence-associated β-galactosidase staining 54
2.9.2.2 Cell morphology 55
2.10 Human cell culture: senescence modulating compound discovery 55
2.10.1 Compound exposures 56
2.10.2 Apoptosis assay 56
2.11 Tissue sectioning and staining 57
2.11.1 Tissue sectioning 57
2.11.2 Tissue staining 57
2.11.2.1 p16 Staining 57
2.11.2.2 Stained tissue image analysis 59
2.12 Immune phenotyping 59
2.13 Statistical analysis and figure generation 61
2.13.1 Accessibility 61
3. Immune senescence following trauma 62
3.1 Introduction 62
3.1.1 Immune ageing in injury 62
3.1.1.1 Changes to the innate and adaptive immune system with age 62
3.1.1.2 Inflammaging 64
3.1.1.3 Quantifying immune ageing 65
3.1.1.4 Immune phenotype changes with injury 65
3.1.2 Injury factors that could affect immune ageing 66
3.1.2.1 Total burn surface area (TBSA) 66
3.1.2.2 rBaux score 67
3.1.2.3 Sequential organ failure assessment score 67
3.1.2.4 Acute physiology and chronic health evaluation II (APACHE II) score 67
3.1.2.5 Body mass index 68
3.1.2.6 Length of stay 68
3.1.3 Aims of the chapter 68
3.2 Results 69
3.2.1 Telomere length following injury 69
3.2.1.1 Participant demographics 69

3.2.1.2 Absolute telomere length analysis 70
3.2.2 Immune ageing following injury 73
3.2.2.1 Acknowledgement 73
3.2.2.2 Participant demographics 73
3.2.2.3 Differences in immune phenotype in burns patients compared to non-injured controls 74
3.2.2.3.1 T cell subsets 74
3.2.2.3.2 B cell sub cells 80
3.2.2.3.3 Natural Killer Cells 81
3.2.2.3.4 The relationship between chronological age and immune cell sub-populations 82
3.2.2.4 Clinical parameters and immune ageing 84
3.2.2.5 IMM-AGE immune ageing 87
3.3 Discussion 89
3.3.1 Absolute telomere length 89
3.3.1.1 The impact of ageing on absolute telomere length 90
3.3.1.2 The impact of BMI on absolute telomere length 91
3.3.1.3 The impact of Injury severity on absolute telomere length 91
3.3.1.4 Does injury impact absolute telomere length 92
3.3.2 Immune ageing 93
3.3.2.1 Immune differences between non-burned individuals and long-term burn-injured individuals 93
3.3.2.1.1 Primary T cell groups 93
3.3.2.1.2 Senescent T cell groups 94
3.3.2.1.3 B cell sub-groups 95
3.3.2.1.4 Regulatory T cells and NK cells 96
3.3.2.1.5 Chronological age associated changes in cell populations 96
3.3.2.2 Does injury severity or biological age impact immune phenotype 97
3.3.2.2.1 BMI, length of stay and immune phenotype 97
3.3.2.2.2 Injury severity scoring and immune phenotype 98
3.3.2.3 IMM-AGE immune age scoring 100
3.3.2.3.1 Does burn injury cause immune ageing 100
3.4 Conclusions 101
3.5 Appendix 102
3.5.1 Absolute telomere length additional figures 102
3.5.2 Immune phenotyping gating strategy 103

3.5.3 Immune ageing cell counts 109
4. Senescent cells as therapeutic targets 115
4.1 Introduction 115
4.1.1 Targeting senescent cells as a therapy for the ageing phenotype 115
4.1.2 Senolytic discovery and action 116
4.1.3 A model for cellular senescence 117
4.1.4 Aims of the chapter 119
4.2 Results 119
4.2.1 Does traumatic injury affect senescent cell numbers within the skin 119
4.2.1.1 Senescent cell load following trauma 119
4.2.1.2 Senescent cell load cohort information 120
4.2.1.3 Changes in $p16^{INK4A}$ expressing cell percentage over time following burn injury ... 121
4.2.2 Senescence modulating compound discovery 125
4.2.2.1 Compound exposure 125
4.2.2.2 Induction of senescence following X-ray radiation exposure 127
4.2.2.3 Cell viability following treatment with epigenetic compounds 130
4.2.2.4 Effects of compounds on Senescence associated β-galactosidase positive fibroblasts 136
4.3 Discussion 138
4.3.1 Mode of action of epigenetic compounds 138
4.3.1.1 Compounds with a significant effect on cell viability 138
4.3.1.2 Compounds with a significant effect on SA-βGal positive senescent cells 144
4.3.1.3 Compounds with a significant effect on the percentage of SA-βGal positive cells and on cell viability in senescent cells 146
4.3.2 Does traumatic injury influence senescent cell numbers in skin 146
4.4 Conclusion 149
5. Epigenetic age following critical illness 151
5.1 Introduction to epigenetics and DNA methylation 151
5.1.1 DNA methylation and ageing 151
5.1.1.1 Measuring epigenetic age 152
5.1.1.1.1 The use of epigenetic clocks within research 152
5.1.1.2 Critical illness and epigenetic age 152
5.1.1.2.1 The impact of injury and critical illness 153
5.1.1 Aims of the chapter 155
5.2 Results 155
5.2.1 DNA methylation analysis 155

5.2.1.1 DNA methylation analysis: Burns cohort 155
5.2.1.1.1 Patient information 156
5.2.1.1.2 Burns: epigenetic age and chronological age 157
5.2.1.1.3 Burns: differential methylation analysis 169
5.2.1.2 DNA methylation analysis: Sepsis cohort 177
5.2.1.2.1 Sample type 177
5.2.1.2.2 Patient information 177
5.2.1.2.3 Sepsis in the critical care environment: epigenetic age and chronological age 179
5.2.1.3 DNA methylation analysis: COVID-19 cohort 194
5.2.1.3.1 Sample type 194
5.2.1.3.2 Patient information 194
5.2.1.3.3 COVID-19: Epigenetic age and chronological age 195
5.2.1.3.4 COVID-19: Epigenetic age, disease severity and clinical parameters 198
5.2.1.3.5 COVID-19: differential methylation analysis 201
5.3 Discussion 206
5.3.1 Burns 206
5.3.2 Sepsis 213
5.3.3 COVID-19 216
5.4 Conclusion 219
5.5 Appendix 222
5.5.1 Differentially methylated genes 222
6. Unexpected survivors of traumatic injury 225
6.1 Introduction 225
6.1.1 What is an unexpected survivor? 225
6.1.2 The response to injury 226
6.1.3 Possible factors influencing survival 227
6.1.4 Study aims 228
6.2 Results 228
6.2.1 Cytokine differences in patients who unexpectedly died compared with unexpected survivors. 229
6.2.1.1 Cytokine cohort information 229
6.2.1.2 Cytokine and neutrophil analysis comparing unexpected survivors and unexpected deaths 230
6.2.2 Differential methylation between patients who died vs unexpected survivors 234
6.2.2.1 Differential methylation cohort information 234

6.2.2.2 Differential methylation analysis 235
6.2.3 RNA Sequencing analysis 237
6.2.3.1 RNA Sequencing cohort information 238
6.2.3.2 RNA sequencing analysis 239
6.3 Discussion 244
6.3.1 Cytokine analysis 244
6.3.2 DNA methylation and transcriptome analysis 245
6.4 Conclusion 247
7. General discussion 249
7.1 Key findings and interpretation 249
7.2 Study limitations 256
7.3 Recommendations for future work 258
7.4 Concluding remarks 259
8. Glossary 261
9. Bibliography 263

1. Introduction

Please note that a majority of this introductory chapter is based upon a review that I wrote in my first year and published in the journal Ageing Research Reviews (Sullivan et al., 2018).

1.1 General introduction to ageing

Since the advent of the modern industrial era in the mid-19th century there has been a sustained increase in life expectancy at birth, with average life expectancy rising from the mid 40's to late-70's within the past 250 years. This change has meant that the global population has never been older. This increase in lifespan is even larger within western Europe and some Asian countries where the average life expectancy is now reaching the early to mid-80s, with Japan still leading the world with a combined life expectancy at birth for both genders of 83.7 (WHO, 2017). If these trends continue, when paired with decreasing birth rates the United Nations predicts that the number of people aged 60+ is set to reach over 1.5 billion, increasing from 9.3% to 16% of the global population (United Nations et al., 2020).

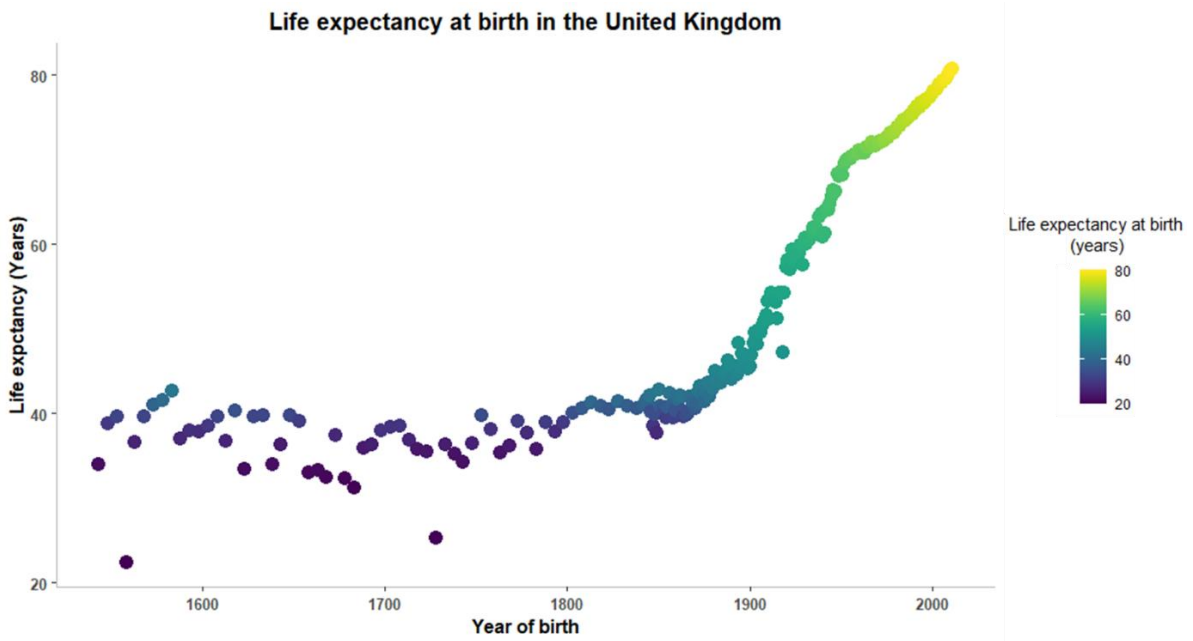


Figure 1.1: Life expectancy at birth in the United Kingdom. This figure was generated using publicly available data from the 'How was life?' publication, produced by 'Clio Infra' a 'Netherlands organization for scientific research' (Zanden et al., 2014; Zijdeman and Ribeira da Silva, 2015). Shown is the average life expectancy at birth in years for both sexes in the United Kingdom over the last 500 years.

Although average lifespan is increasing, the period of life spent in good health, termed "Healthspan", has not kept pace, with people now spending longer portions of their life in ill health. In the United Kingdom the current time spent in ill health is 16.1 years for men and 19.2 years for women (Public Health England, 2016). Understanding the factors influencing the ageing trajectory is required if we are to be better equipped to deal with the effects of demographic change. Whilst genetics and lifestyle have received much attention as influencers of the ageing trajectory (Khaw et al., 2008; Steves et al., 2012), there are other factors largely beyond our control that can have a devastating impact on health across the life course.

This thesis has considered the potential impact of major trauma, with its associated critical illness, on the ageing trajectory and ageing processes. This chapter aims to introduce the potential links between ageing, traumatic injury and the outcomes of injury and critical illness. This will include discussion of the long-term health implications of critical injury as well as highlighting the biological similarities

between the response to injury and the ageing process. The effect the response to injury potentially has on several of the core biological ageing processes will also be discussed together with the potential of targeting these processes for novel therapies.

1.1.1 Ageing as a malleable process

Ageing is perhaps best described in biological terms as an increased inability with time to cope with biological stress resulting in increased risk of disease and death. The biological changes which occur during ageing and drive the aged phenotype have been referred to as the 'Hallmarks of Ageing', and were described in a landmark paper by Lopez-Otin and colleagues (Lopez-Otin et al., 2013). This paper described processes as either core drivers, or downstream mediators of the ageing process. The upstream processes initiating ageing are suggested to be related to damage namely: genomic instability, telomere attrition, loss of proteostasis and epigenetic changes. The more downstream effectors reflect the response to this damage and include mitochondrial dysfunction, cell senescence, altered nutrient sensing, loss of stem cell function and altered intercellular communication, largely related to increased inflammation, as illustrated in Figure 1.2 (Lopez-Otin et al., 2013). These original nine hallmarks have been updated recently to include microbial dysbiosis, disabled macroautophagy and to specifically cite increased systemic inflammation as a distinct biological ageing process (López-Otín et al., 2023). All of these processes increase in the tissues, organs and cells of the body with age, importantly a wide range of studies have now revealed that counteracting these processes extends lifespan and healthspan in a range of species from fruit flies to primates (Colman et al., 2009; Newgard and Sharpless, 2013; Tchkonia et al., 2013).

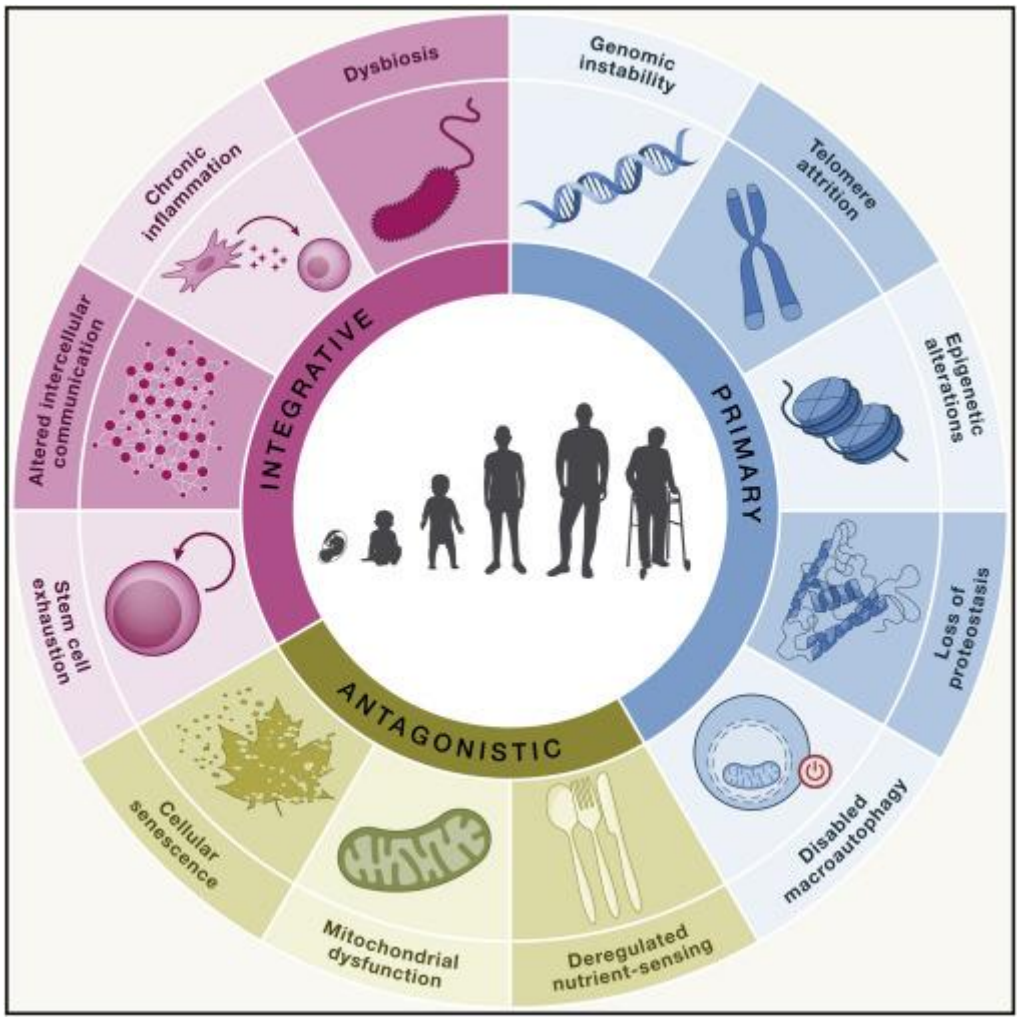


Figure 1.2: The Hallmarks of Ageing. An illustration of "The hallmarks of ageing" which are the driving factors of the ageing phenotype. The hallmarks are divided into five Primary upstream drivers, then the response to the primary causes termed the Antagonistic hallmarks, and finally four downstream mediators of the aged phenotype, termed the Integrative hallmarks. Taken from Lopez-Otin et al., 2023.

Ageing is characterized by a progressive loss of physiological integrity, leading to impaired function and increased vulnerability to death. This deterioration is the primary risk factor for virtually every major human pathology, including cancer, diabetes, cardiovascular disorders, and neurodegenerative diseases. Ageing research has experienced an unprecedented advance over recent years, particularly with the discovery that the rate of ageing is controlled, at least to some extent, by genetic pathways

and biochemical processes conserved across evolution. A major challenge is to dissect the interconnectedness between the candidate hallmarks and their relative contributions to ageing, with the final goal of identifying pharmaceutical targets to improve human health during ageing, with minimal side effects (Lopez-Otin et al., 2023).

Ageing has been shown to be a malleable process with the ageing trajectory showing a high degree of plasticity. Ageing in humans is affected in large part by lifestyle choices, disease, environmental and genetic factors (Langie et al., 2012). Maintaining high levels of physical activity for example is able to preserve the function of several major body systems, including the musculoskeletal (Pollock et al., 2015) and immune systems into old age (Duggal, 2018a, 2018b). Intermittent fasting and calorie restriction have also been shown to reduce both inflammation and the accumulation of senescent cells (Blagosklonny, 2010; Cuervo et al., 2005) and extend both life and healthspan in primates (Colman et al., 2009). The malleability of longevity has also been demonstrated using compounds such as rapamycin, resveratrol and metformin which target some of the core ageing processes directly to extend life span in mice and other model organisms (Harrison et al., 2009; Mouchiroud et al., 2010). Conversely, various biomarkers of ageing appear to be accelerated with poor lifestyle, including increased senescent cell load observed in obesity (Schafer et al., 2016) and raised systemic inflammation with obesity and inactivity (DeBoer, 2013).

Ageing has thus been shown to be a variable process which is affected by virtually every aspect of life. One external factor that can have a significant impact on both lifespan and healthspan, which has so far received little attention from biogerontologists, is major traumatic injury and associated critical illness. Trauma whether physical or emotional is generally described as an injury or damage to a biological organism, or to the psyche of an organism, as a result of a traumatic event such as blunt force trauma, burn, acts of terrorism or exposure to combat. These kinds of events can have long-term impacts on health in later life as well as longevity, regardless of how well the person initially recovers from their injury.

1.1.2 Impact of major trauma on morbidity and mortality

According to the World Health Organisation, death from injury accounts for 10% of annual global deaths, equivalent to approximately 5.8 million people (WHO, 2010). Trauma disproportionately affects the young, being the leading cause of death for under 45s in the US (Lenz et al., 2007). While 5.8 million is an extremely large number of people, a much greater number are injured and survive, providing a new challenge to medicine to improve the long-term health of survivors of traumatic injury.

Perhaps the most apparent long-term impact of surviving a major traumatic injury is the resulting long-term disability experienced by many patients. Evans et al., 2003, studied the prevalence of disability following trauma in a cohort of 109 young adults in the UK (90 male, 19 female. Aged 16-31 years) who were admitted to the hospital with an injury severity score of >15, classifying the injury as major trauma (Palmer, 2007). Of the 109 young adults admitted during the study, 80% experienced a disability which affected their daily activities five years post-injury (Evans et al., 2003).

Importantly, surviving an injury may have long term health consequences that go beyond being left with a disability. Casey and Ballantyne investigated the impact of sustaining a workplace injury on the development of chronic disease (Casey and Ballantyne, 2017), using data on 251 women and 243 men in the 'Canadian community health survey' who were injured between the 2003 and 2008/9 surveys. The prevalence of chronic disease was compared between the injured and non-injured cohorts (n=4495). The study revealed that five years after sustaining a workplace injury the injured workers developed chronic health conditions, including migraine headaches, arthritis, hypertension, asthma, intestinal or stomach ulcers, depression/mood problems, back problems and urinary or bowel disorders at a significantly higher incidence than their matched controls. The authors concluded by stating that suffering a workplace injury is sufficient to increase the risk of developing chronic diseases, many of which are strongly associated with the ageing process. This is in line with the observation that around 16 percent of all disability burden globally is the result of an injury (Krug et al., 2000).

Several retrospective analyses of linked hospital morbidity data for over 30,000 patients admitted with a burn injury between 1980 and 2012 in Western Australia by Duke and co-workers revealed increased admissions for a broad range of classically age-related conditions including cardiovascular disease (Duke et al., 2017), diabetes (Duke et al., 2016) and musculoskeletal conditions (Randall et al., 2015). These studies all suggest a long-term impact on health after surviving a major injury, including an increased risk of diseases most usually seen in older adults.

Not only does major injury increase the risk of chronic disease, there is growing literature providing evidence that a major traumatic injury may also have a negative impact on long term survival. Duke and colleagues also carried out two retrospective analyses of mortality rates in adults aged below and above 45 years with a burn injury using the hospital records of 6,014 patients and 25,759 matched controls. The data revealed increased mortality rate ratios of 1.4 in the over 45 years group and 1.8 in the under 45s (Duke et al., 2015a, 2015c). It is claimed in the papers that these results are likely an underestimate of the impact of burn injury on mortality as the data also included inhospital deaths. The authors suggested that the deaths occurring after discharge from the hospital were potentially due to prolonged oxidative stress, hormone dysregulation and an increased risk of cancer due to the chronic hypermetabolic state often present for years following thermal injury.

Another study investigated the impact of traumatic brain injury (TBI). A TBI is an injury to the brain resulting from sudden trauma such as a blow to the head, or an object piercing the skull and brain tissue directly, TBIs are often accompanied by secondary injury such as hypoxia and herniation resulting from the initial injury (Ghajar, 2000). Brooks *et al* showed in a large-scale study (N=7228) across twenty US hospitals, that after a TBI men aged 40 or under had a 10% increase in mortality over a 20 year period compared to a control population (Brooks et al., 2013).This supports the conclusion of earlier studies which also found that long-term there is a significant increase in mortality among those who have received a TBI (Brown et al., 2004).

What these findings, and the literature more generally show is that a significant physical injury and subsequent critical illness, whether resulting in disability or not, has the potential to increase risk of disease and death. It is possible that this outcome may be due, in part, to an acceleration of the ageing process.

1.2 How might trauma impact the ageing processes?

While the exact mechanisms responsible for increasing the risk of disease and death following a critical trauma are yet to be fully elucidated, it is likely that there are multiple processes at work, many of which may be common between the response to traumatic injury and the physiological ageing process. Thermal injury and many forms of traumatic injury result in a cascade of metabolic changes which result in increased oxidative stress, inflammation, multiorgan damage, tissue loss, changes to body composition and increasing frailty (Duke et al., 2015c). The changes just described are also often associated with ageing and the immediate response of the body to traumatic injury includes processes that also drive the ageing process, including inflammation, metabolic dysregulation, and epigenetic changes.

1.2.1 The inflammatory response to trauma

One common factor between ageing and the response to trauma is increased inflammation. There is a growing consensus within the literature that inflammation, as well as being a consequence of ageing, may also be one of the driving forces behind it (Lopez-Otin et al., 2023). The basal, chronic inflammation that develops and persists as a part of normal ageing has been dubbed 'inflammaging' (Franceschi et al., 2000). As we age there is an increase in chronic low-grade basal inflammation, with raised serum levels of CRP and pro-inflammatory cytokines such IL6, TNFα and reduced levels of anti-inflammatory cytokines such as IL10. The presence and amount of inflammaging is associated with increased mortality (Franceschi et al., 2007) as well as age-related frailty (Baylis et al., 2014) and several age-related diseases (Chung et al., 2009; Franceschi and Campisi, 2014).

There are many factors influencing inflammaging including environmental factors such as physical inactivity (Burini et al., 2020; Phillips et al., 2017), adiposity (Ellulu et al., 2017; Zatterale et al., 2020), ageing of the immune system (Bartlett et al., 2012) as well as the accumulation of senescent cells which have a pro-inflammatory secretory profile (Freund et al., 2010). Any form of tissue damage that occurs during trauma will generate a sterile inflammatory response initiated by the Damage-associated Molecular Patterns, DAMPs, released from the injured site (Zhang et al., 2010; Lord et al., 2014). These DAMPs bind to the same receptors on immune cells that recognise pathogens, such as the Toll Like receptors in the case of some injuries such as burns, this inflammation persists at a low level for many years (Jeschke et al., 2011). In addition, the initial inflammatory response to injury results in compromised immunity, increasing susceptibility to infections and sepsis (Lord et al., 2014), the mechanisms of which remain poorly understood (Figure 1.3). This increased and chronic inflammatory burden may well mimic and contribute to accelerating the ageing process.

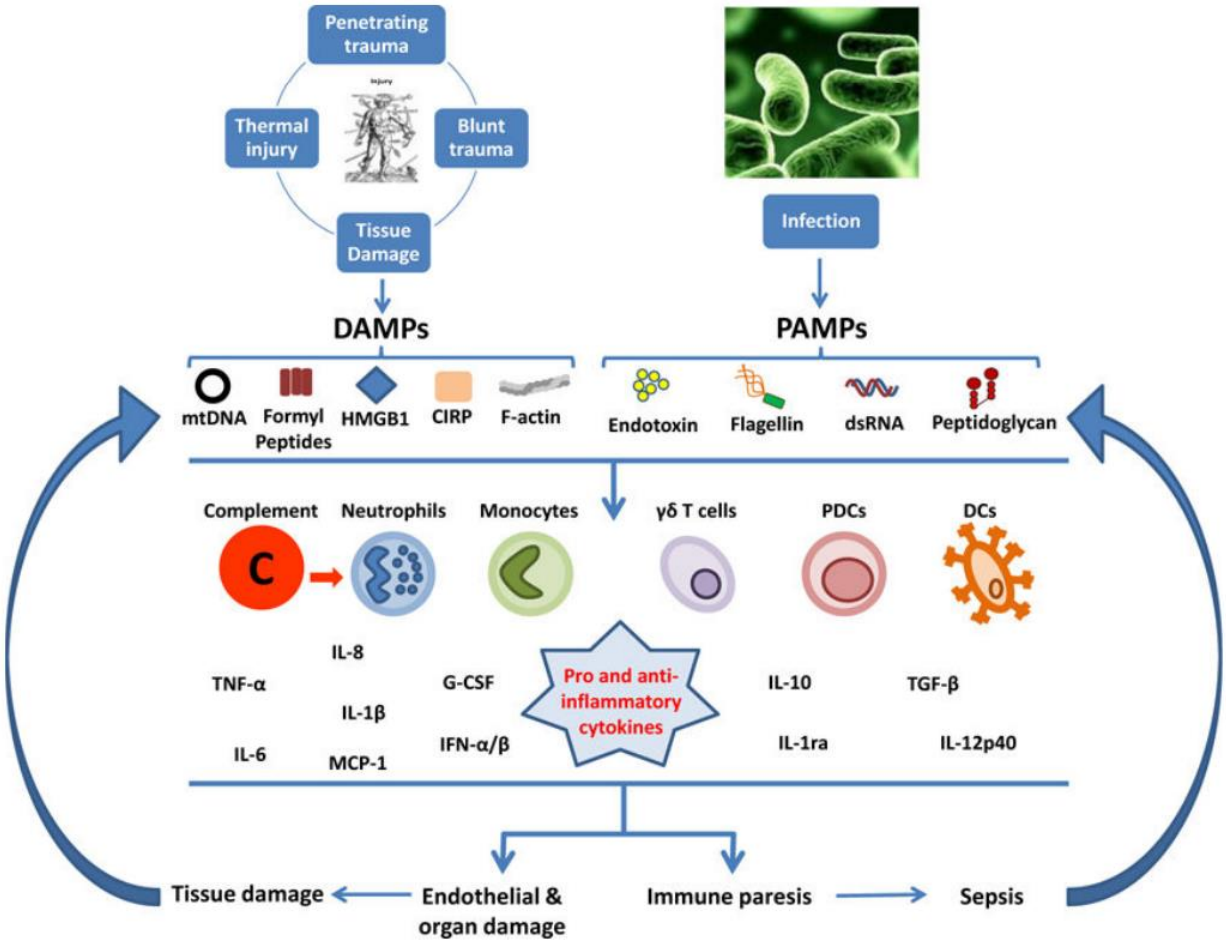


Figure 1.3: Activation of the immune system after trauma. The figure illustrates that both damage and infection release molecular signals, DAMPs and PAMPs respectively, that activate a broad range of immune cells. These in turn produce a range of cytokines that can induce both tissue damage and immune paresis if produced in excess. Taken from Lord et al., 2014.

Inflammation has been shown to increase the number of DNA lesions present within a tissue as a direct result of the increase in reactive oxygen (ROS) and nitrogen species (RNS) present during chronic inflammation (Meira et al., 2008). Trauma which often includes significant blood loss and then tissue reperfusion injury after restoration of blood volume, leads to extended ischaemia in body tissues which in turn generates ROS and RNS and leads to damage to mitochondrial DNA with long lasting impact on mitochondrial function (Ruchko et al., 2005; Papadopoulos et al., 2013). This is one possible mechanism for accelerating the ageing process after trauma as dysregulated mitochondrial function has also been described as a hallmark of ageing (Lopez-Otin et al., 2013).

1.2.2 Telomere attrition and trauma

Telomere length has frequently been used as a biomarker of ageing (Mather et al., 2011). Telomeres are hexanucleotide repeats that aid in maintaining genomic integrity and 'cap' the ends of the chromosomes to reduce the risk of the coding portion of the genome being exposed. Due to the sequence being incompletely replicated during each cellular division, the length of a telomere is shortened by 25-200 bases with each cell division. Telomere length can therefore be used to establish the relative biological age of a cell and to a certain extent of the whole organism. For example shorter leukocyte and total PBMC telomere length has been shown to be associated with increased risk of disease such as cancer, diabetes and heart disease (Blackburn et al., 2015) as well as mortality (Cawthon et al., 2003). Wang et al., performed a meta-analysis of 25 studies which reported associations between leukocyte telomere length and all-cause mortality encompassing 121,749 individuals with a total of 21,763 deaths. They concluded that short telomere length corresponded to a high risk of all-cause mortality, with those falling in the shortest 25% for telomere length having a 26% higher hazard ratio than those participants with the longest telomeres (Wang *et al.*, 2018). Another meta-analysis, including 43,725 participants across 24 studies found an inverse relationship between leukocyte telomere length and cardiovascular disease risk (Haycock et al., 2014). The authors concluded that across all of the studies that being in the shortest 33.3% of relative telomere length imparted a relative risk of cardiovascular disease of 1.4 compared to being in the longest 33.3%.

It is worth mentioning that while telomere length has for a long time been a standard biomarker for cellular ageing, the reliability of telomere length alone as a marker for organismal ageing is in doubt as many studies have shown an inconsistent link between telomere length and many aspects of the ageing process in humans (Sanders and Newman, 2013).

Traumatic stress, such as PTSD whether in combat exposed veterans or victims of childhood abuse is now understood to not only have a lasting psychological impact but a physical one. This is reflected both in the culture in "popular science" books discussing the subject such as "The body keeps the

score" - Bessel, 2014, and within the research literature. PTSD, as well as increasing the risk of disease and mortality (Ahmadi et al., 2011), impacts telomere length. O'Donovan and colleagues conducted a study into telomere length consisting of 43 adults with chronic PTSD and 47 adults without. They found that participants with PTSD, especially those with childhood trauma had significantly shorter telomere lengths than those without (O'Donovan et al., 2011). This finding has been corroborated in more recent studies which have also have concluded that PTSD has a significant impact on telomere length, causing attrition (Kim et al., 2017), and by Aas et al, who found childhood trauma to have a negative impact on telomere length in participants with schizophrenia and bipolar disorder (Aas et al., 2019). There is some contradicting evidence within the literature however, with others reporting contradictory findings, i.e., telomere elongation in trauma victims (Boks et al., 2015).

However, in two recent meta-analyses, one of which was focused on PTSD (X. Li et al., 2017) and one on the long term impact of childhood trauma (Z. Li et al., 2017), both concluded that these stressors were associated with significant telomere shortening. It is worth mentioning that there are multiple co-factors such as substance abuse which are commonly associated with childhood trauma and PTSD generally (De Bellis, 2002). These factors may also contribute to prematurely shortened telomeres making it difficult to attribute any telomere attrition purely to the presence of PTSD.

The little research that has been done on the impact of physical traumatic injury is in repeat mild traumatic brain injury models in rats, which showed telomere shortening was associated with brain injury confirmed by MRI (Wright et al., 2018). However, one study of Dutch military veterans reported no impact of physical injury on telomere length (Boks et al. 2015). So, while there is evidence to suggest that telomere shortening is present to some degree following both emotional and physical trauma, there is clearly a major research gap which needs to be filled by further clinical studies.

Again it is likely that inflammation contributes to a reduction in telomere length as telomere attrition has been associated with systemic and chronic inflammation (D'Aiuto et al., 2010; Masi et al., 2011). While the exact relationship between inflammation and telomere shortening is yet to be fully

understood, it is likely that they have a bi-directional influence (Jurk et al., 2014; Kordinas et al., 2016). Damaged tissue itself has been shown to have decreased telomere length and increased ROS production (Felice et al., 2009), which may be mediated by the direct actions of cytokines or ROS. The downstream effector of cytokine actions, NFκB can regulate telomerase expression (Zhang et al., 2016) and ROS can damage DNA triggering a DNA Damage Repair response and eventually senescence (Correia-Melo et al., 2014). Furthermore, in mice chronic inflammation can directly cause ROS-mediated telomeric DNA damage, and this dysfunction can be prevented anti-inflammatory drugs (Jurk et al, 2014).

1.2.3 Cellular senescence and trauma

Cell senescence, characterised by permanent cell cycle arrest, while synonymous with ageing, is also a vital mechanism used to prevent tumorigenesis in cells which reach their replicative limit or have damaged DNA (Childs et al., 2015). These cells are also important for wound healing (Demaria et al., 2014; Jun and Lau, 2010). Senescent cells remain metabolically active and secrete growth factors (VEGF), matrix metalloproteinases and proinflammatory cytokines, termed the Senescence Associated Secretory Phenotype (SASP) (Freund et al., 2010), these secretions are a consequence of the changes in gene expression following cell cycle arrest (Coppe et al., 2008).

Cellular senescence was first observed in vitro, the concept of cells reaching a replicative limit after which they enter a state of arrest was described by Hayflick and Moorhead, in 1961. We now know that the phenomenon they described is replicative senescence and is due to the telomere attrition which occurs during each cellular division as discussed in the previous section. It is also now known that cellular senescence also occurs in vivo as well as in vitro, and that senescent cells accumulate in tissues with age (Campisi, 2005).

As well as telomere attrition, cellular senescence can also be induced via biological stress. Cellular or genomic damage can all be the result of internal or external biological stressors such as radiation or ROS (Zdanov et al., 2006; Rodier et al., 2009). A damaged cell has multiple options, repair, apoptosis,

necroptosis or senescence (Surova and Zhivotovsky, 2013). Stressors induce senescence predominantly via the activation of two cell cycle arrest pathways, the p53/p21$^{WAF1/CIP1}$ and p16^{INK4A}/pRB pathways (reviewed by Kumari and Jat, 2021). This was also described by Mijit *et al*, as in Figure 1.4. These pathways mediate the multi-step process that leads to the senescent phenotype which differs between cell types but will often include: an enlarged and flattened morphology (Campisi and d'Adda di Fagagna, 2007), an increase in lysosomal content with β-galactosidase activity (Lee et al., 2006), resistance to apoptosis (Zhu et al., 2015), altered gene expression resulting in a complex secretome (SASP) (Saleh et al., 2018), and chromatin remodelling (Chandra et al., 2015). These features of the senescent phenotype allow the identification of senescent cells in vitro and can permit assessment of senescent cell load in vivo, for example by measuring SASP components in serum, though the latter is still a developing field as many SASP components such as pro-inflammatory cytokines are not specific to senescent cells.

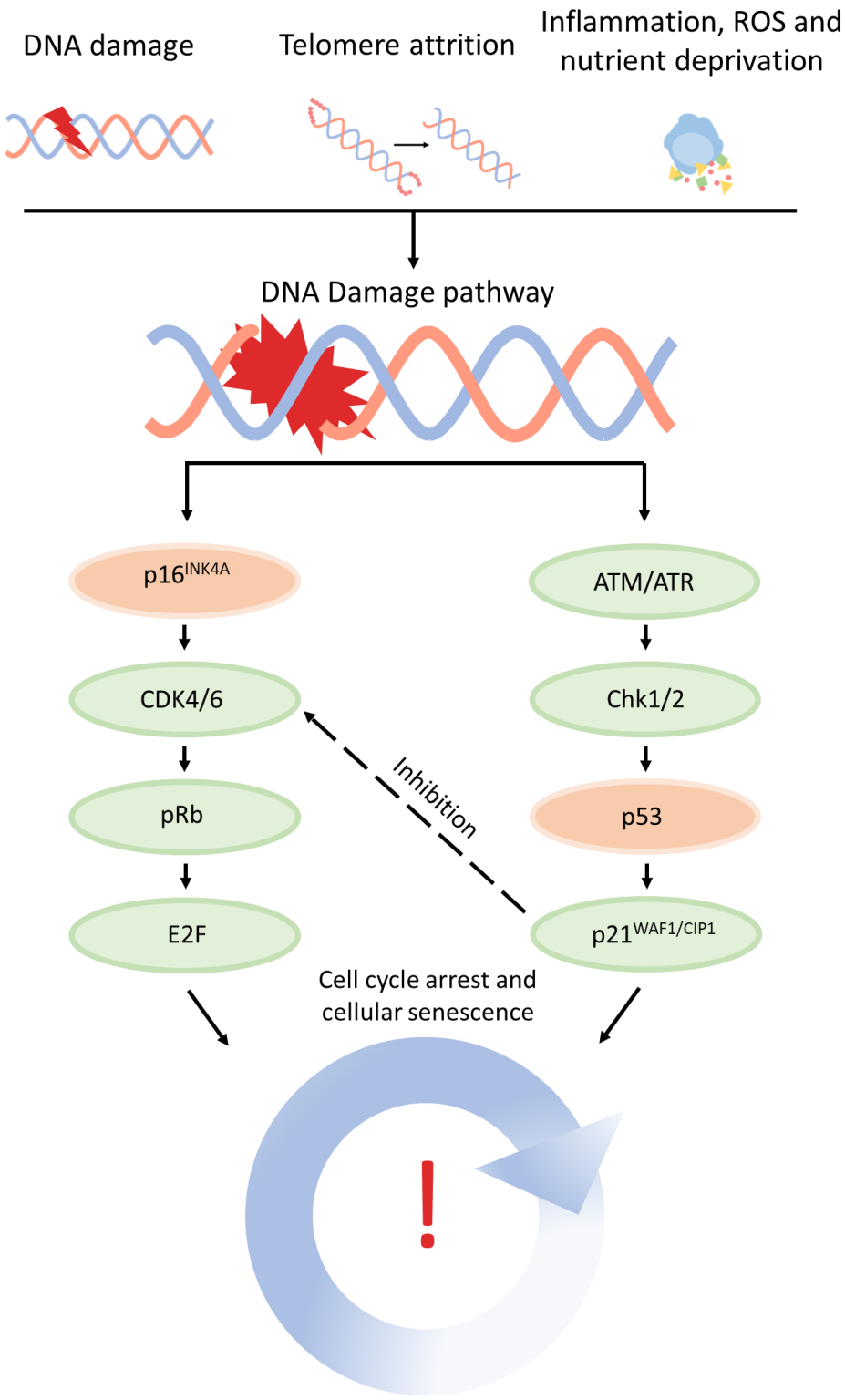


Figure 1.4: Cell cycle arrest and cellular senescence as a response to genomic damage. Shown is the activation of the cell cycle arrest and cellular senescence p16 and p53 pathways following DNA damage from a variety of sources. ROS; reactive oxygen species.

1.2.3.1 Measuring cellular senescence

There are myriad ways to measure cellular senescence and most techniques focus on looking for the presence of senescence biomarkers, usually proteins involved in cell cycle arrest, or a protein only found within senescent cells. There is also increasing interest in extracellular vesicles that are shed by senescent cells (Misawa et al., 2020) as these could offer a route to assessing cell load via a serum measure. Due to the increasing senescent cell load with age, monitoring the number of senescent cells could eventually be used as a tool to measure biological age, though current methods do not permit this. The following section describes some of the most common markers used to determine a senescent state.

1.2.3.1.1 $p21^{WAF1/CIP1}$ and $p16^{INK4A}$

The cyclin-dependent kinase inhibitor p21 ($p21^{WAF1/CIP1}$) protein mediates p53 cell cycle arrest in cells during the G1/S phase of the cell cycle as a response to stimuli including oxidative stress or DNA damage by inhibiting the activity of CDK4/cyclin D and CDK2/cyclin E (Abbas and Dutta, 2009). The $p16^{INK4A}$ protein is encoded by the tumour suppressor gene CDKN2A and its primary role is as a CDK (cyclin-dependent kinase) inhibitor during cell cycle arrest during the G1 phase, inhibiting the binding of CDK4/6 with cyclin D1 (Agarwal et al., 2013; Mijit et al., 2020), thereby preventing proliferation. The presence of either $p16^{INK4A}$ or $p21^{WAF1/CIP1}$ in cells has therefore been associated with cellular senescence during ageing, as well as cellular damage and cancer more generally (Muss et al., 2020). As they are expressed in any arrested cell, they cannot by themselves be used to confirm cell senescence.

1.2.3.1.2 γH2AX

γH2AX is the phosphorylated form of the histone variant H2AX, H2AX becomes phosphorylated at the omega-4 serine residue in response to DNA double strand breaks (Dickey et al., 2009). Cell cycle arrest

whether induced by DNA double strand breaks or telomere attrition involves the ATR-dependent phosphorylation pathway of which γH2AX plays a role (Bernadotte et al., 2016). γH2AX is involved in chromatin remodelling allowing DNA repair machinery access to the damaged section of the genome (Jiang et al., 2010), its phosphorylation also has the downstream effect of recruiting homologous recombination DNA repair proteins such as RAD51 (Anand et al., 2017).

As well as γH2AX being present during the presence of DNA damage, which may lead to cell cycle arrest, senescent cells are often positive for DNA damage proteins in the absence of detectable genomic damage. This term has been referred to as a "pseudo-DNA damage response" and is theorised to be a marker of the over-activated phenotype synonymous with senescent cells (Pospelova et al., 2009). Its association with DNA damage, telomere attrition and ageing have made γH2AX a popular senescence biomarker (Bernadotte et al., 2016).

1.2.3.1.3 Senescence associated β-Galactosidase (SA-βGal)

The presence of a high level of senescence associated β-galactosidase (SA-βGal) in the large number of lysosomes that develop during cell senescence has long been used for the identification of senescent cells (Lee et al., 2006). This is especially used in *in vitro* studies where the process is fast and easy to analyse on cells in culture. The SA-βGal assays can be colorimetric and based upon the cleavage of a labelled galactosidase which changes colour, usually to a blue or brown product, when cleaved by β-galactosidase.

1.2.4 The impact of cellular senescence

Senescent cells are not exclusively negative for human health; as well as playing a role in development and being anti-tumorigenic they also have a role vital to wound healing (Jun and Lau, 2010). Inflammation is important for recruitment of immune cells required to prevent infection after tissue injury, and the SASP also contains factors required to limit fibrosis and scarring, notably PDGF-aa (Demaria et al., 2014). Fibroblasts are present at wound sites during healing to replace damaged skin

and secrete the extracellular matrix found in fibrotic scar tissue. Cellular senescence is the mechanism by which the proliferation of different cell types, such as the satellite cells which produce extracellular matrix in scar tissue is regulated (Soto-Gamez and Demaria, 2017). Mice deficient in senescent cells show compromised wound healing (Demaria et al., 2014). One possible unintended consequence of the evolved wound healing response requirement for senescent cells may be an increased burden of senescent cells in trauma survivors, contributing to acceleration of the ageing process.

Although senescent cells can be removed by immune cells such as NK cells (Sagiv and Krizhanovsky, 2013) and CD8 T cells (Pereira et al., 2019), the immune system undergoes substantial remodelling with age resulting in reduced effectiveness, referred to as immune senescence (Duggal, 2018). In addition, senescent cells can also reduce the ability of NK and CD8 T cells to kill them by expressing HLA-E, which blocks the cytotoxic receptor NKG2D which recognises senescent cells (Pereira et al, 2019). As a result, with advancing age the senescent population of cells increases.

Another feature of senescent cells is called the bystander effect in which senescent cells induce senescence in neighbouring healthy cells (Nelson et al., 2018). This occurs as senescent cells accumulate within a tissue, causing the micro-environment to change. An increase of pro inflammatory cytokines produced by senescent cells in their SASP, such as Interleukin (IL)-1, IL-6, IL-8 begins to contribute to localised inflammation within the area. This, paired with the increase in growth factors such as VEGF within the SASP and the presence of mitochondrial derived ROS (Passos et al., 2007) creates an environment in which senescent cells induce senescence in neighbouring cells. This, as well as having a detrimental effect at the tissue and organismal level creates a negative cycle of increasing levels of SASP which increase the numbers of senescent cells which again, in turn, increases the levels of SASP and senescent cell burden.

The detrimental physiological effects of accumulating senescent cells are well illustrated by a series of experiments in mouse models. Xu et al., 2018, showed that transplanting what they described as a small number of senescent cells (0.5×10^6) into young mice reduced their physical function, as well as

inducing the development of senescent cells within previously senescent cell free tissue. This suggests that cellular senescence is one of the key driving factors of the reduced physical function associated with ageing. This was confirmed within the same study when the targeted removal of senescent cells using a combination dasatinib and quercetin rescued the physical function in young mice as well as improving overall physical function and survival in naturally aged mice. Interestingly, a recent study from the Mittelbrunn lab showed that just inducing senescence in T cells in mice was sufficient to induce an aged and multimorbid phenotype (Desdín-Micó et al., 2020), a similar finding was also observed by Yousefzadeh et al., 2021, who observed an aged immune phenotype was able to promote systemic ageing within mice. This suggests a key role for the senescence of the immune system in the ageing process.

As well as improving survival, reduced disease burden following the ablation of senescent cells has also been demonstrated in mice. Baker *et al,* used a progeroid mouse model to illustrate how the life-long ablation of senescent cells can delay the onset of diseases such as cataracts and sarcopenia, while treatment in later life slowed their progression (Baker et al., 2011). This shows the detrimental impact senescent cells play with regards to multiple age associated pathologies. These effects of senescent cell removal, which have for a long time been demonstrated in animal models, are now beginning to show promise within human trials.

The association between human disease and cellular senescence is well reported, though causality is not yet as well established as in animal models. Cellular senescence has been suggested to play a key role in many pathologies including but not limited to obesity and type-2 diabetes, Alzheimer's disease, fibrotic and vascular disorders (Boccardi et al., 2015; Childs et al., 2018; Conley et al., 2020). Some of the best evidence for a causal role comes from the human progeroid syndromes such as Werner's Syndrome. In this disease the WRN gene, which encodes a DNA repair helicase, is mutated and produces a shortened protein resulting in impaired DNA repair, causing senescent cells to accumulate leading to early development of an aged phenotype and mortality (Cox and Boubriak, 2016).

As was initially shown in mice, the effects of some senolytics appear to be both effective and well tolerated in early human trials. A senolytic is a compound which selectively targets and induces cell death in senescent cells. The preliminary report from a clinical trial of a 3 day course of previously identified senolytic agents Dasatinib and Quercetin showed a significant reduction of 62% of SA-βgal^{+} cells within the adipose tissue in individuals with diabetic kidney disease, a reduction was also noted when looking at p16 and p21 expressing cells (Hickson et al., 2019). Another study using Dasatinib and Quercetin, this time looking at physical function in an idiopathic pulmonary fibrosis cohort, also saw a positive effect. Following the administration of the senolytic agents three days a week over three weeks, measures of physical function, including 6-min walk distance, 4-m gait speed and chair-stands time were significantly and "clinically-meaningfully" improved (Justice et al., 2019).

The evidence is now accumulating that senescent cells are a key driver in the ageing process and these therapies offer a potential method of treatment for trauma patients if injury is in fact shown to increase senescent cell populations over the long term within the tissue, and for the age associated increase in senescent cells more generally. However, increased senescent cell burden within the tissue of trauma patients has not yet been demonstrated and represents a novel area of investigation that could result in new therapies to improve long term outcomes for critically injured adults.

1.2.5 Immune senescence

As well as senescent cells accumulating within tissues as we age, there is an accompanying increase in senescent immune cells, as well as a more general age associated remodelling to both the adaptive and innate immune systems referred to as immune senescence (Aiello et al., 2019). The result of immune senescence is a reduced ability to recognise and kill pathogens, compromised immune surveillance of pre-cancerous cells, poor responses to vaccines and an increased risk of autoimmune disease (Tarazona et al., 2002). In addition, as senescent immune cells resemble non-immune senescent cells in many ways they also produce as SASP (Callender et al., 2018a) and so contribute to

the common, basal, pro-inflammatory phenotype observed in old age, termed inflammaging (Franceschi, 2008). Many of the major changes outlined in this section are summarised in Figure 1.5.

In T cells senescence is usually characterised by the presence of the surface marker CD57 in combination with other cell type specific surface proteins (Ng et al., 2015) such as the loss of CD28 and acquisition of NK cell proteins such as KLRG1, as well as expression of proteins like PD-1 which are responsible for reduced response to signals, termed immune exhaustion (Callender et al, 2017). T cell "exhaustion" is a description of late-stage differentiation which is characterised by a loss of functionality, including cell cycle arrest and a cessation of cytokine production (Pawelec, 2019). While both exhausted and senescent T cells enter cell cycle arrest (Shive et al., 2021), senescent cells remain functionally active, and continue to produce pro-inflammatory cytokines (Pawelec, 2019).

Immune senescence is also characterised by a reduction in antigen-naïve cells, and an accumulation of memory cell subsets (Duggal et al, 2018). The reduction in naïve T cells is because the thymus, which is the source of newly released T cells, begins to atrophy and increase in adiposity during puberty, a process which continues throughout life such that less than 5% of the thymus remains by the age of 65 (Palmer, 2013). This age-associated thymic atrophy has been shown to correspond to the reduced number of newly produced naïve T cells, a classic feature of immune ageing (Pido-Lopez et al., 2001). Evidence suggests that other T cell subsets are modulated in both frequency and function during the ageing process.

Naïve T cells increase in their propensity to differentiate into Th17 cells in aged individuals, leading to a higher prevalence of proinflammatory Th17 cells in older individuals (Bhadricha et al., 2021; Mitsdoerffer et al., 2010). Regulatory T cells or "Tregs", have been shown to accumulate with age (Jagger et al., 2014), but the anti-inflammatory capacity of Tregs is reduced with ageing (Fessler et al., 2013). There is an increase in Treg senescence due to the increase in peripheral expansion of Tregs to compensate for reduced thymic output (Fessler et al., 2013). This increase in pro-inflammatory cells

and decreased anti-inflammatory function is both a sign and cause of immune ageing and inflammaging.

Like what is observed within the T cell compartment, immune remodelling of the B cell population also occurs during the ageing process. There is a decline in overall B cell function with age, resulting in a reduced immune response to infection, vaccination and increased incidence of autoimmunity (Ademokun et al., 2010a). This reduced efficacy observed in the B cell population is due in large part to the reduction in naïve B cells as well switched memory B cells which play a major role in maintaining a protective humoral response (Pinti et al., 2021). This decrease in naïve and switched memory B cells is accompanied by an increase in the presence of late stage differentiated and exhausted B cells (Ademokun et al., 2010a; Frasca et al., 2012).

Monocyte and neutrophil function also reduce with age. Neutrophils have been shown to become more pro-inflammatory and show a decrease in chemotaxis during ageing (Sapey et al., 2014). Monocytes also become more pro-inflammatory, releasing cytokines in the absence of infection, due to increasing TLR4 mediated cytokine production (Shaw et al., 2013). This contributes to local and systemic inflammation and can result in chronicity of inflammation as pro-inflammatory cells fail to leave a tissue promptly (Brubaker et al., 2013).

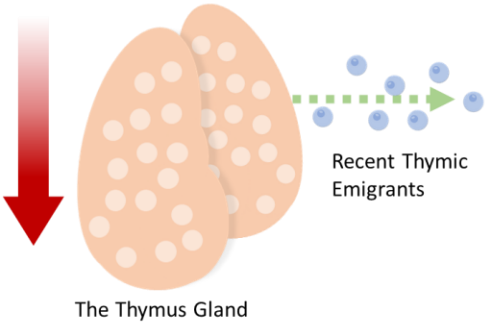
The chronic, low-grade systemic inflammatory phenotype which develops during the ageing process, inflammaging, is characterised by increased levels of pro-inflammatory molecules (IL1β, TNFα, IL6, IL8, IL17) and a reduced level of anti-inflammatory cytokines (IL1ra, IL10) (Bartlett et al., 2012). Infection, chronic stimulation, dysregulated gene expression, damage associated molecular patterns (DAMPs), adiposity and microbial dysbiosis all play a role in driving Inflammaging (Lopez-Otin et al., 2023) and are inexorably linked to gradual shift towards an immune-senescent phenotype (Pinti et al., 2021).

The potential primary role of immune ageing in driving the ageing process has been suggested by a recent study in mice. Yousefzadeh et al., (2021b) demonstrated in a lymphocyte specific *Ercc1* knockout mouse model that immune ageing was sufficient to promote systemic ageing in non-

lymphoid tissues, increasing the numbers of senescent cells, and driving the ageing phenotype. This was also true in wild type mice implanted with splenocytes from the prematurely immune aged mice. This study also showed a rescue of the ageing phenotype in both knockout and wild mice when the mice were treated with rapamycin, an mTOR inhibitor (Yousefzadeh et al., 2021).

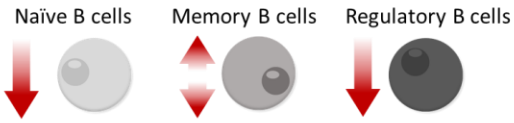
The aged phenotype observed in mice with immune senescence is also observable in humans. Immune senescence has been shown to be increased in multiple age-associated pathologies such as COPD and pulmonary fibrosis (Murray and Chotirmall, 2015). As well as being responsible for disease and blunted vaccine response (Cox et al., 2020), immune senescence results in an increased susceptibility to and increased severity of infection such as sepsis (Martín et al., 2017). which is of relevance within the trauma setting as sepsis mortality is approximately one in three patients. If critical trauma increases immune senescence this may contribute to an accelerated ageing trajectory in trauma survivors.

Thymic involution



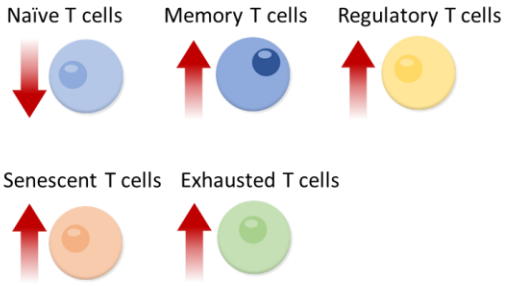
During the ageing process thymic involution occurs, the thymus decreases in size, becomes more fibrotic and has an increasing proportion of adipocytes[1]. This is associated with a decrease in the production of naïve T cells[2].

Changes to B cell populations



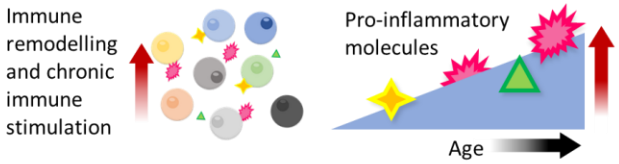
Ageing causes a reduction in the proportion of naïve and switched memory B cells along with an increase in the proportion of unswitched memory B cells[7,8]. There is also a decrease in the proportions of regulatory B cells (CD24+, CD38+) with age[7].

Changes to T cell populations



During the ageing process there is a gradual decrease in the proportion of naïve T cells (CCR7+, CD45RA+), this is accompanied by an increased proportion of different memory T cell subsets such as central memory (CCR7+, CD45RA-), effector memory (CCR7-, CD45RA-) and EMRA (CCR7-, CD45RA+) T cells[3]. Regulatory T cells also accumulate with age (CD25+, Foxp3+) forming a greater percentage of the total T cell population, with reduced function[4]. There is an age associated increase in the proportion of senescent (CD57+, CD28-) and exhausted CD4 and CD8 T cells[5] as well as an increase in senescent NK cells (CD56+, CD57+)[6].

Inflammaging



The immune remodelling which occurs with age is associated with a chronic, low-grade inflammation. Pro-inflammatory molecules such as CRP, IL-1, IL-6, IL-15 and TNF-α are elevated[8], this is accompanied by a change in innate immune cell sub-populations such as an increase in pro-inflammatory monocytes[9]. There is also blunted immune response to stress and dysregulated chemotaxis which effects both the adaptive and innate immune systems[8,10]. This process is referred to as "Inflammaging"[11].

Figure 1.5: The remodelling of the immune system with ageing. Illustrative figures depicting some of the major changes to the immune system which occur during the ageing process. CRP; C-Reactive protein. [1]Dixit, 2010, [2]Palmer, 2013, [3]Li et al., 2019, [4]Xu and Larbi, 2017, [5]Garg et al., 2014,[6]Hazeldine and Lord, 2013, [7]Duggal et al., 2018, [8]Pinti et al., 2021, [9]Seidler et al., 2010, [10]Shaw et al., 2013, [11]Franceschi et al., 2000.

The degree of immune ageing within a person has historically been quantified by profiling cell subsets which are known to change with age such as naïve and memory T cells (Qin et al., 2016) and comparing the findings between groups of interest. This may reveal differences but does not quantify the ageing of the immune system as a whole. In other words, there was no composite measure that could give an overall indication of how the immune system had aged in an individual. However, in 2019 Shen-Orr's team produced a composite set of biomarkers with an associated algorithm to estimate the degree of overall immune ageing, termed IMM-AGE (Alpert et al., 2019). Although this algorithm does not consider neutrophils or NK cells, it was shown to change with increasing age in a longitudinal study and was associated with mortality, thus indicating it as a good marker of immune ageing. A similar composite score based on 51 inflammatory biomarkers has also been developed, termed iAGE (Sayed et al., 2021), this score was associated with increased frailty.

Immune ageing may therefore not only be a result of the ageing phenotype but a driving factor in the ageing process itself, and one which may be influenced by injury. Importantly there are now tools to assess the degree of immune ageing after trauma.

1.3 Epigenetics: a way to measure biological ageing

There are now many potential biomarkers for monitoring the progression of the ageing process, such as the panel of 'healthy ageing biomarkers' proposed by Lara *et al* (Lara et al., 2015), and those discussed so far. These combinations of biomarkers which characterise physical and cognitive function, inflammatory cytokines and immune cell characteristics while valid have some limitations. Notably they require non-standard laboratory techniques (Alpert et al, 2019; Sayed et al, 2020) so could not easily be scaled up for general health checks or involved a broad range of assessments that whilst simple could not be done in a routine GP setting (Lara et al, 2015). Until recently there was no

method of measuring overall, non-tissue dependent biological ageing but this problem is being overcome by the burgeoning field of epigenetics.

Epigenetics describes any modification to DNA or chromatin which does not affect the DNA sequence itself. Of specific interest with regards to ageing is the epigenetic modification of DNA methylation. DNA methylation is the covalent addition of a methyl group by a DNA methyltransferase enzyme (DNMT), usually, to the 5th carbon atom of the pyrimidine ring of cytosine, forming 5-methylecytosine (Kumar et al., 2018). DNA Methylation is a mechanism which regulates gene expression by preventing the adherence of translational machinery to the DNA (Medvedeva et al., 2014). Increased methylation within the promotor region of a gene has been shown to reduce expression (Suzuki and Bird, 2008). This may explain why there is an abundance of CpG islands within the promotor regions of genes, with over 50% of human genes containing CpG rich promotor regions (Vavouri and Lehner, 2012). This is further supported by observations of increased promotor methylation reducing gene expression, with gene body methylation having the inverse effect (Moore et al., 2013; Yang et al., 2014).

DNA methylation patterns gradually change and become more dysregulated during ageing; along with a global trend of hypomethylation in previously methylated CpG rich regions, although some regions do become hypermethylated (Heyn et al., 2012; Johnson et al., 2012). This is believed to be due to the phenomenon known as “epigenetic drift” and is thought to contribute to the ageing process itself (Teschendorff et al., 2013). This ‘drift’ occurs as methyl groups are erroneously added or removed which may be due to mutation, repair, or failure to copy the methylation pattern during replication, as illustrated in Figure 1.6. As well as affecting the gene expression profile of an individual, their levels of ‘epigenetic drift’ can be used to accurately predict their chronological age.

While sites becoming unmethylated due to error is a random process, certain sites change predictability with age. These regions which become hyper and hypomethylated with age are utilised by many of the popular “epigenetic clocks”. The reasoning behind how a seemingly random process can produce predictable results is likened to the presence of DNA damage within the genome,

transcribing regions are preferably repaired compared to those within non-transcribed regions of the genome, a similar process of selective DNA methylation maintenance and repair may be responsible for these “random but predictable” changes (Issa, 2014).

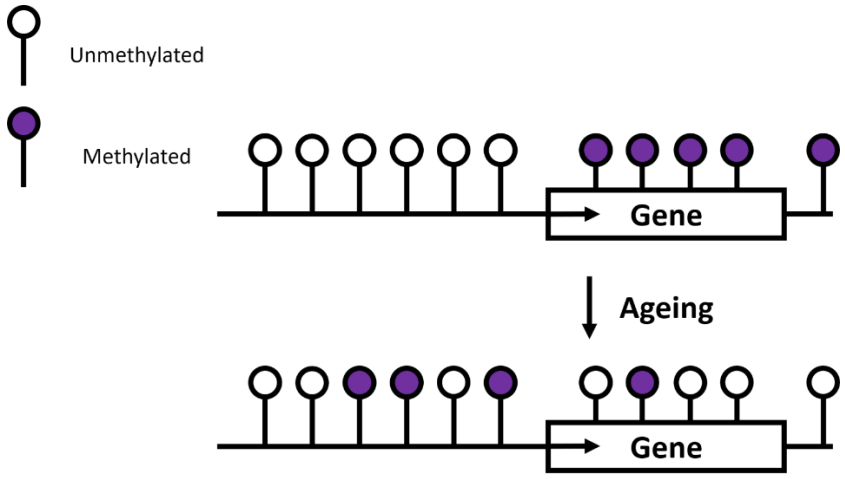


Figure 1.6: Epigenetic drift. An illustration depicting the age associated changes to the methylome known as “epigenetic drift”. Sites within the genome can be seen to become methylated or unmethylated during the ageing process.

This epigenetic age prediction is done using an ‘epigenetic clock’ to analyse methylation data gathered on an illumina 450 or 850/EPIC methylation array. Different research groups have found that methylation intensity values from different sites within the genome are strongly predictive of chronological age in healthy populations. The corresponding values within a given sample are compared and a “biological age” is generated. A person’s biological age differing from their chronological age suggested that their ageing trajectory has been altered. The methylation sites are usually within CpG islands, and the degree of methylation is associated with increased mortality and is therefore a measure of biological age (Horvath, 2013). Epigenetic clocks have been developed by many different groups, using different sample types and different probes, as well as different end points such as either death or disease. This means that each clock will generate a different epigenetic age and may be sensitive to different factors, such as cell type, although no one clock is more ‘correct’

than the other. Some of the most popular clocks within the field are currently the Horvath (S. Horvath, 2013), the Hannum (G. Hannum et al., 2013) and DNAm PhenoAge (Levine et al., 2018). Interestingly other clocks are also being developed that do not rely upon DNA methylation measurement, these include a version of PhenoAge which uses routine clinical biochemistry data (Levine et al, 2018) and one based on metabolomics (Robinson et al., 2020).

1.3.1 The Horvath epigenetic clock

The Horvath epigenetic clock was first published in the landmark paper "DNA methylation age of human tissues" (Horvath, 2013). The paper explains in detail how Horvath developed his epigenetic clock using publicly available DNA methylation data from 8,000 samples including 51 different tissue types, using the now defunct Illumina 27k methylation array. It remains the clock generated on the highest number of samples and different tissue types. Horvath identified 353 probes on the Illumina array corresponding to specific sites within the genome (mostly at CpG sites) which showed changes correlated with chronological age across all tissue types. This multi-tissue approach makes Horvath's clock suitable for age analysis on most cell types. There are however some notable exceptions which have high levels of error such as breast tissue which Horvath suggests may somehow be related to the high hormone sensitivity of breast tissue (Sehl et al., 2017). Skeletal and cardiac muscle also deviate, which may be due in part to the presence of myosatellite cells and stem cell populations respectively (S. Horvath, 2013). One other element of the clock development which is favourable is the age range of the sample used, varying from people aged over 100 years of age to cord blood samples from new-borns, ensuring that Horvath's clock is accurate in the young as well as the elderly.

1.3.2 The Hannum epigenetic clock

Unlike the Horvath clock, the Hannum clock was developed using only whole blood, this time using DNA methylation data generated on the last generation of methylation arrays, the Illumina 450k array. 656 patients with ages ranging from 19 to 101 were analysed and 71 CpGs were found to be predictive of age. These 71 probes are what constitute the Hannum clock (G. Hannum et al., 2013).

1.3.3 The DNAm PhenoAge epigenetic clock

The DNAm PhenoAge epigenetic clock is perhaps the most unique epigenetic clock widely used today (Levine et al., 2018). Rather than setting out to find probes with methylation levels which change with chronological age, the DNAm PhenoAge epigenetic clock was reverse engineered to correspond with the age-predicting values of several clinical markers which make up the non-epigenetic phenological ageing clock (Liu et al., 2018), confusingly referred to simply as the "PhenoAge clock" (Kuo et al., 2020).

A Cox penalised regression model was used on 42 clinical markers across a cohort of 9,926 patients with 24-year mortality data. 10 of those markers, including white blood cell count, albumin and C-reactive protein were identified as being predictive of chronological age. The PhenoAge clock was then validated on a second cohort of 6,209 participants, where it demonstrated a predictive ability when looking at the risk of all-cause mortality, with a 1-year increase in phenotypic age being associated with a 9% increase in all-cause mortality, 7% increase in cancer mortality and a 20% increase in diabetes related mortality (Levine et al., 2018).

To generate an epigenetic version of this blood biomarker based phenotypic clock, DNA methylation data from 456 patients was then used to relate the DNA methylation levels to a generated phenotypic age. Only probes available across the 27k, 450k and 850/EPIC array were considered to maximise the applicability of the newly developed clock. 513 CpGs were identified, and these form the basis of the PhenoAge epigenetic clock. Due to the unique development of the PhenoAge epigenetic clock, its age

prediction shows a strong relationship to all-cause mortality, with a 1-year increase in PhenoAge epigenetic age resulted in a 4.5% all-cause mortality risk (Levine et al., 2018).

1.3.4 The use of epigenetic clocks

Due to being developed on now defunct Illumina array platforms (27k and 450k), 19 of the 353 CpGs Horvath included in his original clock (S. Horvath, 2013) and 6 of the 71 Hannum probes (G. Hannum et al., 2013) are no longer available on the current generation of Illumina platform, the 850/EPIC array. Despite these missing CpGs, the clocks have been shown to perform well and still remain robust and are widely used within the field (McEwen et al., 2018).

It has been suggested that Horvath's original clock is a measure of fundamental intrinsic biological age, as opposed to the Hannum and PhenoAge clocks which may instead reflect extrinsic influences on the trajectory of ageing (Gibson et al., 2019), with the DNAm PhenoAge being more closely related to mortality risk. By using one or more of these epigenetic clocks, it is possible to estimate an individual's biological age, which when compared to the individual's chronological age, reveals the rate at which ageing is occurring. We can surmise that a high epigenetic age represents more rapid biological ageing and may also be a driving factor in the ageing process as many diseases and conditions which show accelerated epigenetic age also exhibit an ageing phenotype. These include Down's syndrome (Horvath et al., 2015a), obesity (Horvath et al., 2014), HIV infection (Horvath and Levine, 2015). Increased epigenetic age has also been shown to correlate with increased risk of multiple age associated diseases as well as mortality (Chung et al., 2020; Fransquet et al., 2019).

Interestingly, those who live into the extreme upper percentiles of human life expectancy (100+ years) often show a decelerated rate of epigenetic ageing (Horvath et al., 2015b). This suggests that these super-centenarians are not merely living longer but are in fact ageing more slowly. It isn't yet clear if a well-regulated methylome is what has contributed to their longevity or is instead a by-product of other processes such as DNA repair or autophagy being well maintained with advancing age. A meta-

analysis of studies of time to death predictions based on DNA methylation concluded that epigenetic regulation plays some role in longevity (B. H. Chen et al., 2016).

1.3.4.1 Reversibility of the epigenetic clock

Until recently the permanence of epigenetic ageing was unknown, i.e., is accelerated epigenetic ageing permanent and unmodifiable? However one recent study demonstrated that 1 year of treatment with a combination of metformin, dehydroepiandrosterone and human growth hormone was able to reduce the epigenetic age of participants by 1.5 years compared to their epigenetic age at the start of the study (a total reduction of 2.5 years) according to the Horvath epigenetic clock (Fahy et al., 2019). Following treatment there was also a significant decrease in the number of exhausted PD-1- positive CD8 T cells and an increase in naïve CD4 and CD8 T cells as well as CD4+ recent thymic emigrants showing a reversal of the immune ageing phenotype. Another study in 43 healthy adults aged 50-72 years suggested that a lifestyle intervention including diet, sleep, exercise and relaxation was sufficient to result in a 3.23 year reduction in Horvath epigenetic age compared to controls (Fitzgerald et al., 2021). There is thus growing evidence that biological age can be reversed and represents a potential therapeutic intervention for a broad range of conditions with accelerated ageing.

1.3.5 What we know so far about the impact of trauma on the epigenetic clock

At this time there is currently only one study describing the impact of physical trauma on epigenetic ageing as measured by an epigenetic clock algorithm. This study of Dutch military veterans of the Afghanistan conflict found an increase in biological age of 1.9 years, using the Horvath clock, in those soldiers who sustained a physical injury (Boks et al, 2015). The analysis was carried out six months

after injury. Although this study found no impact of psychological trauma, PTSD, other studies have reported that emotional/psychological trauma accelerates the ageing process.

The few studies in this area have focussed mainly upon PTSD. The current literature shows that just like physical trauma, psychological trauma also has a negative impact on mortality and health outcomes. Adults who have been exposed to 6 or more 'adverse childhood experiences' (ACEs) lived on average 20 years less than age-matched controls who reported no ACEs (Brown et al., 2009). This significant decrease in life expectancy may be due in part to the poorer mental health outcomes of people who experience a traumatic childhood (i.e., schizophrenia, depression, self-harm), which in turn is associated with an increased risk of behaviour-based mortality (Hiroeh et al., 2001). Psychological trauma and PTSD also have an association with increased risk of disease, including classically age-related conditions such as cardiovascular disease (Dedert et al., 2010), as well as increased levels of inflammation (Baumeister et al., 2016). Recent research has now shown evidence of epigenetic age acceleration which may go some way to explaining the early onset of age-associated diseases and increased risk of mortality following trauma.

One study used a cohort of 339 genotyped, non-Hispanic white military veterans with a median age of 52.5 years who had previously completed a PTSD assessment. The researchers found that while overall PTSD severity was not associated with an accelerated epigenetic age, experiencing certain symptoms, specifically 'hyperarousal' was associated with an accelerated DNA methylation age, hyperarousal in turn, was associated with reduced survival (Wolf et al., 2017a). In the study of military veterans performed by Wolf et al., (2017a) there was no age acceleration in the study participants experiencing PTSD. This suggests that within a military setting, PTSD symptoms alone are not predictive of epigenetic age acceleration. In a meta-analysis of psychological trauma and its association with epigenetic age acceleration there was a small but significant increase in epigenetic age overall linked to childhood trauma and PTSD (Wolf et al., 2017b). While this meta-analysis does not offer a mechanistic insight into what is driving the ageing process forward, it does lend credence

to the proposal that psychological stress may accelerate the ageing process if the trauma is experienced in childhood.

Recent data suggest that an increased biological age may be linked to COVID-19 disease severity. Data from The United Kingdom Biobank (UKB) was used to estimate biological age using the PhenoAge biochemical clock. The study showed that those UKB participants who developed severed COVID-19 were 10-14 years older biologically (Kuo et al., 2020). While this was done using the metabolomic and clinical data, given that the DNAm PhenoAge clock was developed as an epigenetic version of the PhenoAge clinical data clock, it is likely that there is also epigenetic age acceleration occurring. A similar observation was made within a study of age-related changes to the methylome in older adults and how these changes influence susceptibility to sepsis (Lang et al., 2022). This study identified specific CpG sites which showed age-associated changes associated with increased susceptibility to sepsis as well as mortality.

What the literature has undoubtedly suggested is that ageing, disease, and biological stress are inexorably linked, whether due to hyperinflammation, adverse conditions in some way impact the rate of biological ageing.

1.4 Trauma and ageing, commonalities, and differences

While it may be the case that both ageing and trauma share multiple pathogenic mechanisms, as outlined in Table 1, there are also some notable differences that largely relate to the scale and severity of the disturbance. For example, the extensive tissue damage and risk of multiple organ dysfunction (Durham et al., 2003) associated with a physical traumatic injury are not seen in physiological ageing, though there is a gradual decline in many body systems resulting in multimorbidity (Ryan et al., 2015). Functional decline is thus a feature of both, but it is the trajectory and rate of decline that differs. There are also some shared features such as sarcopenia, which is driven by several factors including

physical inactivity, endocrine changes and inflammation (Bano et al., 2017; Foster et al., 2020; Parry and Puthucheary, 2015).

In relation to inflammation, another feature of trauma and ageing, the level and chronicity of this increase is drastically different. In trauma, systemic inflammation is elevated and at a level similar to a major infection (J. Lu et al., 2009; Namas et al., 2009) and the onset is sudden. In contrast the inflammation associated with the ageing process is at a low level, only 2-4 fold that seen in young adults, and is chronic, persisting potentially for decades (Franceschi et al., 2007; Bartlett et al., 2012). It is worth mentioning however that low level chronic inflammation does occur following some injuries such as burns, here chronic low grade inflammation can persist for years in a similar way to the chronic inflammation we classically associate with ageing (Jeschke et al., 2011).

The accumulation of senescent cells, something associated with ageing, also occurs following trauma, although similar to inflammation, the scale and timeframe of this accumulation differs. Following trauma, there is an increase in the presence of senescent cells near the injury site, which aids in tissue repair (Deursen, 2014), in contrast, with ageing the increasing number of senescent cells is not tissue specific and occurs globally at a gradual rate (Burton, 2009).

Here, it is argued not that age and trauma related physiological changes are identical, rather, they share some common mechanisms and while their magnitude and kinetics differ, they achieve the same end – a predisposition to an aged phenotype. Furthermore, it bears mentioning some of the gaps in our understanding of the relationship between trauma and ageing, and limitations in the existing data. Ideally there would be multiple studies within the literature examining the effect of trauma on multiple biomarkers of ageing (S. Horvath, 2013; Lara et al., 2015) in healthy adults of all ages with no confounding comorbidities or health behaviours. Due to the nature of trauma research, this is not the case. Many of the cohorts who feature in the studies described are heterogeneous, of differing ethnicity, sex, injury severity, BMI and comorbidities. Many of the people enrolled into trauma research studies may already be showing many of the phenotypic changes we associate with

ageing prior to their injury, particularly the frail older patient whose injury may well be the result of a fall. In the case of the younger patient, their injury may be the result of, or lead to, risky lifestyle behaviours such as substance abuse. Therefore, more clinical work is needed to assess the influence these cofactors have on the relationship between trauma and ageing.

Characteristic	Presence in Trauma	Presence in Ageing	Shared Characteristic
Inflammation	Acute, high level inflammation (J. Lu et al., 2009; Namas et al., 2009).	Chronic low-level inflammation (Franceschi, 2008).	Chronic inflammation in burn injury (Jeschke et al., 2008).
Functional decline in organ systems	Multiple organ dysfunction (Durham et al., 2003).	Gradual decline in many body systems over time; multimorbidity (Ryan et al., 2015).	Reduced lean body mass, (Bano et al., 2017; Morley et al., 2010; Parry and Puthucheary, 2015) fatigue; disability (Evans et al., 2003; WHO, 2011).
Immune compromise	Acute immuneparesis and increased susceptibility to infection and sepsis (Hietbrink et al., 2006).	Immune remodelling with broad compromise to immunity (Dorshkind et al., 2009).	Reduced neutrophil function (Butcher et al., 2001; Hampson et al., 2017); increased risk of infection.
Genomic alterations	Acute and large scale genomic change ((Xiao et al., 2011).	Genome instability (Moskalev et al., 2013).	Epigenetic alterations after psychological trauma (E J. Wolf et al., 2017) and with age (S. Horvath, 2013); Telomere attrition (Jiang et al., 2007; X. Li et al., 2017; Z. Li et al., 2017).
Metabolic disturbance	Acute Increase in catabolism (Şimşek et al., 2014).	Insulin resistance due to changes in body composition (Karakelides et al., 2010), anabolic resistance (Roubenoff, 2003).	Long term metabolic disturbance after burn – catabolism (Hart et al., 2000), insulin resistance (F. N. Williams et al., 2009).
Cell senescence	Acute Senescence (Deursen, 2014).	Increase in cell senescence over time (Velarde and Demaria, 2016).	Senescent cells primarily at wound site (Campisi, 2005; Deursen, 2014).

Table 1.1: Ageing and trauma, shared characteristics - Examples of some characteristics of ageing which are present in both ageing and the trauma patient.

1.5 Conclusions and directions for research

Outlined throughout this introduction are the long-term health consequences of major trauma for survivors of both physical and psychological trauma, including shortened lifespan and increased risk of early onset of age-related diseases. At the clinical level this would support the argument that trauma accelerates the ageing process and suggests that processes known to drive the ageing phenotype, such as chronic systemic inflammation, immune compromise, and epigenetic change are involved. However further research is required at the cellular and molecular level with reliable and quantitative biomarkers of biological ageing to answer the question "does traumatic injury accelerate the ageing process?".

The benefit of knowing if ageing is accelerated after trauma and disease is not merely to expand our understanding of the consequences of trauma and disease. The field of biogerontology has now advanced to such a stage that anti-ageing therapeutics are now in clinical trials (Fahy et al., 2019; Hofer et al., 2021) and research suggests that epigenetic changes may also be reversible as explained above. Through these interventions we may be able to improve long term outcomes for survivors of major trauma.

1.6 Hypothesis, Aims and Objectives of the thesis

The overall hypothesis to be tested in this thesis is that a traumatic injury or a critical illness will increase morbidity and mortality by accelerating the ageing process. The aim is to test the hypothesis by assessing DNA methylation and/or immune ageing in cohorts of injured or critically ill patients, including those with COVID-19. A secondary aim is to determine if cell senescence can be reversed.

The aims will be met by the following objectives:

1. To determine immune ageing and epigenetic age in burn injured patients.
2. To determine epigenetic age in both moderate and severe COVID-19 patients.
3. To determine epigenetic age in critically ill patients with and without sepsis.
4. To determine whether epigenetic modulators can reverse senescent phenotypes in fibroblasts.

2. Methods

2.1 Burn study participant recruitment

Acknowledgement: The details of the recruitment, consent, sample collection as well as SIFTI study design discussed below have previously been published by the Lord group, sections of this text are based on these previous publications (Hampson et al., 2017; Hazeldine et al., 2021).

All burn injury patients whose samples were analysed as part of this investigation were collected as part of the SIFTI I and SIFTI II studies. These are longitudinal observational studies originally created to investigate the relationship between severe thermal injury and immune function. "**S**cientific **i**nvestigation of the Biological Pathways **F**ollowing **T**hermal **I**njury" I & II (SIFTI I & II).

The studies were approved by UK Research Ethics Committees, references 12/EM/0432 and 16/WM/0217 for SIFTI I and SIFTI II, respectively.

2.1.1 Inclusion criteria

Adult patients were included in SIFTI I if they had a full thickness burn with a total burn surface area (TBSA) of >1%. For SIFTI II, adult patients were included if they had a burn with a TBSA of ≥15%.

2.1.2 Exclusion criteria

Patients were excluded from the studies if they met any of the following criteria: Associated multiple injuries with an injury severity score (ISS) >25 or if a decision not to treat the patient was made due to injury severity; Patients with chemical and deep electrical burns; Patients receiving glucocorticoid treatments, with any active malignant conditions, an active infection such as HIV or hepatitis. Those with limb amputations were also excluded due to unreliable TBSA% scoring.

2.1.3 Consent procedure

Patients who met the inclusion criteria were consented using an approved informed consent process. The consent system used is outlined in Figure 2.1. If the patient is conscious and able to consent, then

they will provide consent. If not a patient's personal consultee is used, they will be a relative, carer or friend. In the event that a personal consultee is not available, a consultee will be appointed. An example of an appointed consultee would be a medical professional, such as an emergency doctor or other member of the burns team, who are not directly involved with the research study but understand its impact on any potential participant. A signed declaration is made by any patient or consultee following access to a leaflet containing specific study information. Participants enrolled by a consultee are approached if they regain capacity (e.g., consciousness) and are asked to give their approval for involvement in the study and to sign the declaration of consent. If the participant declines to do so, they are un-enrolled in the study, and any samples or data collected from them are destroyed.

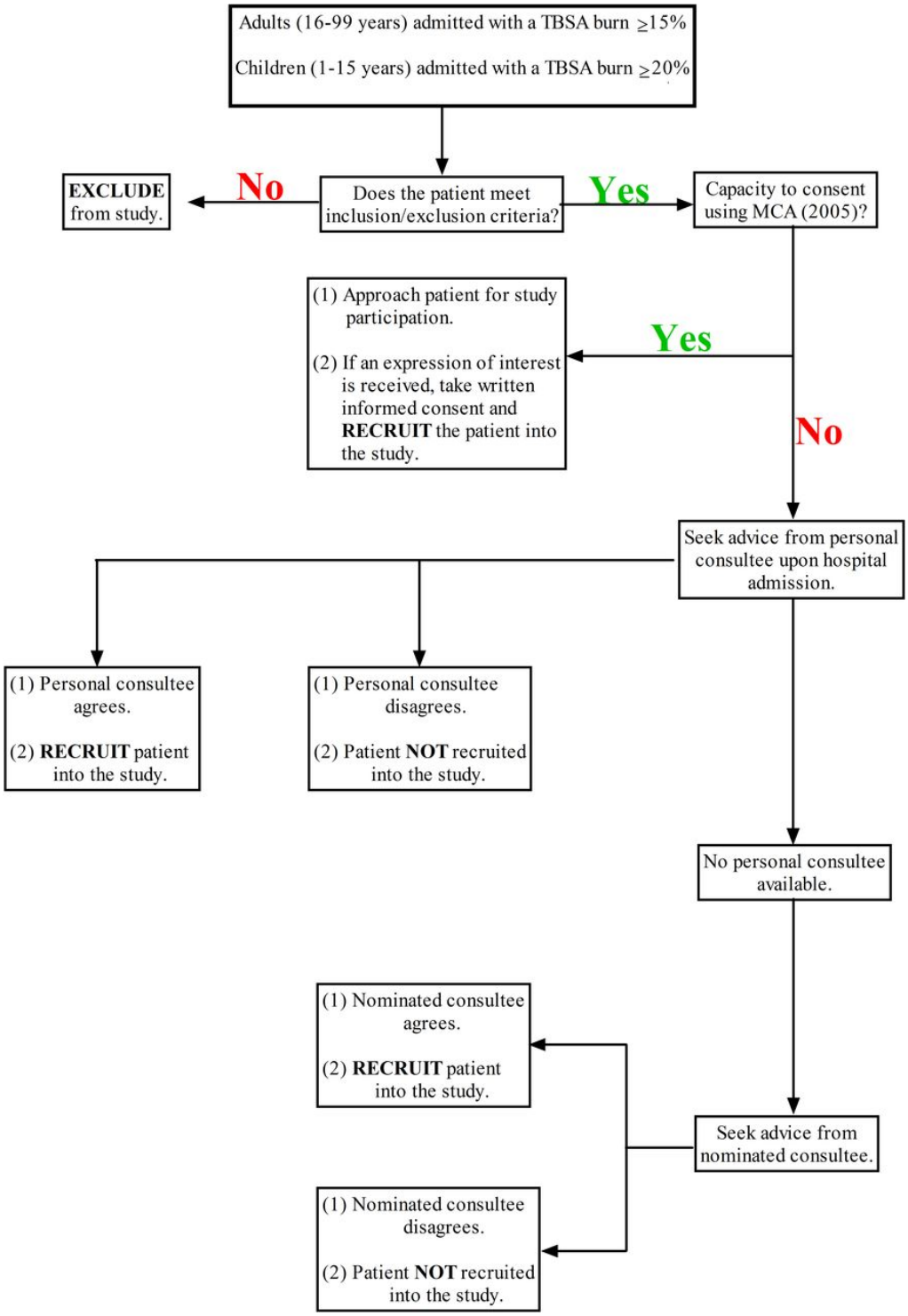


Figure 2.1: SIFTI Recruitment, consent and exclusion protocol. A flow chart showing the recruitment and consent process used for the SIFTI I and II studies. MCA, Mental Capacity Act; TBSA, total body surface area. This figure was originally published by Hazeldine et al., 2021.

2.1.4 Sample collection and storage

Blood samples were collected from patients in BD Vacutainers (Becton Dickinson, Oxford, UK) containing lithium heparin. Blood samples were collected at predetermined time points following injury: day 1 (<24 h post-injury), day 3 (±1 d), day 7 (±1 d), day 14 (±3 d), day 21 (±3 d), day 28 (±3 d), month 2 (±3 d), month 3 (±7 d), month 6 (±7 d) and at month 12 (±7 d).

2.1.5 Clinical data collection

Within 24 hours of injury and following admission to hospital demographic information was recorded, this included information such as: Age, sex, presence of comorbidities, body mass index (BMI), ethnicity and time since injury. Also recorded were injury characteristics such as total burn surface area (TBSA%) method of burn injury as well as various injury scores (ISS, APACHE II, rBaux). Baseline physiological data were also recorded as part of the patient care pathway, including heart rate, blood pressure, temperature and respiratory information. Length of stay (LOS) and death before discharge were also recorded. These data were accessible via the Case Report Form (CRF) or via the University of Birmingham REDCap database (REDCap, Vanderbilt University, Tennessee, USA) which contained all the study data.

2.1.6 PBMC Isolation

All Phosphate buffered saline (PBS) used in this thesis was made by combining a single 5g PBS tablet (Gibco – Thermo Fisher Scientific, Loughborough, UK) with 500ml of distilled water. This PBS does not contain calcium, magnesium, or phenol red.

Patient and control PBMCs were isolated from whole blood collected in lithium heparin vacutainers (Becton Dickinson, Oxford, UK). Whole blood was diluted 1:1 with RPMI 1640 media (Gibco - Thermo Fisher Scientific, Loughborough, UK) supplemented with glutamine plus penicillin and streptomycin (100U/ml) (Gibco – Thermo Fisher Scientific, Loughborough, UK) and mixed via inversion. The RPMI:Blood mixture was then layered over 6ml of Ficoll-Plaque^{TM} PLUS (GE healthcare, Uppsala, Sweden) in a 25ml universal container (Sarstedt, Leicester, UK) and centrifuged at 400 xg for 30 minutes

at room temperature (RT) with no brakes. After centrifugation, the mononuclear cells were collected and transferred into a fresh universal tube using a sterile Pasteur pipette (Thermo Fisher Scientific, Loughborough, UK). The cells were then washed twice in MACS buffer (MACS; PBS, 2 mM Ethylenediamine-tetraacetic Acid (EDTA), 0.5% bovine serum albumin (BSA) and 0.09% azide; Miltenyi Biotec, Bergisch Gladbach, Germany) with centrifugation at 300 xg for 10 minutes at RT. The supernatant was then remove, and the pellet resuspended in 1ml of 'Freezing solution' which consisted of Heat-Inactivated Fetal Bovine Serum (Sigma-Aldrich, Gillingham, UK) 45ml + 5ml DMSO (Final volume of 10%) (Sigma-Aldrich, Gillingham, UK). The 1ml PBMC suspension was divided into 2 green Cryo.S storage vials (Greiner bio-one, Stonehouse UK) and placed into a freezing container (Corning, New York, USA) and stored at -80^{o}C.

2.2 Sepsis group study

Acknowledgement: The details of the recruitment, consent, sample collection and the study design for the "Epigenetic profiling in severe sepsis (EPSIS)" described below are based on the supplementary material published as part of "Epigenetic Profiling in Severe Sepsis: A Pilot Study of DNA Methylation Profiles in Critical Illness" paper (Binnie et al., 2019). Some sections of text were copied directly from the supplementary information included in the publication and are in quotation marks. The EPSIS study is part of the broader parent study "Studies of blood DNA in patients with severe infection (DYNAMICS)" investigating how blood plasma DNA levels may be predictive of patient outcomes.

The studies were approved by the Research Ethics Board at the Hamilton Health Sciences in November 2010 (NCT01355042) and access to the data was approved by the PI Dr Claudia Dos Santos (University of Toronto).

2.2.1 Inclusion criteria

Patients were recruited into the septic group if they: had suspected or a confirmed infection based on their clinical information at the time of screening, had one or more dysfunctional organ systems, 3 or more signs of systemic inflammatory response syndrome (SIRS) and were also predicted to be in the

ICU for 72 hours or more. For this investigation of organ dysfunction was defined as: "(1) SBP ≤90 mm Hg or MAP ≤70 mm Hg or SBP < 40 mm Hg for at least 1 hour despite fluid resuscitation, adequate intravascular volume status, or use of vasopressor in attempt to maintain systolic BP ≥90 or MAP ≥ 70 mm Hg, (2) P/F Ratio ≤ 250 in the presence of other dysfunctional organs or systems, or ≤ 200 if lung is the only dysfunctional organ, (3) acute rise in creatinine > 171 mM or urine output 1.5 times the upper limit of normal, and (4) platelet count < 50,000 or a 50% drop over the 3 days prior to ICU admission.". The inclusion criteria for septic shock were the same as for sepsis with one difference: the patients had to have received vasopressors in the last 24-hour period.

Non-septic ICU patients were recruited and matched for illness severity and mortality.

2.2.2 Exclusion criteria

Patients were excluded if they were under the age of 18, were currently pregnant or breast feeding, or were receiving only palliative care.

2.2.3 Consent procedure

Patients who met the inclusion criteria were consented using approved informed consent process. This meant that written and informed consent was obtained from eligible patients or their appointed consultee (e.g., family, carer, appointed medical professional).

2.2.4 Clinical data collection

Demographic data were collected following admission to ICU, this included patient age and sex. Clinical data recorded included multi-organ dysfunction scores (MODS) as well as comorbidities. Patient outcomes such as survival to discharge and death before discharge were also recorded.

2.2.5 Sample collection and storage

Samples used for DNA methylation analysis were collected on "Day 1" following admission to ICU. Whole blood was collected as whole blood in DNA PaxGENE tubes (PreAnalytiX GmbH, Hombrechtikon, Switzerland) or buffy coat. DNA was extracted using the QIAquick DNA purification kit (Qiagen, Hilden, Germany).

2.2.6 DNA methylation processing

Genomic DNA was run on the 450K Illumina array system. For the subsequent analysis, a pre-processed methylation dataset was provided by the original research group, rather than the raw IDAT files used for the burns and COVID-19 DNA methylation analysis.

2.3 COVID-19 group study

The severe COVID-19 patients were recruited in Birmingham as part of the Coronavirus Immunological Analysis study approved by Northwest Preston Research Ethics Committee (20/NW/0240). The moderate disease patients were recruited as part of the Post-hospitalisation COVID-19 (PHOSP-COVID) study approved by Leeds West Research Ethics Committee (20/YH/0225).

2.3.1 Inclusion criteria:

Patients were recruited 2-7 months post PCR confirmed SARS-CoV-2 infection. Patients were grouped into 'moderate' or 'severe' based on their fraction of inspired oxygen (FiO2) during their admission as well as their ventilation requirement status. Those patients requiring between 28-60% FiO2 were classified as 'moderate'. Patients who required above 60% FiO2 or were admitted to intensive care were classified as 'severe'.

2.3.2 Exclusion criteria:

Patients were excluded if they had a positive diagnosis for a pathogen unrelated to the objectives of the study, i.e., SARS-Cov2, who were not admitted to hospital following arrival at the hospital, or who had a life limiting illness with a life expectancy of 6 months or less. The exclusion criteria for the healthy control group were self-reported infection or co-morbidity (e.g., diabetes, heart disease, arthritis).

2.3.3 Consent procedure

Written informed consent was obtained from all study participants.

2.3.4 Clinical data collection

Demographic data were collected including age, ethnicity and sex were recorded. Clinical data such as BMI, length of stay (LOS), time on oxygen and disease severity (based on fraction of inspired oxygen) were also recorded.

2.3.5 Sample collection and storage

Blood samples were collected from patients in BD Vacutainers containing lithium heparin (Becton Dickinson, Oxford, UK). PBMCs were isolated and stored under the same procedures outlined in section 2.1.4.

2.4 DNA extraction and quality checks

All DNA used throughout this investigation, for genomic analysis and telomere length analysis, was extracted from PBMCs and checked for quality using the steps outlined below.

2.4.1 DNA Extraction

Genomic DNA was extracted from stored PBMCs or whole blood using the Qiagen DNeasy Blood and tissue kit (Qiagen, Hilden, Germany) with the additional on membrane RNase treatment (Qiagen, Hilden, Germany). The maximum recommended starting number of cells (5 x 10^6) was used, when possible, with a minimum of 1 x 10^6 cells used for each extraction. DNA quality and concentration was determined.

2.4.2 DNA Quality control

2.4.2.1 Nanodrop DNA presence and quality checks

1.5µl of Isolated DNA was analysed using the Nanodrop 2000 (Thermo Fisher Scientific, Loughborough, UK) to establish Initial DNA concentration and signs of contamination.

2.4.2.2 Qubit fluorometer and DNA quantification

Absolute DNA concentration was measured using the high sensitivity (HS) double stranded DNA (dsDNA) assay kit from Qubit in conjunction with the Qubit 3 Fluorimeter (Invitrogen, Massachusetts, USA) according to manufacturer's instructions.

2.4.2.3 DNA integrity

DNA integrity was quantified using the Agilent genomic DNA reagents and genomic DNA ScreenTape in conjunction with the Agilent 2200 TapeStation system (Agilent Technologies, California, USA). 1µl of genomic DNA was added to 10µl of the 'Agilent genomic DNA reagents' sample buffer inside a 0.2ml PCR tube (Abgene, New Hampshire, USA) for each sample. Samples were spun down using a benchtop PCR strip microcentrifuge (SciQuip, Shropshire, UK) briefly vortexed at 2000rpm on a microplate mixer (Camlab, Over, UK) and spun down again. A DNA ladder was also included for each run. A representative image showing the TapeStation DNA integrity results can be seen in Figure 2.2.

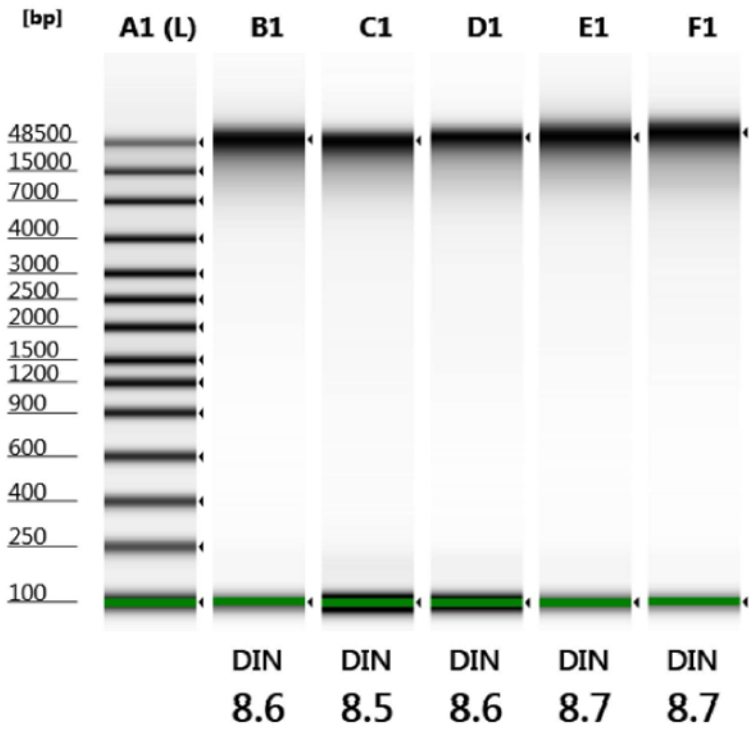


Figure 2.2: DNA microgel electrophoresis result from the Agilent 2200 TapeStation. Genomic DNA samples are loaded into lanes B1-F1, and the DNA ladder is loaded into lane A1(L). There are thick bands in the sample lanes in line with the 48500 bp band in the ladder, this along with minimal banding or smudging across the rest of the sample lanes indicates a high degree of integrity within the samples. This is confirmed by high DNA integrity numbers of >8 (DIN). DNA integrity numbers range from 0-10 with 0 being the lowest and 10 being the highest (best). DIN; DNA integrity number, BP; base pair.

2.5 DNA methylation

Methylation analysis of extracted genomic DNA was performed by external suppliers.

2.5.1 Illumina 450K array

Initial Burn injured patient samples were run on the array that was still in use at the time, namely the Illumina 450k array (Illumina, California, USA). Genomic DNA was shipped to Oxford genomics for further processing using the Illumina 450K array in line with their submission requirements 12ng/µl, with no less than 500ng total genomic DNA.

2.5.2 Illumina Infinium EPIC array

Subsequent samples were all run on Illumina Infinium EPIC 850k arrays which superseded the 450k arrays (Illumina, California, USA). Genomic DNA was shipped to Diagenode Dianostics (Liege, Belgium) for further processing using the Illumina Infinium EPIC array in line with their submission requirements; a minimum concentration of 10ng/µl, with no less than 500ng total genomic DNA.

2.5.3 DNA methylation analysis

Methylation analysis was performed using raw IDAT files supplied from Oxford genomics or Diagenode Diagnostics unless stated otherwise.

2.5.3.1 Quality control and processing

All DNA processing and statistical analysis was performed with R Studio 2022.02.3+492. DNA QC and Noob pre-processing was performed using the Minfi package. Loci with SNPS were identified and removed using the Minfi. Cross-reactive probes were removed using the markgene/maxprobes package.

2.5.3.2 Normalisation and epigenetic age generation

The ENmix package was used for low quality probe removal, missing probe imputation, and beta value generation. The ENmix package 'methyage' function was used for BMIQ normalisation and to generate epigenetic age calculations using the Horvath (Horvath, 2013), Hannum (Hannum, 2013) and DNAm PhenoAge (Levine et al., 2018) clocks.

2.5.3.3 Pathway enrichment analysis

The ReactomePA package was used for BH false discovery p value adjustment (Benjamini and Hochberg, 1995) and pathway enrichment analysis.

2.6 Absolute Telomere length analysis

The absolute telomere length of PBMCs from patients at admission and 6 months post injury was measured using qPCR on extracted genomic DNA using the ScienCell absolute human telomere length quantification qPCR assay kit (ScienCell, California, USA) along with the SYBR green master mix (Roche, Basel, Switzerland). The ScienCell absolute human telomere length quantification PCR assay kit has previously been used to quantify telomere length in the literature (Bruno et al., 2019; Lazzarini et al., 2018; Martin et al., 2019). Samples were run on the Bio-Rad CFX384 Real-Time System thermocycler using 384-well thin well Hard-Shell PCR Plates (Bio-Rad, California, USA). 1µl of genomic DNA normalised to 5ng/µl and was used for each PCR reaction, the manufacturer's recommended cycle conditions as well as the reagent volumes per reaction are listed below in Table 2.1.

Reagent	Volume (µl)
DNA sample (Genomic or reference)	1
Primer stock solution (Telomere or SCR)	2
qPCR master mix	10
Nuclease-free H2O	7
Total Volume	20

Step	Temperature	Time	Number of Cycles
Initial Denaturation	95°C	10 min	1
Denaturation	95°C	20 sec	32
Annealing	52°C	20 sec	
Extension	72°C	45sec	
Data acquisition	Plate read		
Optional	Melting curve analysis		1
Hold	20°C	Indefinite	1

Table 2.1: qPCR reagents and cycle conditions. A table showing the qPCR reagent mixture and cycle conditions used for absolute telomere length per diploid cell using the "ScienCell absolute human telomere length quantification qPCR assay kit".

Each participant sample was used for two reactions. One reaction using telomere specific primers to amplify the telomeric sequence (referred to in calculations as TEL), and one reaction containing single copy reference gene primers which are used to control for the number of genomic copies within the total DNA sample (referred to in calculations as SCR). This allows for the absolute telomere lengths of each sample to be calculated. Run alongside the participant samples is a reference DNA sample (supplied with the kit) with a telomere length of 524kb (per dl/cell).

The calculation used to calculate the telomere length per diploid cell is described within the ScienCell kit as follows:

1. For telomere (TEL), ΔCq (TEL) is the quantification cycle number difference of TEL between the target and the reference genomic DNA samples.

ΔCq (TEL) = Cq (TEL, target sample) - Cq (TEL, reference sample)

Note: the value of ΔCq (TEL) can be positive, 0, or negative.

2. For single copy reference (SCR), ΔCq (SCR) is the quantification cycle number difference of SCR between the target and the reference genomic DNA samples.

ΔCq (SCR) = Cq (SCR, target sample) - Cq (SCR, reference sample)

Note: the value of ΔCq (SCR) can be positive, 0, or negative.

3. ΔΔCq = ΔCq (TEL) - ΔCq (SCR)

4. Relative telomere length of the target sample to the reference sample (fold) = $2^{-\Delta\Delta Cq}$

5. The total telomere length of the target sample = Reference sample telomere length x $2^{-\Delta\Delta Cq}$

This provides the absolute telomere length per diploid cell. The number can be divided by 92 to show the telomere per chromosome end.

2.7 RNA Extraction and quality checks

All RNA used throughout this investigation for gene expression analysis was extracted and checked using the steps outlined below.

2.7.1 RNA extraction

RNA was extracted from thawed PBMCs using the Qiagen RNeasy Mini kit (Qiagen, Hilden, Germany) according to their standard mammalian cell extraction method. The additional DNA digestion step was done using the Qiagen DNase set (Qiagen, Hilden, Germany). Due to the nature of using previously stored cells the starting number of cells available for RNA isolation varied. The maximum number of available cells were used, ranging from 1 x 10^6 to the recommended maximum of 1 x 10^7. RNA, quality, and concentration was determined.

2.7.2 RNA Quality control

2.7.2.1 Nanodrop RNA presence and quality

1.5µl of Isolated RNA was analysed using the Nanodrop 2000 (Thermo Fisher Scientific, Loughborough, UK) to establish RNA concentration and signs of contamination.

2.7.2.2 Qubit fluorometer RNA quantification

Absolute RNA concentration was established using the RNA high sensitivity (HS) assay kit from Qbit in conjunction with the Qubit 3 Fluorimeter (Invitrogen, Massachusetts, USA) according to the manufacturer's instructions.

2.7.2.3 RNA integrity

RNA integrity (RIN) was quantified using the Agilent genomic RNA reagents and genomic RNA ScreenTape in conjunction with the Agilent 2200 TapeStation system (Agilent Technologies, California, USA). RNA samples were defrosted on ice. 5µl of sample buffer was mixed with either 1µl of sample

or 1µl of RNA ladder. Samples were spun down in a benchtop microcentrifuge (SciQuip, Shropshire, UK) then vortexed at 2000 rpm on a microplate mixer (Camlab, Over, UK) for 1 minute. Samples were spun down again using a benchtop microcentrifuge, heated to 72°C for 3 minutes then placed back on ice for 2 minutes. Samples were spun down a final time using a benchtop microcentrifuge before being loaded into the Agilent 2200 TapeStation.

RNA sequencing usually requires high quality minimally degraded RNA. Due to RNA being extracted from PBMCs stored in a phenotyping buffer and not an RNA preservation buffer combined, with their time spent in frozen, sample quality was observed to be low but usable. The low quality of the RNA can be seen in Figure 2.3 as illustrated by the low RNA integrity numbers (RIN).

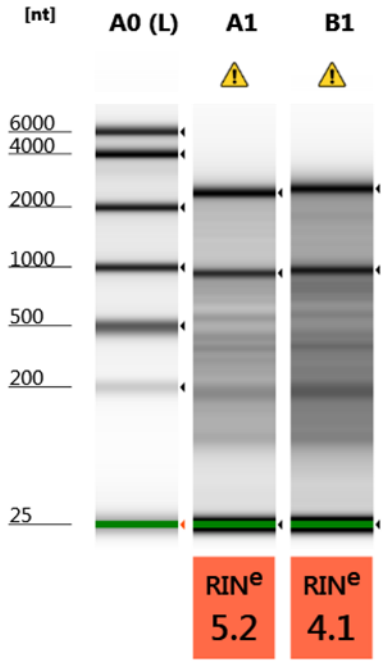


Figure 2.3: RNA microgel electrophoresis result from the Agilent 2200 TapeStation. RNA samples were loaded into lanes A1 and B1 and the RNA ladder was loaded into lane A0(L). There are multiple thick bands as well as a high level or smudging within the sample lanes indicating a high degree of fragmentation within each sample. This fragmentation is reflected in low RNA integrity numbers (RIN). RNA integrity numbers range from 0-10.

2.8 RNA Sequencing

RNA from two subsets of burns admission patients was sequenced from a group of “unexpected survivors” in the burn injury study and severely injured patients who died following admission.

2.8.1 Library preparation

Multiplex Library prep was performed using the QuantSeq 3’ mRNA-Seq FWD Library Generation Module, Lexogen Library Amplification Module, Lexogen UDI 12nt Set A1 and Purification Module with Magnetic Beads (Lexogen, Wien, Austria), chosen for their ability to generate viable libraries from low quality clinical samples.

2.8.2 sequencing platform and data

The samples were run on the Illumina HiSeq Xten platform (Illumina, California, USA). This widely used platform was chosen to ensure that the data generated could be used in conjunction with future studies using a similar platform. Due to low sample quality (low RNA integrity number), many reads from the run remain unassigned. Due to this issue, samples had a slightly lower read depth than expected. However, the achieved read depth of around 10 million is still suitable for mammalian expression studies.

2.8.3 RNA sequencing analysis

RNA sequencing data analysis was performed on the University of Birmingham BlueBEAR high performance Linux computing cluster. Alignment was performed using STAR, FastQ files were trimmed using Trim_Galore with ASCII+33 quality scores used for quality trimming. The subsequent count matrix was generated using HTSeq. Differential expression analysis was done, and associated figures were generated in R Studio using DESeq2 and limma.

2.9 Human cell culture and senescence induction

All cell culture work was performed on virally transfected hTert-HRAS, BJ human dermal foreskin fibroblasts kindly provided by Dr Eva Petermann (University of Birmingham) (Kotsantis et al., 2016).

2.9.1 Human cell culture

Human dermal fibroblasts were cultured in modified DMEM (Gibco - Thermo Fisher Scientific, Loughborough, UK) containing 10% heat inactivated bovine serum albumin (Sigma-Aldrich, Gillingham, UK) and 1% penicillin-streptomycin (Gibco - Fisher Scientific, Loughborough, UK). They were re-seeded as required in T75 flasks (Greiner bio-one, Stonehouse UK) following disassociation with TrypLE express (Gibco - Fisher Scientific, Loughborough, UK).

2.9.2 Senescence induction using X-ray irradiation

To induce senescence fibroblasts were exposed to a dose of 10Gy of ionising radiation using the "CellRad+ Benchtop system" (Precision X-Ray, Connecticut, USA).

2.9.2.1 Senescence-associated β-galactosidase staining

Senescence was confirmed post day 10 by senescence-associated (SA) beta-galactosidase (SAβ-Gal) staining using the "senescent cells histochemical staining kit" (Sigma-Aldrich, Gillingham, UK) and according to manufacturer's instruction. Cells were Incubated with the provided staining solution for 4.5 hours at 37^{o}C without CO_2.

Bright-field images of stained cells were taken using the Axio Vert.A1 and AxioCam ERc5s (Zeiss, Jena, Germany). Images were processed using ZEISS ZEN (Blue edition) (Zeiss, Jena, Germany). 5 fields of view at 10x magnification were taken of each of the 3 cell culture replicates in 12 well flat-bottomed plates (Corning, New York, USA). The total number of cells within each field of view was counted as were the number of these cells which showed positive, blue, SA beta-galactosidase staining. The

proportion of positive cells was then reported as a percentage of the total cells with a minimum of 100 cells counted.

2.9.2.2 Cell morphology

Senescent and non-senescent cell size was calculated, using fluorescence microscopy and image analysis, as additional characteristics of senescence. The Initial protocol used for investigating cell morphology were provided by Dr Nikhil Jain. Cells were first grown on standard 22x22mm glass cover slips (Camlab, Over, UK) to enable clear imaging and staining. Cells were first washed with 0.3 Triton-x (Sigma-Aldrich, Gillingham, UK) for 10 minutes before washing once with PBS. 6µl of phalloidin-FITC to stain F-actin (40x dilution in DMSO, ~26.8 nM, TOCRIS: 5782) and 3µl of DAPI stock (1000 µg/ml) (Thermo Fisher Scientific, Loughborough, UK) was added to 1.5ml of 1% BSA in PBS to create a cocktail. 200µl of this cocktail was added to each cover slip and incubated for 1 hour in the dark in a humidity chamber. The cover slips were washed with PBS and placed face down onto a single drop of mounting media on generic microscope slides. The slides were incubated for 2 hours in the dark to allow the Anti-Fade mounting media (Abcam, Cambridge, UK) to set. Finally, the cover slip edges were coated with clear varnish to prevent drying out. The samples were kept in the dark at 4°C before viewing.

Cells were imaged on the Leica DM6000 microscope (Leica Microsystems, Wetzlar, Germany), the 358-461 and 540-545 excitation range lasers were used. Images were recorded at 10x, 20x and 40x magnification. Cell images were analysed using FIJI (Schindelin et al., 2012). The cell area was measured for a minimum of 100 cells at each time point. These data were used to calculate the mean cell area.

2.10 Human cell culture: senescence modulating compound discovery

Acknowledgement: The compound library and EC_{50} values used in this investigation into the effect epigenetic compounds have on senescent fibroblasts were provided by Dr Annette von Delft, Centre for Medicines Discovery, University of Oxford.

2.10.1 Compound exposures

BJ human dermal fibroblasts were treated with 10Gy of X-ray radiation to induce senescence. These cells were fed 3 times weekly (see section 2.9.1 for media information) and seeded from T75 flasks (Greiner bio-one, Stonehouse UK) into 12 well flat bottomed plates (Corning, New York, USA) at day 10 post irradiation. The non-X-rayed, non-senescent control cells were also seeded onto 12 well plates on day 10. Cells were given 48 hours to adhere to the plates, bringing the day of culture to day 12 post-irradiation for the senescent cells. Cells were then treated with the compounds of interest or solvent control for 48 hours before analysis on day 14. Non-senescent cells were seeded at seeding density (approximately $0.1x10^6$) and senescent cells were seeded at near confluency (approximately $0.5x10^6$).

2.10.2 Apoptosis assay

Apoptosis was determined by binding of Annexin V with exclusion of propidium iodide (PI), staining with both Annexin V and PI was indicative of necrosis (Rieger et al., 2011). 10x Annexin binding buffer stock solution comprised 0.1M Hepes pH 7.4 containing 1.4M NaCl and 25mM CaCl2. Annexin binding buffer was prepared by diluting the Annexin binding buffer stock 1:10 with ddH_2O. Annexin binding buffer + Annexin V FITC stain was prepared by adding Annexin V FITC (Miltenyi Biotec, Bergisch Gladbach, Germany) to the Annexin binding buffer at a ratio of 1:500.

Cells were dissociated from the plates using trypsin (TrypLE Express, Gibco – Thermo Fisher Scientific, Loughborough, UK) and washed with iced 1% BSA by centrifugation at 400xG for 4 minutes as 4°C. Cell pellets were washed in 3ml iced Annexin V binding buffer and spun at 400xg for 4 minutes at 4°C, supernatant was removed. 200 µl of Annexin binding buffer + Annexin V FITC stain was added to each tube, tubes were vortexed and incubated for 15 minutes on ice in the dark. Cells were then washed twice with 3µl of Annexin binding buffer, with centrifugation at 400xg for 4 minutes as 4°C. Cells were resuspended in 200 µl of Annexin binding buffer and kept on ice. 1µl of propidium iodide solution (Sigma-Aldrich, Gillingham, UK) was added to each tube and vortexed gently for ~1 minute before

analysis. All samples were analysed by flow cytometry on the BD FACSVia C6 Flow cytometry system for a minimum of 2500 captured events.

2.11 Tissue sectioning and staining

2.11.1 Tissue sectioning

Paraffin mounted human skin biopsies (full thickness, punch, 2.5-5mm) were sectioned at a thickness of 5µm. They were mounted on "Plus+Frost positive charged slides" (Solmedia, Shrewsbury, UK) and baked at 65°C for one hour.

2.11.2 Tissue staining

Prior to staining, sections were rehydrated using 3 x 3-minute 100% xylene wash, followed by a 3 x 3-minute 100% ethanol wash followed by 2 x 2-minute H_2O wash. Sections were microwaved at "high" (800W) for 3 minutes in a microwave safe container containing a sodium citrate retrieval solution (eBioscience – Thermo Fisher Scientific, Loughborough, UK) diluted 1:100 with ddH_2O. Sections were allowed to cool for 10 minutes and were then placed into cold running tap water for 3 minutes before being washed in 1 x PBS for 5 minutes.

2.11.2.1 p16 Staining

The BLOXALL, DAB, ABC reagents as well as the secondary antibody and Hematoxylin were all part of the VectaStain Elite ABC-HRP Kit (Vector Laboratories, California, UK).

Slides were removed from PBS and the edges of the slides were carefully dried with a paper towel; a wax pen was then used to mark a barrier around the sample taking care not to draw over the sample edge. A drop of the peroxidase BLOXALL blocking solution was added, enough to cover the sample for 10 minutes. The blocking agent was poured off and the slide washed in PBS for 10 minutes. 3-5 drops of 5% BSA (enough to cover sample) was added, this was left to incubate for 1 hour and 30 minutes at RT. 200µl of p16 antibody (enough to cover the tissue section) at a working concentration was added

(See table below). 200µl of an isotype control antibody was added to an additional sample (enough to cover the tissue section) to check for non-specific staining. Sections were incubated with the primary antibody/isotype control at room temperature for 30 minutes.

P16							
Antibody Target	**Manufacturer**	**Product code**	**Clone**	**Source/Iso**	**Stock concentration**	**Dilution**	**Working concentration**
P16	abcam	ab54210	2D9A12	Mouse IgG2b	1mg/ml	1:500 5% BSA	2µl/ml
Isotype control	abcam	ab18413	MG2B-57	Mouse IgG2b	1mg/ml	1:500 5% BSA	

Table 2.2: p16ink4A and isotype control antibodies. Details of antibodies used for p16ink4A tissue staining, with supplier and dilutions used.

Sections were then washed in 0.05 PBST (1x PBS + 0.05% v/v TWEEN 20) for 5 minutes 5 times. The secondary antibody was then added, and slides were incubated for 30 minutes at room temperature. The secondary antibody was poured off and samples were washed in PBS for 5 minutes, 5 times. The ABC reagent was added and left for 30 minutes. Slides were washed in plenty of PBS for 5 minutes, 5 times. 200µl of the DAB stain was added to each slide and they were incubated for 30 seconds before being placed under cold tap water for 3 minutes. Hematoxylin counterstain was added and incubated for 3 minutes at room temperature. Slides were rinsed gently with distilled water before being placed into cold running tap water for 3 minutes, followed by hot running tap water for 5 minutes. Slides were then placed into a 100% EtOH wash for 3 minutes, 3 time before being placed in a 100% xylene wash for 3 minutes 3 times. Slides were then placed flat and DPX mounting solution (Sigma-Aldrich, Gillingham, UK) was added, covering the section, a cover slip was applied and slides were left over night in a ventilation hood.

Imaging of tissue sections was done on the Zeiss Axio slide scanner (Zeiss, Jena, Germany). Samples were scanned at 20x magnification.

2.11.2.2 Stained tissue image analysis

All image analysis was performed using QuPath 3.0 histology analysis software (QuPath: Open-source software for digital pathology image analysis). A representative image of $p16^{ink4A}$ positive cell staining within a skin biopsy section can be seen in Figure 2.4.

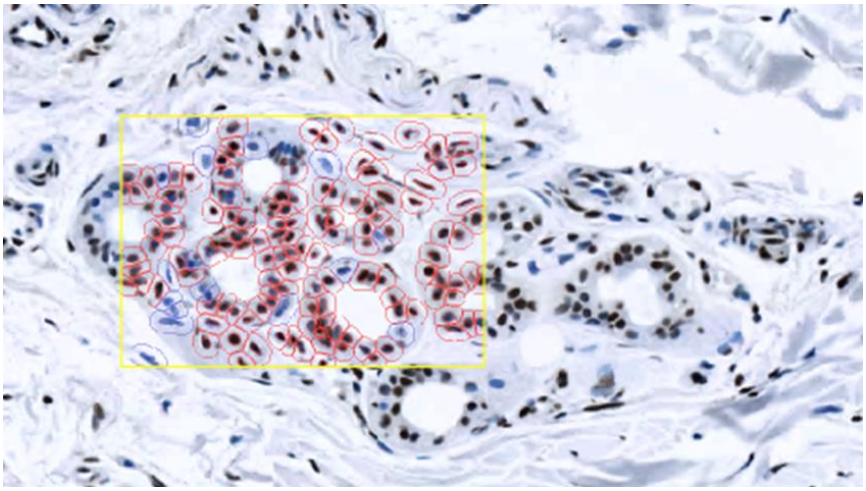


Figure 2.4: Automated $p16^{INK4A}$ positive cell detection in skin using QuPath 3.0 histology analysis software. After optimising the detection parameters, the software can differentiate positive and negative cells. This is shown within the yellow box where positive cells have been identified, shown here in red, and negative cells have been identified, shown here in blue.

2.12 Immune phenotyping

Flow cytometry of immunostained PBMCs was done on the Milteny Biotec MACSQuant Analyzer 10 (Miltenyi Biotec, Bergisch Gladbach, Germany).PBMC samples were defrosted from -80°C and washed with iced 1% BSA-PBS (Fisher Scientific, Loughborough, UK) and resuspended in 1% BSA-PBS and divided equally between the tubes required for each panel. Antibodies and isotype controls were added at the concentrations listed in the Table 2.3 and incubated at 2-8°C in the dark for ten minutes. Unlike many conventional antibodies, Reafinity antibodies and Reafinity isotype controls are not provided with a recommended concentration given in mass per microlitre (e.g., ng/µl). They are instead provided with an effective concentration, for example 1:50, with isotype controls

recommended to be used at the same effective concentration. Samples were topped up with 1ml of ice cold 1% BSA in PBS and spun at 300xg for 10 minutes. Supernatant was removed and cells were resuspended in 200µl of MACSQuant Running buffer (Miltenyi Biotec, Bergisch Gladbach, Germany) and kept on ice in the dark until use. Intra-cellular staining (FoxP3) was performed using the FoxP3 Staining buffer set (Miltenyi Biotec, Bergisch Gladbach, Germany).

A minimum number of evens were captured by flow cytometry for each panel. For the T cell subset panel, a minimum of 20,000 events were captured within the CD3+ gate. For the Treg panel, a minimum of 20,000 events were captured within the CD3+/CD4+ gate. A minimum of 20,000 events were also captured within the CD3+ gate for the senescence panel. For the B cell panel, a minimum of 5,000 events were captured within the CD19+ gate. A minimum of 5,000 events were captured within the CD3+/CD56+ gate for the NK panel.

The gating strategies used were based on previously published and widely accepted methodologies. The T cell subset gating strategy used has been published multiple times within the literature (De Biasi et al., 2020; Duggal et al., 2018b), as has the T cell senescence gating strategy (Duggal et al., 2018b; H.-S. Yi et al., 2019), B cell (Asito et al., 2011; Duggal et al., 2018b) and B Reg (Niharika A. Duggal et al., 2013; Hayashi et al., 2016) gating strategies as well as for NK cells (Björkström et al., 2010; Lorenzi et al., 2013; Moreira et al., 2019; Wijaya et al., 2019) and regulatory T cell populations (Haas et al., 2019; Hori and Sakaguchi, 2004).

Isotype controls were used where appropriate and are listed along with the other antibodies used in Table 2.3.

Flow cytometry gating plots and cell population counts were generated using FlowJo 10.7.2 (FlowJo LLC).

T Cell Sub-Set Panel					
Antibody Target	Fluorophore	Manufacturer	Product code	Clone	Concentration (x µl : 50)
CD3	PE-Vio770	Miltenyi Biotec	130-113-140	REA613	1
CD4	VioBlue	Miltenyi Biotec	130-114-534	REA623	1
CCR7	APC	Miltenyi Biotec	130-120-466	REA546	2
CD45RA	PerCP-Vio700	Miltenyi Biotec	130-113-368	REA562	1
PTK7	PE	Miltenyi Biotec	130-112-677	REA836	4
CD8	VioGreen	Miltenyi Biotec	130-110-684	REA734	1
ISO Control IgG1	APC	Miltenyi Biotec	130-113-284	REA293	2
ISO Control IgG1	PerCP-Vio700	Miltenyi Biotec	130-113-368	REA293	1
ISO Control IgG1	PE	Miltenyi Biotec	130-113-640	REA293	4

Senescence Panel					
Antibody Target	Fluorophore	Manufacturer	Product code	Clone	Concentration (x µl : 50)
CD3	PE-Vio770	Miltenyi Biotec	130-113-140	REA613	1
CD4	VioBlue	Miltenyi Biotec	130-114-534	REA623	1
CD28	APC	Miltenyi Biotec	130-118-343	REA612	2
CD57	PE-Vio615	Miltenyi Biotec	130-111-815	REA769	2
PD-1 (CD279)	PE	Miltenyi Biotec	130-120-382	REA1165	2
CD8	VioGreen	Miltenyi Biotec	130-110-684	REA734	1
ISO Control IgG1	APC	Miltenyi Biotec	130-113-284	REA293	2
ISO Control IgG1	PE-Vio615	Miltenyi Biotec	130-113-451	REA293	2
ISO Control IgG1	PE	Miltenyi Biotec	130-113-640	REA293	2

Regulatory T Cell Panel					
Antibody Target	Fluorophore	Manufacturer	Product code	Clone	Concentration (x µl : 50)
CD3	PE-Vio770	Miltenyi Biotec	130-113-140	REA613	1
CD4	VioBlue	Miltenyi Biotec	130-114-534	REA623	1
CD25	APC	Miltenyi Biotec	130-113-284	REA570	4
FoxP3	PE	Miltenyi Biotec	130-125-579	REA1253	2
ISO Control IgG1	APC	Miltenyi Biotec	130-113-284	REA293	4
ISO Control IgG1	PE	Miltenyi Biotec	130-113-640	REA293	2

NK Panel					
Antibody Target	Fluorophore	Manufacturer	Product code	Clone	Concentration (x µl : 50)
CD3	PE-Vio770	Miltenyi Biotec	130-113-140	REA613	1
CD57	PE-Vio615	Miltenyi Biotec	130-111-815	REA769	2
CD56	APC	Miltenyi Biotec	130-113-310	REA196	2
ISO Control IgG1	PE-Vio615	Miltenyi Biotec	130-113-451	REA261	3

B Cell Panel					
Antibody Target	Fluorophore	Manufacturer	Product code	Clone	Concentration (x µl : 50)
IgD	VioBlue	Miltenyi Biotec	130-110-648	REA740	2
CD27	PE	Miltenyi Biotec	130-113-640	REA499	2
CD24	PE-Vio770	Miltenyi Biotec	130-112-658	REA843	1
CD38	APC	Miltenyi Biotec	130-123-852	REA671	2
CD19	FITC	Miltenyi Biotec	130-113-645	REA675	2
ISO Control IgG1	VioBlue	Miltenyi Biotec	130-110-648	REA293	2
ISO Control IgG1	PE	Miltenyi Biotec	130-113-640	REA293	2
ISO Control IgG1	PE-Vio770	Miltenyi Biotec	130-112-658	REA293	1
ISO Control IgG1	APC	Miltenyi Biotec	130-113-284	REA293	2

Table 2.3: Immune ageing flow antibodies - The antibodies used for each flow cytometry panel as well as their conjugated fluorophore, product code, and relative concentration used and colour matched isotype control.

2.13 Statistical analysis and figure generation

All statistical analysis carried out, unless stated otherwise was performed using R Studio 2022.02.3+492. The statistical packages used were either the inbuilt R Studio statistical functions or the ggplot2 statistical analysis functions (Villanueva and Chen, 2019).

2.13.1 Accessibility

All colour figures were generated using the Viridis R package and accompanying colour schemes. To ensure that all figures are distinguishable for people with the 4 most common forms of colour blindness.

3. Immune senescence following trauma

3.1 Introduction

3.1.1 Immune ageing in injury

The innate and adaptive immune systems undergo continuous and wide-ranging remodelling during physiological chronological ageing (Niharika A Duggal et al., 2013; Franceschi et al., 2020; Shaw et al., 2010). These changes are often referred to as "immune ageing" or "immunosenescence." Immunosenescence results in a reduced ability to respond to challenge as well as a change in the circulating cell subtypes (Yan et al., 2010). The clinical implications of immunosenescence are negative, and include reduced pathogen clearance and vaccine responses (Allen et al., 2020), increased cancer risk (Lian et al., 2020). Immunosenescence has also been implicated in multiple age-associated diseases, ranging from cardiovascular disease to neurological diseases (Barbé-Tuana et al., 2020).

3.1.1.1 Changes to the innate and adaptive immune system with age

The role of the innate immune system is to mount a broad and rapid response to pathogens via the pattern recognition receptors (PRR) present on the cells of the innate immune system (Fulop et al., 2018). These PRR can be markers of internal danger and damage termed "damage-associated molecular patterns" (DAMPs) (Roh and Sohn, 2018) or external markers present on pathogens termed "pathogen-associated molecular patters" (PAMPs) (Akira and Hemmi, 2003). The innate immunity compartment contains multiple cell types including monocytes, macrophages and neutrophils which facilitate the rapid recruitment of different immune cell subtypes to the site of damage or infection. This is done by via the production of chemokines and cytokines such as TNF and IL-6 (Marshall et al., 2018). Cells within the innate immune system such as macrophages also clear threats such as bacteria directly via phagocytosis as well as presenting antigens to T cells (Turvey and Broide, 2010). These processes become less effective during ageing, leading to a kind of "immune paralysis" developing.

This immune paralysis is also characterised by a baseline of chronic stimulation causing the overproduction of cytokines, leading to systemic inflammation alongside a reduction in activity when specific cell functions are needed (Fulop et al., 2016). The dysregulation of innate cell behaviour, with factors such as reduced antigen presentation and raised systemic inflammation, has a direct effect on the adaptive immune response.

The adaptive compartment of the immune system, containing T and B cells, targets and eliminates threats and has the ability to respond more effectively to previous infections upon repeat exposure, so-called immune memory (Blanchard et al., 2020). T cells are broadly divided into CD4+ and CD8+ expressing cells. Both T cell types can be categorised further into memory, effector and naïve subtypes, each with a distinct function (Luckheeram et al., 2012). CD4+ T cells help to regulate the behaviour of other immune cells (Das et al., 2017), such as the CD8+ cytotoxic T cells which destroy threats including virally infected and pre-cancerous cells (Raskov et al., 2021). During the ageing process there is a gradual reduction in the proportion of antigen naïve cells and an increase in circulating memory cells leading to a reduced ability or respond to new threats or vaccines. This reduction in naïve CD4+ T cells is due to the gradual atrophy of the thymus which begins in early adulthood. The thymus becomes populated by more adipose tissue, reducing its T cell producing function (Araki et al., 2016). There is also a noted involution of the lymph nodes with age, this has been theorised to directly impact the immunological response (Pan et al., 2008). Another example of the remodelling of the immune system is the observed shift in the CD4+ and CD8+ populations with the CD4:CD8 ratio reducing (Li et al., 2019).

As T cells gradually develop from naïve T cells through to effector and memory cells following antigen exposure, they shorten their telomeres and eventually enter a state that resembles senescence in non-immune cells, though they do retail some proliferative capacity. Senescent T cells produce a senescence associated secretory phenotype (SASP) that is very similar to that seen in non-immune cells (Callender et al., 2018b). The increased presence of the pro-inflammatory SASP paired with a

reduction in the anti-inflammatory capacity of regulatory T cells (Fessler et al., 2013) may further drive the aged immune phenotype. Recently studies in mice have revealed that introducing senescent T cells in to young mice is enough to induce an aged phenotype suggesting they make a major contribution to poor health outcomes in ageing, at least in mice (Yousefzadeh et al., 2021c).

Overall, this immune ageing results in an increased threat from new infections, cancer and inflammation, reduced ability to benefit from vaccination and increased poor health in old age (Fulop et al., 2005).

3.1.1.2 Inflammaging

It is impossible to discuss immunosenescence without discussing the pro-inflammatory phenotype or "inflammaging" which accompanies it. Inflammaging put simply is the low level but chronic inflammatory phenotype which continually develops as we age, and contributes to the pathogenesis of many age associated diseases (Franceschi et al., 2018). Its link with immunosenescence forms the basis of a negative feedback loop wherein less new naive immune cells are produced, due to the negative influence of inflammatory cytokines on thymic atrophy (Gruver and Sempowski, 2008). The existing T cells become senescent and then increase production of pro-inflammatory cytokines via their SASP, which in turn drives senescence, as confirmed in a recent meta-analysis (Rodriguez et al., 2021). Where lifestyle and genetics intersect, for example obesity, there is an observed increase in inflammation (DeBoer, 2013), this coincides with an increased presence of the immunosenescent phenotype (Shirakawa and Sano, 2021).

As injury can result in chronic inflammation, it is possible that this will also increase immunosenescence. Interestingly, an inflammation specific universal clock has been developed to quantify inflammaging from study to study. The iAGE clock was built on cytokine profiles that predicted frailty, it has therefore been taken as an estimate of the degree of inflammatory ageing and may also relate to a person's biological age (Sayed et al., 2021).

3.1.1.3 Quantifying immune ageing

Given the multitude of changes which occur within the immune system during the ageing process, there is a clear need for standard immune ageing scoring method rather than the current system which sees different groups looking at different sub-populations using different markers. This would function in the same way as an injury severity score might, providing a repeatable framework for analysis that can be used universally, and can allow for accurate comparisons between studies. One such method is the IMM-AGE scoring system which has been developed by Alpert et al. 135 individuals had their immune systems phenotyped over a 9 year period using time of flight cytometry (CyTOF). The changes in their immune profiles were used to create an immune "trajectory", tracking the ways in which different immune cell populations change over time and how this related to mortality, generating an "IMM-AGE" score. (Alpert et al., 2019). This technique offers a useful universal scoring system for immune ageing. IMM-AGE was developed to incorporate 71 cell sub-populations, a number too high for most conventional flow cytometry studies, thanks to a recent collaboration with the authors of IMM-AGE, we have been able to reduce the number of cell sub-populations to 8 to generate an equally valid but more practical modified IMM-AGE score (Foster et al., 2022).

3.1.1.4 Immune phenotype changes with injury

To date there is a paucity of data in the literature with regards to the effect of traumatic injury on immune ageing. One study which did look into the effect an injury could have on immunosenescence was that of Pavlicek et al., in 2017. This study determined the impact of spinal cord injury (SCI) on immunosenescence. A comparison was made between the immune phenotypes of 85 participants with SCI and 84 non-injured controls. It was observed that those participants with SCI had a reduced proportion of naïve T cells and increased memory T cells (Pavlicek et al., 2017). While this study is looking at an injury specific effect on the immune system, the pathology of SCI is drastically different from that of a burn injury. This is because SCI can drastically reduce a person's mobility depending on the position of the injury, sometimes limiting it almost completely. The enforced immobility could

itself result in immune ageing, as physical activity is known to have profound influences on immunosenescence (Duggal et al., 2018a).

While there is limited research on physical injury and immunosenescence there has been research into the effect of psychological trauma and stress. Caregiving can be an incredibly stressful, long-term activity. The impact that high-stress caregiving had on the immune phenotype was investigated by Prather et al., in 2018. The immune phenotype of 91 primary caregivers (all female, aged 20-50) of young children with some form of autism spectrum disorder (aged 2 - 6) were compared to those of age matched primary care givers of neurotypical children of the same age. They found that the chronically stressed caregivers displayed lower percentages of naïve T cells and greater memory T cells than the controls (Prather et al., 2018). A similar finding has been observed within hip fracture patients, who, following the development of depressive symptoms showed an increased frequency of senescent and exhausted T cells compared with healthy controls (Duggal et al., 2014). While these data may not be related to burn injury it supports the suggestion that immunosenescence can be induced by a stressor, a life changing injury such as a large burn may have a similar if not greater effect.

3.1.2 Injury factors that could affect immune ageing

The study presented in this chapter was performed using samples taken from participants in the SIFTI 1 & 2 studies (Hazeldine et al., 2021), these participants were admitted to hospital with a major burn injury. The clinical markers of interest that will be used in this chapter, as well as several markers of particular interest to ageing research are outlined below.

3.1.2.1 Total burn surface area (TBSA)

TBSA percentage is the total percentage of the skin on the body which has been affected by a burn injury. It is usually estimated not by measuring the exact area of burn and total surface area of the patient's skin but is determined using the assumption that the skin covering different portions of the body generally make up the same percentage across the population. This is done using a chart such as the Lund and Browder (Lund, 1944), or some variation thereof (Murari and Singh, 2019). Although

more modern techniques are aiming to use images and accompanying software to more accurately calculate TBSA (Barnes et al., 2015).

3.1.2.2 rBaux score

The revised Baux score (rBaux) is a clinical scoring method used to predict mortality following burn. It is a combination of the factors which most contribute to patient outcome following burn injury. The formula is age (years) + TBSA% (+ 17 if inhalation injury was sustained) (Lam et al., 2021). An rBaux score of ~130 is deemed to be un-survivable although this number varies depending on the level of care available.

3.1.2.3 Sequential organ failure assessment score

The sequential organ failure assessment score (SOFA) is an ICU mortality prediction score which has been shown to be strongly predictive of ICU patient outcomes globally. The total SOFA score can be generated after 24 hours of ICU admission and is calculated by monitoring the respiratory system, nervous system, cardiovascular system, liver, coagulation, and kidneys. Regular clinical scores are taken such as the Glasgow coma scale, which is used to assess the neurological condition of a patient. These values are then converted to a 'SOFA' score ranging from 0 to 4, a 15 on the Glasgow coma scale for example is given a SOFA score of 4. Another example is that for coagulation, where a platelet count of < 15 $x10^3$/ml would earn a SOFA score of 0. This is done for all clinical scores looking at the areas described above and the total SOFA score is recorded (Lambden et al., 2019). This method is not injury specific and allows for predictions and comparisons between patient groups. This makes SOFA score a valuable biomarker when investigating the injury effect on patient outcomes.

3.1.2.4 Acute physiology and chronic health evaluation II (APACHE II) score

Like the SOFA score, the APACHE II is also a clinical ICU scoring system which is used to classify disease severity. It too is an accurate patient outcome prediction tool. As well as using several clinical markers such as blood pH and heart rate, the APACHE II score also attributes points for age and chronic health conditions such as heart failure or immunosuppression (Knaus et al., 1985). This inclusion of serious

comorbidities means that the APACHE II scoring system may offer a clearer picture of patient outcomes in the injury setting due to considering their pre-injury health.

3.1.2.5 Body mass index

Obesity is known to mimic the ageing process in many ways. Obesity increases inflammation (DeBoer, 2013), senescent cell accumulation (Conley et al., 2020), and has been shown to accelerate the biological ageing process as measured using DNA methylation clocks (Horvath et al., 2014; Nevalainen et al., 2017). Adiposity is not easily measured within a standard hospital environment, so BMI is used instead. It is calculated by dividing a person's mass in kg by the square of their height in metres (Weir and Jan, 2021). A score of 18.5 to 24.9 is considered a normal weight, with a BMI of 30 or more being considered obese. Higher BMI is also correlated with poorer patient outcomes, as was highlighted by the disproportionately poorer outcomes of obese patients following COVID-19 hospital admissions (Soeroto et al., 2020).

3.1.2.6 Length of stay

A patient's length of stay within hospital can often be used as a measure of how ill or seriously injured a patient is, with extended periods of stay being predictive of poor outcomes and mortality (Lingsma et al., 2018), the relationship between length of stay and outcome therefore making it another valuable marker of patient injury severity and potential impact.

3.1.3 Aims of the chapter

This chapter aimed to address the following questions:

1. Does burn injury cause short and long-term changes in telomere length in peripheral blood mononuclear cells (PBMCs)?
2. Does burn injury cause long-term immune ageing?

To answer these questions, PBMC telomere length was measured by quantitative PCR at admission, 6 months post injury and in a healthy control population. Flow cytometry immune profiling was also

performed on PBMCs from burn injured patients 6 months post injury and compared to a healthy control population to look for signs of immune ageing.

3.2 Results

3.2.1 Telomere length following injury

Telomere attrition occurs during the ageing process and is considered a hallmark of ageing (Lopez-Otin et al., 2013). To investigate how burn injury affects this ageing hallmark the absolute telomere length of PBMCs of burn injured patients was measured following admission and 6 months post injury. The absolute telomere length of burn-injured patients was also compared to those of a healthy control population.

3.2.1.1 Participant demographics

Absolute telomere length (ATL) per diploid cell was measured using isolated DNA from PBMCs taken at admission to hospital with burns at day one and again at month 6 in 33 participants in the SIFTI 1 and 2 studies. ATL was also measured in an age matched un-injured control group (Table 1). The injured cohort had a mean TBSA% of 32.15% and a mean length of stay (LOS) of 53.59 days. The mean age of the burn group was 41.17 compared with 39.64 in the control group. Mean body mass index (BMI) of the burn group was 26.37 compared with 23.99 in the control group, with a similar split of sexes between the groups, although the burn group contains more men, a result of more men presenting to hospital with burn injury than women.

The ATL analysis was performed using the Sciencell Absolute telomere length quantification qPCR assay kit. As well as primers for the telomere sequence this kit includes a reference sequence of DNA of a known length as well as single copy reference gene primers so that telomere length per genome can be calculated.

	n	Age	Sex	M : F	BMI	rBaux	TBSA%	LOS	APACHE II	SOFA
Burn group	33	41.17 (16.44 - 79.57)	26	: 9	26.37 (19.4 - 35.2)	81.80 (21 - 126.8)	32.15 (13 - 66)	53.59 (8.63 - 226)	17.88 (0 - 36)	5.36 (0 - 15)
Control group	28	39.64 (19 - 85)	18	: 10	23.99 (17.52 - 30)	n/a	n/a	n/a	n/a	n/a

Table 3.1: Absolute telomere length analysis cohort information - Table showing the cohort information of the participant groups used for telomere length analysis. This includes participant number, age, sex at birth, BMI and for the injured burn group the clinical markers rBaux score, total burn surface area percentage (TBSA %), length of stay (LOS), acute physiology and chronic health evaluation II score (APACHE II) and sequential organ failure score (SOFA). Data are mean, ranges shown where appropriate.

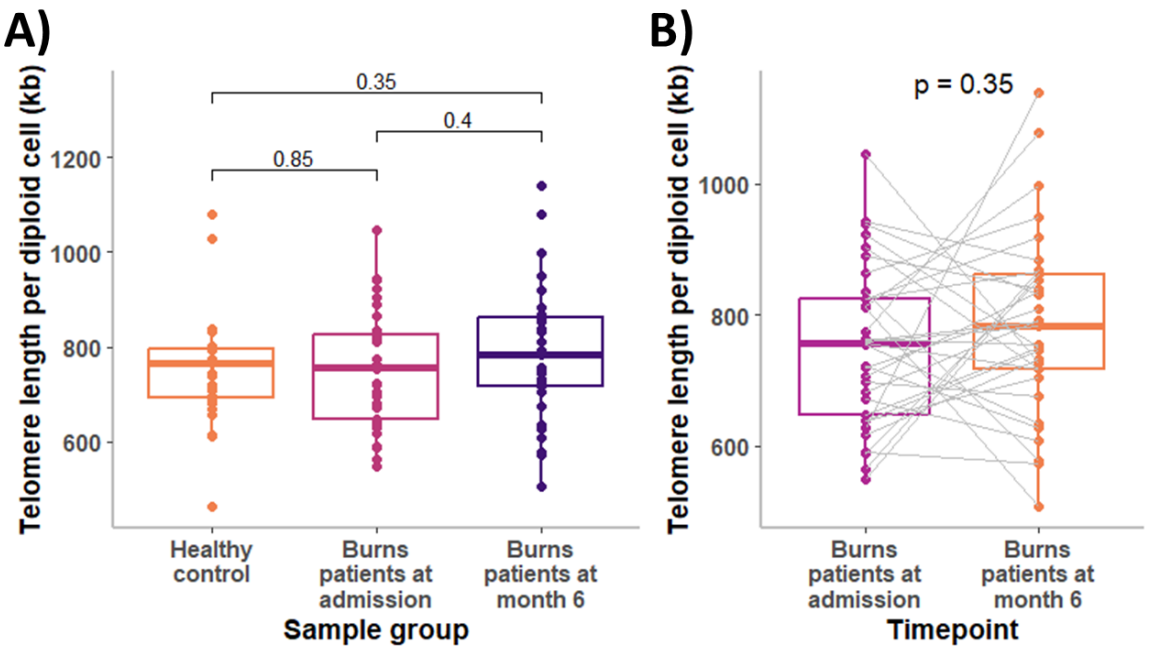
3.2.1.2 Absolute telomere length analysis

The absolute telomere length per diploid cell (ATL), specifically PBMCs, of the control group (755kb), and patient group at admission (752kb) and 6 months post injury (783kb) were compared. There was no significant difference between the ATL of any of the groups (Figure 3.1 A).

A paired analysis of the participants at admission and the same participants at month 6 showed a non-significant increase (p=0.35) in the mean ATL of 30kb (Figure 3.1 B). Therefore, burn injury does not cause a difference in ATL in the acute (day 1) or chronic (6 months) post injury phases.

The absolute telomere length of the individuals was compared to several clinical parameters. There was no significant correlation between ATL and chronological age in any of the groups (Figure 3.1 C), although there was a trend towards shorter telomeres at older age within the control group, Figure 3.3 A ($R = -0.32$, $p = 0.094$, Spearman correlation). Consistent with reports of short telomeres in patients with obesity there was a statistically significant, but weak negative correlation between ATL and BMI in the burn cohort at admission (Figure 3.1 C; $R = -0.36$, $p = 0.036$, Spearman correlation). There was no correlation between ATL at admission or month 6 and TBSA% (Spearman). The R values were 0.033 and -0.0047 suggesting that there was essentially no correlation between the two values (Figure 3.1 C). There was also no significant correlation between ATL and rBaux score in either group

(Figure 3.1 C) and no correlation between ATL at admission or month 6 and LOS (Spearman). The R values were 0.0059 and -0.11 suggesting that there was as virtually no correlation between the two values. There was also no significant correlation between ATL and SOFA score in either group, although in the month 6 samples there was a trend towards significance and a weak positive correlation ($R = 0.32$, $p = 0.072$).



C)

	Participant group					
	Burn Admission		Burn Month 6		Healthy Control	
Clinical parameter	R	P value	R	P value	R	P value
Chronological Age	-0.15	0.39	-0.25	0.15	-0.32	0.094
BMI	-0.37	**0.036**	-0.28	0.12	-0.28	0.16
TBSA %	0.033	0.86	-0.005	0.98		
rBaux	-0.027	0.88	-0.11	0.55		
LOS	0.0059	0.97	-0.11	0.56		
SOFA	0.0032	0.99	0.32	0.07		
APACHE II	-0.067	0.71	0.26	0.16		

Figure 3.1: Absolute telomere length in burn injured individuals at admission and 6 months post injury compared with healthy controls and clinical parameters. The figure shows absolute telomere length in burn injured participants (n = 33) following admission to hospital and 6 months post injury as well in healthy controls (n = 28). **A** is a comparison between the absolute telomere length per diploid cell in healthy controls and patients at admission and 6 months post injury (Wilcoxon). **B** is a paired comparison of the participants at admission and 6 months post injury, the lines between points link the data from the same participant at each time point (paired Wilcoxon). For each box plot (**A** & **B**) each point is one participant. The central line is median, the bottom line is the 1st quartile (Q1), the upper the 3rd quartile (Q3). The whiskers represent calculated minimum and maximum values using the interquartile range (IQR). Whiskers are calculated using the formula Q1 + 1.5 x IQR or Q3 + 1.5 x IQR. **C** is a table showing the correlation (Spearman) between absolute telomere length and clinical parameters of interest, significant correlations are highlighted in green and bold. BMI = body mass index; TBSA % = total burn surface area percentage; rBaux = revised Baux score; LOS = length of stay; SOFA = sequential organ failure score; APACHE II = acute physiology and chronic health evaluation II score.

3.2.2 Immune ageing following injury

3.2.2.1 Acknowledgement

The healthy control immune phenotyping data used below was gathered and provided by Dr Niharika Duggal.

3.2.2.2 Participant demographics

Injured participant samples were collected as part of the SIFTI 1 and 2 studies. PBMCs were isolated from the whole blood of 31 burn injured participants 6 months post injury and analysed using immunostaining and flow cytometry. These data were then compared to data from 27 age matched healthy control individuals. General cohort demographic information can be seen in Table 2.

Immune ageing data were compared to clinical markers including burn area and injury severity to see if there was any relationship between the extent of the injury and any changes in immune phenotype.

	n	Age	Sex M : F	BMI	rBaux	TBSA%	LOS	APACHE II	SOFA
Burn group	31	41.87 (16.94 - 74.73)	31 : 0	26.30 (19.40 - 43.50)	77.53 (21 - 137)	31.94 (4 - 71)	45.71 (6 - 216)	17.82 (0 - 36)	4.90 (0 - 15)
Control group	27	42.44 (20 - 70)	27 : 0	n/a	n/a	n/a	n/a	n/a	n/a

Table 3.2: Immune ageing cohort information. Table showing the cohort information of the participant groups used for immune ageing flow cytometry analysis. This includes participant number, age, sex at birth, body mass index (BMI) and for the injured burn group the clinical markers rBaux score (revised Baux), total burn surface area percentage (TBSA %), length of stay (LOS), chronic health evaluation II score (APACHE II) and sequential organ failure score (SOFA). Data are mean, ranges shown where appropriate.

3.2.2.3 Differences in immune phenotype in burns patients compared to non-injured controls

Burn injury is associated multiple negative long-term health outcomes often associated with the ageing process, such as increased risk of cancer, cardiovascular disease, and increased risk of mortality. One possible explanation is that this is the result of accelerated ageing. Immune ageing is a classic hallmark of ageing (Lopez-Otin et al., 2013), to see if burn injury can cause long term immune aging, PBMCs from burn injured patients 6 months post injury and healthy controls were profiled using flow cytometry and cell populations were compared.

3.2.2.3.1 T cell subsets

T cells are broadly divided into CD4+ helper T cells and CD8+ cytotoxic T cells. Within each compartment (CD4+ or CD8+) there are multiple cell sub-populations, broadly divided into naïve, central memory, effector memory, and effector memory cells re-expressing CD45RA (EMRA). There are also some additional further sub-populations such as recent thymic emigrants (Naïve T cells expressing PTK7), senescent T cells (CD28-, CD57+) and regulatory T cells (CD25+, FoxP3+). Each cell sub-population is functionally distinct and has a unique impact in the immune system. As well as comparing the sub-populations between healthy and long-term burn injured participants groups such as the total T cell populations are also compared in order to estimate the IMM-AGE score (Foster et al., 2022).

While there was no difference in the percentage of CD4+ T cells as a proportion of all CD3+ T cells between burn injured and control groups (Figure 3.2, A), there were significant differences detected in other CD4+ cell sub-populations. In the burn group there were significantly lower percentages of PTK7 expressing recent thymic emigrants (RTE) (Figure 3.2B; $p = 0.00024$) as well as CD4+ naïve (Figure 3.2C; $p = 5.6e-07$) T cells as well as and EMRA T cells (Figure 3.2F; $p = 5.3e-08$) compared to the healthy control group. Within the burn group there were also significantly higher percentages of CD4+ central

memory (Figure 3.2D; p = 4.4e-08), effector memory (Figure 3.2E; p = 7.3e-09) and total memory (Figure 3.2G; p = 1.1e-07) T cells compared to the healthy control group.

Regulatory T cells' role is to suppress and regulate T cell responses, largely through secretion of anti-inflammatory cytokines such as IL-10 (Kondělková et al., 2010). When comparing the healthy control and burn group, there was no significant difference in the proportions of Treg cells between groups, though there was a trend towards an increase in Tregs (Figure 3.2H; p = 0.051).

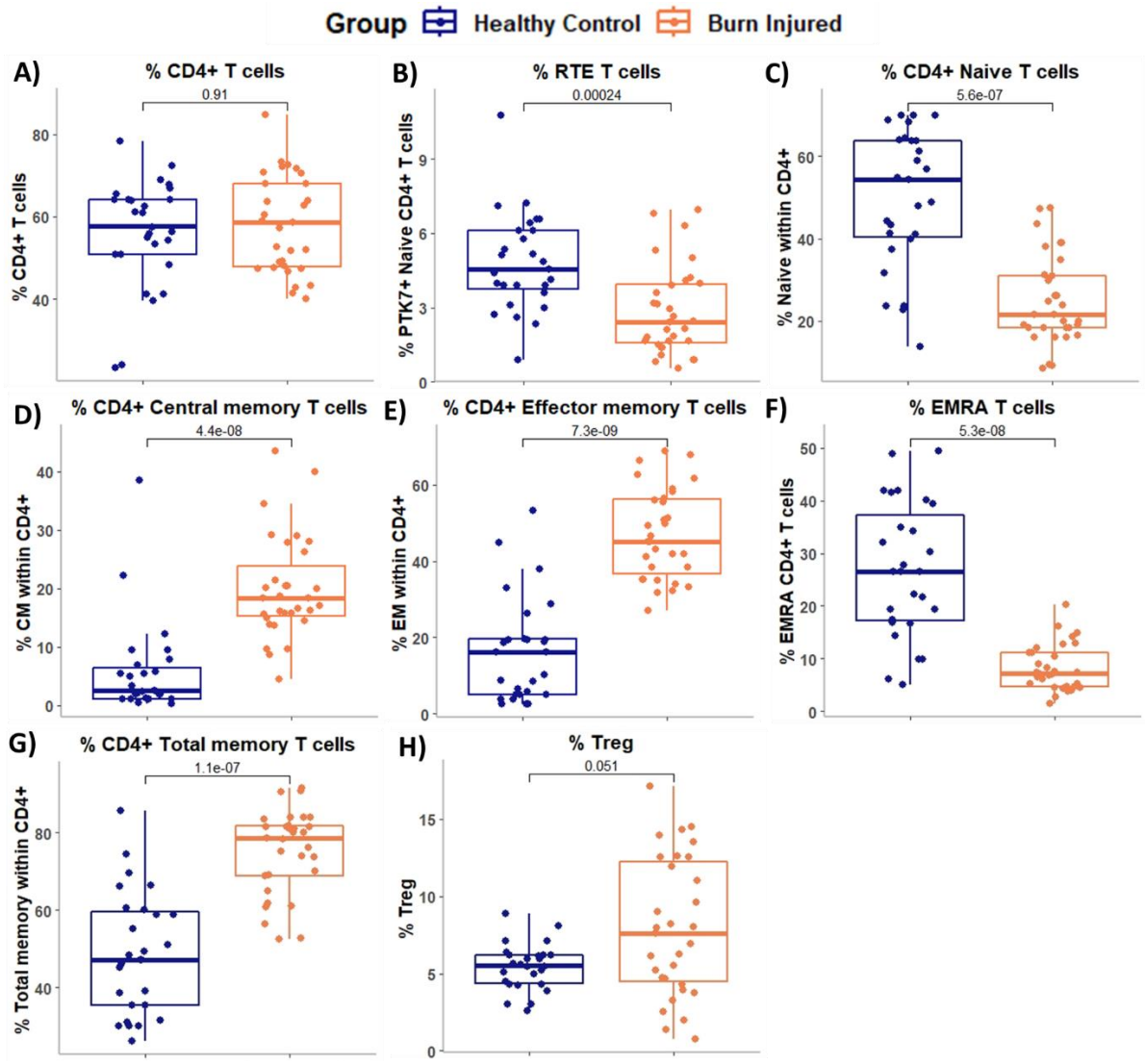


Figure 3.2: Differences in CD4+ T cell subsets between long-term burn injured participants and healthy controls. The figure shows the proportions of several CD4+ T cell subtypes in burn injured participants (n = 31) 6 months post injury compared to a healthy control group (n = 27) (Wilcoxon). Shown are the CD4+ T cells as a proportion of all lymphocytes (**A**); then as a proportion of CD4+ T cells are the percentage of recent thymic emigrants (RTEs) (**B**), naïve (**C**), central memory (**D**), effector memory (**E**), effector memory re-expressing CD45RA (**F**) and total memory (**G**) T cells. Shown as a proportion of all lymphocytes are regulatory T cells (Treg) (**H**). For each box plot each point is one participant. The central line is the median, the bottom line is the 1st quartile (Q1), the upper the 3rd quartile (Q3). The whiskers represent calculated minimum and maximum values using the interquartile range (IQR). Whiskers are calculated using the formula Q1 + 1.5 x IQR or Q3 + 1.5 x IQR.

There were significant differences in CD8+ cell phenotype detected between controls and burn participants 6 months post injury (Figure 3.3). In the burn group there were significantly lower percentages of total CD8+ T cells (Figure 3.3A; p = 7.5e-05) as a proportion of CD3+ T cells compared to the healthy control population. In the burn injured group there were also fewer CD8+ central memory T cells (Figure 3.12E; p = 0.00048) as well as and CD8+ EMRA (Figure 3.12E; p = 0.048) T cells within the CD8+ T cell population compared to the control group, but there was a higher percentage of CD8+ effector memory cells (Figure 3.12C; p = 3.2e-07). The EMRA group is the one that contains most senescent or exhausted T cells. There was no significant difference between the burn and control groups with regards to the CD8+ naïve subpopulation. Despite the differences observed in memory subpopulations between groups, there was no significant difference in the total CD8+ memory T cell population between the groups (Figure 3.2F; p=0.73).

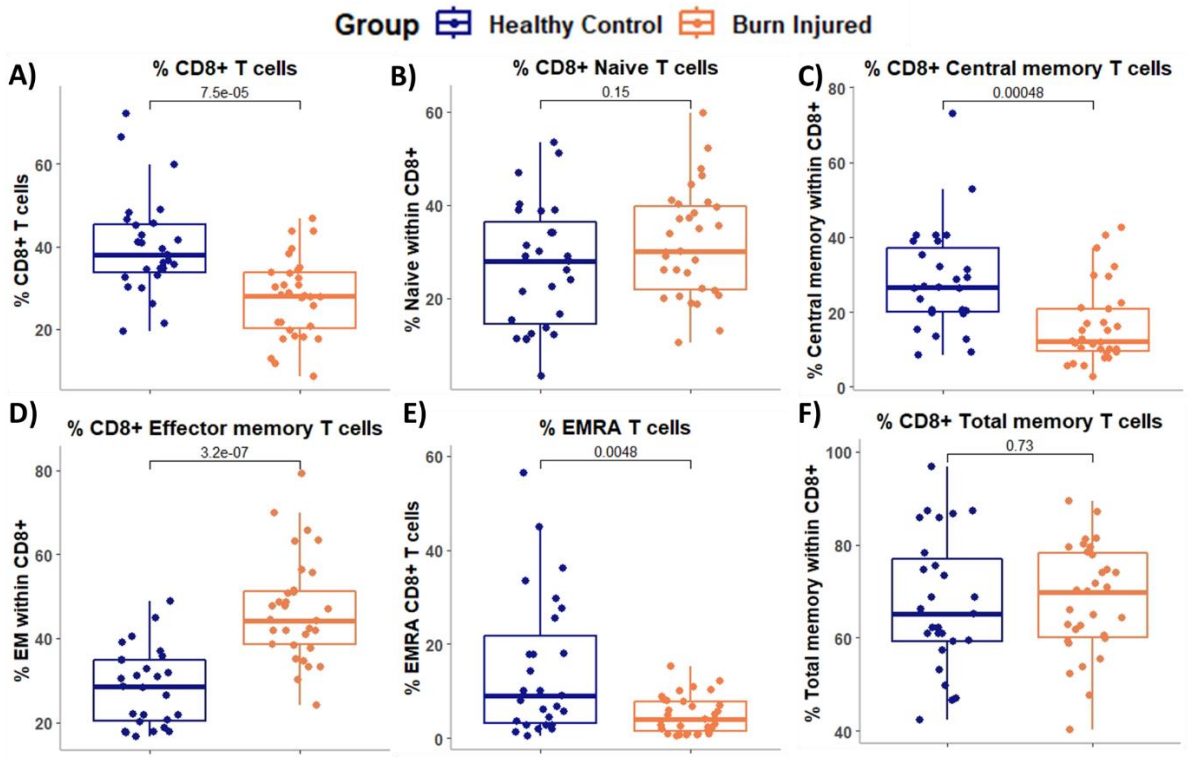


Figure 3.3: Differences in CD8+ T cell subsets between long-term burn injured participants and healthy controls. The figure shows the proportions of multiple CD8+ T cell subtypes in burn injured participants (n = 31) 6 months post injury compared to a healthy control group (n = 27) (Wilcoxon). Shown are the CD8+ T cells as a proportion of all lymphocytes (**A**). Also shown as a proportion of CD8+ T Cells are the percentage of naïve (**B**), central memory (**C**), effector memory (**D**), effector memory re-expressing CD45RA (**E**) and total memory (**F**) T cells. For each box plot each point is one participant. The central line is median, the bottom line is the 1st quartile (Q1), the upper the 3rd quartile (Q3). The whiskers represent calculated minimum and maximum values using the interquartile range (IQR). Whiskers are calculated using the formula Q1 + 1.5 x IQR or Q3 + 1.5 x IQR.

As stated above the senescent T cell population is largely found in the EMRA population. To more specifically assess their presence, cells lacking CD28 and expressing CD57 were measured. There was no significant difference in the percentage of CD4+ and CD8+ senescent cells in the burn injured group or the control group (Figure 3.4, A &B). This agrees with the observation in the telomere data shown in Figure 3.1, where there was likewise no evidence of increased senescence in the form of telomere shortening.

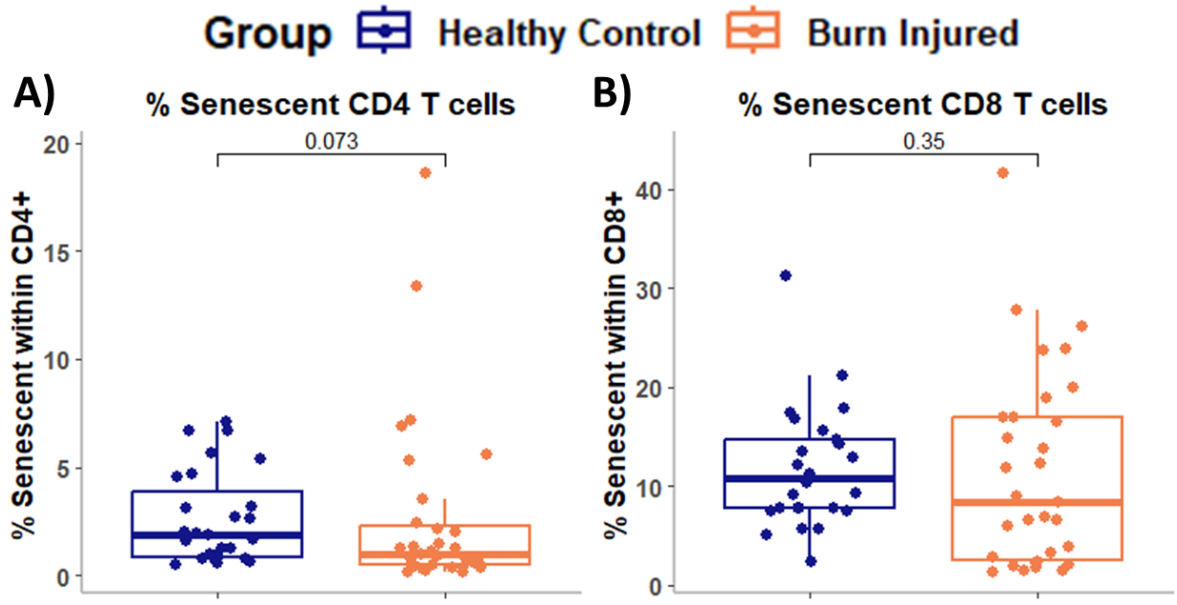


Figure 3.4: Differences in senescent CD4+ and CD8+ T cell subsets between long-term burn injured participants and healthy controls - Shown are the proportions of senescent (CD57+, CD28-) CD4+ and CD8+ T cells in burn injured participants (n = 31) 6 months post injury compared to a healthy control group (n = 27) (Wilcoxon). Shown are the percentage of senescent T cells (CD57+, CD28-, **A** & **B**) within the CD4+ & CD8+ T cell compartments. For each box plot each point is one participant. The central line is median, the bottom line is the 1st quartile (Q1), the upper the 3rd quartile (Q3). The whiskers represent calculated minimum and maximum values using the interquartile range (IQR). Whiskers are calculated using the formula Q1 + 1.5 x IQR or Q3 + 1.5 x IQR.

3.2.2.3.2 B cell sub cells

B Cells here have been divided into naïve, class switched memory, non-class switched memory and regulatory B cells, all of which have distinct immune functions. There were significant differences between the burn and control group in some B cell subsets examined (Figure 3.5). There was a significantly lower percentage of both total B cells (Figure 3.5A; p = 0.00059), naïve (Figure 3.5B; p = 8.7e-05) and unswitched memory B cells (Figure 3.5C; p = 0.02) in the burn group compared to the control group, with an increase in regulatory B cells (Figure 3.5E; p = .0013). There was no significant difference in the percentage of switched memory B cells between burn injured participants and healthy controls (Figure 3.5D; p=0.21).

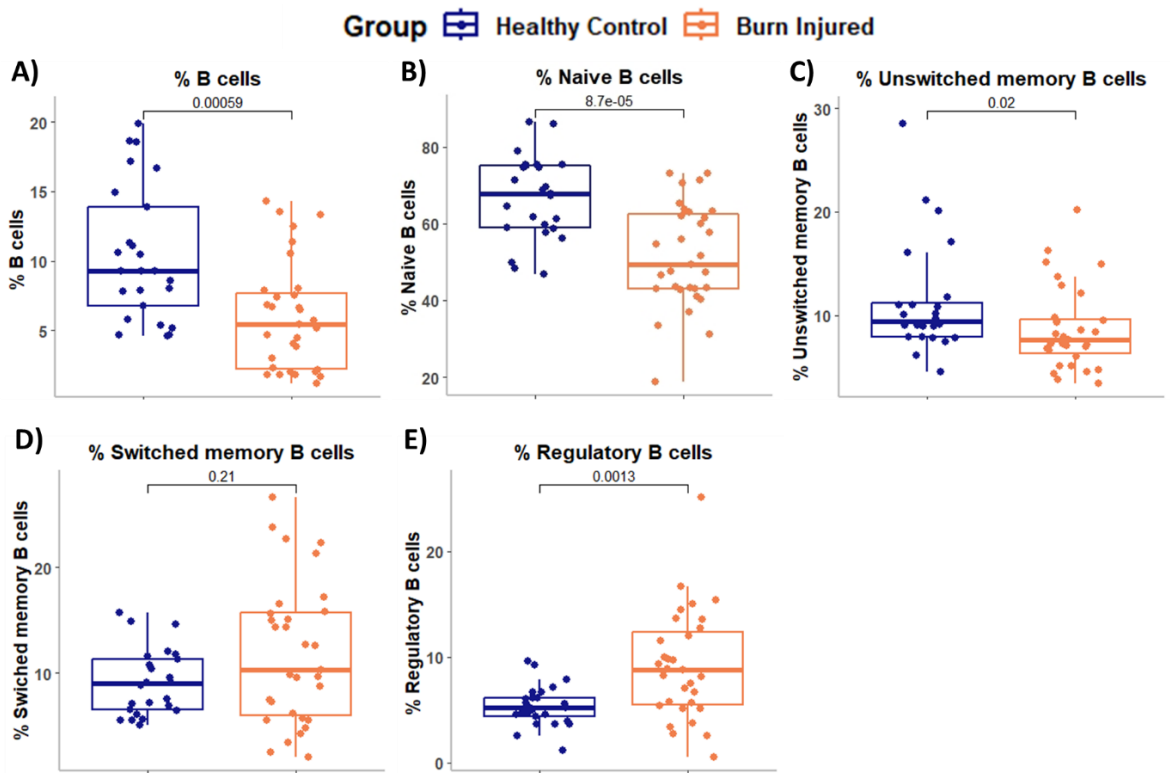


Figure 3.5: Differences in B cell subsets between long-term burn injured participants and healthy controls. The figure shows the percentage of B cells (CD19-, **A**) as a proportion of the total lymphocytes in burn injured participants (n = 31) 6 months post injury compared to a healthy control group (n = 27) (Wilcoxon). Also shown are the are the percentage of B cells which are naive (IgD+, CD27-, **B**), unswitched memory (IgD+, CD27+, **C**), switched memory (IgD-, CD27+, **D**) or regulatory B cells (Breg, $CD24^{Hi}$, $CD38^{Hi}$, **E**). For each box plot each point is one participant. The central line is median, the bottom line is the 1st quartile (Q1), the upper the 3rd quartile (Q3). The whiskers represent calculated minimum and maximum values using the interquartile range (IQR). Whiskers are calculated using the formula Q1 + 1.5 x IQR or Q3 + 1.5 x IQR.

3.2.2.3.3 Natural Killer Cells

Natural killer (NK) cells play a primary role in the innate defence against viral infections and also remove senescent cells (Gotthardt and Sexl, 2017). When comparing the healthy control and burn group there was no significant difference in the proportions of NK cells as a percentage of lymphocytes between groups, neither was there a significant difference in the proportion of cytotoxic CD56+ bright or regulatory CD56+dim subsets (Figure 3.6).

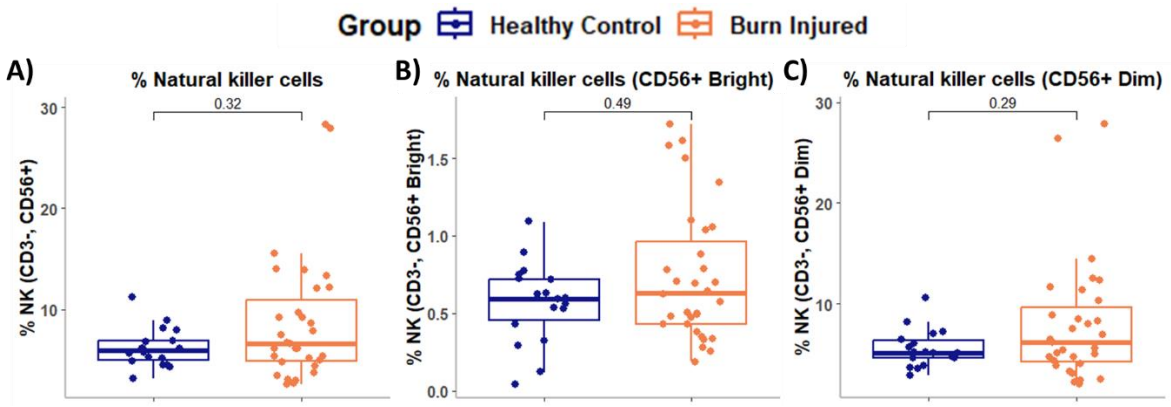


Figure 3.6: Differences in NK cell subsets between long-term burn injured participants and healthy control. The figure shows the proportions of natural killer (NK) cells (CD3-, CD56+) in burn injured participants (n = 31) 6 months post injury compared to a healthy control group (n = 27) (Wilcoxon). Shown are the percentage of lymphocytes which are NK cells (**A**), CD56+ bright NK cells (**B**), and CD56+ dim NK cells (**C**). For each box plot each point is one participant. The central line is median, the bottom line is the 1st quartile (Q1), the upper the 3rd quartile (Q3). The whiskers represent calculated minimum and maximum values using the interquartile range (IQR). Whiskers are calculated using the formula Q1 + 1.5 x IQR or Q3 + 1.5 x IQR.

3.2.2.3.4 The relationship between chronological age and immune cell sub-populations

Multiple immune cell sub-populations change during ageing. The relationship between age and cell percentages and numbers were compared to chronological age.

Table 3.3 shows that there was a significant negative correlation between chronological age and CD4+ naïve T cell percentage in both groups. There was also a significant positive correlation between CD4+ central memory T cell percentage and age within the burn group (Table 3.3, R = 0.5, p = 0.0038), this relationship was not observed in the control group. Additionally, there was no significant relationship between age and CD4+ effector memory or RTE percentages in either group.

Table 3.3 also shows the relationship between age and several CD8+ T cell subsets. There was no significant correlation between chronological age and naïve CD8+ cell frequency in the burn cohort, whereas there was a strong negative correlation within the control cohort (R = -0.43, p = 0.026). There was also a significant chronological age associated decline in CD8 central memory T cells (R = -0.52, p = 0.0027), as well as a strong positive association between effector memory T cells wand chronological age (R = 0.54, p = 0.0019) within the burn group. There was no detectable correlation between senescent CD4+ and CD8+ T cell percentage and chronological age in either group, although there was a tend towards significance in the moderate correlation in the burn injured group (R = 0.35, p = 0.055).

No B cell subtypes showed any significant relationship with chronological age in either group other than classical memory B cells in the burn group. There was a significant positive moderate correlation between chronological age and the percentage of switched memory B cells (Table 3.3, R = 0.39, p = 0.03, Spearman correlation). This change was not observed within the healthy control cohort.

There was no significant relationship observed between chronological age and NK or Treg percentage in either group. The NK cell percentage was approaching significance in the burn group, with a moderate positive correlation (R = 0.32, p = 0.078). There were more correlations observed between chronological age and the percentage of cells in the burn injured group compared to the control group.

This was also true when comparing the numbers of cells as opposed to their percentages. Within the burn group there were significant correlations between chronological age and the number of CD4+ central memory (R = 0.41, p = 0.021), CD4+ effector memory (R = 0.44, p = 0.016), CD4+ total memory (R = 0.42, p = 0.02) as well as C28- (R = 0.45, p = 0.012) and CD57+ CD4+ T cells (R = 0.44, p = 0.015). There was also a significant relationship between the number of CD8+ central memory T cells (R = -0.51, p = 0.004) in the burn group. There was a significant correlation between age and as CD8+ naïve T cells in the burn (R = 0.42, p = 0.021) and control group (R = 0.5, p = 0.008). The control group also showed a correlation between CD4+ naïve T cell number and chronological age (R = -0.43, p = 0.025)

	Percentage				Number			
	Control		Burn		Control		Burn	
Cell population	**R**	**p**	**R**	**p**	**R**	**p**	**R**	**p**
CD3+ Lympocytes	-0.47	0.013	-	-	-	-	-	-
CD4+	-	-	0.38	0.035	-	-	-	-
CD4+ Naïve	-0.43	0.025	-0.58	7E-04	-0.43	0.025	-	-
CD4+ Central memory	-	-	0.5	0.004	-	-	0.41	0.024
CD4+ Effector memory	-	-	-	-	-	-	0.44	0.016
CD4+ EMRA	0.43	0.024	-	-	-	-	-	-
CD4+ Total memory	-	-	0.58	7E-04	-	-	0.42	0.02
CD4+ CD28-	-	-	0.46	0.009	-	-	0.45	0.012
CD4+ CD57+	-	-	0.45	0.011	-	-	0.44	0.015
CD8+	-	-	-0.57	9E-04	-	-	-	-
CD8+ Naïve	-0.43	0.026	-	-	-0.5	0.008	-0.42	0.021
CD8+ Central memory	-	-	-0.52	0.003	-	-	-0.51	0.004
CD8+ Effector memory	-	-	0.54	0.002	-	-	-	-
CD8+ EMRA	-	-	0.37	0.042	-	-	-	-
CD8+ CD57+	-	-	0.42	0.02	-	-	-	-
Switched memory B cell	-	-	0.39	0.03	-	-	-	-

Table 3.3: The correlation between cell sub-populations and chronological age. The table shows the correlation (Spearman) between chronological age, the percentage, and number of immune cell sub-populations in burn injured participants (n = 31) 6 months post injury and in healthy controls (n = 27).

3.2.2.4 Clinical parameters and immune ageing

The immune phenotyping data of the burn participants 6 months post injury was compared to several clinically relevant clinical parameters to look for any significant relationship. The variables included body mass index (BMI), the participant's length of stay in hospital (LOS) and total burn surface area % (TBSA %). Additionally, the comparison was made to three relevant clinical scoring methods: rBaux, SOFA and APACHE II scoring systems. All cell types profiled were compared against all parameters.

Table 3.4 shows any relationships between cell type and clinical markers showing a significant positive (highlighted in green) or negative (highlighted in orange) relationship are included in the table. Relationships nearing significance are highlighted in grey. Any cell types not shown in the table showed no significant relationships with any clinical markers.

CD4+ naïve T cells, CD4+ central memory T cells, CD4+ RTE, CD4+ total memory, exhausted CD4+ T cells, CD4+ EMRA and CD4+ senescent T cells all showed no significant relationship with any of the clinical parameters examined. Exhausted CD8+ T cells, as well as CD8+ EMRA T cells also showed no relationship with any parameter. This was also true for regulatory T cells as well as naïve and central memory B cells. CD4+ effector memory T cell percentage showed a strong negative correlation with APACHE II ($R = -0.41$, $p = 0.033$) and a positive correlation with BMI ($R = 0.36$, $p = 0.048$).

There was no significant relationship between naïve CD8+ T cell percentage and any parameter other than rBaux score, which showed a significant moderate negative correlation ($R = -0.36$, $p = 0.046$). CD8+ central memory T cell percentage showed a significant, strong, negative relationship with BMI ($R = -0.47$, $p = 0.0084$) and there was a significant strong correlation between CD8+ effector memory cell percentage rBaux score ($R = 0.51$, $p = 0.0038$). rBaux also showed a significant moderate positive correlation with CD8+ total memory T cell frequency ($R = 0.36$, $p = 0.046$). rBaux score again had a significant moderate positive correlation with senescent CD8+ T cell percentage ($R= 0.29$, $p = 0.028$).

APACHE II score showed a strong negative correlation with NK cell percentage (R = 0.4, p = 0.038), as did BMI (R = 0.39, p = 0.029) and SOFA score was approaching significance (R = -0.32, p = 0.089). BMI also showed a positive correlation with the CD56 dim NK percentage (R = 0.4, p = 0.024). No other parameters had a significant relationship to NK cell percentage in the burn group.

Regulatory B cells cell percentage showed a positive correlation with every parameter which could be used to quantify injury severity (Table 3.4). TBSA % showed a strong and significant correlation (R = 0.5, p = 0.004) and a significant positive correlation was observed with LOS (R = 0.48, p = 0.0059), rBaux (R = 0.46, p = 0.0098), APACHE II (R = 0.42, p = 0.031) and SOFA (R = 0.46, p = 0.011) scores (Table 3.4).

When investigating the impact clinical parameters had on cell counts as opposed to percentages the results were slightly different, only BMI and rBaux showed any significant impact (Table 3.4). rBaux showed a significant positive relationship with Tregs (R = 0.37, p = 0.043) as well as CD57+ CD4+ (R = 0.36, p = 0.049) and CD57+ CD8+ (R = 0.41, p = 0.02), which may be related to the fact the rBaux scoring is weighted by chronological age. BMI only impacted NK cell count, showing a positive correlation with NK (R = 0.47, p = 0.01), NK CD56 dim (R = 0.45, p = 0.013) and senescent NK count (R = 0.5, p = 0.005).

		TBSA%		BMI		LOS		rBaux		APACHE II		SOFA	
Cell Percentage	**Cell population**	**R**	**p**	**R**	**p**	**R**	**p**	**R**	**p**	**R**	**p**	**R**	**p**
	CD3+ Lymphocytes	-	-	-	-	0.32	0.078	-	-	-	-	-	-
	CD4+ Effector memory	-	-	0.36	0.048	-	-	-	-	-0.41	0.033	-	-
	CD8+ Naïve	-	-	-	-	-	-	-0.36	0.046	-	-	-	-
	CD8+ Central memory	-	-	-0.47	0.008	-	-	-	-	-	-	-	-
	CD8+ Effector memory	-	-	-	-	-	-	0.51	0.004	-	-	-	-
	CD8+ Total memory	-	-	-	-	-	-	0.36	0.046	-	-	-	-
	CD8+ Senescent	-	-	-	-	-	-	0.39	0.028	-	-	-	-
	NK	-	-	0.39	0.029	-	-	-	-	-0.4	0.038	-0.32	0.089
	NK CD56 Dim	-	-	0.4	0.024	-	-	-	-	-	-	-	-
	NK Senescent	-	-	-	-	-	-	0.33	0.069	-	-	-	-
	B Switched memory	-	-	-	-	-	-	-	-	-0.46	0.033	-	-
	B Regulatory	0.5	0.004	-	-	0.48	0.006	0.46	0.01	0.42	0.031	0.46	0.011
		TBSA%		**BMI**		**LOS**		**rBaux**		**APACHE II**		**SOFA**	
Cell Number	**Cell population**	**R**	**p**	**R**	**p**	**R**	**p**	**R**	**p**	**R**	**p**	**R**	**p**
	CD4+ Naïve	-	-	-	-	0.32	0.089	-	-	0.42	0.061	0.35	0.065
	CD4+ CD57+	-	-	-	-	-	-	0.36	0.049	-	-	-	-
	CD8+ Effector memory	-	-	-	-	-	-	0.34	0.064	-	-	-	-
	CD8+ Senescent	-	-	-	-	-	-	0.34	0.065	-	-	-	-
	CD8+ CD57+	-	-	-	-	-	-	0.41	0.02	-	-	-	-
	TREG	0.31	0.095	-	-	-	-	0.37	0.043	-	-	-	-
	NK	-	-	0.47	0.01	-	-	-	-	-	-	-	-
	NK CD56 Dim	-	-	0.45	0.013	-	-	-	-	-	-	-	-
	NK Senescent	-	-	0.5	0.005	-	-	-	-	-	-	-	-

Table 3.4: The correlation between cell sub-population number, percentage, and chronological age. The table shows the correlation (Spearman) between clinical parameters and the percentage, and number of immune cell sub-populations in burn injured participants (n = 31) 6 months post injury. Positive correlations are highlighted in green, negative correlations are highlighted in red. Those which were only approaching significance are highlighted in grey.

3.2.2.5 IMM-AGE immune ageing

The IMM-AGE score is a scoring system which plots the trajectory of the immune systems of individuals, with mortality as the outcome (Alpert et al., 2019). Here a modified version of this algorithm was used to generate a modified IMM-AGE score using just 8 immune cell subtypes (Foster et al., 2022). These included total T cells, effector memory CD4+ T cells, effector memory CD8+ T cells, CD57+ effector memory CD8+ T cells, regulatory T cells, CD28- CD8+ T cells and naïve CD4+ T cells. The samples analysed are scored from 0 to 1 with 0 being the "youngest" and 1 being the "oldest" for immune age.

Figure 3.7A shows the immune trajectory of the participants separated by group, there is a clear separation between the two groups with minimal overlapping indicating a high degree of difference in the immune profiles of the control and burn participants. Figure 3.7B shows the immune trajectory of the participants coloured by participant age. There is no clear direction to the immune trajectory with relation to age, this is further analysed in Figure 3.7C., which shows there is no clear correlation between IMM-AGE and chronological age in either group. This is contrary to what was found in the original publication (Foster et al., 2022), where IMM-AGE score would be expected to increase with chronological age. However, there was a significant difference between the IMM-AGE scores of the two groups (Figure 3.7D, $p = 1.8e\text{-}13$, Wilcoxon). This result however should be taken with caution, as the lack of any relationship between IMM-AGE score and chronological age in either group suggests that this reduced panel of cell markers may not be sufficient to accurately assess immune age in this cohort.

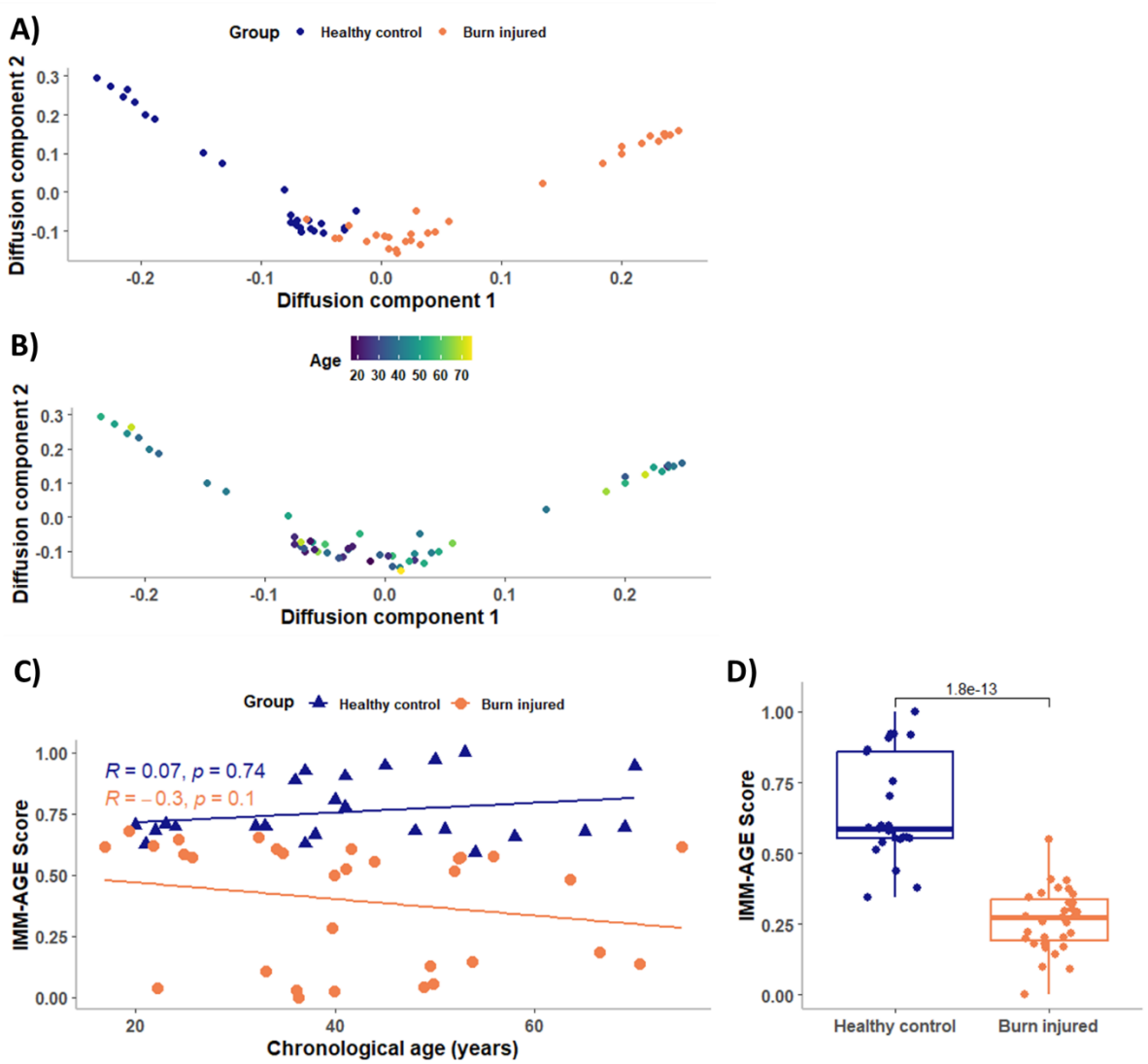


Figure 3.7: IMM-AGE analysis of healthy control and long-term burn-injured participants. The figure shows IMM-AGE analysis performed on burn-injured participants (n = 31) 6 months post injury compared to a healthy control group (n = 27). **A** shows the trajectory of IMM-AGE scores based on the participants group. **B** shows the same data coloured for the age of the participant. **C** shows the correlation between IMM-AGE score and chronological age (Spearman). **D** is a comparison of the IMM-AGE scores generated for each group (Wilcoxon). For each box plot each point is one participant. The central line is median, the bottom line is the 1st quartile (Q1), the upper the 3rd quartile (Q3). The whiskers represent calculated minimum and maximum values using the interquartile range (IQR). Whiskers are calculated using the formula Q1 + 1.5 x IQR or Q3 + 1.5 x IQR.

3.3 Discussion

3.3.1 Absolute telomere length

Telomere attrition is a hallmark of ageing (Lopez-Otin et al., 2013), premature telomere attrition is correlated with poor health outcomes such as disease and increased mortality risk (Schneider et al., 2022) and is present in multiple diseases and conditions with an accelerated ageing phenotype including Down syndrome, PTSD and schizophrenia (Jenkins et al., 2006; Polho et al., 2015; Roberts et al., 2017). In this study there was no difference in the telomere length of PBMCs between the control and burn injury group at admission or after 6 months from injury. Paired longitudinal analysis in the same patient between admission and 6 months also showed no shortening of telomeres.

The evidence surrounding the impact of physical injury on telomere length is limited. A mild traumatic brain injury model of concussion has been shown to reduce telomere length in a rats (Hehar and Mychasiuk, 2016), something which was also predictive of their behavioural performance pre and post injury. In humans the literature is even more limited. A study by Monroe *et al* investigated the effect chronic spinal cord injury had on telomere length in 278 patients. However, they found no effect of injury (Monroe et al., 2019), with only some clinical characteristics such as the most severely injured or wheelchair users edging towards significance. However, a lack of data from a non-injured control group somewhat diminishes the scope of that study. There is so far no research examining the long-term relationship between thermal injury and telomere length in an adult population.

The only work citing telomere length in relation to burn injury at the time of writing is a paper by Gürünlüoğlu et al., 2019. This study observed longer leukocyte telomeres in their burn groups compared to their controls, although this study was not long term, and focussed on the effect of different wound dressings in children. This difference in design and objective makes their conclusions hard to apply to the results in this investigation and leaves a clear gap within the literature regarding the long-term impact burn injury has on telomere length in adults.

Within the critical care environment a negative relationship has been reported between telomere length and patient survival and acute respiratory distress syndrome (ARDS) severity in septic patients (S. Liu et al., 2020). Quantitative PCR is widely used within the literature to analyse telomere length, with the previously discussed Monroe et al., Gürünlüoğlu et al., and Liu et al,. all using this technique. The lack of meaningful correlations between telomere length and clinical markers of injury severity presented in this chapter may be reflective of a bias within the data as only participants who survived to 6 months post injury were included, excluding those who succumbed to their injuries.

Overall, the data from this thesis and the existing literature do not suggest an effect of injury upon telomere length.

3.3.1.1 The impact of ageing on absolute telomere length

Telomere length has been shown to shorten with age in multiple tissues, including PBMCs (Zglinicki et al., 2000). Therefore, the fact that there was a trend towards significance between chronological age and ATL in the control cohort but not in the burn cohort at day one or month six is interesting. Although there is a known negative correlation between telomere length and age, it is only described as weak to moderate due to the high levels of interpersonal variation (Azcona-Sanjulian, 2021; Müezzinler et al., 2013). This is due to the overwhelming impact lifestyle and heritability can have on telomere length (Kim et al., 2020; Shammas, 2011). This variability and the relatively small cohort assessed here may explain why there was no significant correlation between ATL and age within this cohort.

Of the three groups examined, the burn samples taken at admission had the weakest and least significant relationship with chronological age of any group. This suggests that on admission to hospital the activated immune response and altered cell type (significant neutrophil and monocyte numbers and lymphocytopenia) following injury may have a disruptive effect on ATL. This change in cell populations being in part responsible for changes in telomere length has been reported by others (Mazidi et al., 2017), with notably a positive relationship between telomere length and basophil ratio,

and a negative relationship between telomere length and monocyte count and red cell distribution width. Zribi et al., 2019 showed that telomere length was negatively correlated with WBC count. Despite a large increase in WBC count in burns patients, controls having a mean WBC count 6.07 [10^9/L] compared to 21.97 [10^9/L] in SIFTI participants at admission (Figure A.3.1), a significant relationship between telomere length and WBC count was not observed in our investigation.

3.3.1.2 The impact of BMI on absolute telomere length

BMI had a larger effect on telomere length than chronological age, within the injured cohort. BMI has previously been shown to have a negative impact on telomere length, with an increased BMI having a negative correlation with telomere length (Kim et al., 2009). It is unclear why there is only a significant correlation between ATL and BMI at admission and in no other group. One hypothesis is that BMI, which as well as being a biomarker for obesity, which influences telomere length (Weisell, 2002), is also considered to be an intermediate health indicator (Contoyannis and Jones, 2004). The greater BMI of the burn injured participants compared to the control group may be related to poorer general health pre-injury, which in turn could negatively influence telomere length (Njajou et al., 2009), therefore resulting in less scope for shortening post injury.

3.3.1.3 The impact of Injury severity on absolute telomere length

To date, there have been no studies investigating the link between burn injury and telomere length. There have also been no investigations looking at the relationship between hospital LOS, SOFA, APACHE II score and telomere length in any injury group. These data therefore represent a novel preliminary look into the impact traumatic injury has on telomere length.

Interestingly there was no relationship between LOS and ATL at 6 months. Physical activity has been shown to have a protective effect on telomere length, with a meta-analysis of 11 studies of 19,292 participants showing physical activity had a positive correlation with telomere length (Lin et al., 2019). The patients with longer LOS will have been severely reduced in the amount of physical activity they

were able to perform, both due to their injuries and the hospital environment. Despite this inactivity, there was no observable impact on telomere length (Figure 3.1). The mean LOS was 53 days for the SIFTI participants (Figure 3.5). 20 of the burn injured participants were in hospital for 45 days or less, with 12 exceeding a 50-day LOS. This may mean that a telomere modulating effect may only be present in more long-stay patients which were not adequately represented in this study.

The ICU scoring methods, SOFA and APACHE II likewise had no predictive power when it came to telomere length. One reason that the clinical markers investigated here do not seem to have an impact on telomere length may be the time frames that were examined. To look for evidence of accelerated ageing one would ideally examine participants before they were injured and after to monitor the effects. As it is not logistically possible to collect samples for a huge population and wait for some to become injured, or ethically imaginable to, collect samples and then injure participants, we are left to analyse samples taken only post injury or compare to a separate uninjured cohort. Samples taken at admission were considered to be a potential baseline, although the speed at which telomeres can become shortened following insult is not yet understood, so a non-injured control cohort was also included.

3.3.1.4 Does injury impact absolute telomere length

These findings suggest that burn injury was not sufficient to cause a significant change in absolute telomere length in PBMCs in this study. It is worth noting however that the mean telomere length in the burns patients at day one was lower than the controls and appeared longer at month six. This may suggest that patients had recovered from this six-months post injury, likely because the blood cell type changes immediately post-injury had resolved. Other studies have reported a significant shortening of telomere length following ICU admission (Zribi et al., 2019). Zribi and co-workers were interested in the short-term changes in telomere length, investigating 41 patients within 72 hours of admission and 1-2 weeks post admission. They observed significant telomere shortening in some of their patients. This suggests that telomere shortening is possible within the hospital environment. However,

our study aimed to look at the long-term impacts, as any persisting changes are likely to be representative of changes to the ageing phenotype, as opposed to some kind of injury response. This supports the hypothesis stated above that telomere shortening may be occurring, but that it is likely resolved 6 months post injury.

This telomere data measured at admission and 6 months post injury, combined with what is known in the literature suggests that burn injury does not have a long-term impact on the telomere length of burn injured participants.

3.3.2 Immune ageing

3.3.2.1 Immune differences between non-burned individuals and long-term burn-injured individuals

3.3.2.1.1 Primary T cell groups

T cell sub-populations change during the ageing process, with decreasing naïve populations and increasing memory populations, this study asked whether burn injury could cause some of these changes to occur.

During the ageing process thymic output decreases reducing the numbers of recent thymic emigrants (RTE), this also leads to the gradual reduction in naïve populations (Goronzy and Weyand, 2019) and increasing representation of memory subsets, something observed within this study. Thymic involution has been shown to occur in the critical care environment, whether as a result of physical injury, such as traumatic brain injury (TBI) (Ritzel et al., 2018) or as a result of infection, a not uncommon occurrence in any burns cohort, accelerating natural atrophy which occurs with age (Duah et al., 2021; Luo et al., 2021). Reduced thymic output has been observed in critically ill patients, who have a lower number of PTK7+ T cells compared with controls (Duggal et al., 2018c), thymic atrophy and reduced thymic output has also been shown in conditions such as sepsis, in cohorts ranging from neonatal to adult and in other species such as mice (Basu et al., 2012; Ito et al., 2021; Sommer et al.,

2020), suggesting that hyperinflammatory conditions in critical illness have a negative impact on thymic function. As burn injury is considered a pro/hyperinflammatory injury, it is not surprising to see that there is a significant reduction in naïve and RTE sub-populations.

Unlike the CD4+ population there was a significant difference in the CD8+ total T cell percentage when comparing the SIFTI and control group as well as a difference in some of the sub-populations, namely central and effector memory T cells. Additionally, there was a lower percentage of CD4+ and CD8+ EMRA cell in the burn group compared with the healthy controls which was unexpected after the decline in naïve T cells. This may be explained by the increased percentages of effector and central memory populations, effectively reducing the proportion of the EMRA cells in the total T cell population. As EMRA are effectively the final stage of T cell development it may be that after 6 months the central memory and effector memory T cells had not yet progressed through to the EMRA stage.

These findings support what has been reported within the literature where insults such PTSD, an age accelerating condition, have been shown to reduce naïve T cell populations and increase memory cell populations when compared with healthy controls (Sommershof et al., 2009). This has also been observed within paediatric trauma patients, where CD4+ central memory populations have been shown to be increased in the long term and other sub-populations have been altered compared to controls (Johnson et al., 2020).

3.3.2.1.2 Senescent T cell groups

Given that burn injury appears to have no effect on telomere length and EMRA T cells, which are thought to contain the senescent cells, declined it is perhaps unsurprising that there was no significant difference in the percentage of senescent CD4+ or CD8+ T cells between the groups. Other studies have shown that chronic inflammatory diseases can increase the proportion of senescent T cell sub-types (González-Osuna et al., 2022) despite the pro-inflammatory nature of burn injury (Mulder et al., 2021), this does not appear to be the case within this patient cohort.

This suggests that although burn injury is causing signs of immune ageing it is not doing it via an increase in the senescent cell populations and instead the effect may be focussed on the reduction in naïve T cells. This is plausible as the hyperinflammatory state of burn patients, which persists for at least a year, would be a negative influence on thymic output (Gruver and Sempowski, 2008). One other possibility is that the circulating NK cells are functionally active and are clearing out the senescent T cell population, a well characterised NK cell function (Antonangeli et al., 2019).

3.3.2.1.3 B cell sub-groups

The hypothesis that burn-injury may cause immune ageing is supported by the lower percentage of naïve B cells seen in the burn group, as this reduction in naïve B cells during ageing has been reported previously (Duggal et al., 2013). The B cell specific decline in naïve cells is attributed to the reduced numbers of hematopoietic stem cells seen in the elderly, as well as reduced effectiveness of IL-7 producing stromal cells within the bone marrow and reduced sensitivity of pro-B cells, blunting B cell proliferation (Ma et al., 2019). The reduction in naïve B cell observed within the burn injured cohort is evidence of an age associated immune phenotype present following burn injury. It would be interesting to measure IL-7 levels in this cohort to determine possible mechanisms involved.

Interestingly, there was also a lower percentage of the unswitched memory B cells compared to control, a change which has been now described as occurring during the ageing, although there is some contradictory evidence regarding the age-associated increase in memory B cell percentage (Ademokun et al., 2010b). This reduced percentage of two primary B cell subsets is accompanied by a much higher percentage of regulatory B cells observed in the burn group compared to the controls. B regs have immuno-suppressive and inflammation-inhibiting effects (Bueno et al., 2016), it therefore follows that they may remain elevated following an injury with a chronic proinflammatory pathology such as a burn (Mulder et al., 2021) to try to combat the systemic inflammation, although how effectively they are able to do so within this burn cohort is not known. Going forward we could measure IL-10 levels to at least see if this theory may be correct.

This observation again shows evidence of long-term immune remodelling following burn injury, even if these changes are not completely aligned with age-related effects.

3.3.2.1.4 Regulatory T cells and NK cells

Regulatory T cells or Tregs, like Bregs also have an immune modulatory phenotype. Tregs function by restraining the inflammatory response by reducing T cell proliferation and cytokine production and play a vital role in regulating immune tolerance and autoimmunity (Luo and Li, 2013). There was an increase in the Treg percentage in the burn group which was approaching significance (Figure 3.15B, $p = 0.051$). Other literature has shown the acute activation of CD4+ regulatory T cells in patients with traumatic injury (Sturm et al., 2020; Yamakawa et al., 2021) owing to their role in regulating inflammation via the upregulation of immunosuppressive molecules (IL-10) and other anti-inflammatory mediators (van der Veeken et al., 2016). It may be that given a larger sample size, significance may have been reached. There was also no significant difference in NK or NK sub-population percentages between group. NK function has been shown to be reduced in humans following surgical trauma (Müller-Heck et al., 2021), with some literature reporting an increase in the number of NK cells present within burn injured skin up to 3 weeks post injury (Mulder et al., 2022), despite this there is little long-term data regarding circulating NK cell number following burn injury. This again is further evidence of immune remodelling, perhaps to combat the long-term inflammation present following burn injury which mirrors the chronic low-grade inflammation present with ageing, dubbed, Inflammaging.

3.3.2.1.5 Chronological age associated changes in cell populations

Chronological age showed a relationship with multiple changes in cell composition. Naïve T cell populations declined with age in the burn and control groups, and memory T cell sub-populations also changed (Figure 3.2, 3.3). Similar changes are widely observed within the ageing population and have

been discussed in the introduction. Interestingly the age-associated memory sub type remodelling was only observed within the burn cohort. While there was no observed difference in the senescent cell percentages between the control and burn injured groups (Figure 3.4), the senescent CD8+ T cell percentage showed a strong positive correlation with chronological age, nearing significance ($p = 0.055$). This suggest that in this population the ageing trajectory was present in both cohorts but not accelerated by injury.

3.3.2.2 Does injury severity or biological age impact immune phenotype

3.3.2.2.1 BMI, length of stay and immune phenotype

BMI is regularly used as a substitute measure of adiposity and is considered a marker for obesity (Weisell, 2002). Adiposity, has been shown to mimic many aspects of the ageing process, including driving low grade systemic inflammation and reduced nutrient sensing (Karczewski et al., 2018). High BMI and increased adiposity have also been shown to negatively affect the innate and adaptive immune response in a similar way to ageing (Frasca et al., 2017). There are multiple immune characteristics found in both an aged and obese individuals' immune systems, such as a reduced vaccination response (Milner and Beck, 2012), reduced thymic output and naïve T cells (Yang et al., 2009) and a greater proportion of memory T cells (Mauro et al., 2017; Misumi et al., 2019).

It is unsurprising then that BMI, like chronological age, has been shown to be predictive of patient outcomes following critical care (Schetz et al., 2019), as was highlighted during the COVID-19 pandemic (Sanchis-Gomar et al., 2020). Increased adiposity, as measured via BMI, can therefore be seen as accelerating ageing (Salvestrini et al., 2019). The observation that BMI correlates with some although not all the cell type changes seen with chronological age, including effector memory, central memory, and NK cell percentage, supports this suggestion.

3.3.2.2.2 Injury severity scoring and immune phenotype

It is interesting for example that CD8+ naïve T cell percentage in the burn group showed no significant relationship to chronological age, or any clinical parameter other than rBaux score. The rBaux score, as discussed above, considers, age, TBSA % and any inhalation injury sustained. This was surprising as we had predicted that injury would compound naïve T cell reduction in line with the degree of severity. Such reductions have been observed in other studies, for example those looking at PTSD (Sommershof et al., 2009) and a short term study in mice, showing a 50% reduction in naïve CD4+ T cells 5 and 10 days post burn injury (Patenaude et al., 2005).

In contrast, the proportion of CD8 effector and central memory T cells showed an increase with an increasing rBaux score. This relative increase in memory cell subtypes following stress was also reported by Sommershof et al., 2009 in their PTSD investigation.

Exhausted CD4+ T cells and to some extent senescent NK cells both showed a positive relationship with rBaux score. i.e., cell numbers increased with greater clinical score of severity. However, both cell types showed no relationship with any other clinical marker of injury severity suggesting that this positive relationship may be due to age as rBaux is heavily weighted by chronological age. The same is also true of senescent CD8 cells.

NK cells and NK cell sub-population percentages appeared to be correlated with the APACHE II, SOFA and rBaux scoring systems. The total NK percentage in the burn injured group showed a negative correlation with the APACHE II scoring system, while senescent and exhausted NK cells showed a positive correlation, suggesting that while numbers reduced as APACHE II score increased, the cells that remained were more senescent and exhausted (Table 3.4). The relationship between NK cells and APACHE II score have been studied in other patient populations before. Within elderly patients, NK cell count has been shown to be more predictive of sepsis-associated delirium than APACHE II scoring or lymphocyte counts (Li et al., 2020), suggesting that NK cell numbers perhaps provide a better perspective on patient outcomes and potentially insult severity than some current scoring systems.

NK cell numbers have also been reported to increase with age (Gounder et al., 2018), as has the proportion of senescent NK cells (Przemska-Kosicka et al., 2018). The findings of the investigation presented in this chapter show an age-associated increase in NK cells in burn patients, although non-significant ($r = 0.32$, $p = 0.078$), increasing injury severity as measured by APACHE II score however seems to show the opposite finding. This suggests that injury severity is not impacting immune ageing as observed within the NK cell population. Within the exhausted and senescent populations, which as discussed increase with age, APACHE II and rBaux do suggest that there is a relationship between injury severity and senescent NK cell percentages, which is a sign of immune ageing.

It is important to remember however that the rBaux scoring system includes the patients age, which is obviously a contributing factor to immune senescence (Aiello et al., 2019; Lam et al., 2021). The APACHE II score also showed a negative correlation with CD4+ effector memory (EM) populations. This is surprising given that the CD4+ EM population was elevated in the burn cohort compared with the control group. This suggests that the APACHE II injury score, while being predictive of mortality, does not offer any predictive power with regards to CD4+ T cell immunosenescence.

All measures of injury severity (TBSA %, LOS, rBaux, APACHE II and SOFA score) showed a strong positive correlation with regulatory B cell numbers. This again is likely due to the inflammation regulating role they play within the immune system and the acute and chronic inflammatory pathology of burn injury (Mulder et al., 2021). Regulatory B cell number and function has been shown to decline with age (Niharika A Duggal et al., 2013), a decline which can be ameliorated by positive lifestyle factors such as high levels of physical activity (Duggal et al., 2018a).

The data presented in this chapter then suggests that within the B cell population that injury is causing long term re-modelling, but that this is not necessarily evidence of immune ageing.

3.3.2.3 IMM-AGE immune age scoring

The reduced IMM-AGE panel of 8 markers as opposed to 71 (Alpert et al., 2019), may be insufficient to accurately detect immune age in this cohort given the findings presented here. The IMM-AGE score of the burn group appeared to be lower than that of the control group. This may be due to the fact that immune cells often associated with immune ageing which were used in the age estimation, such as CD57+ CD8+ T cells were slightly higher in the control group, despite there being no significant difference in senescent T cell percentage. Another Issue raised by these results is a lack of relationship between chronological age and IMM-AGE score, as an increased age would be expected to correlate with in increased IMM-AGE score in any valid measure of an ageing biomarker. It may be suggested that an expanded panel be used for future analysis to increase the likelihood of a successful IMM-AGE calculation.

3.3.2.3.1 Does burn injury cause immune ageing

It has been reported in the literature that burn injury causes long term remodelling of the immune system. Some of the changes to the immune system observed following burn injury are also seen during ageing such as diminished vaccine response and increased proportions of memory T cells (Johnson et al., 2020). It is also well established that there is a strong interaction between immune ageing and inflammation. The inflammation which occurs during ageing is a driver of immunosenescence, which then in turn further increases inflammation, resulting in inflammaging (Teissier et al., 2022). While not all classic signs of immune ageing are present in the data reported here, it is clear that there is a shift in the immune profiles of burn injured individuals, with a decreasing proportion of naïve cells and increasing proportions of memory cells. Burn injury appears to be inducing some, but not all features of an aged immune phenotype 6 months post injury, which is likely driven by the well described persistent, pro-inflammatory state in burn injured patients (Mulder et al.,

2021). This pro-inflammatory state and associated stress is likely to be key in driving the immune remodelling outlined in this investigation.

3.4 Conclusions

This study was novel with regards to considering the effect of traumatic burn injury on long-term telomere length and immune phenotype, revealing some features of an aged immune system and a potential anti-inflammatory response via raised Bregs. However, it was somewhat limited by patient sample availability, due to the relative rarity of burns patients, and the even greater difficulty of attaining samples from the same individuals 6 months post injury. It would therefore be desirable to have a more comprehensive and broader investigation before any definitive conclusions are drawn.

The modulation of the immune ageing phenotype, especially to reduce thymic atrophy, could be beneficial in burn patients. This has been demonstrated in recent clinical trials in which a cocktail of human growth hormone, metformin and DHEA which demonstrated reversing thymic atrophy and immunosenescence in a group of 51-65 year old adult men over a 12 month period (Fahy et al., 2019). The TRIIM trial showed that thymic involution and immunosenescent trends could be reversed. A promising option for improving patient outcomes following an injury such as burns.

3.5 Appendix

3.5.1 Absolute telomere length additional figures

The absolute telomere length of SIFTI burn participants and controls compared to their WBC count as measure by the SYSMEX NV whole blood profiler Figure S.1.1. The WBC count is only available for a sub-set of the total participants as the SYSMEX NV was not in use at the start of the first arm of the study (SIFTI participants, n = 24, control group, n = 14).

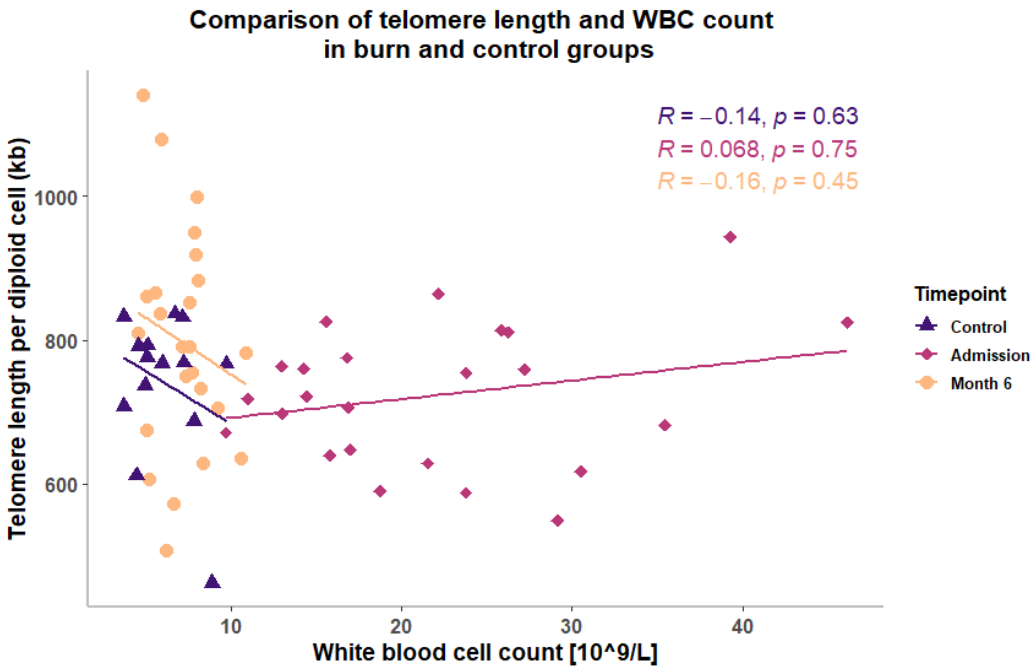


Figure A.3.1: Telomere length and white blood cell count - A scatter graph showing relationship between absolute telomere length and white blood cell count (WBC) in control burn injured participants following admission (n = 24), 6 months post injury (n = 24) and in healthy controls (n = 14). There was no significant relationship between telomere length and WBC and ATL in any group.

3.5.2 Immune phenotyping gating strategy

Shown below is the general gating strategy that was used for each panel. Section A of each figure shows the basic gating strategy, from lymphocyte selection to single cell selection followed by the cell subtype gating. Shown in Figure A.3.2, section A shows the T cell subset gating strategy from lymphocyte selection to single cell selection, to CD3+ T cell selection followed by CD4+ or CD8+ positive T cell selection (Figure A.3.2, A). Shown in section B is CD4+ and CD8+ subtype gating. CD4+ and CD8+ T cells are subcategorised as, naïve (CCR7+, CD45RA+), central memory (CCR7+, CD45RA-), effector memory (CCR7-, CD45RA-) effector memory re-expressing CD45RA (EMRA: CCR7-, CD45RA+) and recent thymic emigrants (RTE: CCR7+, CD45RA+, PTK7+).

Shown in Figure A.3.3, section A shows the T cell senescence gating strategy from lymphocyte selection to single cell selection, to CD3+ T cell selection followed by CD4+ or CD8+ positive T cell selection (Figure A.3.3, A). Shown in section B & C is CD4+ and CD8+ subtype gating. CD4+ and CD8+ T cells are subcategorised as senescent (CD57+, CD28-, Figure A.3.3, B) and exhausted (PD1+, Figure A.3.3, C).

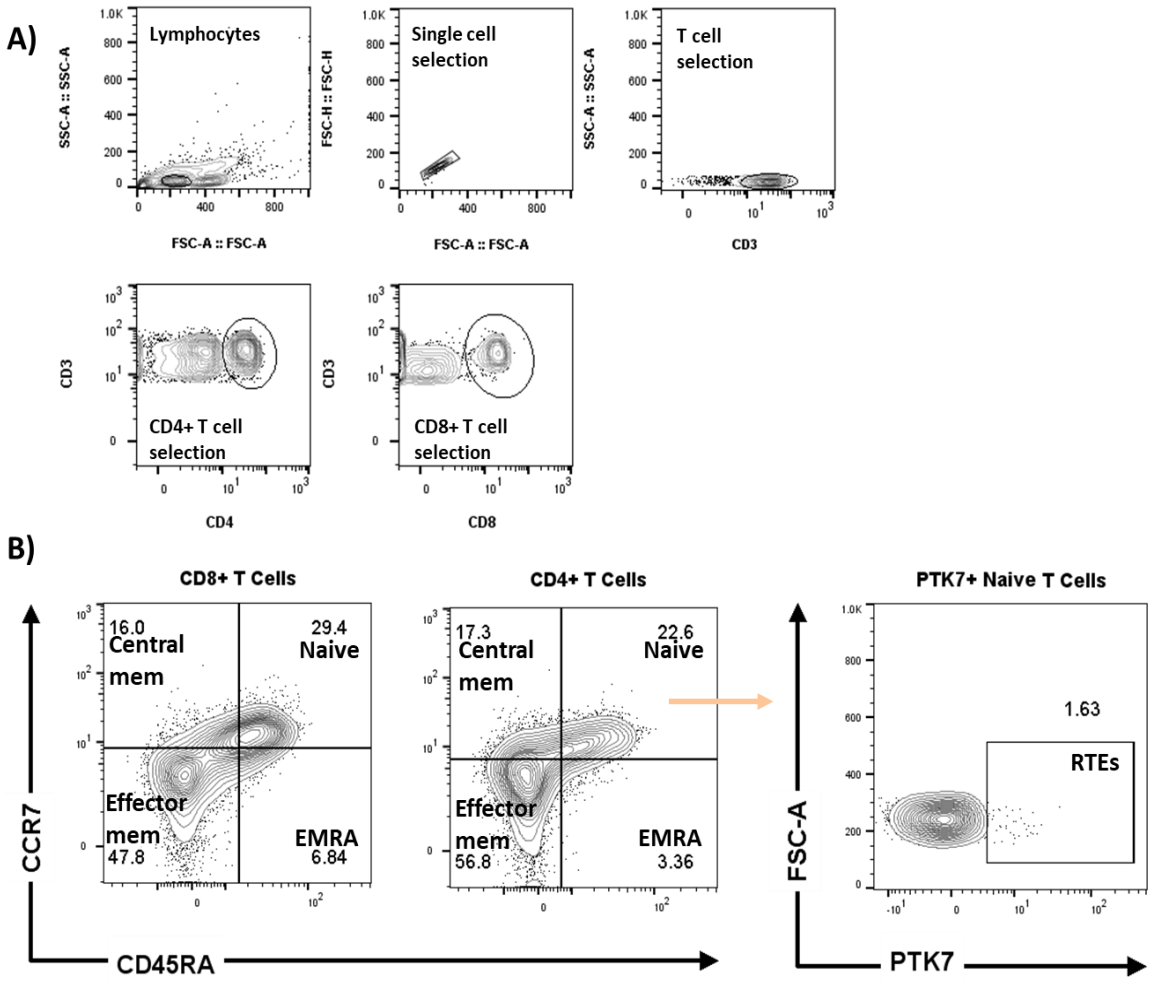


Figure A.3.2: T Cell subset gating strategy - The gating strategy used to phenotype the T cell subsets. **A** shows the basic gating strategy from lymphocyte selection, doublet exclusion and total T cell selection (CD3+) as well as the gating used to isolate CD4+ or CD8+ positive T cells. **B** shows how Naïve, central memory and effector memory CD4+ and CD8+ T cells were identified. Also shown in section B is how the recent thymic emigrant (RTE) cell subset (PTK7+) was gated from within the Naïve CD4+ cell population. Representative images shown are from a burn injured participant.

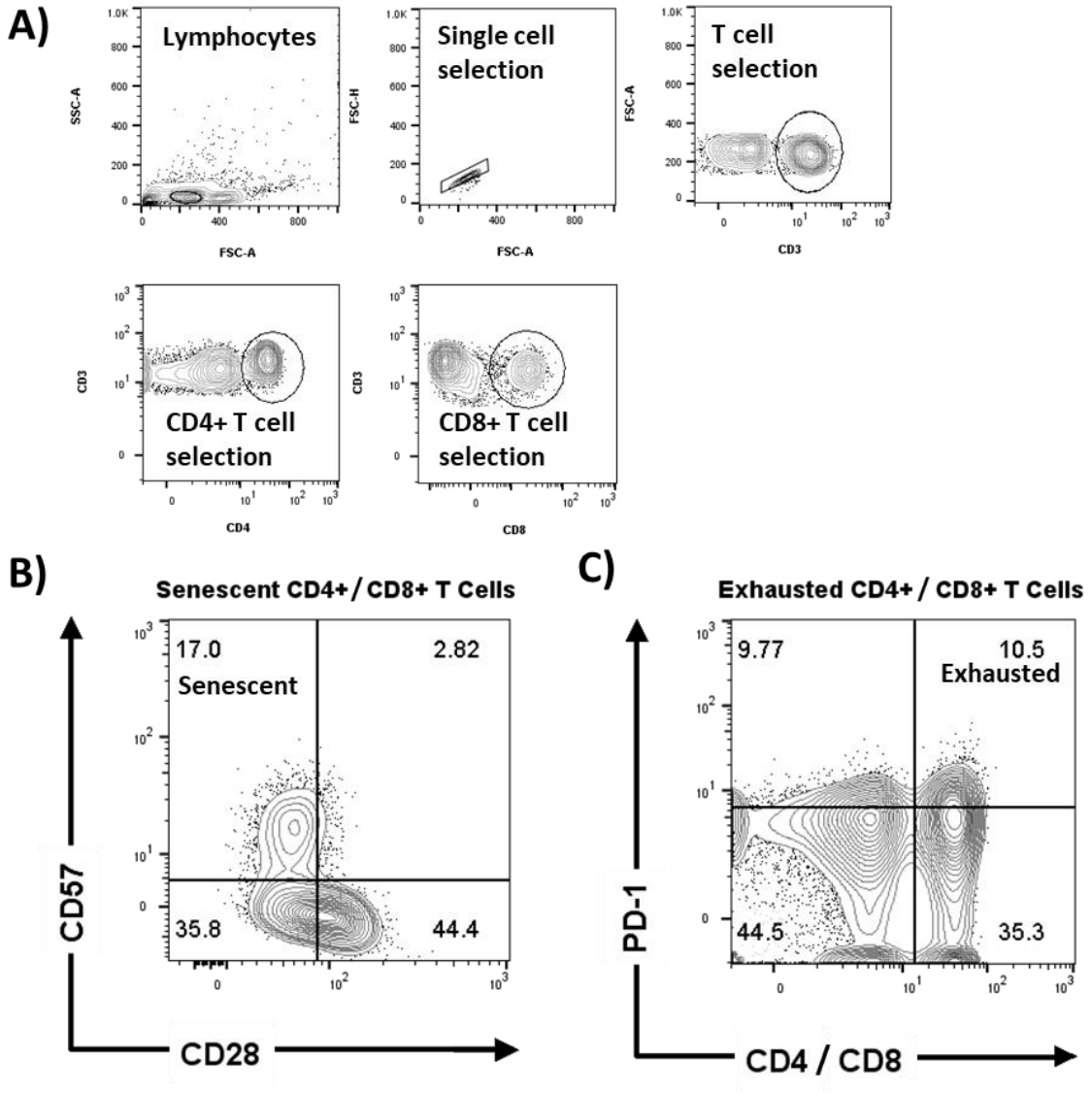


Figure A.3.3: T Cell senescence gating strategy - The gating strategy used to phenotype the senescent and exhausted T cell subsets. Section **A** shows the basic gating strategy from lymphocyte selection, doublet exclusion and total T cell selection (CD3+) as well as the gating used to isolate CD4+ or CD8+ positive T cells. Section **B** shows how the senescent (CD57+, CD28-) CD4+ and CD8+ T cells were identified. Section **C** shows how the Exhausted (PD-1+) CD4+ and CD8+ T cells were identified. Representative images shown are from a burn injured participant.

Shown in Figure A.3.4, section A shows the B cell gating strategy from lymphocyte selection to single cell selection, to B cell selection (CD19+) followed (Figure A.3.3, A). Shown in section B is the B cell subtype gating. B cells (CD19+) are further subcategorised as naive (CD19+, IgD+, CD27-), unswitched memory (IgD+, CD27+), switched memory (IgD-, CD27+) and regulatory B cells ($CD24^{Hi}$, $CD38^{Hi}$).

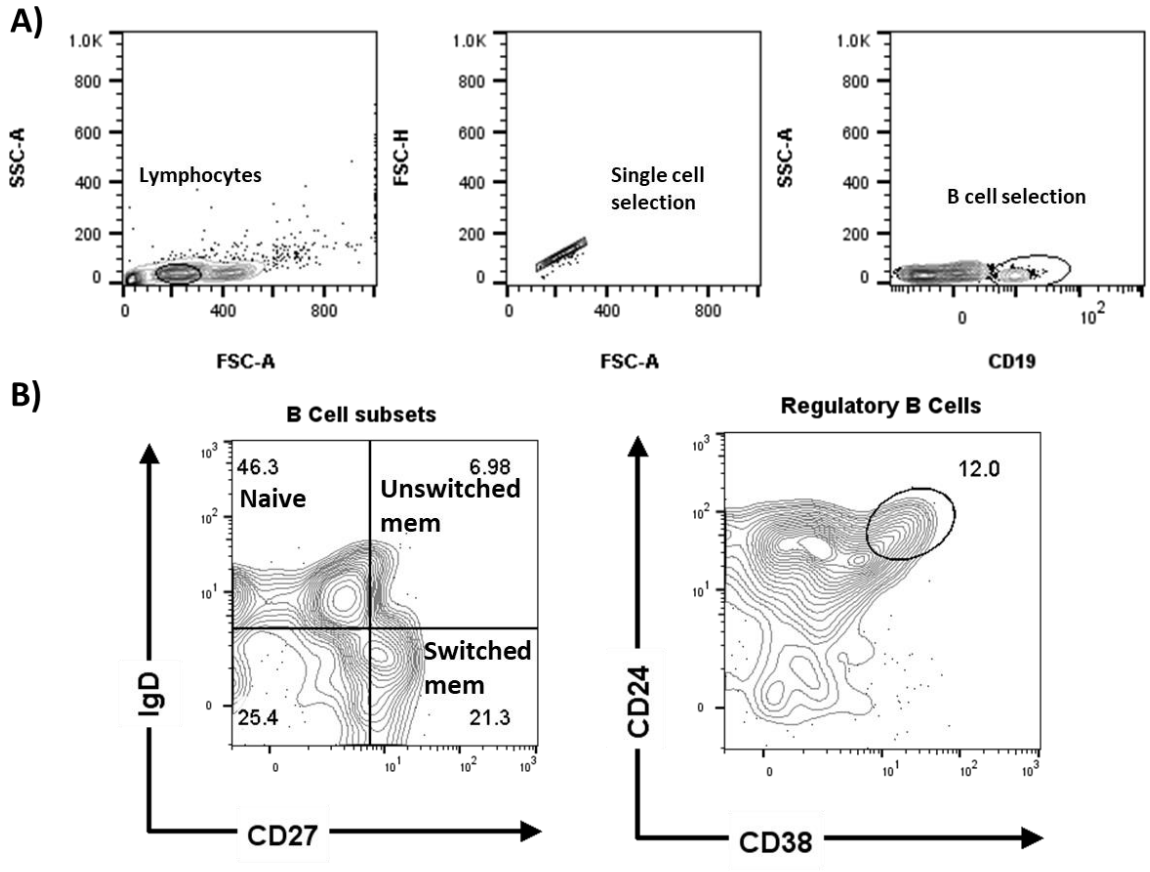


Figure A.3.4: B Cell subset gating strategy - The gating strategy used to phenotype the B cell subsets. Section **A** shows the basic gating strategy from lymphocyte selection, doublet exclusion and total **B** cell selection (CD19+). Section B shows how the naïve (CD19+, IgD+, CD27-), unswitched memory (Unswitched mem: CD19+, IgD+, CD27+) switched memory (Switched mem: CD19+ IgD-, CD27+), IgD- & CD27- B cells (CD19+, IgD-, CD27-) and regulatory B cells (CD19+, $CD24^{Hi}$, $CD38^{Hi}$) were identified. Representative images shown are from a burn injured participant.

Shown in Figure A.3.5, section A shows the NK cell gating strategy, from lymphocyte selection to single cell selection. Section B shows NK cell selection (CD3-, CD56+) and NK subtype gating. NK cells are subcategorised as NK dim (CD3+ $CD56^{Lo}$) and NK bright (CD3+ $CD56^{Hi}$), senescent NK Cells (CD3-, CD56+, CD57+).

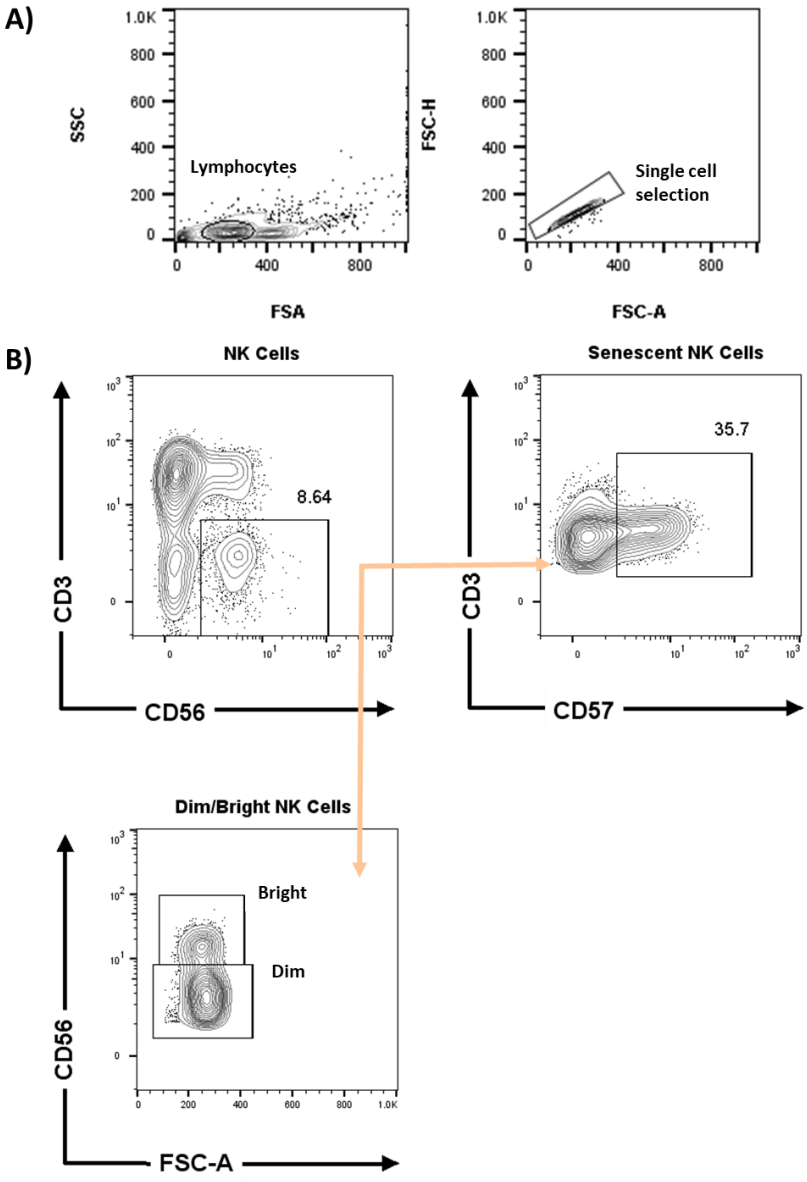


Figure A.3.5: NK Cell gating strategy - The gating strategy used to phenotype the NK cell subsets. Section **A** shows the basic gating strategy from lymphocyte selection, doublet exclusion. Section **B** shows NK cell selection (CD3-, CD56+), NK dim (CD3+ $CD56^{Lo}$) and NK bright (CD3+ $CD56^{Hi}$), senescent NK cells (CD3-, CD56+, CD57+). Representative images shown are from a burn injured participant.

Shown in Figure A.3.6, section A shows the regulatory T cell (Treg) gating strategy from lymphocyte selection, to CD4+ T cell selection. Section B shows Treg selection (CD4+, D25+, FoxP3+).

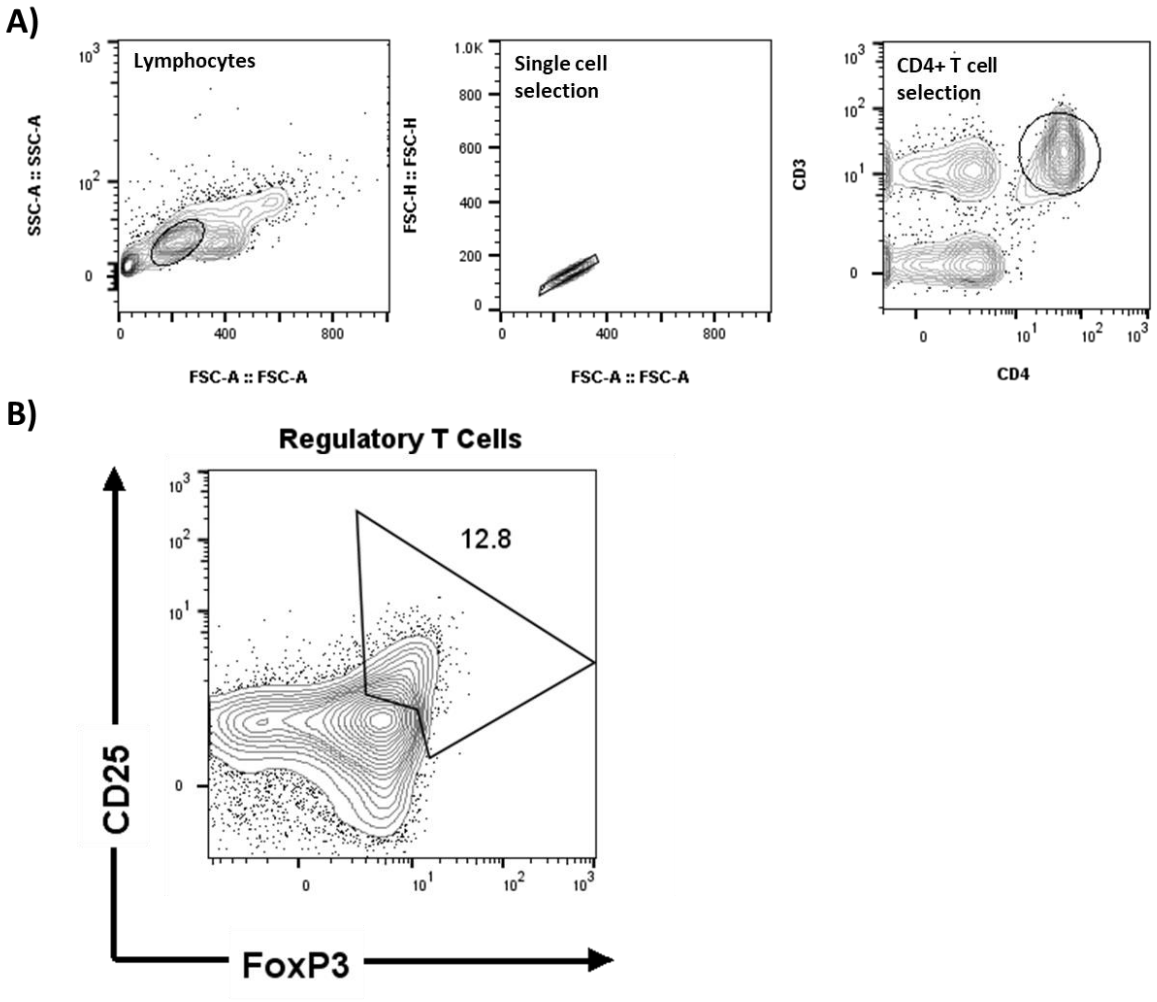


Figure A.3.6: Regulatory T cell gating strategy - The gating strategy used to phenotype regulatory T cells. Section **A** shows the basic gating strategy from lymphocyte selection, doublet exclusion and appropriate T Cell selection (CD3+, CD4+). Section **B** shows regulatory T cell selection (CD3+, CD4+, CD25+, FoxP3+). Representative images shown are from a burn injured participant.

3.5.3 Immune ageing cell counts

To avoid repetition of results, the cell counts for the month 6 and healthy control samples are listed here. Shown are the absolute counts for each cell sub-population for each group. The absolute number of lymphocytes present within the long-term burn injured participants was significantly greater than those present within the healthy control population. The burn injured group had a mean Lymphocyte count of 2.1 (10^9/L) compared to 1.5 (10^9/L) in the control group ($p = 0.001$, Wilcoxon).

With the exception of CD4+ cells, RTE T cells and Naïve T cells, all other CD4+ T cell subsets showed the same relationships with regards to the number of cells, as was observed when cells were examined as a percentage (Figure 3.2). While there were no significant differences in the percentage of T cells which were CD4+ (Figure 3.2), there was a significant difference in the numbers, with CD4+ T cell numbers being greater in the burn injured Cohort (Figure A.3.7, $p = 0.00024$, Wilcoxon). There were also no significant differences in the numbers of RTE T cells and naïve T cells between groups. The greater number of CD4+ T cells in the burn group, but no differences in the RTE and naïve CD4 sub-populations, explains the significantly lower percentage of RTE and naïve CD4+ T cells shown in Figure 3.2.

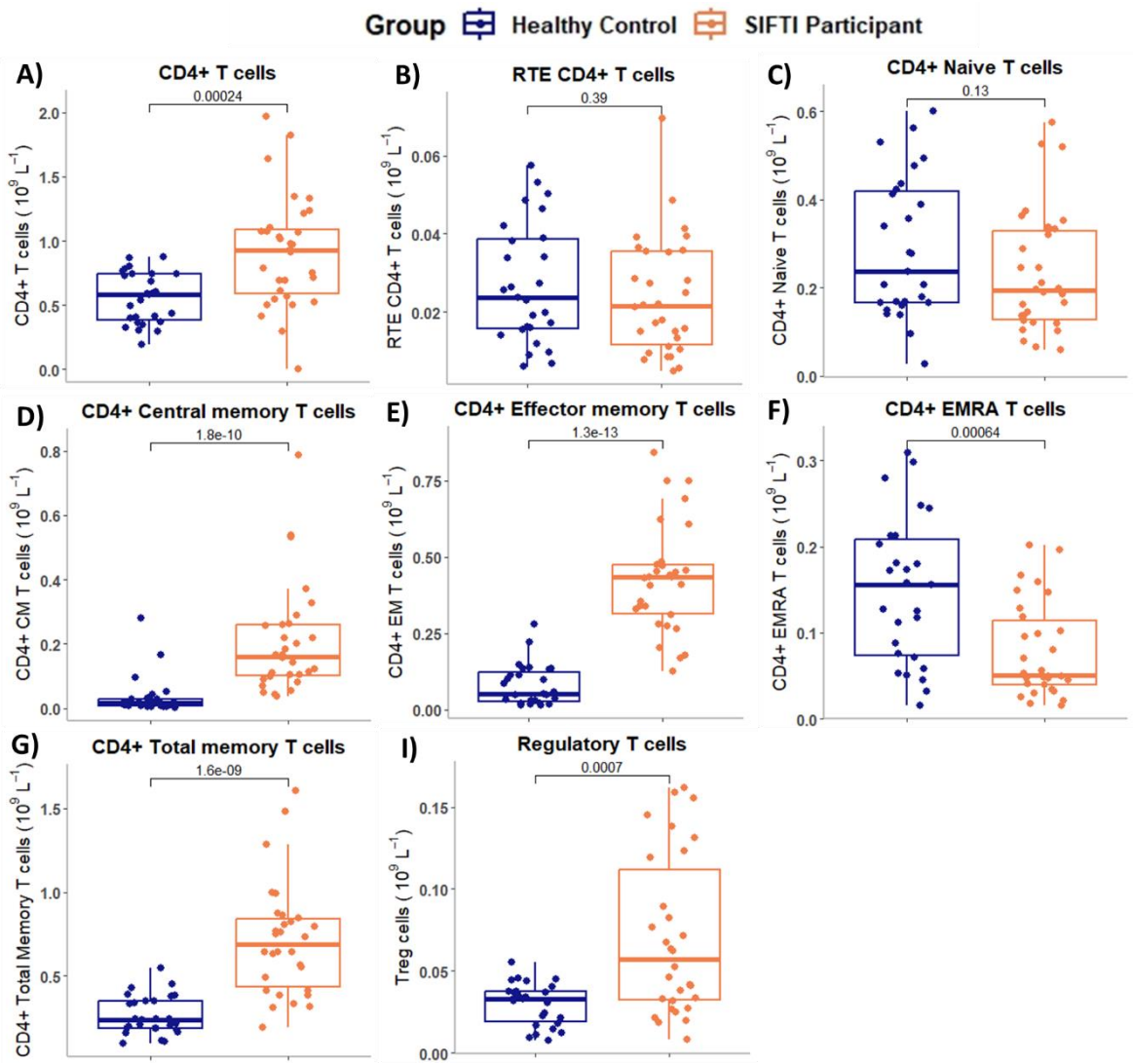


Figure A.3.7: Differences in CD4+ T cell subsets between long-term burn injured participants and healthy controls - Shown are the numbers of various CD4+ T cell subtypes in burn injured participants (n = 31) 6 months post injury compared to a healthy control group (n = 27) (Wilcoxon). Shown are the number of CD4+ T cells (**A**). Also shown are the number of recent thymic emigrants (RTEs) (**B**), naïve (**C**), central memory (**D**), effector memory (**E**), effector memory re-expressing CD45RA (**F**), total memory (**G**) T cells and regulatory T cells (Treg) (**H**). For each box plot each point is one participant. The central line is median, the bottom line is the 1st quartile (Q1), the upper the 3rd quartile (Q3). The whiskers represent calculated minimum and maximum values using the interquartile range (IQR). Whiskers are calculated using the formula Q1 + 1.5 x IQR or Q3 + 1.5 x IQR.

The numbers of CD8+ T cells and cell subsets shown in Figure A.3.8 show the same trends as when the cells were represented as percentages (Figure 3.3) with the exception of the total CD8+ T cells (Figure A.3.8, A). There was no significant difference in the total number of CD8+ T cells (Figure A.3.8, p = 0.99, Wilcoxon) however there was a significant difference in the percentage of T cells which were CD8+ (Figure 3.3). This can likely be explained by the lower total number of lymphocytes present within the control group, making a greater proportion of a smaller total number (CD8+ as a percentage of total T cells in the control group) the same as a smaller percentage of a greater number (CD8+ of total T cells in the burn injured group).

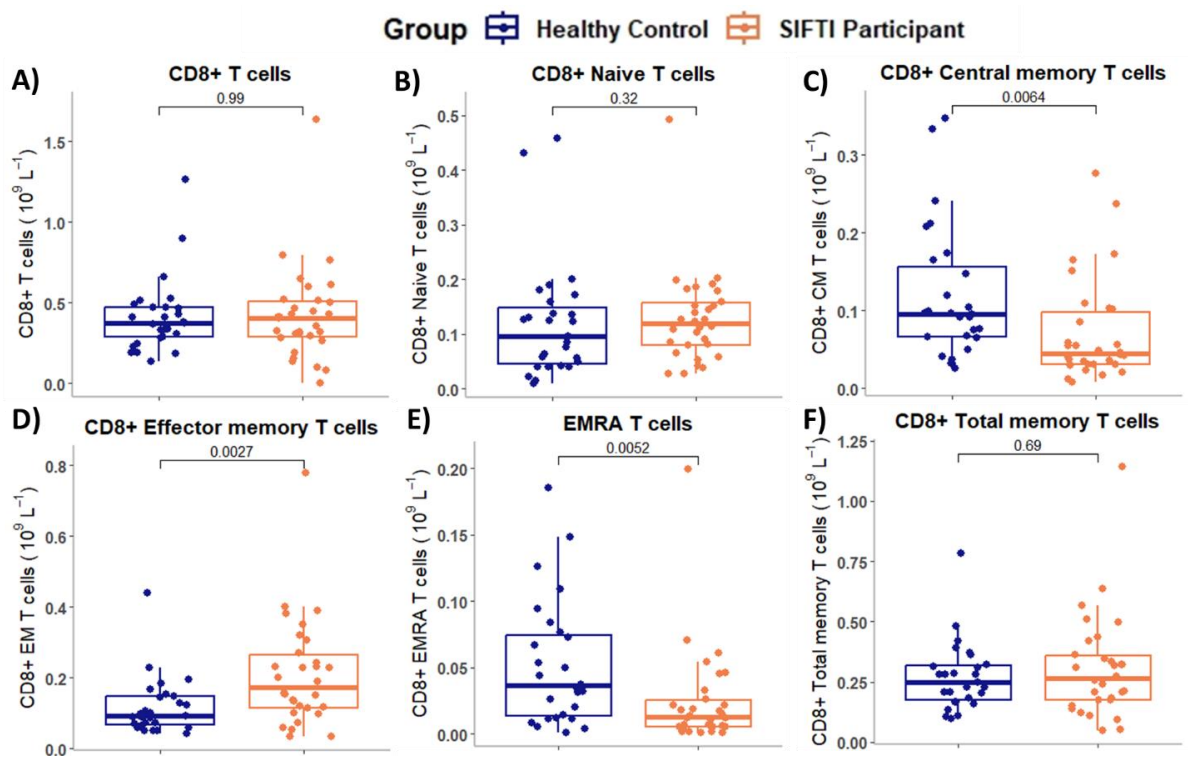


Figure A.3.8: Differences in CD8+ T cell subsets between long-term burn injured participants and healthy controls - Shown are the numbers of several CD8+ T cell subtypes in burn injured participants (n = 31) 6 months post injury compared to a healthy control group (n = 27) (Wilcoxon). Shown are the CD8+ T cell numbers (**A**) as well as CD8+ naïve (**B**), central memory (**C**), effector memory (**D**), effector memory re-expressing CD45RA (**E**) and total memory (**F**) T cells. For each box plot each point is one participant. The central line is median, the bottom line is the 1st quartile (Q1), the upper the 3rd quartile (Q3). The whiskers represent calculated minimum and maximum values using the interquartile range (IQR). Whiskers are calculated using the formula Q1 + 1.5 x IQR or Q3 + 1.5 x IQR.

The results when comparing the number of senescent and senescent sub-population of CD4+ and CD8+ T cells, the results mirrored those shown when comparing the cells as percentages (Figure 3.4).

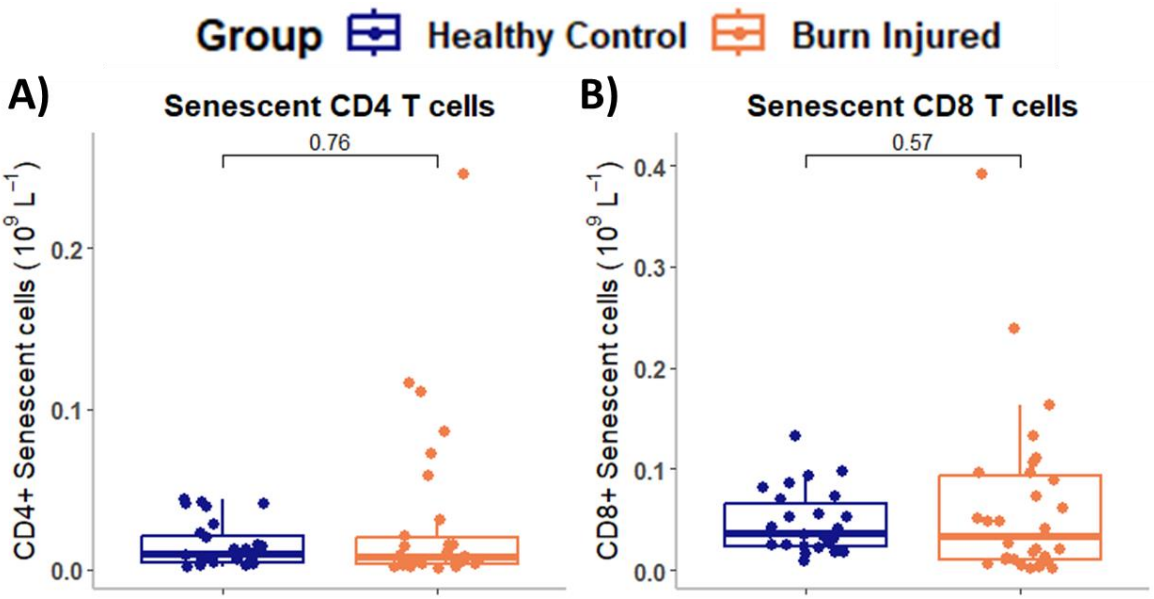


Figure A.3.9: Differences in senescent CD4+ & CD8+ T cell subsets between long-term burn injured participants and healthy controls - Shown are the number of senescent (CD57+, CD28-) CD4+ and CD8+ T cells in burn injured participants (n = 31) 6 months post injury compared to a healthy control group (n = 27) (Wilcoxon). Shown are the number of senescent T cells (CD57+, CD28-, **A** & **B**) within the CD4+ & CD8+ T cell compartments. For each box plot each point is one participant. The central line is median, the bottom line is the 1st quartile (Q1), the upper the 3rd quartile (Q3). The whiskers represent calculated minimum and maximum values using the interquartile range (IQR). Whiskers are calculated using the formula Q1 + 1.5 x IQR or Q3 + 1.5 x IQR.

The results when comparing the number of B cells and B cell sub-populations (Figure A.3.10) closely resembled those shown when comparing the cells as percentages (Figure 3.5) with the exception of the regulatory B cell (Breg) population. While the percentage of B cells which were greater in the burn group (Figure 3.5, E) when represented as the cell counts, there was no significant difference between burn injured individuals and healthy controls (p = 0.48, Wilcoxon).

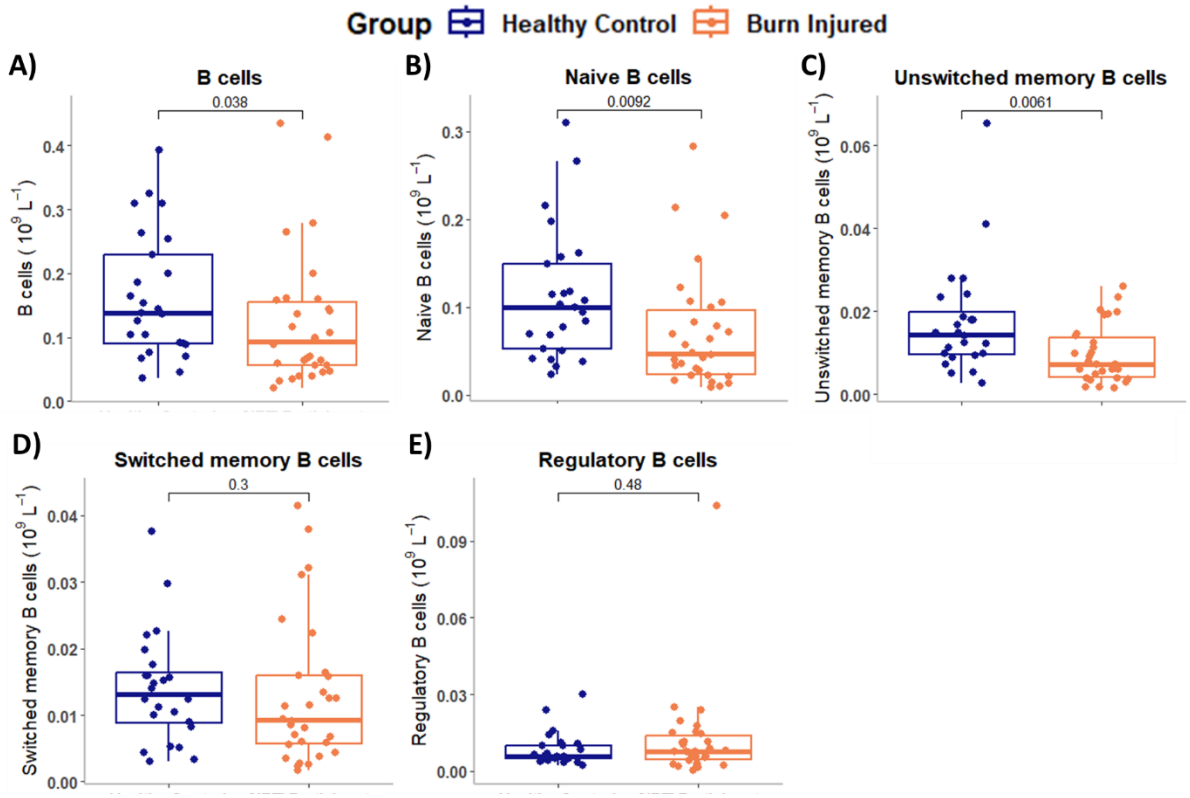


Figure A.3.10: Differences in B cell subsets between long-term burn injured participants and healthy controls - Shown are the number of B cells (CD19-, **A**) in burn injured participants (n = 31) 6 months post injury compared to a healthy control group (n = 27) (Wilcoxon). Also shown are the are the number of B cells which are naive (IgD+, CD27-, **B**), unswitched memory (IgD+, CD27+, **C**), switched memory (IgD-, CD27+, **D**) or regulatory B cells (Breg, $CD24^{Hi}$, $CD38^{Hi}$, **E**). For each box plot each point is one participant. The central line is median, the bottom line is the 1st quartile (Q1), the upper the 3rd quartile (Q3). The whiskers represent calculated minimum and maximum values using the interquartile range (IQR). Whiskers are calculated using the formula Q1 + 1.5 x IQR or Q3 + 1.5 x IQR.

Within the burn injured group there were significantly more NK Cells (Figure A.3.11, A, p = 0.0043, Wilcoxon), NK CD56+ bright (Figure A.3.11, B, p = 0.0014, Wilcoxon) and CD56+ dim cells (Figure A.3.11, C, p = 0.0093, Wilcoxon). This is in contrast to the percentage data shown in Figure 3.6 where no significant differences between the groups was observed.

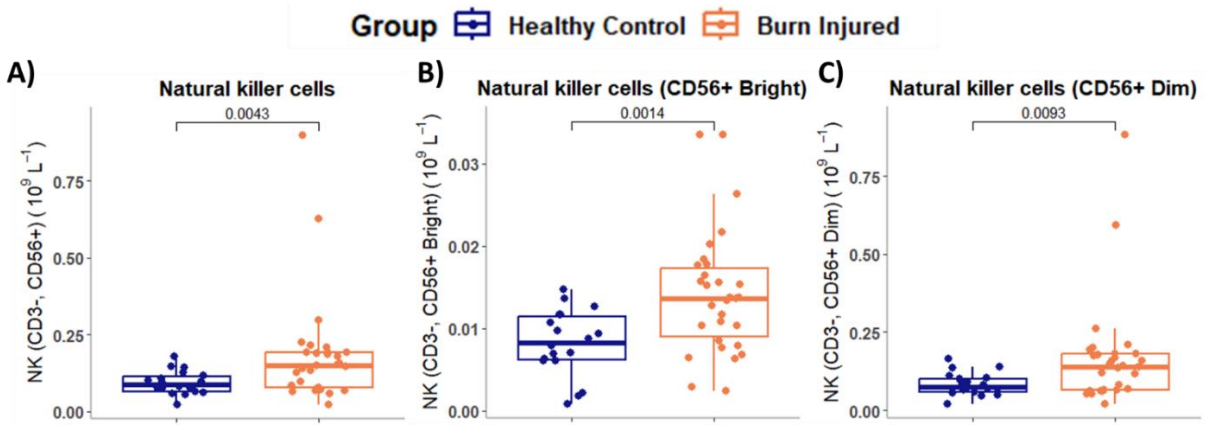


Figure A.3.11: Differences in natural killer cell subsets between long-term burn injured participants and healthy controls - Shown are the number of natural killer (NK) cells (CD3-, CD56+, **A**) in burn injured participants (n = 31) 6 months post injury compared to a healthy control group (n = 27) as well as the number of, CD56+ bright NK cells (**B**), and CD56+ dim NK cells (**C**). For each box plot each point is one participant. The central line is median, the bottom line is the 1st quartile (Q1), the upper the 3rd quartile (Q3). The whiskers represent calculated minimum and maximum values using the interquartile range (IQR). Whiskers are calculated using the formula Q1 + 1.5 x IQR or Q3 + 1.5 x IQR.

4. Senescent cells as therapeutic targets

4.1 Introduction

4.1.1 Targeting senescent cells as a therapy for the ageing phenotype

As well as accumulating during normal ageing, senescent cells can appear during the wound healing process (Jun and Lau, 2010, Demaria et al., 2014), as well as during prolonged pro-inflammatory and hyper-metabolic conditions (Papaconstantinou, 2019), which are all features of severe burn injury (Mulder et al., 2021). They also form a negative cycle of inflammation and senescent cell development due to their own pro-inflammatory and pro-senescent phenotype (Nelson et al., 2018). Their presence, while needed in some conditions, has been shown to contribute to the ageing phenotype in mice, and their ablation has been shown to restore physical function and increase lifespan (Baker et al., 2011). Despite the role of senescent cells in the development of the aged phenotype (Lopez-Otin et al., 2013), little is known about the impact injury has on senescent cell load. An increase in senescent cells after injury may be contributing to the increased morbidity and mortality in trauma survivors reminiscent of an aged phenotype. If so, removal of these cells could offer a new therapeutic route to improve long term patient outcomes.

Research has shown that several drugs such as Dasatinib, Quercetin and Fisetin are able to overcome the anti-apoptotic mechanisms in senescent cells to induce cell death (Wissler Gerdes et al., 2020; Zhu et al., 2017). These senolytic agents therefore offer one option for modulating the aged phenotype, the benefits of which have been discussed at length within the literature and in the introduction to this thesis. Removing or altering the phenotype of senescent cells, for example by reducing their SASP, has also become a key area of interest in the field of drug discovery and the burgeoning field of anti-ageing research (Birch and Gil, 2020; Robbins et al., 2021; Xu et al., 2018).

One combination of compounds which has been shown to be effective both in-vivo and in-vitro is that of dasatinib and quercetin. This combination, used in this thesis as a positive control, has been shown be effective at selectively killing senescent cells in culture, resulting in a subsequent reduction in pro-inflammatory factors in the SASP (Xu et al., 2018). These compounds have also been shown to be well tolerated and effective in improving physical function such as gait speed and chair stand times in early human trials in patients with idiopathic pulmonary fibrosis (Justice et al., 2019)

If trauma and critical illness increase the rate of ageing or one feature of the ageing process such as cell senescence, it is logical to develop a treatment pathway for patients which includes the use of therapeutics which have been shown to be beneficial in the reduction of senescent cells or their SASP, resulting in reduced inflammation and improved physical function and potentially extended healthspan. Senolytics therefore offer a potential treatment opportunity in patients exhibiting signs of accelerated ageing by targeting one of ageing's driving forces, senescent cells.

4.1.2 Senolytic discovery and action

It has previously been discussed that the use of senolytics in different age-related diseases is a rapidly growing area of research with the number of publications increasing significantly in recent years. In 2015 there were 28 publications including mention of the word senolytic (including the coining of the term) and the early proof of concept work, by the Kirkland group at the Mayo clinic (Kirkland and Tchkonia, 2015; Zhu et al., 2015). The number of publications including reference to senolytics has grown to 3753 in 2021 ("'Senolytic' in Publications - Dimensions.ai," 2022), confirming a burgeoning interest in the field.

The first senolytic drugs to be discovered were Navitoclax, Fisetin, Dasatinib and Quercetin (Reviewed in: Kirkland and Tchkonia, 2020). The list of identified senolytic compounds has grown from those initial four, now including both novel drugs such as SSK1, a compound which induces apoptosis in senescent cells via activation of the p38 MAPK pathway (Cai et al., 2020), and previously known compounds such as curcumin which has been shown to reduce senescent cell number in-vitro

(Robbins et al., 2021; Yousefzadeh et al., 2018). This modest increase suggests scope for more novel compounds to be discovered that specifically target senescent cells.

One common, time effective method of drug discovery is to screen a compound library in a high throughput fashion, often utilising robotic systems to maintain accuracy across plates containing over 1500+ wells (Michael et al., 2008) to look for compounds which then have the desired effect within a model system (Szymański et al., 2011). This involves developing a biological model of the disease or condition of interest such as a cell line exhibiting the desired phenotype and exposing the model to the library of compounds. While a high throughput system was not available for use in this study, the same principles were followed. A model system, cells induced to enter senescence, was exposed to 40 compounds as part of two highly repeatable assays and any potential 'hits' were recorded for further investigation as early lead compounds.

4.1.3 A model for cellular senescence

For use in this study a model of cellular senescence was needed. One option would be to use naturally aged mice or knockout mice with a progeroid condition (Carrero et al., 2016). These models would undoubtedly provide valuable data about not only the senescence clearing properties of a compound but the physiological impact they have, as senolytic studies in the past have also shown the positive impact senolytic compounds can have on animal health (Xu et al., 2018). However, such animal work can be both labour intensive and costly and could only be justified ethically once a lead compound had been identified in an initial in vitro screening protocol.

This study used the hTert immortalised BJ human foreskin fibroblast cell line, a kind gift from Dr Eva Petermann (Kotsantis et al., 2016). This cell line is used in the Lord lab as a model of oncogene induced senescence as these cells express a 4-hydroxytamoxifen (4-OHT) inducible HRas construct (Kotsantis et al., 2016). Senescence in this cell line can also be induced via oxidative stress, following timed exposure to hydrogen peroxide. However, for this study DNA damage was selected as the method of

senescence induction due to the high degree of reproducibility of the kinetics of senescence induction and the shorter time taken by the cells to reach senescence following DNA damage.

Senescence was induced via DNA damage caused by exposure to ionising radiation, in this case a 10Gy via X-ray (see methods chapter for details). Cell cycle arrest occurred as a response to DNA damage. Exposure to a non-lethal DNA damaging condition will initiate the DNA damage response, characterised by the increased expression of p53 and p21 and temporary cell cycle arrest. While DNA damage can be repaired and cells can return to the cell cycle, sufficient damage particularly in the form of multiple double and single strand breaks can force the cells into permanent cell cycle arrest and cellular senescence (Chen et al., 2019). While X-ray radiation exposure at relatively high doses is not a perfect replication of the natural ageing process, the DNA damage theory of ageing posits that accumulated genomic damage plays at least a partial role in driving the ageing process (López-Otín et al., 2013), with markers of genomic instability increasing with age (Petr et al., 2020).

In this exploratory study a library of compounds all targeting epigenetic processes, kindly provided by Professor Annette von Delft (University of Oxford), was used to identify agents that may have senolytic potential. I was also interested to determine if cell senescence could be reversed epigenetically and therefore measured both the induction of apoptosis and reduced presence of SA-βgal in the screening programme. The cell line used had no detectable SA-βGal positive cells during normal non-irradiated cell culture as is shown in Figure 4.3 (Day 0). These untreated fibroblasts made up a non-senescent control group to test for any non-senescence specific cytotoxic effects of the compounds in the test library.

That such a rescue from senescence might be possible has previously been demonstrated by Walters et al, who demonstrated that when human dermal fibroblasts were treated with a pan-mTOR inhibitor (AZD8005), many of the classic hallmarks of cellular senescence such as increased cell size and SA-βGal activity were reversed (Walters et al., 2016). The Harries group also had success showing that features of senescence can be reversed; they demonstrated that small molecule compounds based on

resveratrol that target mRNA splicing factors were able to reverse many features of senescence in human primary fibroblasts, including re-entry into cell cycle and lengthening of telomeres (Latorre et al., 2017).

4.1.4 Aims of the chapter

This chapter set out to address two separate experimental aims:
Aim one: To assess the senescent cell load within skin samples taken from burn injured patients.
Aim two: To identify compounds which modify aspects of the senescent cell phenotype in human dermal fibroblast culture.

4.2 Results

4.2.1 Does traumatic injury affect senescent cell numbers within the skin

4.2.1.1 Senescent cell load following trauma

To investigate if traumatic injury influences senescent cell load across the body, several skin biopsies were taken from burn injured patients over a 6–12-month period. Skin biopsy samples were taken from the burn affected area via a 5mm full thickness punch biopsy on the day of admission, day 14 and at a long term follow up (6 or 12 months). Samples were taken both at the site of injury and from non-injured skin at each time point. On the day of admission, the biopsy was only taken once the burned area had been debrided and cleaned to avoid necrotic tissue in the sample.

Each skin sample was formalin fixed and paraffin mounted, sections were then stained using IHC to determine the number of $p16^{INK4A}$ positive cells. The expression of $p16^{INK4A}$ was considered evidence of cellular senescence. Samples from the site of injury and from non-injured tissue were compared to establish if there were changes in senescent cell load following injury and during the healing phase.

4.2.1.2 Senescent cell load cohort information

Listed below is the cohort demographic and clinical information for the patients included in the long-term study of senescent cell load quantification following burn injury. Long-term samples were obtained at 12 months post-injury for 2 patients and at 6 months for 5 patients.

Patient ID	Age	Sex	TBSA%	rBaux	Sample timepoints
A012	51.8	M	17	68.8	Day 1, Day 14, Month 6
A018	47.61	M	35	82.61	Day 1, Day 14, Month 6
A020	52.09	M	22	91.09	Day 1, Day 14, Month 6
A028	47.53	F	51.5	129.5	Day 1, Day 14, Month 12
A030	41.06	M	16	74.06	Day 1, Day 14, Month 6
A034	17.81	M	30	64.81	Day 1, Day 14, Month 6
A038	47.22	M	22	113.22	Day 1, Day 14, Month 12
Mean	43.59	n/a	27.64	89.16	n/a
SD ±	11.06	n/a	11.60	22.32	n/a

Table 4.1: Senescent cell tissue staining cohort information. A table showing the cohort information of the patients used for senescent cell percentage within skin sample analysis. Skin samples were collected at the time points shown. TBSA% is the total burn surface area as a percentage of the total area of the individual, rBaux (Revised Baux score) is a burn severity score composed of the TBSA% + age (+17 if there is an inhalation injury). TBSA; Total burn surface area.

4.2.1.3 Changes in $p16^{INK4A}$ expressing cell percentage over time following burn injury

Figure 4.1 is a representative image showing a sub-section of p16 stained tissue collected as part of a 5mm full thickness punch biopsy of the skin. Negative cells are stained in blue, positive cells are dark brown (Figure 4.1 **A**). Highlighted in Figure 4.1 **B** is an example of how cells were quantified as positive or negative, with positive cells circled in red, and negative circled in blue. Figures 4.1 **C** and **D** show the same tissue stained with an isotype control, showing no positive cells, this confirms antibody specificity. Multiple sections were treated with isotype controls during each batch of staining. Positive $p16^{INK4A}$ staining appeared to mainly be localised to the nucleus with low levels of cytoplasmic staining, p16 localisation has been shown to be related to survival probability in some kinds of cancer, with high cytoplasmic expression correlating with lower survival than high nuclear staining (Zhao et al., 2012). For detailed information on how this quantification was done and the software used, please refer to the methods section.

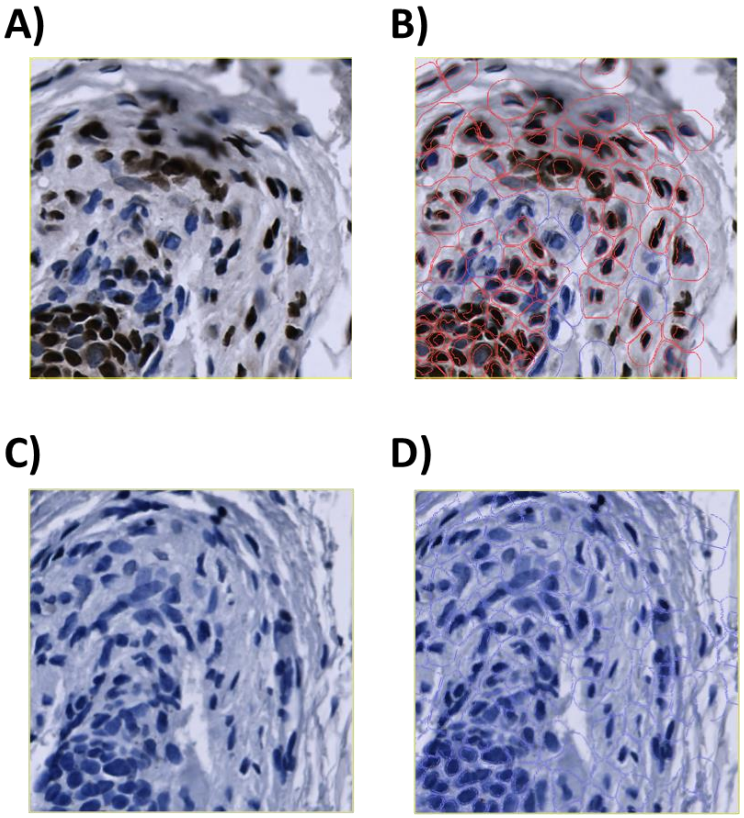


Figure 4.1: p16 positive and negative cell selection with isotype control. A set of images showing a section human dermal tissue section stained for $p16^{INK4A}$ (**A** & **B**) with **B** showing automated positive and negative cell selection using QuPath software, positive cells are circled in red, negative in blue. Shown in **C** & **D** is another section taken from the same tissue stained using an isotype control, **D** shows the automated positive and negative cell detection showing no positively stained cells as all cells are circled in blue.

A paired Wilcoxon analysis showed that within burn injured skin tissue there was a modest but significant increase in the percentage of $p16^{INK4A}$ positive cells at day 14 compared to admission following injury ($p = 0.047$). There was no significant difference between the percentage positive cells at day 14 and at long term follow up ($p = 0.3$), or between admission and long term follow up ($p = 1.0$) (Figure 4.2 **A**). The mean percentage of $p16^{INK4A}$ positive cells across all patients increased from 73.4% at day one to 82.9% at day 14 and back down to 71.4 at long-term follow up within burn injured tissue (Figure 4.2 **A**).

In healthy non-burn injured skin taken from burn injured patients a paired Wilcoxon analysis showed that there was a no difference between the percentage of $p16^{INK4A}$ positive cells at day 14 and day 1 ($p = 0.22$) or between day 14 the long-term follow-up ($p = 0.11$) (Figure 4.2 **B**). There was however a significant decrease in the percentage of $p16^{INK4A}$ positive cells between day 1 and at the long term follow up ($p = 0.031$). The mean percentage of $p16^{INK4A}$ positive cells at day 1 was 84.5% decreasing to 79.2% at day 14 before decreasing further to 69.49% in non-burn injured skin taken from burn patients (Figure 4.2 **B**).

Despite the proposed active role of senescent cells in the wound healing process there was no significant difference observed in the percentage of $p16^{INK4A}$ positive cells when comparing burn-injured and non-burn injured tissue at any time point (Wilcoxon), (Figure 4.2 **C**).

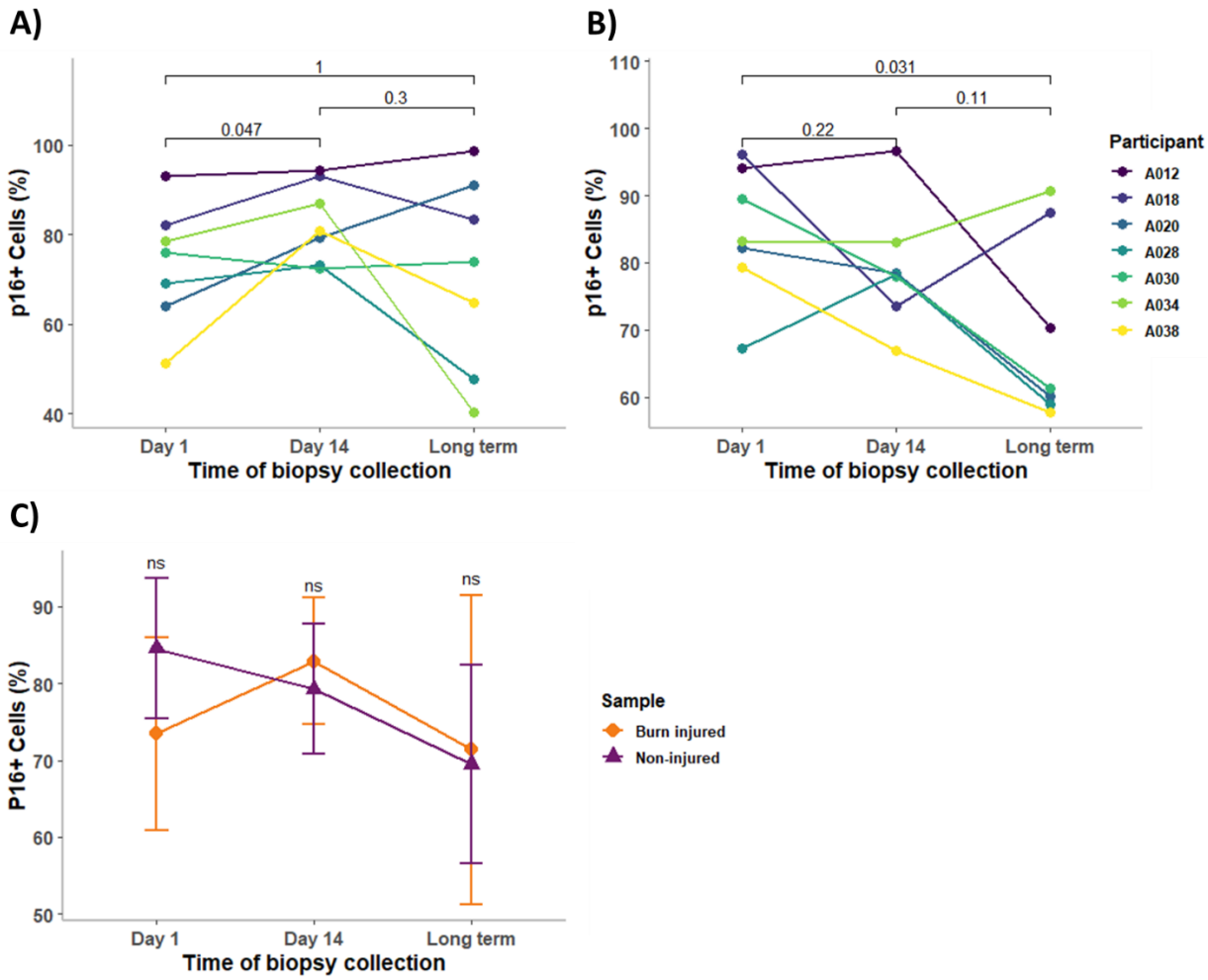


Figure 4.2: The percentage of p16^{INK4A} positive cells within burn injured and non-injured skin over time following injury. Plot **A** is a dot and line plot showing the percentage of p16^{INK4A} positive cells within skin tissue of burn injured patients taken from a burn injured site, at the day of admission, day 14 and at a long-term follow-up (n = 7). Plot **B** is dot and line plot showing the percentage of p16^{INK4A} positive cells within skin tissue of burn injured patients taken from a non-injured site, at the day of admission, day 14 and at a long-term follow-up (n = 7). **C** shows a dot and line plot showing a comparison of the percentage of p16 positive cells within skin tissue from burn injured patients (n = 7) taken from a burn injured and a non-burn injured site at the day of admission, day 14 and at a long-term follow-up. Data are mean, bars indicate ±SD.

4.2.2 Senescence modulating compound discovery

4.2.2.1 Compound exposure

A single dose of ionising radiation (10Gy) in the form of X-rays was used to induce senescence in hTert transformed BJ fibroblasts. The cells were analysed using Annexin V + PI staining and flow cytometry to look for evidence of apoptosis and necrosis. Annexin V + PI staining in conjunction with flow cytometry is an established method of investigating cell death in fibroblasts (Gary and Rochette, 2020). An SA-βGal expression assay and brightfield microscopy were used to monitor the development of a senescent phenotype as previously described (Deng et al., 2018; Gu et al., 2011). Any compound which increased cell death only in senescent cells was deemed to have senolytic potential, whereas a compound which increased cell death in both senescent and non-senescent cells was deemed to be generally cytotoxic.

Each compound treatment lasted 48 hours before cell viability and SA-βGal assays were performed. The positive control (1 µM dasatinib + 20 µM Quercetin) has previously been shown to be effective at killing senescent cells in vitro following a 48-hour exposure (Xu et al., 2018), this was also the incubation period that the group who provided the compound library had previously used. It was for these reasons that a 48-hour incubation was selected. Senescent cells were treated on Day 12 post X-ray treatment with cell viability and SA-βGal assays performed on day 14. Each of the 40 compound exposures were run in technical triplicate for the viability and for the SA-βGal assays. A vehicle control of 0.1% DMSO was used alongside each compound exposure as all compounds within the library were suspended in DMSO, concentrations are listed in Table 4.2.

Probe ID	EC50 (nM)
(+)-JQ1	500
SGC 0946	10
UNC 1215	500
SGC-CBP30	1000
I-CBP 112	1000
(R)-PFI2 hydrochloride	100
UNC 1999	124
PFI 3	1000
UNC 0642	130
A 366	100
BAZ2-ICR	1000
OICR 9429	223
OF 1	80
GSK LSD1 dihydrochloride	5
SGC 707	91
NI 57	1000
BI 9564	1000
I-BRD9	159
GSK 2801	1000
MS049 oxalate salt	970
MS 023 dihydrochloride	1000
NVS CECR2 1	255
BAY 299	575
TP 472	323
TP 064	43
GSK 591 dihydrochloride	56
BAY 598	50
A 395	90
GSK 343	174
A 196	500
GSK 6853	20
L Moses dihydrochloride	260
A 485	73
BAY 6035	70
GSK 864	320
LLY 283	30
SGC 3027	1300
MRK 740	800
BI 9321	1200
Control compounds	**Concentration**
DMSO	0.1% (v/v)
Dasatinib + quercetin	1 µM + 20 µM

Table 4.2: Compounds used for cell treatments. A table showing the concentrations used for compound exposures based on their EC50. Negative control was 0.1% (v/v) DMSO and the positive control was Dasatinib (1uM plus quercetin (20uM).

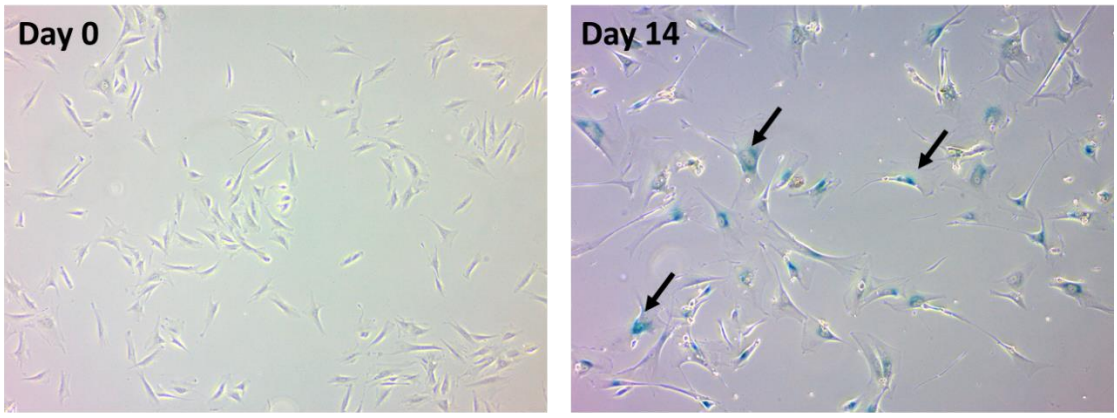
4.2.2.2 Induction of senescence following X-ray radiation exposure

A previously validated method of senescence induction was used, this involved exposing the cells to a single dose of 10Gy of X-ray radiation and assessing senescence 12-14 days later. This method was shown to cause a significant increase in the percentage of SA-βGal positive cells compared to non-irradiated cells (Figure 4.3 **A**) beginning at day 6 (p value = ≤ 0.05, Wilcoxon, Figure 4.3 **B**). By day 12 approximately two thirds of the cells stained positive for SA-βGal, increasing to approximately 90% at day 14 (Figure 4.3 **B)**.

There was also a visible increase in cell size following exposure to 10Gy of X-ray radiation (Figure 4.4 **B**). The mean cell area increased significantly by 4.1-fold at day 14 compared to the pre-exposure area increasing from 3137 μm^2 to 13142 μm^2 (p value ≤ 0.0001, Wilcoxon, Figure 4.4 **A**) with a high degree of variability.

Both SA-βGal activity and Increased cell size have been observed as phenotypic traits present in senescent cells, both in-vitro and in-vivo (Biran et al., 2017; Neurohr et al., 2019). As both increased cell area and SA-βGal activity were present following X-ray exposure in the cells used, this was considered evidence of a successful senescent cell induction.

A)



B)

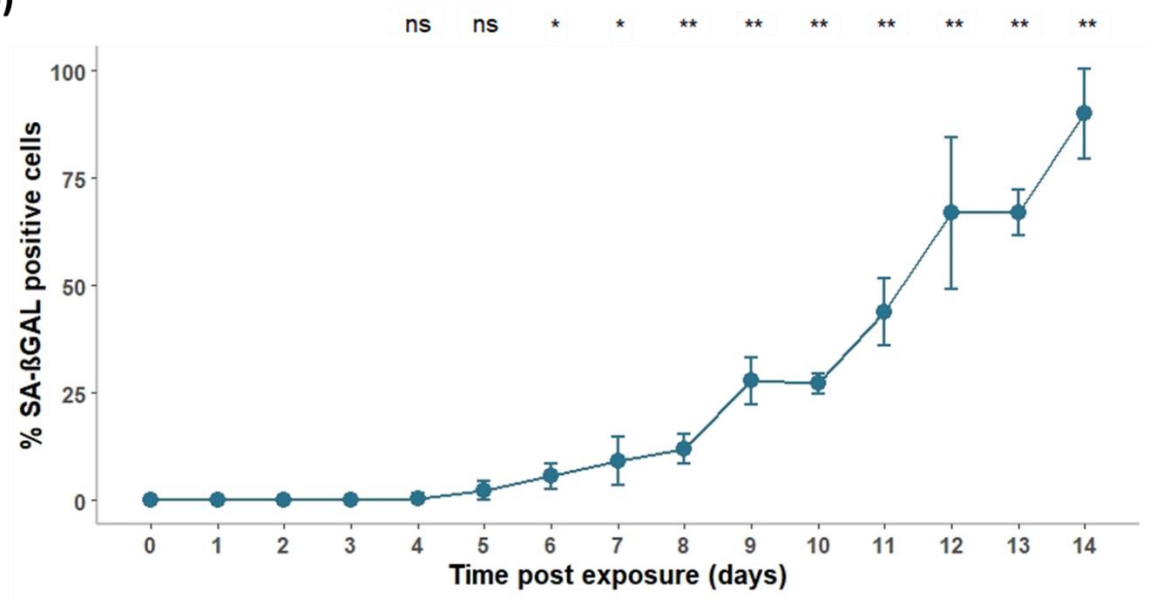


Figure 4.3: SA-βGal positive cells human dermal fibroblasts following exposure to X-ray irradiation. Figure **A** shows two representative images of BJ dermal fibroblasts prior to 10Gy X-ray exposure (Day 0) and 14 days post exposure (Day 14), the cells have been stained for SA-βGal. Positive cells are stained blue, highlighted with arrows. **B** shows the percentage of senescence associated β-galactosidase (SA-βGal) positive fibroblasts pre 10Gy X-ray exposure (day 0) and on each subsequent day following exposure (1-14). Percentages were calculated by imaging 3 technical replicates at each time point and counting the total cells and the number that were SA-βGal positive. Data are mean ± SD. * = $p \leq 0.05$, ** = $p \leq 0.005$. ns= non-significant.

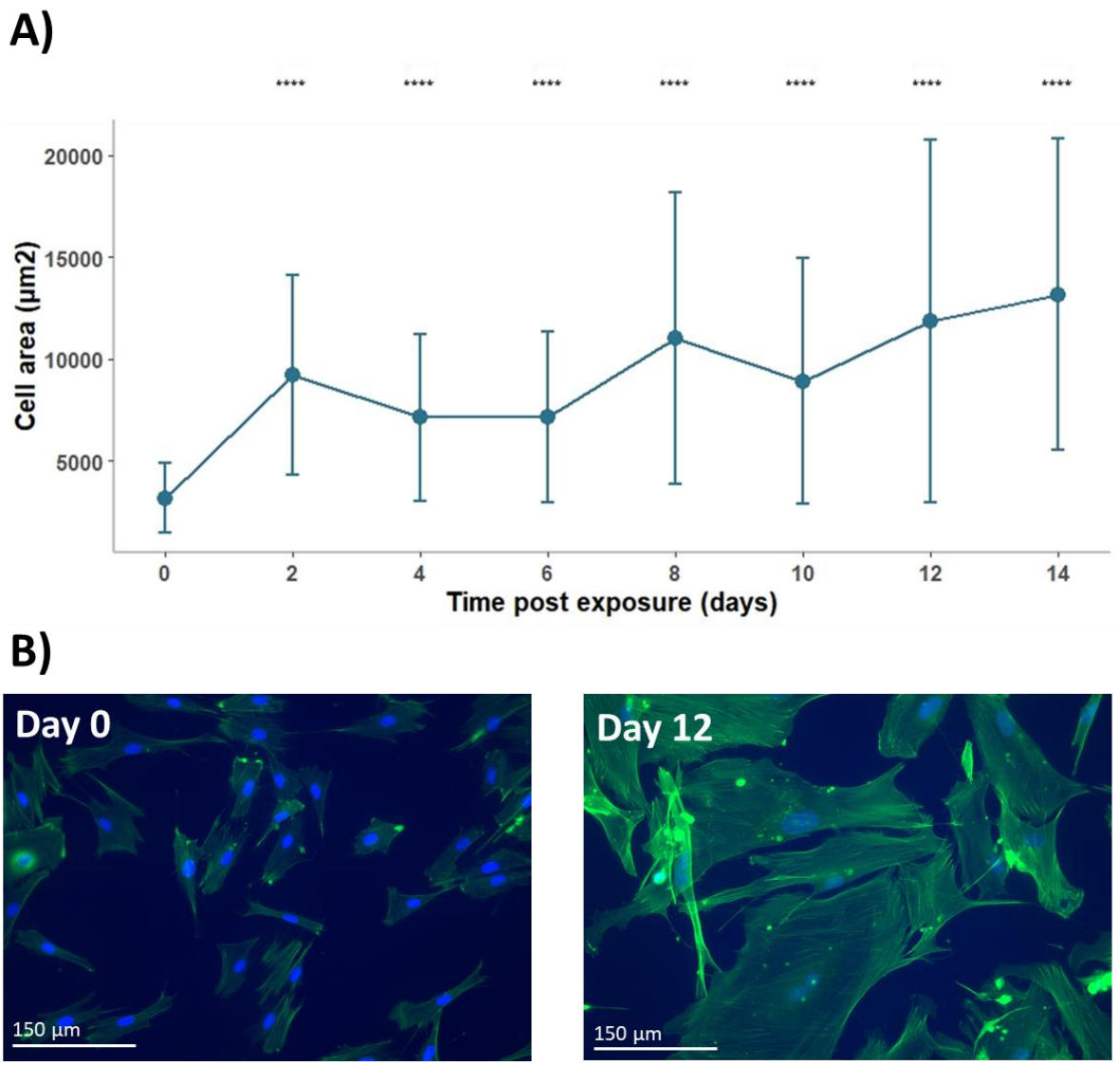


Figure 4.4: Changes in cell area following X-ray irradiation - A) a line graph showing the increase in cell area (μm^2) of BJ dermal fibroblasts following exposure to 10Gy of X-ray radiation. Mean cell size increased from 3137 μm^2 pre-X-ray (day 0) to 13142 μm^2 14 days post X-ray. Data are mean ± SD. **** = $p \leq 0.0001$. **B**) representative images showing the visible difference in size from pre dose (day 0) to day 12. Cell nuclei are counterstained blue with DAPI, the cytoskeleton of the cell is stained green with phalloidin. Cell area was measured on a minimum of 100 cells using images taken from 3 technical replicates at each time point.

4.2.2.3 Cell viability following treatment with epigenetic compounds

Cell viability was measured via flow cytometry using Annexin V + Propidium iodide (PI) staining to test whether exposure of cells to the compounds of interest lead to cell death. PI is a nucleic acid intercalating staining agent only able to enter cells with a non-intact plasma membrane (e.g., late apoptotic, or necrotic cells). Annexin V binds to phosphatidylserine, a phospholipid normally located in the inner layer of the cell membrane, but which flips to the outer membrane of cells in the early stages of apoptosis. In combination these two reagents allow apoptosis and necrotic cell death to be measured (Rieger et al., 2011).

A representative image of the gating strategy used, which has been previously published (Engelbrecht et al., 2021; Korga et al., 2019), is shown in Figure 4.6. Each drug treatment was run in technical triplicate with a vehicle control. Using flow cytometry debris and clumped cells were excluded to improve the reliability of results and ensure that only intact individual cells were being recorded (Figure 4.5 **A** and 4.5 **B**), the subsequent Annexin V + PI data was collected (Figure 4.5 **C**).

A known senolytic, a combination of 1 µM dasatinib and 20 µM quercetin (D + Q) was added to the list of compounds at a concentration previously shown to be effective at killing senescent cells after a 48-hour exposure in in vitro studies (Xu et al., 2018). This was included as a positive control and a means of establishing if the assay was sensitive enough to detect changes in cell viability following exposure to compounds with a known impact on the senescent phenotype. As is clearly illustrated in Figure 4.6, the addition of dasatinib and quercetin caused a significant reduction in the number of non-apoptotic cells from ~50% to less than 25% because of an increase in apoptosis in the senescent cell group compared to a vehicle control ($p = 0.00087$, t-test). In the non-senescent cells, there was no significant difference in the percentage of non-apoptotic cells compared to vehicle control ($p = 0.176$, t-test), as would be expected due to D + Q specifically targeting senescent cells while not affecting non-senescent cells (Zhu et al., 2015). This confirmed the sensitivity of the assay to detect compounds affecting viability in the fibroblast model of senescence.

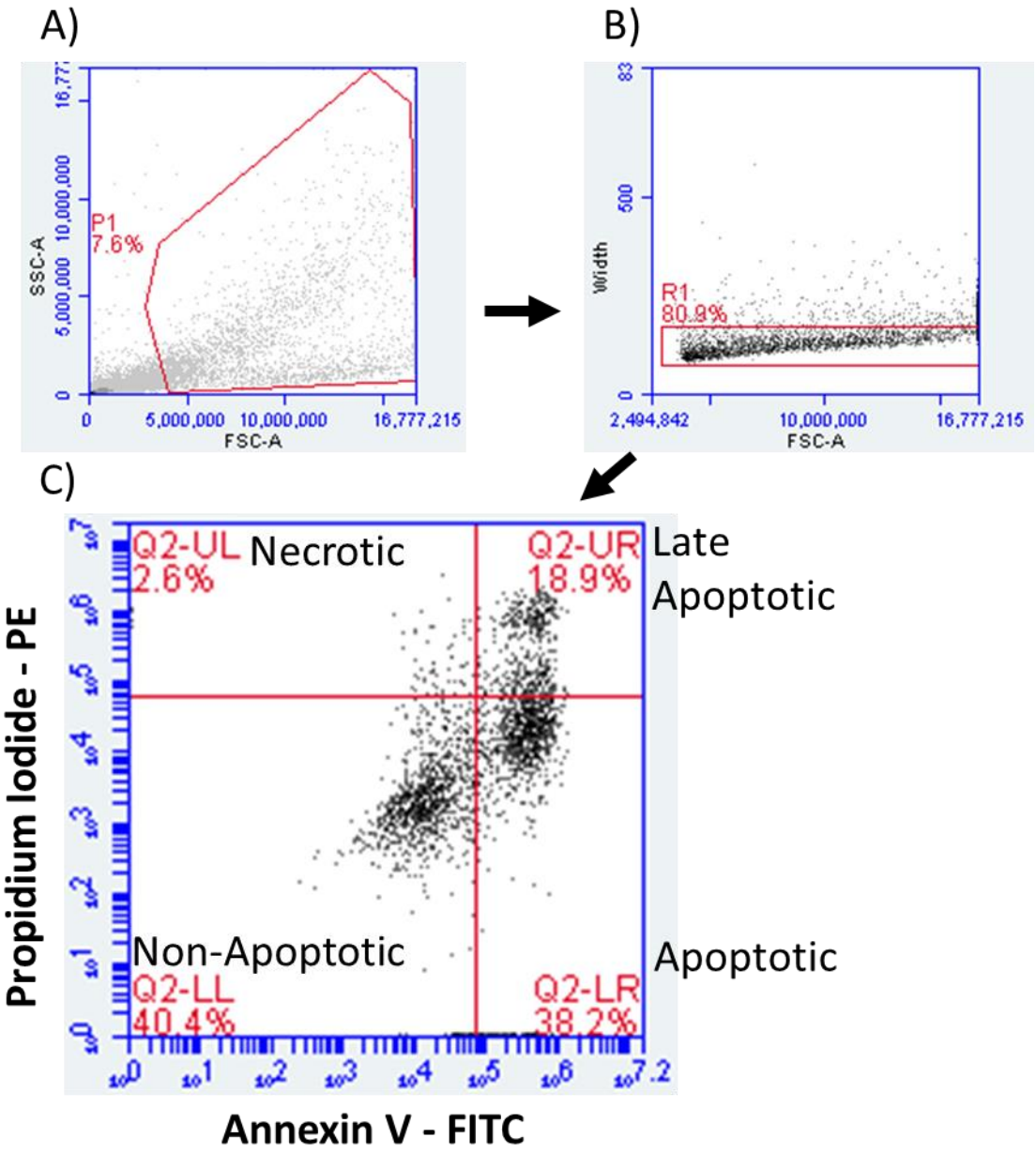


Figure 4.5: Annexin V & PI gating strategy - Flow cytometry plots showing gating strategy and representative data. (A) Debris exclusion. (B) Doublet and clumped cell exclusion, (C) cell viability. 'LL' are non-apoptotic, 'LR' are early apoptotic, 'UR' are late apoptotic, and 'UL' are necrotic.

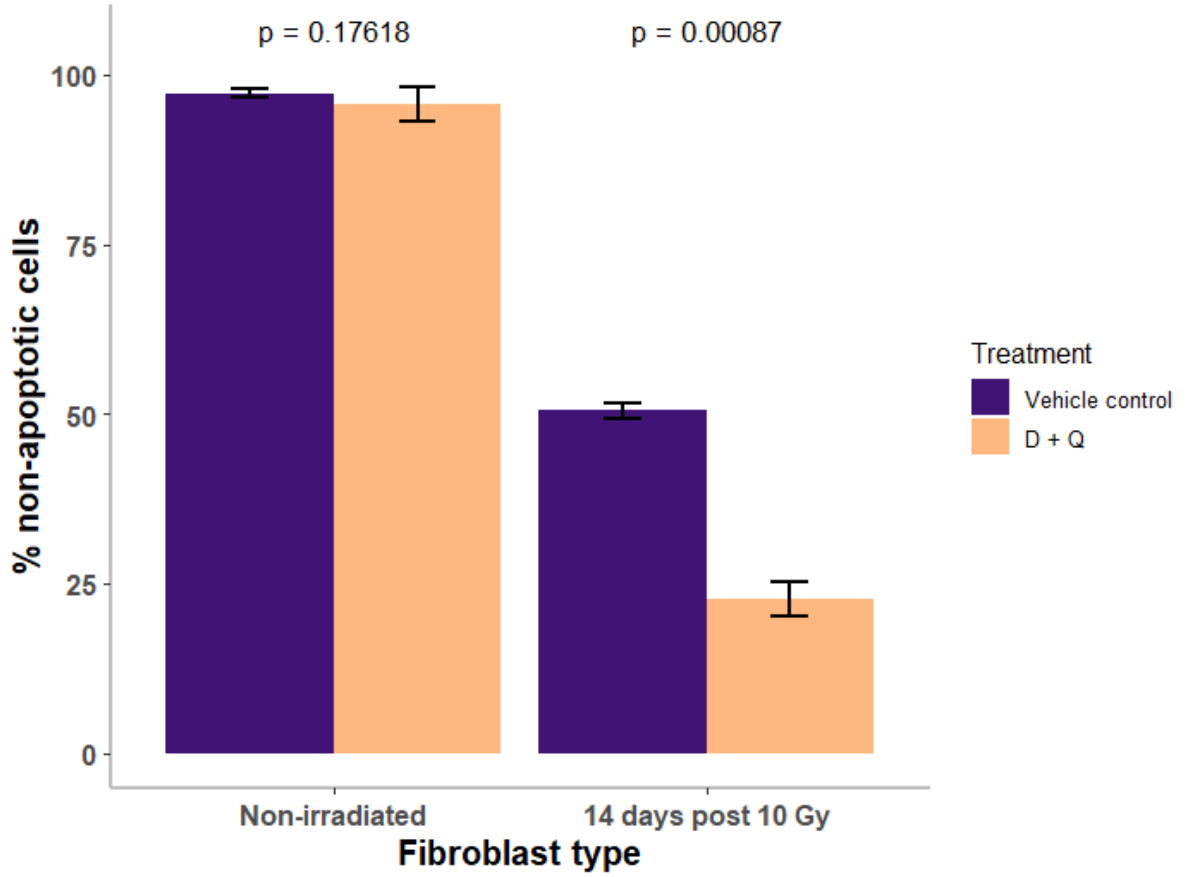


Figure 4.6: Percentage non-apoptotic dermal fibroblasts following treatment with Dasatinib and Quercetin. Bar graph showing the difference in the percentage of non-apoptotic BJ dermal fibroblasts following a 48-hour treatment with dasatinib (1 µM) + quercetin (20 µM) (D + Q) or vehicle control (0.1% DMSO). Non-irradiated, non-senescent cells showed no significant difference in the percentage of non-apoptotic cells following treatment with D + Q compared to vehicle control. Senescent cells showed a significant reduction in the percentage of non-apoptotic cells following treatment with D + Q compared to vehicle control. Each compound was tested in technical triplicate (n=3) and data are mean ± SD.

Each time the compound library exposure data was recorded a DMSO (0.1% v/v) vehicle control exposure was also included for comparison. The slight variation in the % non-apoptotic cells of the vehicle control shown in Figure 4.7 reflects the fact that a vehicle control was measured alongside each compound of interest, occurring over several days.

Of the 39 compounds in the test library only 6 had a significant effect on senescent cell viability compared to vehicle control (0.1% DMSO): GSK 864 ($p = 0.0053$); BI 9321 ($p = 0.0117$); A485 ($p = 0.0221$); OF 1 ($p = 0.0224$); GSK LSD ($p = 0.0325$); MRK 740 ($p = 0.039$) (t-test). Unlike D + Q treatment, these compounds had a positive impact on the number of non-apoptotic cells and reduced the number of apoptotic cells compared with a vehicle control (Figure 4.7 **A**).

Of the 39 compounds in the test library 7 had a significant effect on non-senescent cell viability compared to a vehicle control (0.1% DMSO): UNC 1999 ($p = 0.0040$); SGC 0946 ($p = 0.0073$); (R)-PFI2 HCL ($p = 0.0468$); PFI 3 ($p = 0.0313$). All caused a significant increase in the percentage of non-apoptotic cells, reducing the number of apoptotic cells present compared to a vehicle control (t-test, Figure 4.7 **B**).

Only NI 57 ($p = 0.049$), BAY 598 ($p = 0.0134$) and A 395 ($p = 0.0288$) caused a significant decrease in the number of non-apoptotic cells compared to a vehicle control (t-test, Figure 4.7 **B**).

There was no overlap between the senescent and non-senescent cells with regards to the compounds which had a significant impact on the percentage of non-apoptotic or apoptotic cells and the remaining compounds did not affect cell viability in either cell type (Table 4.3).

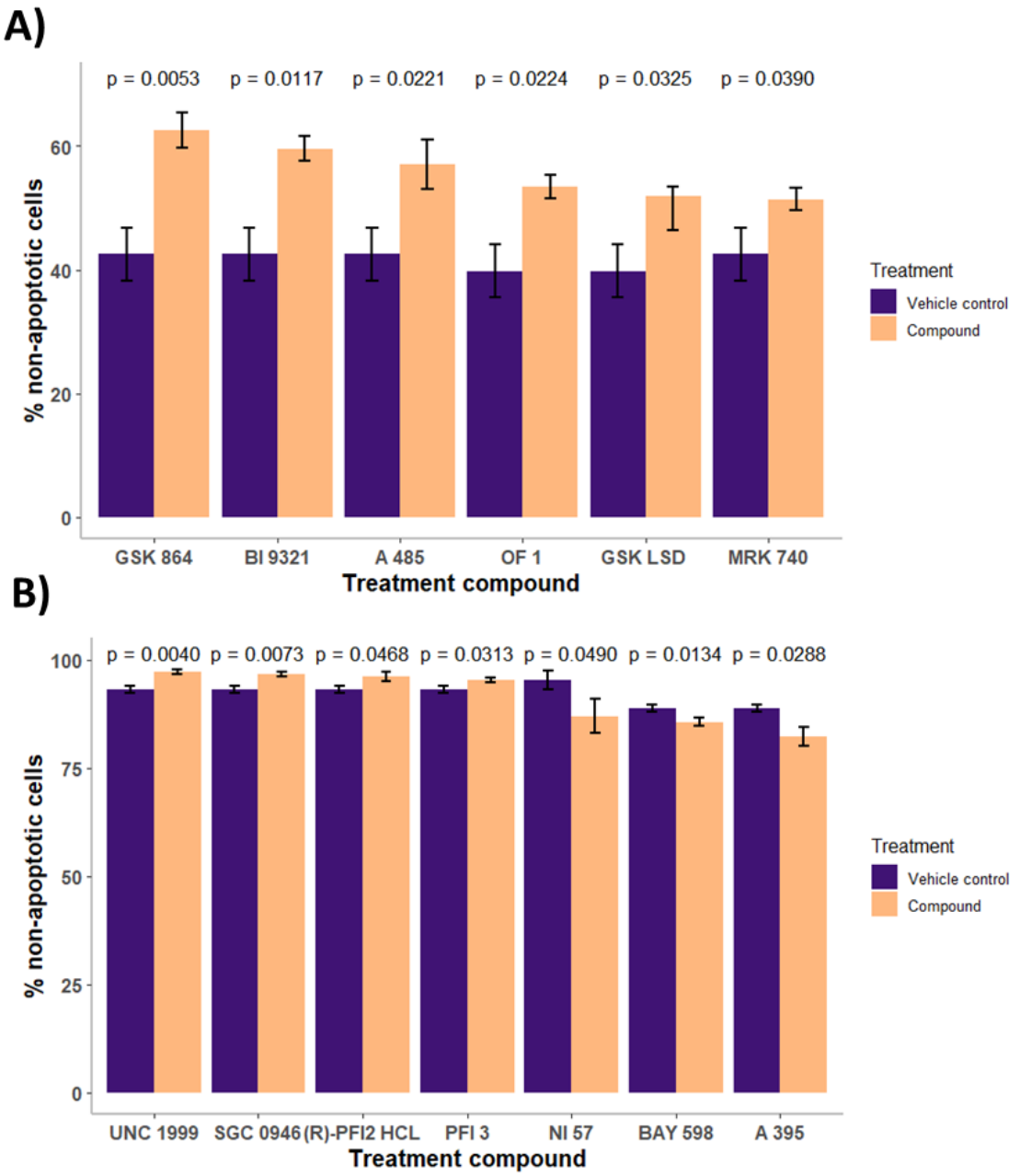


Figure 4.7: Changes in the percentage of non-apoptotic senescent and non-senescent dermal fibroblasts following compound exposure. Compound and vehicle control exposures in BJ dermal fibroblasts lasted 48 hours. Each exposure was performed in technical triplicate (n = 3), vehicle control was 0.1% DMSO (v/v). **A**) Percentage non-apoptotic senescent cells (14 days post 10Gy radiation). **B**) Percentage non-apoptotic non-senescent cells. Data are mean ± SD.

	Senescent cells				Non-senescent cells			
Probe	% Non-apoptotic cells	SD (±)	P.value	Change in % of non-apoptotic cells	% Non-apoptotic cells	SD (±)	P.value	Change in % of non-apoptotic cells
PFI 3	36.23	7.21	0.91	n/a	94.63	0.59	0.03	+
UNC 0642	39.10	0.26	0.37	n/a	95.03	1.42	0.07	n/a
(+)-JQ1	45.30	3.57	0.10	n/a	92.40	1.90	0.98	n/a
SGC 0946	43.97	8.09	0.29	n/a	95.93	0.70	0.01	+
UNC 1215	48.10	2.08	0.05	n/a	91.53	2.28	0.58	n/a
SGC-CBP30	34.73	4.06	0.83	n/a	90.57	4.03	0.51	n/a
I-CBP 112	39.67	1.32	0.32	n/a	93.23	1.34	0.45	n/a
(R)-PFI2 hydrochloride	43.00	2.71	0.12	n/a	95.00	1.21	0.05	+
UNC 1999	35.97	2.62	0.93	n/a	96.60	0.70	0.00	+
I-BRD9	39.80	1.87	0.48	n/a	83.20	7.63	0.16	n/a
GSK 2801	40.17	2.37	0.43	n/a	87.10	3.38	0.11	n/a
A 366	52.43	7.24	0.55	n/a	88.20	5.12	0.30	n/a
BAZ2-ICR	45.43	4.94	0.29	n/a	90.57	0.40	0.38	n/a
OICR 9429	46.10	2.21	0.10	n/a	92.57	2.06	0.93	n/a
OF 1	51.23	2.31	0.02	+	91.30	4.60	0.75	n/a
GSK LSD1 dihydrochloride	48.47	4.24	0.03	+	91.73	2.55	0.79	n/a
SGC 707	47.10	6.50	0.08	n/a	93.17	0.67	0.67	n/a
NI 57	45.40	2.89	0.06	n/a	82.33	4.86	0.05	-
BI 9564	38.03	5.56	0.96	n/a	84.90	5.14	0.11	n/a
A 395	39.70	5.52	0.65	n/a	80.37	2.67	0.03	-
GSK 343	35.73	4.02	0.56	n/a	80.73	3.33	0.05	n/a
MS049 oxalate salt	44.97	4.46	0.10	n/a	87.53	0.91	0.53	n/a
MS 023 dihydrochloride	42.53	4.37	0.23	n/a	86.90	1.75	0.39	n/a
NVS CECR2 1	40.77	2.84	0.35	n/a	84.67	2.48	0.13	n/a
BAY 299	33.93	4.45	0.32	n/a	78.00	8.05	0.16	n/a
TP 472	42.50	0.99	0.16	n/a	88.37	2.45	0.84	n/a
TP 064	29.63	6.65	0.16	n/a	84.70	2.00	0.09	n/a
GSK 591 dihydrochloride	35.63	4.64	0.57	n/a	84.20	5.65	0.36	n/a
BAY 598	39.27	1.17	0.58	n/a	84.50	1.10	0.01	-
MRK 740	49.50	2.26	0.04	+	96.50	0.75	0.79	n/a
BI 9321	56.70	2.43	0.01	+	96.17	1.40	0.62	n/a
A 196	50.37	7.05	0.85	n/a	84.20	5.72	0.37	n/a
GSK 6853	46.43	5.93	0.47	n/a	82.77	3.24	0.10	n/a
L Moses dihydrochloride	51.50	3.97	0.48	n/a	86.53	1.31	0.18	n/a
A 485	43.33	4.80	0.15	n/a	90.63	2.21	0.17	n/a
BAY 6035	52.07	4.81	0.02	+	95.10	0.89	0.08	n/a
GSK 864	59.87	3.42	0.01	+	96.60	1.35	0.94	n/a
LLY 283	51.93	8.75	0.08	n/a	93.37	4.77	0.35	n/a
SGC 3027	46.03	6.49	0.14	n/a	96.23	3.07	0.83	n/a
Dasatinib + Quercetin	20.13	3.09	0.00	-	93.03	3.12	0.18	n/a

Table 4.3: Compounds tested for their effects on senescent cell viability. Table showing change in the percentage of non-apoptotic cells following 48-hour exposure in both senescent and non-senescent BJ dermal fibroblasts for each test compound. The table also shows the standard deviation, p-value (t-test) and if the change in percentage of non-apoptotic cells was an increase, decrease or no change. Significant changes compared to vehicle control (0.1% DMSO (v/v)) are highlighted in red.

4.2.2.4 Effects of compounds on Senescence associated β-galactosidase positive fibroblasts

Exposures were performed in technical triplicate and a minimum of 5 images were taken at random positions in each well containing the treated senescent fibroblasts. The total cell count per image was recorded as was the number of cells which were positive for SA-βGal (Figure 4.9). These data were used to generate the percentage of cells which were positive and likely to be senescent. This number was then compared against a vehicle control (0.1% DMSO) to determine any compound effect.

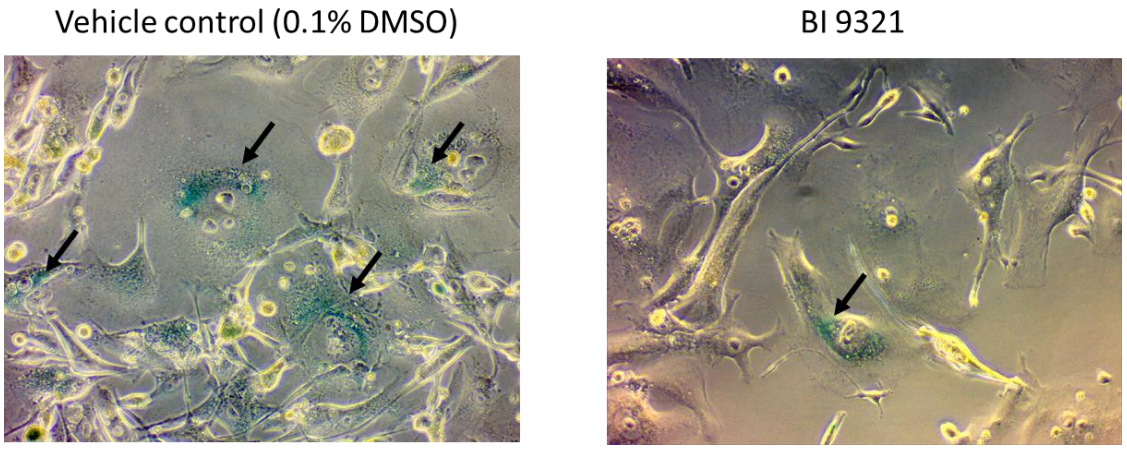


Figure 4.8: Representative images showing senescent dermal fibroblasts following a 48-hour treatment with a compound of interest (BI 9321) or a vehicle control (0.1% DMSO (v/v)). BJ dermal fibroblast cells were stained for SA-βGal using a histochemical stain 14 days post 10gy of X-ray radiation having undergone a 48-hour compound or vehicle control exposure. Cells which stained positive for SA-βGal activity (blue) are marked with arrows.

Of the 39 compounds tested 4 showed a significant change to the percentage of SA-βGal positive cells. MS049 OS (p = 0.04), NVS-CECR2-1 (p=0.02), BI 9564 (p = 0.018) and BI 9321 (p = 0.024) (t-test) all caused a significant reduction in the percentage of senescent cells present following treatment (Figure 4.11).

None of these compounds showed any effect on cell viability in the non-senescent cell group and only BI 9321 showed any effect on cell viability in the senescent group (Table 4.3), suggesting the decline in SA-βGal positive cells is likely due to reversal of cell senescence.

The slight variation observed between the vehicle control bars is likely due to each sample being run alongside a vehicle control on the day of analysis leading to slight differences in positive cell percentages recorded on different days.

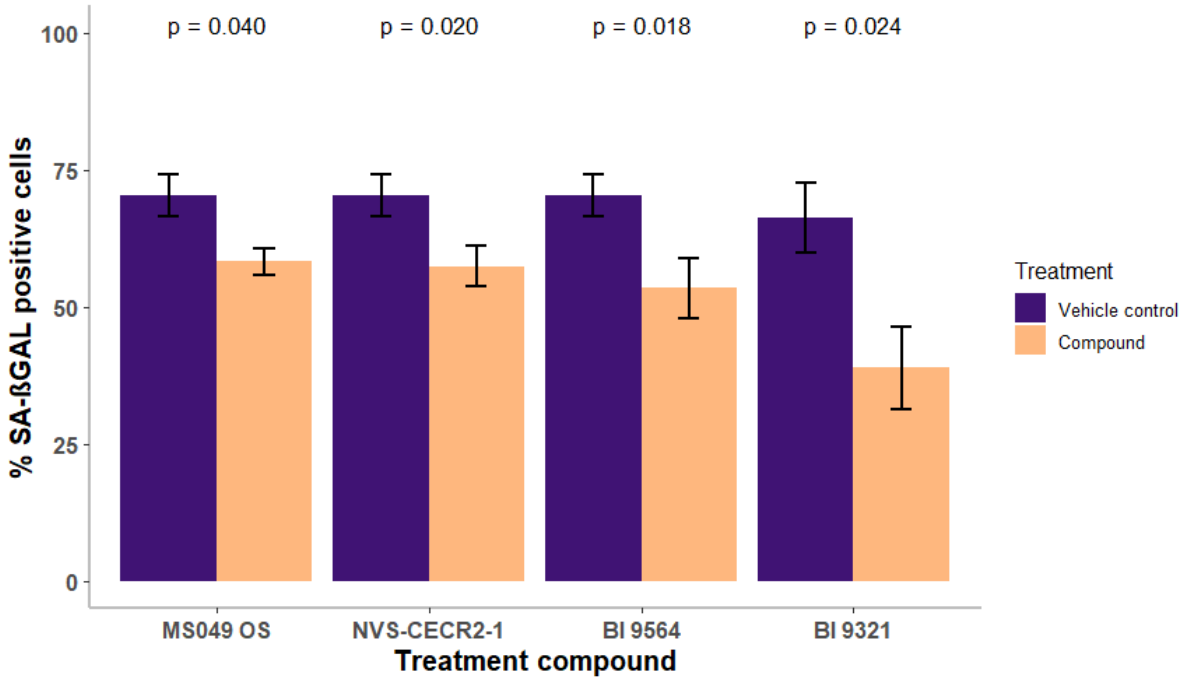


Figure 4.11: Percentage SA-βGal positive senescent dermal fibroblasts following compound exposure. A bar graph showing the changes in the percentage of SA-βGal positive BJ dermal fibroblasts following 48-hour exposure to test compounds in senescent cells. MS049 OS, NVS-CECR2-1, BI 9564 and BI 9321 all caused a significant reduction in the percentage of SA-βGal positive cells compared to the vehicle control (0.1% DMSO (v/v)). Each compound was tested in technical triplicate (n=3) with a minimum of 100 cells counted, data are mean ± SD.

4.3 Discussion

Senescent cells accumulate with age (Kumari and Jat, 2021b), and the benefits of removing them are clear and have been well described. For example, senescent cell removal has been shown to improve physical function, reduce inflammation and decrease disease development in mice (Baker et al., 2011). Data are also emerging from clinical trials in humans showing a similar beneficial effect of senolytic drugs such as Dasatinib and Quercetin (Ellison-Hughes, 2020; Justice et al., 2019). One area of research taking a different approach to senolytic drugs is the field of senescent cell phenotype modulation. While the accumulation of senescent cells within the brain have been associated with Alzheimer's disease (Bhat et al., 2012) and in the cornea this contributes to age-related macular degeneration (Lee KS et al., 2021) the ablation of cells within non-regenerative tissues and organs may impair function and therefore not be desirable. In these tissues it may be more beneficial to investigate ways of reversing cellular senescence or modulating the senescent phenotype, so called senotherapies, keeping the cells alive and eventually restoring their non-senescent, functional phenotype.

Here four compounds which act on epigenetic processes were found that were able to reduce SA-βGal expression and increase the survival of irradiated dermal fibroblast cells, with BI9321 being the most effective. Clearly, future studies will need to confirm if this truly represents a modulation of the senescent cell phenotype by looking at cellular factors such as SASP secretion and ability to proliferate as well as other senescence markers such as telomere associated foci (Hewitt et al., 2012).

4.3.1 Mode of action of epigenetic compounds

4.3.1.1 Compounds with a significant effect on cell viability

A non-senescent cell group was included in the analysis to establish if any compounds had an effect not specific to senescent cells. 7 compounds in total had a significant effect by improving or reducing cell viability in non-senescent cells (Table 4.4). None of these compounds showed any effect on FACS-assessed Annexin V + PI staining of senescent cells. This confirmed that any compounds observed to

affect the senescent cells were acting specifically because of the senescent phenotype. The targets of these 7 compounds are shown in Table 4.3. What is interesting is that 4 of the compounds improved cell viability (PFI 3, SGC 0946, (R)-PFI2 HCL and UNC 1999).

PFI3 is a bromodomain inhibitor which selectively blocks chromatin remodelling proteins SMARCA2/4 (Vangamudi et al., 2015). It has shown some ability to sensitize cancerous cells to DNA damage due to its chromatin remodelling inhibition, although how this would improve cell viability as observed in this study is not clear (Lee D et al., 2021). It has also been shown to alter stem cell lineage specification and lead to an increase in trophoblast differentiation in embryos following exposure (Fedorov et al., 2015), how this mode of action would promote cell viability is also unclear although it may be the result of altered gene expression as suggested by the compounds ability to effect trophoblast differentiation.

SGC 0946 Is a DOT1L histone methyltransferase inhibitor, it has been shown to have no effect on T cell proliferation (Kagoya et al., 2018) but has been shown to increase cell apoptosis in cancer cell lines (Du and Zhang, 2022; Vlaming et al., 2019). How this reduction in methyltransferase activity would promote cell survival is unclear as the inhibition of other methyltransferase enzymes has been shown to increase apoptosis (Nakatsuka et al., 2021; Zhu et al., 2001).

(R)-PFI2 HCL is a SETD7 inhibitor, a gene responsible for histone-lysine methyltransferase activity as well as being involved in regulating the tumour suppressor gene p53's binding activity (Batista and Helguero, 2018). My observation that inhibition of SETD7 promotes cell viability contradicts the findings of Chen et al., (2016), who found that increased SETD7 expression increased cell proliferation. It could however be that by reducing p53 activity, p53-dependent apoptosis is inhibited. A more targeted investigation would be needed to determine if this is indeed the mode of action promoting a decrease in apoptosis (Komarova and Gudkov, 2000).

UNC 1999 is another lysine methyltransferase inhibitor, selective for EZH1/2. EZH1/2 proteins are responsible for Histone H3 Lysine trimethylation and their inhibition has been shown reduce

proliferation in cancer cell lines (Honma et al., 2017). It is likely that UNC 1999's mode of action is similar to the other histone methyltransferase modulating compounds discussed, in that it alters gene expression due to its effect on chromatin.

The three remaining compounds BAY 598, A 395, and NI 57 all caused an increase in non-senescent cell death. BAY 598 is a selective inhibitor of the methyl transferase SMYD2 (Eggert et al., 2016). Like SETD7 mentioned above, SMYD2 has been associated with the p53 DNA binding pathway (Huang et al., 2006). While the full role of the protein methylating enzyme is not known, it could be proposed that the inhibition of any methyltransferase, especially one associated with a tumour suppressor pathway, could have a negative impact on cell survival due to their role in DNA repair. A 395 is an EED/PRC2 inhibitor. PRC2 is a gene, which like some of the other genes discussed above, is a complex which has H3 lysine methyltransferase activity, the inhibition of which, as was discussed in the case of SMYD2, could have a negative impact on cell viability. Increased PRC2 activity has been observed in cancerous cells (Chen et al., 2021), with its expression believed to foster a stem cell like proliferative phenotype(Stafford et al., 2018). It is possible then that inhibiting PRC2 may be preventing some proliferation, therefore increasing the proportion of apoptotic cells within the total population. NI 57 is a BRPF bromodomain inhibitor (Igoe et al., 2017). BRPF has been shown to be upregulated in some cancers, and is the key upstream regulator for several oncogenes (Cheng et al., 2021). If its upregulation is associated with aberrant cell survival, it follows that inhibition may increase cell deaths.

Given that many of these research compounds are newly developed, how they are promoting cell survival remains unknown, with more targeted research needed to elucidate their downstream effects.

Caused a significant increase in non-senescent cell viability

Compound ID	Compound description	Target protein function
UNC 1999	EZH2/EZH1 inhibitor	Maintains repressive chromatin via trimethylation of histone H3 (Margueron et al., 2008).
SGC 0946	DOT1L inhibitor	H3 Histone methyltransferase, implicated in transcription and DNA repair (Kari et al., 2019).
(R)-PFI2 HCL	SETD7 inhibitor	Enables histone-lysine N-methyltransferase activity and is an upstream regulator of p53 activity (Batista and Helguero, 2018).
PFI 3	SMARCA2/4 and polybromo 1 inhibitor	SMARCA2/4 is involved in chromatin remodelling and repair. Polybromo 1 also regulates chromatin remodelling and is a tumour suppressor gene (Kargbo, 2020).

Caused a significant decrease in non-senescent cell viability

Compound ID	Compound description	Target protein function
NI 57	BRPF bromodomain inhibitor	A multivalent chromatin reader which plays a role in epigenetic regulation via the regulation of acetyltransferases (Yan et al., 2017).
BAY 598	SMYD2 inhibitor	A methyl transferase which methylates histone H3 and other nonhistone proteins. SMYD2 dysfunction and inappropriate expression is present in diseases such as cancer and heart disease (Yi et al., 2019).
A 395	EED inhibitor	Plays a role in epigenetic gene repression and cell development as part of a complex which has a histone methylating ability (Imagawa et al., 2017).

Caused a significant increase in senescent cell viability

Compound ID	Compound description	Target protein function
GSK 864	IDH1 inhibitor	Involved in energy production, namely in the Krebs cycle as well as maintaining cell homeostasis due to its ability to catalyse the oxidative decarboxylation of isocitrate (Han et al., 2020).
A 485	Inhibitor of HAT p300/CBP	A family of histone acetylation proteins (Luan et al., 2015).
OF 1	BRPF1B and BRPF2 inhibitor	Subcomponents of multivalent chromatin reader which plays a role in epigenetic regulation via the regulation of acetyltransferases (Mishima et al., 2011).
GSK LSD	LSD1 Inhibitor	Functions as a transcriptional regulator via demethylation. It plays a role in inflammation as well as in several disease pathologies (Kim et al., 2021).
MRK 740	PRDM9 inhibitor	A DNA binding protein which regulates meiotic recombination as well as histone and other protein methylation (Grey et al., 2018)

Caused a significant decrease of SA-βGal positive cell %

Compound ID	Compound description	Target protein function
MS049 OS	PRMT4 & 6 inhibitor	Modulates the accessibility of genes via chromatin remodelling (Nakayama et al., 2018).
BI 9564	BRD9/7 inhibitor	Involved in the restructuring of chromatin and is an oncogene regulator. (Drost et al., 2010; Chen et al., 2021)
NVS-CECR2-1	BRD CECR2 inhibitor	Plays a major role in the regulation of transcription via chromatin remodelling and acetylation (Josling et al., 2012).

Caused both a significant increase in senescent cell viability and decrease in SA-βGal positive cell %

Compound ID	Compound description	Target protein function
BI 9321	NSD3 inhibitor	A histone 3 and transcription regulation protein (Han et al., 2018; Shrestha et al., 2021).

Table 4.4: Targets of compounds which influenced cell apoptosis or the percentage of SA-βGal positive dermal fibroblast cells. A table showing the molecular targets of all compounds which altered cell viability or the percentage of A-βGal positive cells, the proposed mechanism of action for each compound and the function of the proteins they are affecting.

Compounds GSK 864, A485, OF 1, GSK LSD and MRK 740 increased the non-apoptotic cell percentage in the senescent cell culture, their mode of action is shown in Table 4.4. Compounds which increased the number of non-apoptotic senescent cells but had no impact on the percentage of SA-βGal positive senescent cells may be impacting one facet of the senescent phenotype. Senescent cells are already relatively apoptosis-resistant and senolytics act by targeting anti-apoptotic pathways (Kirkland and Tchkonia, 2015; Zhu et al., 2015), here these agents may further enhance this anti-apoptotic aspect of cell senescence.

Another possibility could be that these compounds are increasing the rate of proliferation of non-senescent cells within the senescent cell culture, as at day 12 only ~70% of the cells were senescent. However, these compounds increased the percentage of non-apoptotic cells without changing the percentage of SA-βGal positive cells, something which would change if the proportion of non-senescent cells within the senescent group increased. Also, none of these compounds showed any effect when used on the non-senescent cells (Table 4.2). This tends to support the conclusion that the compounds are in some way altering the anti-apoptotic senescent phenotype rather than increasing the non-senescent cell numbers within the culture.

GSK 864, a compound which improved cell viability in the senescent cells selectively targets and inhibits isocitrate dehydrogenase 1 (IDH1) (Dimitrov et al., 2015). IDH1 is an enzyme which has the primary function of catalysing the oxidative decarboxylation of isocitrate during the TCA cycle. This decarboxylation of isocitrate also forms, as a by-product, α-ketoglutarate and reduces NADP+ to NADPH. This process evolved to limit the impact of oxidative damage in response to ROS (Molenaar et al., 2014), as such inhibition of this process would be expected to reduce cell survival. Mutant IDH1 expression has also been shown to cause downstream accumulation of misfolded collagen which promotes a pro-apoptotic phenotype within cells (Dimitrov et al., 2015). While the interference in the TCA cycle does not appear to offer an explanation as to how this compound is increasing cell viability It may be that the ionising radiation has caused a mutation within the gene body of IDH1 within some

cells, and that by inhibiting its activity, GSK 864 is preventing the downstream effects and avoiding, or reducing, a pro-apoptotic phenotype.

OF-1, which improved cell viability of senescent cells inhibits BRPF1&2, a bromodomain-containing protein (Igoe et al., 2017). BRPF1&2 form part of MOZ/MORF histone acetyltransferase machinery which regulates transcription. Including target gene RUNX2 (Ullah et al., 2008). RUNX2 plays a role in delaying cell proliferation by limiting the ability of the cells to enter S phase of cell cycle, as shown in human osteosarcoma cell lines (Lucero et al., 2013). It may be that by inhibiting this negative regulatory protein that senescent cells are becoming less apoptosis-prone although the exact mechanism behind this change remains unclear.

Of the compounds which affected the senescent cells, those which only affected cell viability, all increased the percentage of non-apoptotic cells. Of these compounds GSK LSD, MRK 740 and BAY 6035 all have targets which impact transcription via methylation or demethylation of histones or chromatin organisation (Allali-Hassani et al., 2019; Gradl et al., 2021; Hong et al., 2020). It is well established that chromatin organisation and meta-structure are dependent on a large number of different post-translational histone modifications including acetylation, methylation, and de-methylation (Javaid and Choi, 2017). GSK LSD specifically targets LSD1, a demethylase enzyme. LSD1 is overexpressed in multiple cancers. When LSD1 is inhibited in conjunction with HDAC it has actually been shown to increase cell apoptosis, the opposite of what was observed in this study (Haydn et al., 2017), although when inhibited on its own Haydn et al., 2017 found that LSD1 inhibition had no cytotoxic impact on cancerous cells. This, while not supporting the findings here of LSD1 inhibition providing a survival benefit, does show that LDS1 inhibition is at least not cytotoxic. MRK 740 inhibits H3K4 histone modification via PRDM9 (Allali-Hassani et al., 2019). The PRDM family of proteins have been hypothesised to play an anti-cancer role, influencing proliferation. While not all members of the PRDM family have been fully characterised, the overexpression of some members has been shown to induce cell cycle arrest and apoptosis (Fog et al., 2012). It may follow then that the inhibition of these

proteins may prevent cell apoptosis, and result in the increased cell viability seen in the senescent cells. BAY 6035 is a SMYD3 inhibitor, a protein which is involved in gene regulation (Gradl et al., 2021). Within the cancer environment, SMYD3 expression is believed to prevent apoptosis and encourage proliferation and migration via hypermethylation of the RIZ1 promoter region, whereas inhibiting SMYD3 prevents this method of survival promotion (Chen et al., 2007). How this would encourage cell survival within the senescent cells is unclear.

It is also known that chromatin is remodelled during apoptosis, becoming more condensed and compact (Füllgrabe et al., 2010) and all of the survival promoting compounds can disrupt the processes which enable this chromatin remodelling in some way. It may be that these compounds are reducing the percentage of cells which are able to enter apoptosis via off-target and downstream effects. It is unsurprising to see that all the compounds which had a pro-survival effect act through similar mechanisms, although how exactly these mechanisms impart this survival advantage remains unknown.

4.3.1.2 Compounds with a significant effect on SA-βGal positive senescent cells

Compounds MS049 OS, NVS-CERC2-1 and BI9564 all decreased the percentage of SA-βGal positive cells within the senescent cell culture. This was not due to the compounds simply causing apoptosis of the senescent cells and allowing any remaining non-senescent cells within the group to proliferate. This can be reasoned as none of these compounds showed any senolytic or cytotoxic effect in either the senescent or non-senescent cultures (Table 4.2). Whether these compounds in some way reverse the senescent cell phenotype or merely interfere with SA-βGal expression remains to be fully elucidated.

MS049 OS inhibits both PRMT 4 and 6 which are both methyltransferases (Lo Piccolo et al., 2019), playing a key role in transcriptional regulation and epigenetic modification. Like many of the other compounds previously mentioned, PRMT4 regulates transcription by binding to several transcriptional activators and methylating the H3 and H4 histones and increasing genomic accessibility for

transcription (Nakayama et al., 2018). It is possible that by modulating chromatin structure in this way expression of SA-βGal activity is reduced, this has been observed in the literature in oocytes and embryos where β-galactosidase activity is correlated with chromatin configuration, and therefore transcriptional activity (Edwards et al., 2015). It is also possible that the signalling pathways upstream in the senescence process are affected. Further work is clearly needed to determine which other aspects of cell senescence are modified by this agent.

BI 9564 Inhibits BRD9 and its ortholog BRD7 (Martin et al., 2016), both of which are bromodomain containing proteins. BRD7 is required for chromatin remodelling via the SWI/SNF chromatin remodelling complex and plays a vital role in embryonic stem cell differentiation (Kaeser et al., 2008). Another, perhaps more relevant function with regards to cellular senescence is BDR7's role in preventing uncontrolled proliferation. BRD7 is a positive regulator of the p53 pathway and is required for oncogene-induced cell cycle arrest (Drost et al., 2010; Chen et al., 2021). Knowing that BRD7 plays a role in promoting oncogene-induced senescence, it is perhaps not surprising that inhibiting it may impact the senescent phenotype. It may be that by inhibiting the p53 tumour suppression pathway, that the cells have reverted to a less senescent phenotype, explaining the reduction in the percentage of SA-βGal positive cells.

NVS-CECR2-1 is a BRD family inhibitor (Park et al., 2020), as are many other compounds discussed here, it specifically targets CECR2 a gene believed to play a role in Cat Eye syndrome. Cay eye syndrome comprises a list of health conditions related to development such as cardiac defects, cleft palate and an eye deformity after which the condition itself is named, it is the result of an additional copy of chromosome 22 (Jafari-Ghahfarokhi et al., 2015). The effects of NVS-CECR2-1 in this study are more likely to be due to its inhibitory effects regarding the chromatin binding of this BRD protein (Park et al., 2020), and may act in a way similar to the other BRD inhibiting compounds mentioned above.

4.3.1.3 Compounds with a significant effect on the percentage of SA-βGal positive cells and on cell viability in senescent cells

BI 9321 was shown not to kill dermal fibroblasts and was the only compound shown to improve senescent cell viability and decrease the percentage of SA-βGal positive cells. BI 9321 is an NSD3 inhibitor which interferes with methyltransferase activity at histone H3 as well as transcription regulation more generally (Han et al., 2018; Shrestha et al., 2021). The NSD3 gene has also been identified as being related to Wolf-Hirschorn syndrome, a condition which stunts growth and as cell senescence is also important in embryonic development this may be relevant (Battaglia et al., 2015). NSD3 is also a regulator of MYC. MYC is an oncogene transcription factor first identified in cancer (Land et al., 1983) and has been shown to have a direct impact on increasing proliferation while elevated levels of MYC leads to an increased sensitivity to apoptosis (Hoffman and Liebermann, 2008; Melnik et al., 2019). It is possible that by inhibiting NSD3 senescent cells have been further de-sensitised to apoptosis, increasing cell viability. How impeding cell proliferation in non-proliferating senescent cells would impact the levels of SA-βGal expression is not clear. It appears that this modification of the epigenetic regulation within the senescent cells is in some way altering the senescent cell phenotype, improving cell viability, and decreasing SA-βGal and warrants greater study to elucidate the exact mechanism by which it is acting.

4.3.2 Does traumatic injury influence senescent cell numbers in skin

It appears that within burned injured skin the number of senescent cells, at least as characterised by being $p16^{INK4A}$ positive, increases in the first 14 days following injury. In some patients the raised percentage of $p16^{INK4A}$ positive cells within the tissue remains elevated 6-12 months later, while in others it declines by the time the long-term samples were collected. The observed initial increase is in line with our current understanding of the role senescent cells play within the wound healing process (Jun and Lau, 2010). Senescence occurs rapidly in local cells following injury to the skin, and promotes wound closure and healing through the secretion of PDGF-AA as part of the senescence associated secretory phenotype (SASP) (Demaria et al., 2014). It is also in agreement with literature showing that

exposure to increased temperatures induces a senescent phenotype in human dermal fibroblasts in vitro, characterised by an increase in SA-βGal positive cells, increased $p16^{INK4A}$ expression and increased SASP (Kerschbaum et al., 2021a).

It is possible that at the site of injury, even after the initial stages of wound healing are complete, senescent cells persist, which may drive the ageing process itself forward via the increased SASP and ROS output and creation of more senescent cells via the "senescent bystander effect" (da Silva et al., 2019). This may in turn contribute to the chronic proinflammatory pathology observed in burn injury (Mulder et al., 2021). Although it is worth noting that all burn injuries heal at different rates, depending on individual factors such as patient health as well as burn injury size, thickness and any associated surgical intervention (Monstrey et al., 2008), it is possible that these factors (i.e. the senescent bystander effect, proinflammatory nature of burn injury and ongoing wound healing and treatment) are also causing an increased presence of senescent cells in and around the site of the burn injury in the long-term.

While there was no increase in the percentage of senescent cells within non-burn injured tissues over time, the fact that it decreases over time may suggest that there may have been some elevation in the numbers of senescent cells in non-burn injured tissue at admission following burn injury. This perhaps may drive the large increase in proinflammatory cytokines and increase in ROS present following burn injury (Parihar et al., 2008), which as previously discussed, can cause non-senescent cells to become senescent. The alternative hypothesis is that senescent cells were not elevated at admission and instead decreased following injury. There are several possible causes; one perhaps less obvious reason could be that following burn injury patients may find that they are spending more time inside and their burn site is bandaged. This would reduce their exposure to UV radiation from the sun, a known driver of cellular senescence, particularly in the dermis and epidermis of the skin (Debacq-Chainiaux et al., 2012; Domaszewska-Szostek et al., 2021). An alternative hypothesis is that the number of p16+ cells decreased as a percentage due to the increased presence of new proliferative cells, something

which occurs during wound healing and is associated with a reduction of p16, as p16 expression suppresses proliferation (Rayess et al., 2012), although this was not observed in every patient and the reduction of p16+ cells was only significant the non-injured skin. While the average percentage of p16 positive cells within the skin are hard to determine based on the literature, with some studies reporting the positive cell percentage by tissue layer, e.g., dermis & epidermis, the levels present in the biopsies analysed in this thesis do seem higher than what has previously been reported (Idda et al., 2020). There are several factors which could be responsible for the high level of p16 positive cells observed in the samples taken from the burn injured patients. One could be that the antibody in question was binding non-specifically, however the images presented in this chapter, along with the isotype control images, show clear and specific binding, with clear positive and negative cells in proximity. The other could be related to the patient cohort. Many of the patients who are recruited following burn injury have multiple co-morbidities. These often include alcohol and substance misuse disorders, metabolic diseases and mental health conditions, all of which have previously been associated with an increase in cellular senescence and accelerated ageing (Chen et al., 2017; Diniz et al., 2019; Palmer et al., 2022; Polho et al., 2015).

It was surprising however to find that there was no significant difference in the percentage of p16 positive cells present in the skin taken from injured and non-injured sites in the patients given the active role senescent cells play in wound healing, although this may be due in part to the large amount of variation observed between individuals.

To know more definitively how injury affects cellular senescence across the body more samples would need to be analysed and importantly more markers of cell senescence should be assessed as the use of only one senescence associated marker (p16) is a limitation. This is in addition to more markers of cellular senescence being used, to see if the increase observed was specific to p16 positive cells, or if the changes are also seen in markers such as γH2AX or p21 or investigating SASP specific markers (Bernadotte et al., 2016; Coppé et al., 2010; Macip et al., 2002).

Given that the percentages of p16 positive cells appeared to change over time following burn injury, and that senescent cells have a long term, detrimental impact on organisms (Robbins et al., 2021), developing methods of clearing senescent cells after the wound healing process is complete, may be a way to improve patient outcomes.

4.4 Conclusion

The data provided shows evidence that burn injury is sufficient to cause initial and long-term changes to the of $p16^{INK4A}$+ cell load within both injured and non-injured skin in burns patients. While more evidence is needed to establish if this corresponds to an increased senescent cell load more broadly across the body, if senescent cell numbers do remain elevated in patients following injury, they may be a potential target for senolytic or senescence modulating compounds as a means of improving patient outcomes.

The compound library employed here specifically contained compounds which were known or suspected to have an epigenetic effect. It is therefore perhaps unsurprising that while they all have different targets, many of them act through related mechanisms or pathways and were able to affect either cell survival positively or negatively. Interfering with chromatin modelling, histone modification, methylation, or transcription more generally, as well as some downstream effects impacting proliferation or apoptosis is a common mode of action. Despite this only a small number were able to modify the SA-βGal phenotype. As this was a pilot study it was not possible to determine mode of action of the compounds that affected either cell viability or SA-βGal expression and it will be important to follow this through and confirm these data. It will also be important to assess whether rother markers of senescent cells are modified by these compounds. Compound BI 9321 is particularly promising as a senotherapeutic. It is also important to determine if cells were truly rescued from senescence by examining proliferative capacity, SASP secretion, as has been demonstrated by others using resveratrol analogues or m-TOR inhibitors (Latorre et al., 2017; Walters et al., 2016). Further, it

will be interesting to see if these compounds also modulate senescence induced by oncogene overexpression or through replicative senescence to indicate broad therapeutic potential.

The compounds discussed above may be the next generation of potential therapeutic compounds for the modulation of the senescent phenotype, which may serve patients who experience an increased senescent cell load following injury, as suggested by this investigation.

5. Epigenetic age following critical illness

5.1 Introduction to epigenetics and DNA methylation

The research question addressed in this chapter is whether critical illness, caused by a traumatic injury or severe infection such as COVID-19, causes an acceleration in the ageing process assessed using an epigenetic approach. Epigenetics encompasses any factor which affects the expression of a gene, without altering the genome itself. Epigenetic methods of gene regulation come under three major categories: non-coding RNA action, histone modification and DNA methylation.

The ways in which histone modification modulates gene expression by controlling genomic access to transcriptional machinery are important, as are the ways in which non-coding RNAs act in a similar manner, and these are covered in chapter 1. However, the most relevant epigenetic modification to this study is DNA methylation. DNA methylation has been pioneered as a method of biological age estimation, as opposed to chronological age, since the pioneering papers of Horvath and Hannum in 2013 (Hannum et al., 2013; Horvath, 2013).

5.1.1 DNA methylation and ageing

There is a predictable change in the methylome with advancing age and the degree of methylation correlates highly with chronological age. Importantly the deviation from this association, described as “epigenetic age acceleration” is associated with increased mortality indicating that “epigenetic age” is a measure of the degree of biological ageing occurring in an individual (Gregory Hannum et al., 2013; Steve Horvath, 2013). These age-associated changes in DNA methylation have been termed ‘epigenetic clocks. Other groups have developed clocks which predict age based on DNA methylation changes associated with metabolic differences (Levine et al., 2018). The different epigenetic clocks used here are described below.

5.1.1.1 Measuring epigenetic age

All of the widely used epigenetic clocks, currently 15 reported, use Illumina array data, primarily due to the ubiquity of the Illumina platform within the field and the relatively low expense when compared to methylome sequencing. The Illumina Infinium platform is a bead chip array, with probes situated on the array itself which are complementary to specific regions within the genome (Illumina inc., 2012). By comparing the fluorescent signals generated by either methylated or unmethylated sites it is possible to build a detailed picture of the methylome.

5.1.1.1.1 The use of epigenetic clocks within research

All epigenetic clocks were developed on different datasets, meaning that they reflect different aspects of the ageing process. Horvath's clock is a measure of fundamental intrinsic biological age, as opposed to the Hannum and DNAm PhenoAge clocks which instead offer a more immune specific or reactive picture of ageing (Gibson et al., 2019), with the DNAm PhenoAge clock being closely related to mortality risk (Levine et al., 2018). By using one or more of these epigenetic clocks, it is possible to estimate a person's biological age, which can then be compared to the person's chronological age. When one is deducted from the other this is known as the epigenetic age "residual", "Δ Age", or age acceleration.

5.1.1.2 Critical illness and epigenetic age

It has been observed that those living to over 100 years have a younger epigenetic age compared to their chronological age (Horvath et al., 2015b). This can be interpreted as meaning that these long-lived people are not simply surviving to old age but are taking longer to reach biological old age. At the time of writing, we don't know if a well maintained methylome is the secret to a long and healthy life or if what we are seeing in these super-centenarians is in fact just a by-product of other well performing vital processes such as DNA repair. Regardless of the mechanism, a large meta-analysis of studies of time to death predictions based on DNA methylation concluded that epigenetic regulation

does play a key role in longevity (B. H. Chen et al., 2016) suggesting that epigenetics and longevity are intertwined.

5.1.1.2.1 The impact of injury and critical illness

Regardless of initial recovery, injury has been shown to increase the incidence of co-morbidities (Casey and Ballantyne, 2017) and increase long term mortality (Brooks et al., 2013; Davidson et al., 2011; Duke et al., 2017). This could suggest that biological age is accelerated after injury or critical illness. Despite these observations, so far there has been very little research investigating how injury impacts epigenetic age. There is also little known of the impact of a critical illness, whether as the result of injury or an infection.

Sepsis is one of the most well researched conditions which occurs in the critical care setting, with advanced age known to be the largest risk factor for poor outcomes (Pinheiro da Silva and Machado, 2017). Despite this, there is a paucity of research looking at whether sepsis affects the ageing process itself, especially from an epigenetic perspective. One study identified 241 loci, the methylation levels of which changed with age within a control group, 161 of these sites maintained their correlation with age within a group of patients with sepsis. The authors proposed that these genetic loci may play some role in explaining why age has such a negative impact on sepsis outcome (Lang et al., 2022). Fundamentally though, they did not investigate how sepsis affects the ageing process itself.

COVID-19 is caused by the coronavirus SARS-CoV2, a member of the SARS family of viruses. The previously most well-known SARS virus was the SARS-CoV virus, responsible for the “severe acute respiratory syndrome” which predominantly affected countries within Asia and which gave the family of viruses its name (Abdelrahman et al., 2020). Individuals who contract the SARS-CoV2 virus and develop COVID-19 can also become critically ill, with age the primary predictor of patient outcomes such as the need for intensive care and ventilation. A meta-analysis of 70 studies showed that age increased the risk of mortality by 7.4% per year, with no age cut off where this rate changed, showing age to be a risk factor at all stages of life (Starke et al., 2021). During sample collection for the data

presented in this chapter, two papers were published by other groups looking at COVID-19 and epigenetic age estimated by DNA methylation analysis. Contradictory conclusions were drawn in the two studies. One study used samples from 152 patients with severe and mild COVID-19 symptoms as well as some pre-pandemic healthy controls. They found there to be little difference between the groups for epigenetic age via principal component analysis following normalisation and saw no real evidence of higher epigenetic age in those with severe disease (Franzen et al., 2021). In contrast, another study showed evidence of higher epigenetic age and telomere attrition in 413 patients with severe or non-severe COVID-19 infection which was somewhat resolved at long term follow up (Cao et al., 2022). While both studies used the same illumina EPIC DNA methylation arrays, Cao et al., suggests that the differing results reported by the two group, may be due to the small sample size in some of the data sets used Franzen et al, as well as some potential differences in the way that the age estimations were used or other unknown differences in the datasets such as unreported or misreported CODIV-19 severity.

5.1.1.2 The long-term implications of detecting increased epigenetic age

As stated earlier, sustaining a major injury, or contracting a serious illness can have a lasting negative impact on a person's health ((Brooks et al., 2013; Davidson et al., 2011; Duke et al., 2017). Despite this, little clinical support is currently available to help change the trajectory of a person's health-span post-critical illness. We know that those injured at work are likely to go on to develop subsequent co-morbidities (Casey and Ballantyne, 2017). Individuals who experience a burn injury are likely to die younger and are more likely to develop heart disease and cancer (Duke et al., 2017, 2015a) yet little is done beyond treating each new disease as it arises. The question arises as to whether the poor long term health outcome of critically ill patients is the result of accelerated epigenetic ageing and if so could therapies shown to reduce epigenetic age (Fahy et al., 2019) be helpful in the future.

5.1.1 Aims of the chapter

The DNA methylation studies which make up this chapter aimed address several key research questions:

1: Does accelerated epigenetic ageing occur within the critical care environment?

2: Does insult severity impact the degree of epigenetic ageing?

3: How long does accelerated epigenetic ageing persist?

4: What is the impact of a changing methylome on patient outcomes?

To answer these questions, samples were taken at different time points and from different patient cohorts who had been in hospital, with or without the need for intensive care, either as the result of an injury or infection. The patient groups included in this study were:

- Patients with a burn injury: at admission (n = 53) and 6 months post injury (n = 34).
- Patients admitted to ICU with (n = 66) or without sepsis (n = 68) (secondary data analysis only).
- Patients with severe (n = 38) or moderate (n = 25) COVID-19.

5.2 Results

5.2.1 DNA methylation analysis

Acknowledgement: Some of the healthy control DNA methylation data were provided by Dr Thomas Nicholson.

5.2.1.1 DNA methylation analysis: Burns cohort

Within the Burns cohort DNA methylation analysis was performed on DNA from PBMCs isolated from whole blood.

5.2.1.1.1 Patient information

Table 5.1 details the clinical and demographic features of the burns patients who participated in the SIFTI I and SIFTI II studies. These studies were established to investigate the relationship between severe thermal injury and immune function over time. The studies were approved by UK research ethics committees, references 12/EM/0432 and 16/WM/0217 for SIFTI 1 and SIFTI II, respectively. Of the 53 patients making up the admission cohort, 45 had samples taken in under 24 hours following admission, with 8 being taken within 72 hours. For a detailed description of the inclusion/exclusion criteria as well as sample collection and consent details, see the methods section. For analysis all of the samples collected up to 72 hours have been grouped together and classified as "admission". Of those patients analysed, not all clinical information was available. The missing information is as follows, injury severity data: **APACHE**: 12 missing, **SOFA**: 9 missing, **TBSA**: 4 missing, and demographic data: **BMI**: 2 missing. The low mean length of stay (LOS) observed in the burns patients at admission cohort is due to the inclusion of patients who died following admission.

All the patients who were analysed at 6 months also had samples taken at admission, thus the paired analysis shown in this chapter consists of this 6-month cohort paired with their admission samples. Of those patients sampled at month 6 not all clinical information was available. The missing information is as follows, injury severity data: **APACHE**: 6 missing, **SOFA**: 3 missing, and demographic data: **LOS**: 1 missing.

At admission to the study the mean chronological age of the patients was 45.4 years, with a mean BMI of 26.6 and there was a preponderance of male patients (49M;4F). 13 patients did not survive their injury and died in hospital. The injuries were considerable with a mean TBSA of 35.7% and an rBaux score of 90.9 (rBaux of 120+ is considered probably not survivable). The mean LOS was 35.5 days. At the 6 month follow up 34 samples were obtained, and the mean age of patients was 40.9 years, and all were male, indicating an attrition of older patients and females, 3 of whom died, and one was lost

to follow-up. The mean BMI was similar at 26.3 but the TBSA of this group was lower (30.9%) with a lower rBaux score too (75.7).

Burns patients at admission

n	Age	F	M	Died	Survived
53	45.44 (16.43 - 85.76)	4	49	13	40

BMI	TBSA%	rBaux	APACHE	SOFA	LOS
26.65 (19.4 - 37.03)	35.70 (4 - 95)	90.97 (38.81 - 155)	27.70 (1 - 46)	6.68 (0 - 16)	35.54 (1 - 216)

Burns patients 6 months post injury

n	Age	F	M	Died	Survived
34	40.95 (16.95 - 74.73)	0	34	0	34

BMI	TBSA%	rBaux	APACHE	SOFA	LOS
26.37 (19.4 - 36.3)	30.91 (4 - 71)	75.70 (38.81 - 137.31)	18 (0 - 46)	4.80 (0 - 15)	43.82 (5 - 216)

Table 5.1: Cohort information for burns patients at admission and 6 months post injury: The table contains the number of patients in each group "n", the mean age, BMI, TBSA%, rBaux, LOS as well as APACHE and SOFA scores as well as the minimum and maximum values for each parameter. The table also contains the number of patients in each group who died or survived to out-patient status, as well as the patient's sex at birth with "F" for female and "M" for male. BMI = Body mass index; TBSA% = Total burn surface area (%); rBaux = Revised Baux score; APACHE = Acute Physiology and Chronic Health Evaluation; SOFA = sequential organ failure assessment score; LOS = Length of stay.

5.2.1.1.2 Burns: epigenetic age and chronological age

All of the epigenetic ages; DNAm PhenoAge (R = 0.73, p = < 4.4e-10, Spearman), Hannum (R = 0.85, p = 5.6e-16, Spearman) and Horvath (R = 0.86, p = < 2.2e-16, Spearman) showed a strong or very strong positive correlation with chronological age at admission (Figure 5.1**A**). This was also true of the epigenetic ages measured 6 months post injury; DNAm PhenoAge (R = 0.88, p = < 2e-08, Spearman),

Hannum (R = 0.92, p = < 2.2e-16, Spearman) and Horvath (R = 0.95, p = < 2.2e-16, Spearman) all showed a strong and significant correlation with chronological age (Figure 5.1**B**).

There was a significant acceleration in epigenetic age at admission of 6.2 years (p = 0.032, Paired Wilcoxon) according to the Horvath epigenetic clock, but a decrease in epigenetic age according to the DNAm PhenoAge clock of 19.6 years (p = 4.5e-07, Paired Wilcoxon) no change was detected using the Hannum clock (p=0.62, Paired Wilcoxon) (Figure 5.1**C**).

There was a significant epigenetic age acceleration of 6.04 years (p=5.2e-0.8, Paired Wilcoxon) at 6 months post injury according to the Horvath epigenetic clock and a trend towards an increase in epigenetic age by the Hannum clock (p=0.1, Paired Wilcoxon). There was again a decrease in epigenetic age of 22.87 years, (p = 1.2e-10, Paired Wilcoxon) according to the DNAm PhenoAge clock (Figure 5.1**D**).

The epigenetic age residuals, the difference between epigenetic and chronological age, of burns patients at admission showed a significant negative correlation with chronological age, showing greater age acceleration in the younger patients according to all epigenetic clocks; DNAm PhenoAge (R = -0.37, p = 0.0064, Spearman), Horvath (R = -0.37, p = 0.0069, Spearman), there was a stronger negative correlation between the Hannum age residual and chronological age (R = -0.62, p = 6.3e-07, Spearman) (Figure 5.1**E**). There was a moderate significant negative correlation between the amount of Hannum epigenetic age acceleration and chronological age 6 months post injury (R = -0.43, p = 0.013, Spearman) (Figure 5.1**F**).

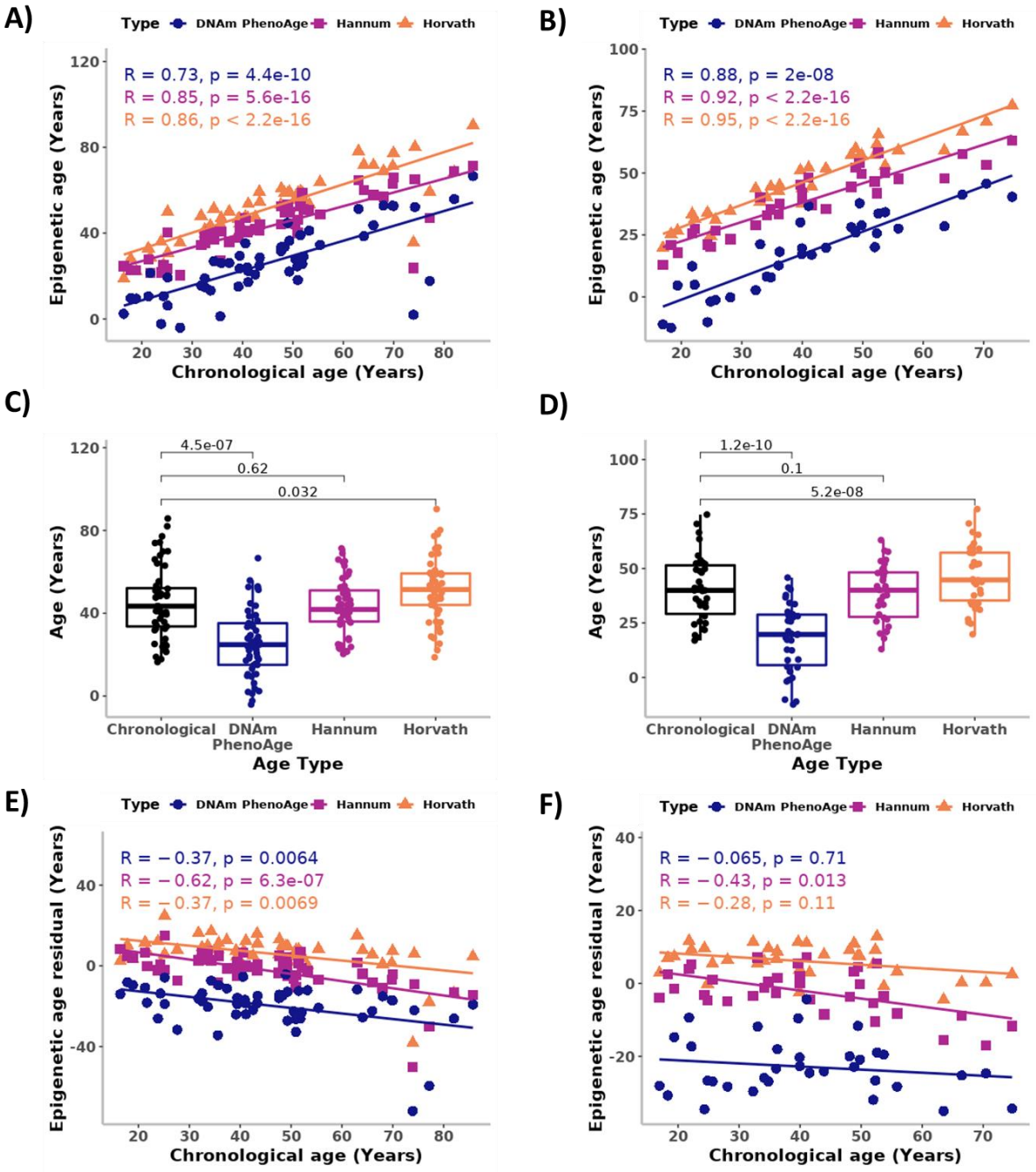


Figure 5.1: Epigenetic age analysis of burns patients at admission and 6 months post injury – This figure shows epigenetic age data following admission to hospital with burn injury (n = 53) and 6 months post injury (n = 34). Each point is one patient. **A** (admission) and **B** (month 6) show the correlation between chronological age and DNAm PhenoAge as well as Hannum and Horvath epigenetic ages, **C** (admission) and **D** (month 6) show the difference between chronological and calculated epigenetic age. **E** (admission) and **F** (month 6) show the correlation between the epigenetic age residual (epigenetic age – chronological age) and chronological age. For each box plot the central line is median, the bottom line is the 1st quartile (Q1), the upper the 3rd quartile (Q3). The whiskers represent calculated minimum and maximum values using the interquartile range (IQR). Whiskers are calculated using the formula Q1 + 1.5 x IQR or Q3 + 1.5 x IQR.

A paired analysis of the epigenetic ages of patients was used to reveal if there was a change in epigenetic age between admission and 6 months post injury. Paired samples were processed at the same time. All clocks showed that patients had a higher epigenetic age following admission with burns injury than they did 6 months later, suggesting some resolution of the accelerated ageing. The DNAm PhenoAge clock showed that there was a significant reduction in epigenetic age from a mean age of 24.84 years at admission to 18.04 years 6 months post injury, a difference of 6.72 years (p=0.00011, Paired Wilcoxon, Figure 5.2**A**). The Hannum clock showed that there was a significant reduction in epigenetic age from a mean age of 41.54 years at admission to 38.78 years six months post injury, a difference of 2.75 years, (p=0.018, Paired Wilcoxon, Figure 5.2**B**). The Horvath clock showed that there was a significant reduction in epigenetic age from a mean age of 48.99 at admission to 46.98 6 months post injury (p=0.034, Paired Wilcoxon, Figure 5.2**C**), a difference of 2 years.

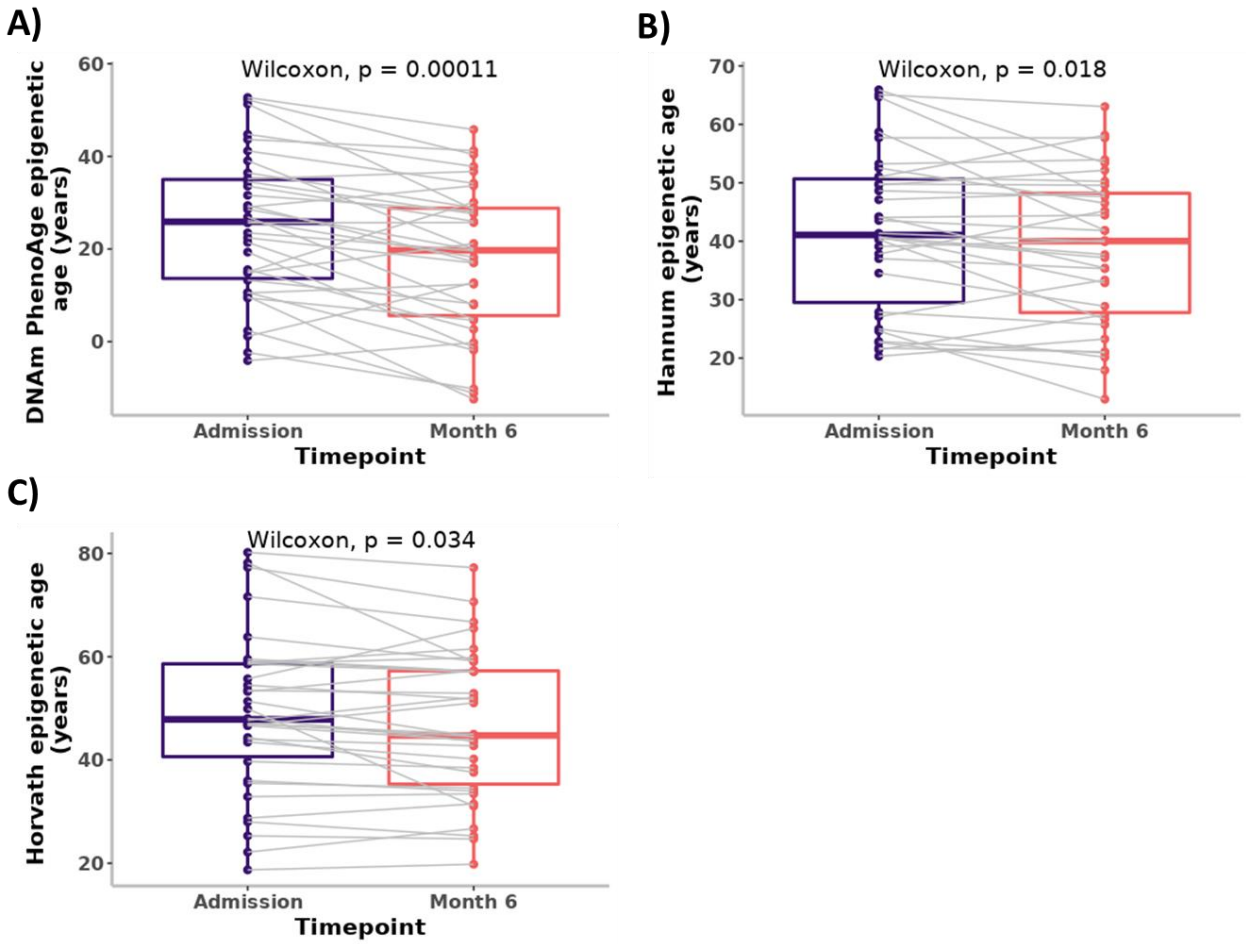


Figure 5.2: A paired comparison of epigenetic age at admission and 6 months post injury in burn injured patients. This figure shows paired epigenetic age data following admission to hospital with burn injury (n = 34) and 6 months post injury (n = 34) from the same individuals. **A** Shows the epigenetic age estimations of individuals at both time points according to the DNAm PhenoAge epigenetic clock. **B** Shows the epigenetic age estimations of individuals at both time points according to the Hannum epigenetic clock. **C** Shows the epigenetic age estimations of individuals at both time points according to the Horvath epigenetic clock. For each box plot the central line is median, the bottom line is the 1st quartile (Q1), the upper the 3rd quartile (Q3). The whiskers represent calculated minimum and maximum values using the interquartile range (IQR). Whiskers are calculated using the formula Q1 + 1.5 x IQR or Q3 + 1.5 x IQR.

Epigenetic age in burn injured individuals is higher at admission than 6 months post injury (Figure 5.3). To see if the epigenetic ages of burn injured patients returned to "normal", meaning the level of age accelerarion observed within the general population, the epigenetic ages of patients 6 months post injury were compared to an age and sex matched non-burn injured control group. The demographic information for the month 6 and healthy control groups are shown in Table 5.2. There was no significant difference in the epigenetic ages of the burn injured group 6 months post injury and a non-injured healthy control group according to the DNAm PhenoAge clock (Wilcoxon, p = 0.82) the Hannum clock (Wilcoxon, p = 0.94) or the Horvath clock (Wilcoxon, p = 0.87) (Figure 5.3).

	Month 6 post injury	Healthy control
n	34	24
Age	40.95 (16.95 - 74.73)	41.67 (19.65-78.00)
F	0	0
M	34	24
TBSA%	30.91 (4 - 71)	n/a
rBaux	75.70 (38.81 - 137.31)	n/a
APACHE	18 (0 - 46)	n/a
SOFA	4.80 (0 - 15)	n/a
LOS	43.82 (5 - 216)	n/a

Table 5.2: Cohort information for burns patients 6 months post injury as well as a healthy control population: The table contains the number of patients in each group "n", the mean age, TBSA%, rBaux, LOS as well as APACHE and SOFA scores where appropriate also shown are minimum and maximum values for each parameter. The table also contains the number of patients in each group who died or survived to out-patient status, as well as the patient's sex at birth with "F" for female and "M" for male. TBSA% = Total burn surface area (%); rBaux = Revised Baux score; APACHE = Acute Physiology and Chronic Health Evaluation; SOFA = sequential organ failure assessment score; LOS = Length of stay.

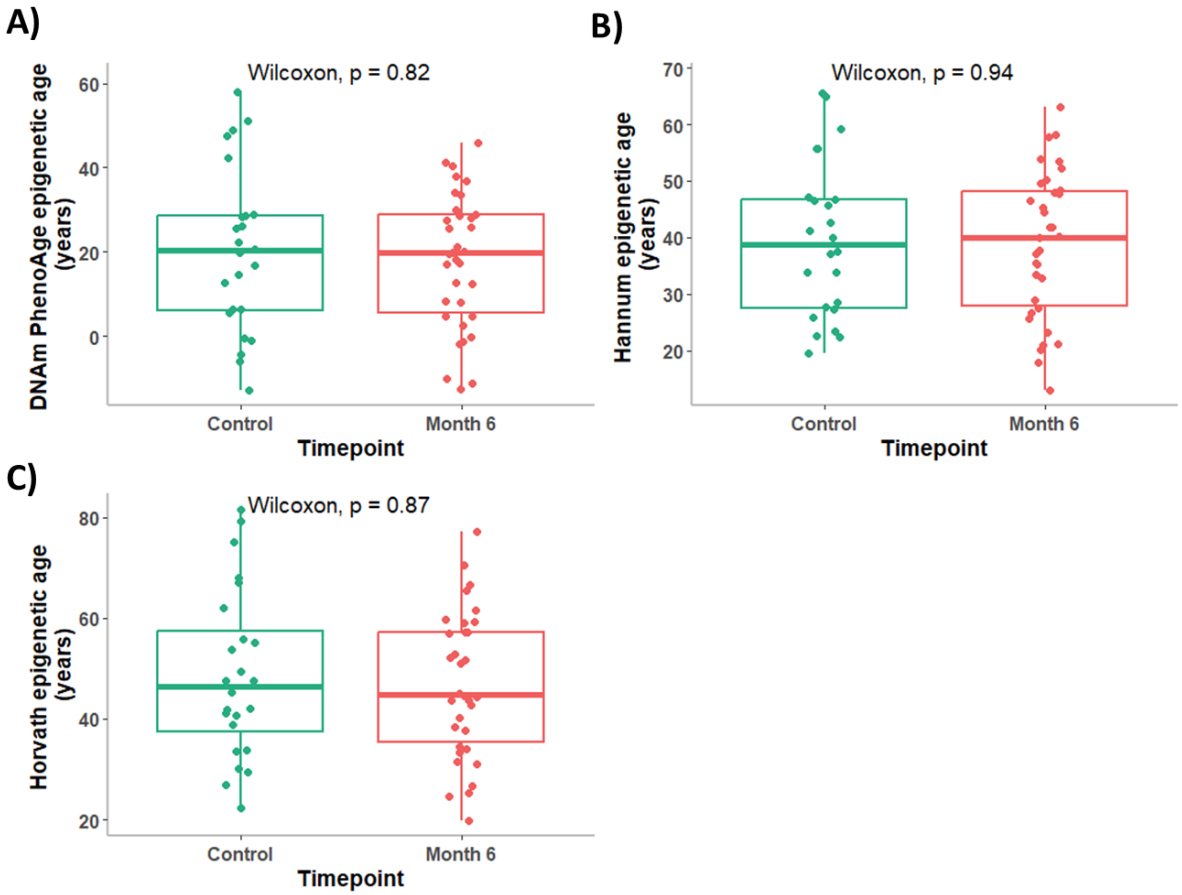


Figure 5.3: Epigenetic age 6 months post burn injury compared to healthy controls. This figure shows paired epigenetic age data 6 months post injury (n = 34) compared to healthy controls (n = 24). **A** Shows the epigenetic age estimations of burn injured individuals 6 months post injury and healthy controls according to the DNAm PhenoAge epigenetic clock. **B** Shows the epigenetic age estimations of burn injured individuals 6 months post injury and healthy controls according to the Hannum epigenetic clock. **C** Shows the epigenetic age estimations of burn injured individuals 6 months post injury and healthy controls according to the Horvath epigenetic clock. For each box plot the central line is median, the bottom line is the 1st quartile (Q1), the upper the 3rd quartile (Q3). The whiskers represent calculated minimum and maximum values using the interquartile range (IQR). Whiskers are calculated using the formula Q1 + 1.5 x IQR or Q3 + 1.5 x IQR.

The degree of epigenetic age acceleration quantified using the epigenetic age residual, meaning the difference between epigenetic and chronological age, of each patient was compared to several clinical parameters of interest, including BMI, TBSA%, injury severity scores and patient survival. At admission there was a significant negative relationship between the Hannum epigenetic age and rBaux ($p = 0.0048$, Spearman, Figure 5.4**D**), the relationship between DNAm PhenoAge and rBaux was approaching significance ($p = 0.071$, Spearman, Figure 5.4**D**). No other clinical parameters showed a correlation with epigenetic age residual at admission.

There was a significant weak positive correlation between epigenetic age acceleration and TBSA% in patients 6 months post injury using the DNAm PhenoAge clock ($p=0.049$, Spearman, Figure 5.5**C**). There were no other significant correlations between epigenetic age acceleration and any clinical marker (Figure 5.5).

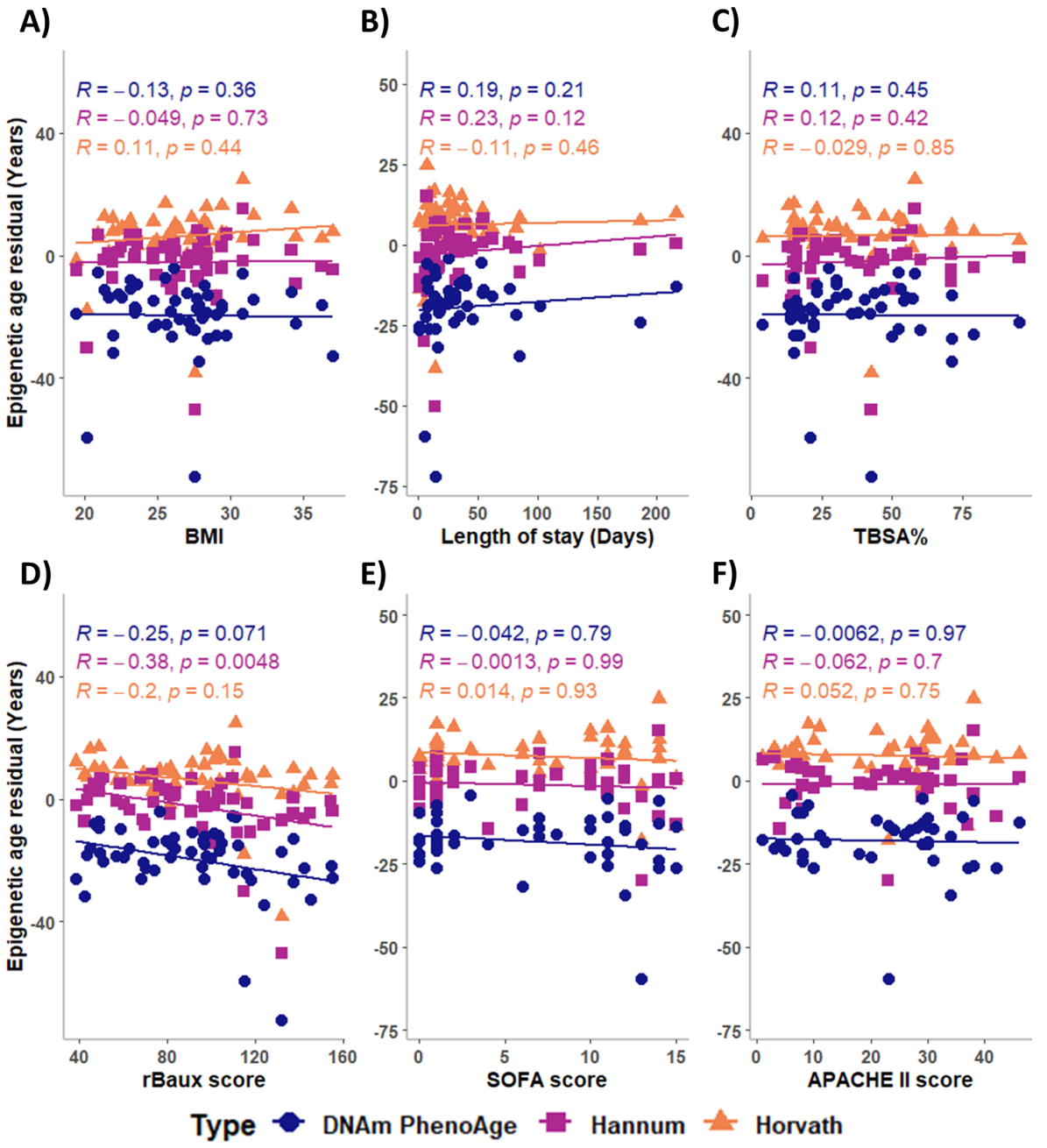


Figure 5.4: Comparison of burns patient epigenetic age residual at admission with several clinical parameters. This compiled figure shows the DNAm PhenoAge, Hannum and Horvath epigenetic age residuals of burn injured patients at admission (n = 53) compared with markers of interest; **A** BMI (n = 51), **B** Length of stay (n = 53), **C** TBSA% (n = 49), **D** rBaux Score (n = 53), **E** SOFA score (n = 44) and **F** APACHEII score (n = 41). BMI = Body mass index; TBSA% = Total burn surface area (%); rBaux = Revised Baux score; SOFA = sequential organ failure assessment; APACHE = Acute Physiology and Chronic Health Evaluation.

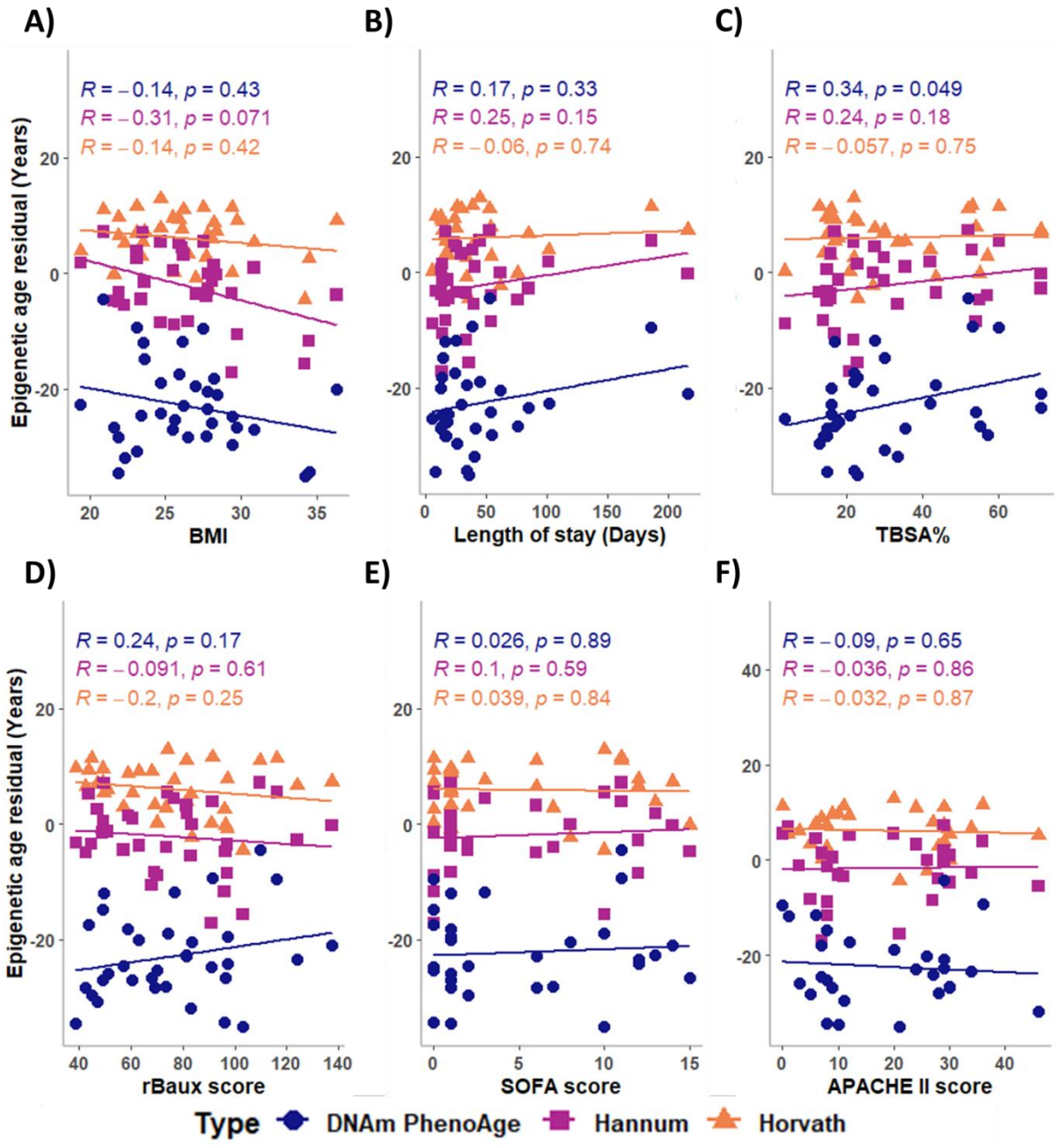


Figure 5.5: Comparison of burns patient epigenetic age 6 months post injury and several clinical parameters. This compiled figure shows the DNAm PhenoAge, Hannum and Horvath epigenetic age residuals of burn injured patients 6 months post injury (n = 34) compared with markers of interest; **A** BMI (n = 34), **B** Length of stay (n = 33), **C** TBSA% (n = 34), **D** rBaux Score (n = 34), **E** SOFA score (n = 31) and **F** APACHEII score (n = 28). BMI = Body mass index; TBSA% = Total burn surface area (%); rBaux = Revised Baux score; SOFA = sequential organ failure assessment; APACHE = Acute Physiology and Chronic Health Evaluation.

A comparison was made between the epigenetic age residuals at admission of patients who died compared with those who survived. The cohort information can be seen in Table 5.3. Some information for the patients was unavailable, the missing information for the patients who died is as follows, **APACHE**: 1 missing, **SOFA**: 1 missing, **BMI**: 1 missing. For patients sampled at admission who survived the missing data is, **APACHE**: 11 missing, **SOFA**: 8 missing, **TBSA**: 4 missing, **BMI**: 1 missing.

Burns patients who died following admission

n	Age	F	M	Time from admission to death (days)
13	53.99 (25.14 - 85.76)	3	10	11.55 (0.91 - 31.83)

BMI	TBSA%	rBaux	APACHE	SOFA	LOS
26.42 (20.13 - 31.60)	35.70 (14 - 79)	109.61 (79.49 - 155)	30.08 (4 - 42)	11.00 (4 - 15)	11.30 (1 - 31)

Burns patients who survived following admission

n	Age	F	M	Time from admission to death (days)
40	42.65 (16.43 - 74.23)	1	39	n/a

BMI	TBSA%	rBaux	APACHE	SOFA	LOS
26.72 (19.4 - 37.03)	33.80 (4 - 95)	84.92 (38.81 - 154.48)	18.27 (1 - 46)	5.06 (0 - 16)	44.53 (6 - 216)

Table 5.3: Table showing cohort information for burns patients who died following admission and those who survived: The table contains the number of patients in each group "n", the mean age, BMI, TBSA%, rBaux, LOS as well as APACHE and SOFA scores as well as the time from admission from death as well as the minimum and maximum values for each parameter. The table also contains the number of patients in each group who died or survived to out-patient status, as well as the patient's sex at birth with "F" for female and "M" for male. BMI = Body mass index; TBSA% = Total burn surface area (%); rBaux = Revised Baux score; APACHE = Acute Physiology and Chronic Health Evaluation; SOFA = sequential organ failure assessment score; LOS = Length of stay.

A comparison between the levels of epigenetic age acceleration between patients who died following admission compared with those who survived revealed that there was no significant difference in the epigenetic age acceleration present between the two patient groups (Figure 5.6).

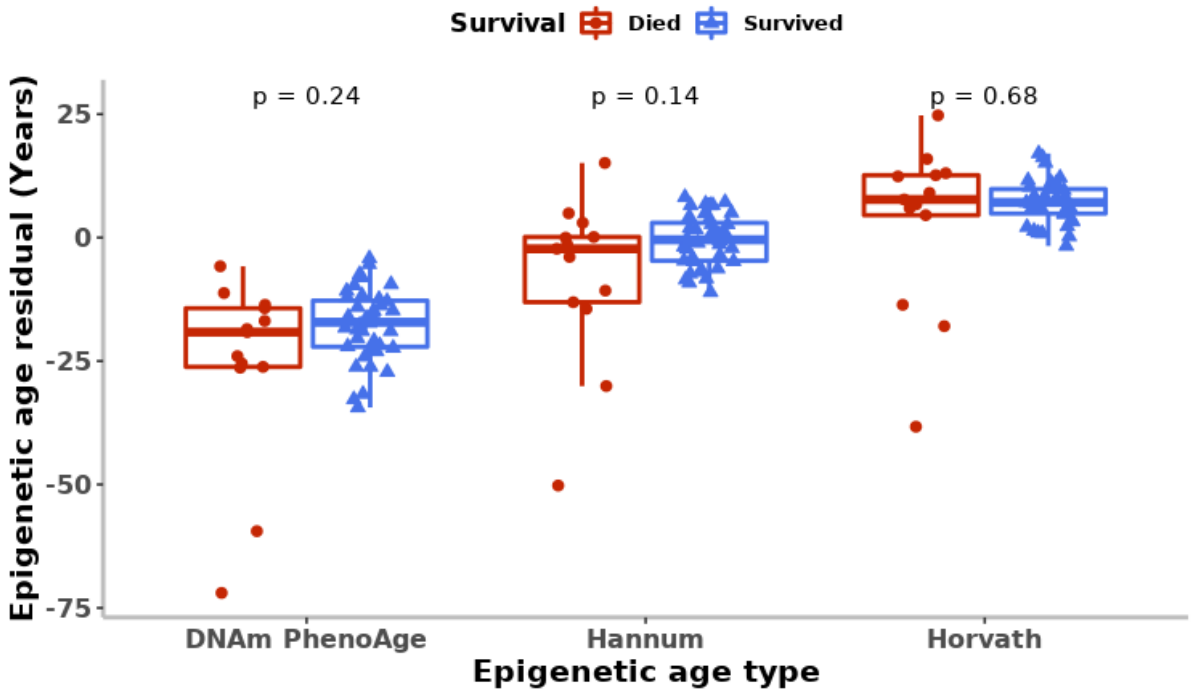


Figure 5.6: Comparison of difference in epigenetic age residuals at admission between burns patients who survived and those who died following admission. A box plot comparing the epigenetic age residuals at admission of patients who died (n = 14) compared with those who survived (n = 40). For each box plot the central line is median, the bottom line is the 1st quartile (Q1), the upper the 3rd quartile (Q3). The whiskers represent calculated minimum and maximum values using the interquartile range (IQR). Whiskers are calculated using the formula Q1 + 1.5 x IQR or Q3 + 1.5 x IQR.

5.2.1.1.3 Burns: differential methylation analysis

The methylation profiles of patients at admission were compared to those of patients 6 months post injury. Figures in this section show the most enriched pathways and each pathway's respective GeneRatio. A GeneRatio is a ratio of significant genes (cut off adjusted P value = < 0.01) compared with all genes which have an overlap in a specific pathway. The map plots show the relationship between the most enriched pathways, these are the pathways with the greatest numbers of associated genes differentially methylated between the admission and month 6 groups.

A pathway enrichment analysis was performed on the differentially methylated genes detected between all samples collected at admission and those samples collected 6 months post injury. A large number of significantly differentially methylated probes and corresponding genes were detected between the two groups, the 10 most differentially methylated are shown in Table A.5.1 (appendix). Subsequent pathway enrichment analysis showed no significantly enriched pathways when ignoring the log fold change of the levels of methylation present. Following this discovery, a slightly relaxed but still significant adjusted p value cut off was used (< 0.05) to generate Figure 5.7 which shows a map plot of the most differentially methylated pathways and their interactions between all admission and month 6 samples as well. These data were also used to generate Figure 5.8 which is a dot plot showing the 10 most differentially methylated pathways, the greatest of which is "Diseases of signal transduction by growth factor receptors and second messengers".

There was only one significantly enriched pathway when examining genes which showed an increase in methylation at admission when compared with the month 6 samples, this was the "Neuronal system" pathway (adjusted p value = 0.0019). Figure 5.9 shows the 10 most significantly enriched pathways when examining genes which showed a decrease in methylation at admission compared to month 6. Pathways most altered were those involved in the cell cycle, growth receptor signalling and transcription.

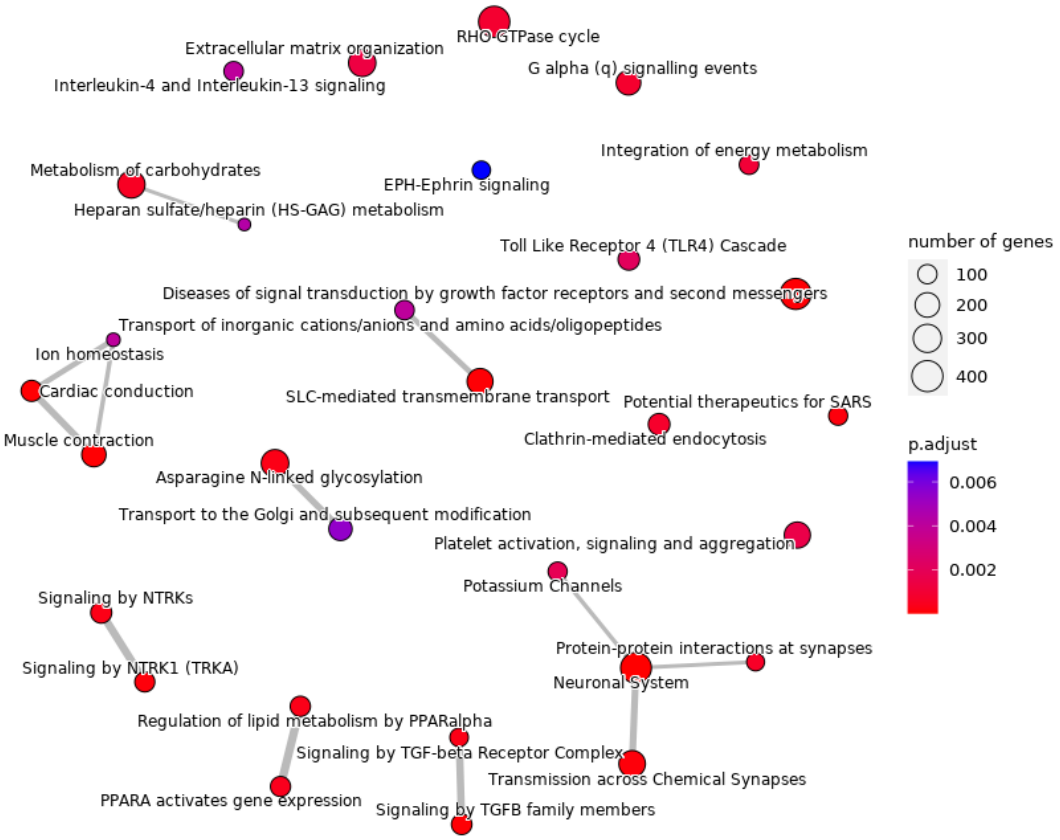


Figure 5.7: The most differentially methylated pathways between all patients at admission and all month 6 patients. A map plot showing the relationships between the most significantly differentially methylated pathways between all burn patients at admission (n = 53) and 6 months post injury (n = 34). Node size denotes the number of genes associated with a specific pathway, with increasing size reflecting as greater number, colour can also be seen to reflect the adjusted p value.

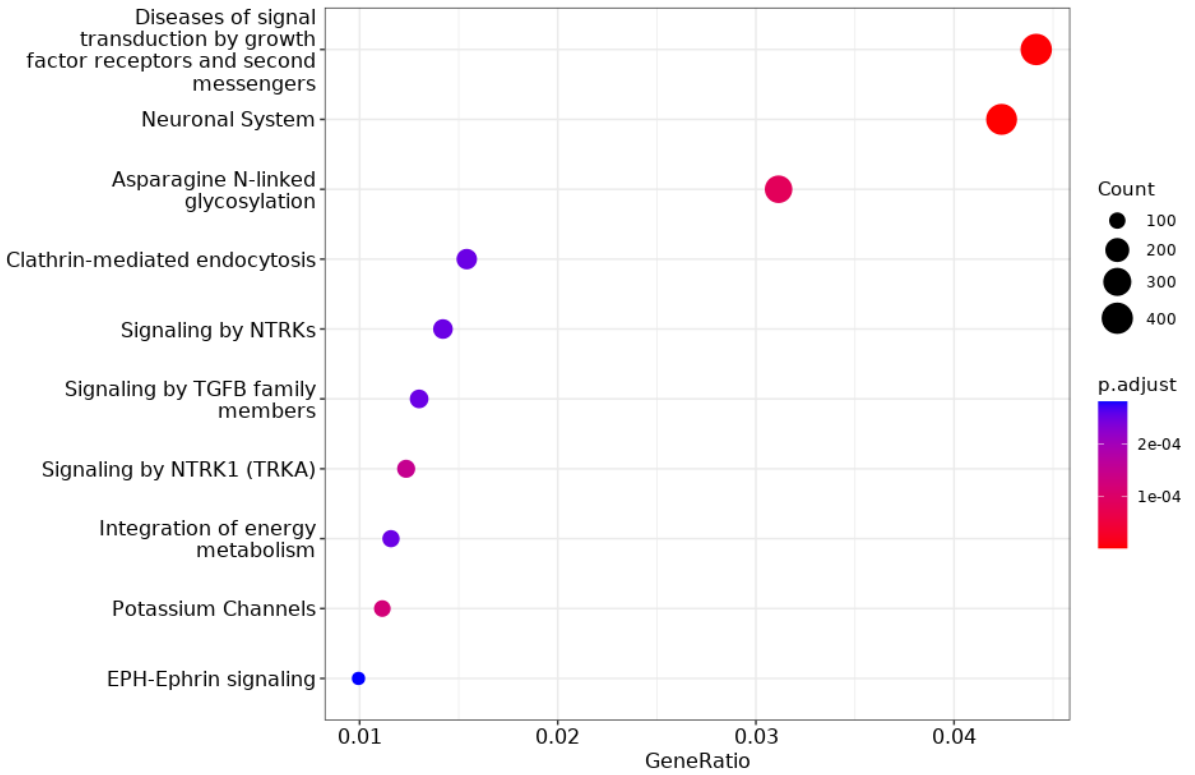


Figure 5.8: The most significantly enriched pathways of differentially methylated genes irrespective of fold change at admission compared with 6 months post injury when comparing all patients. Shown is a dot plot containing are the pathway name, gene count, gene ratio and adjusted p value for the 10 most significantly differentially methylated pathways between all patients at admission (n = 53) and 6 months post injury (n = 34).

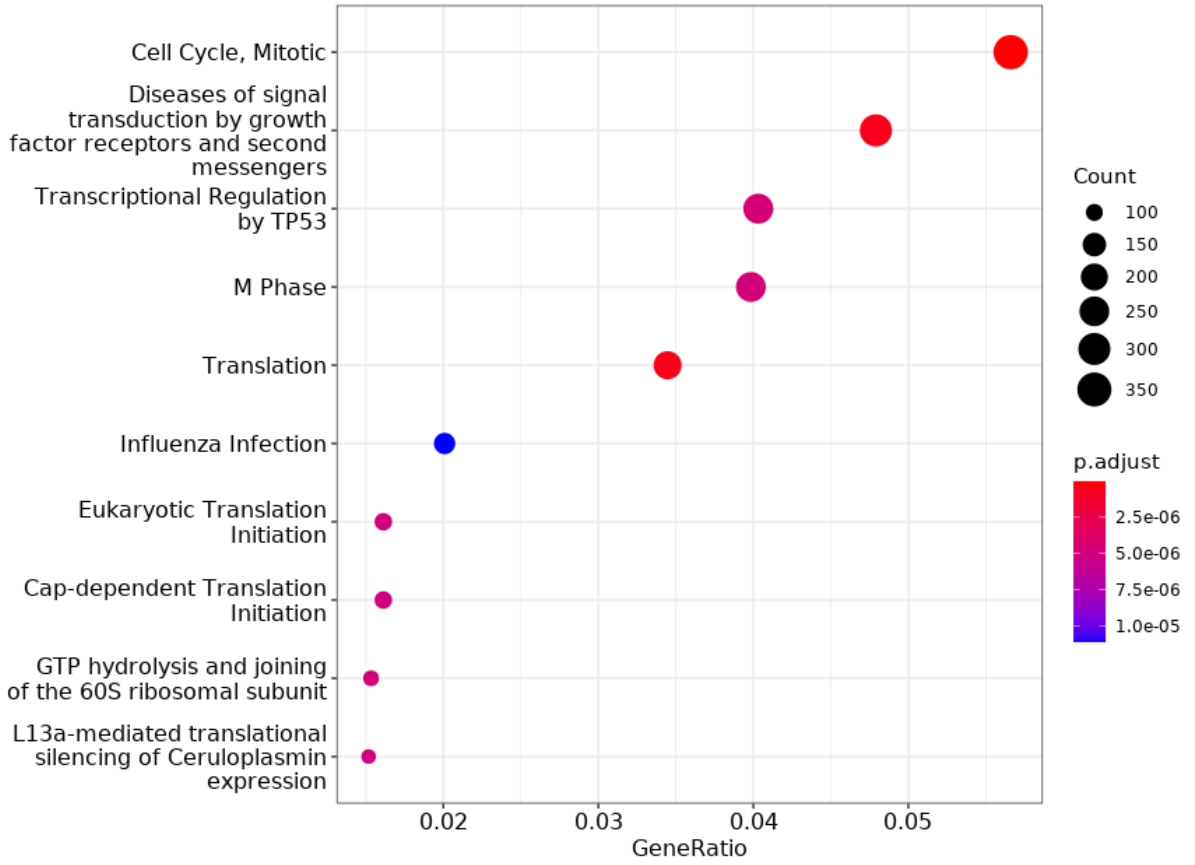


Figure 5.9: The most significantly enriched pathways of genes showing a negative fold change in methylation at admission compared with month 6 when comparing all samples. Shown is a dot plot containing the pathway name, gene count, gene ratio and adjusted p value of the 10 most significantly differentially methylated pathways between all patients at admission (n = 53) and 6 months post injury (n = 34) based on genes showing a negative fold change in methylation.

A pathway enrichment analysis was also performed on the differentially methylated genes detected in the same individuals at admission and 6 months post injury. The most significantly differentially methylated genes detected between the two time points related to 4 pathways following enrichment analysis, regardless of the direction of the fold change in methylation. These related to Rho GTPase, the neuronal system, RHO GTPase, and cardiac conduction (Figure 5.10) a map plot of these pathways and their relationships is shown in Figure 5.13.

The most significantly enriched pathways when examining genes which showed an increase in methylation in patients at admission when compared with month 6 are shown in Figure 5.11. These were dominated by tyrosine kinase signalling, RHO GTPase, the neuronal system, and ECM organisation. Figure 5.12 shows the 10 most significantly enriched pathways when examining genes which showed a decrease in methylation in patients at admission compared to month 6. Pathways for receptor tyrosine kinases, cell cycle, growth receptors and transcription dominated. With the pathways for receptor tyrosine kinases being the pathway experiencing the greatest increase and decrease in methylation.

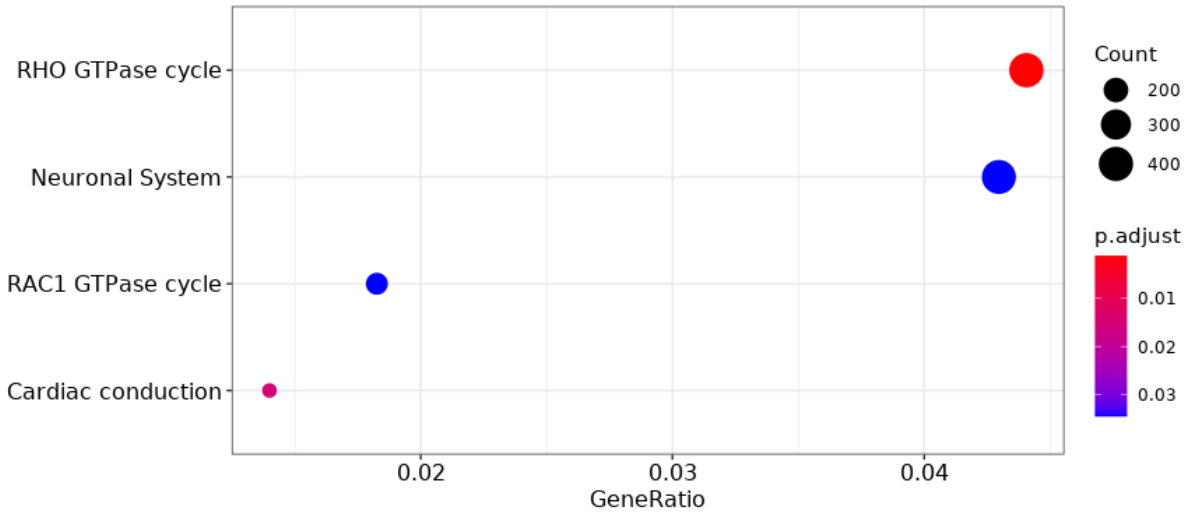


Figure 5.10: The most significantly enriched pathways of differentially methylated genes at admission compared with 6 months post injury in the same patients. Shown is a dot plot containing are the pathway name, gene count, gene ratio and adjusted p value for the most significantly differentially methylated pathways between the same individuals at admission (n = 34) and 6 months post injury (n = 34).

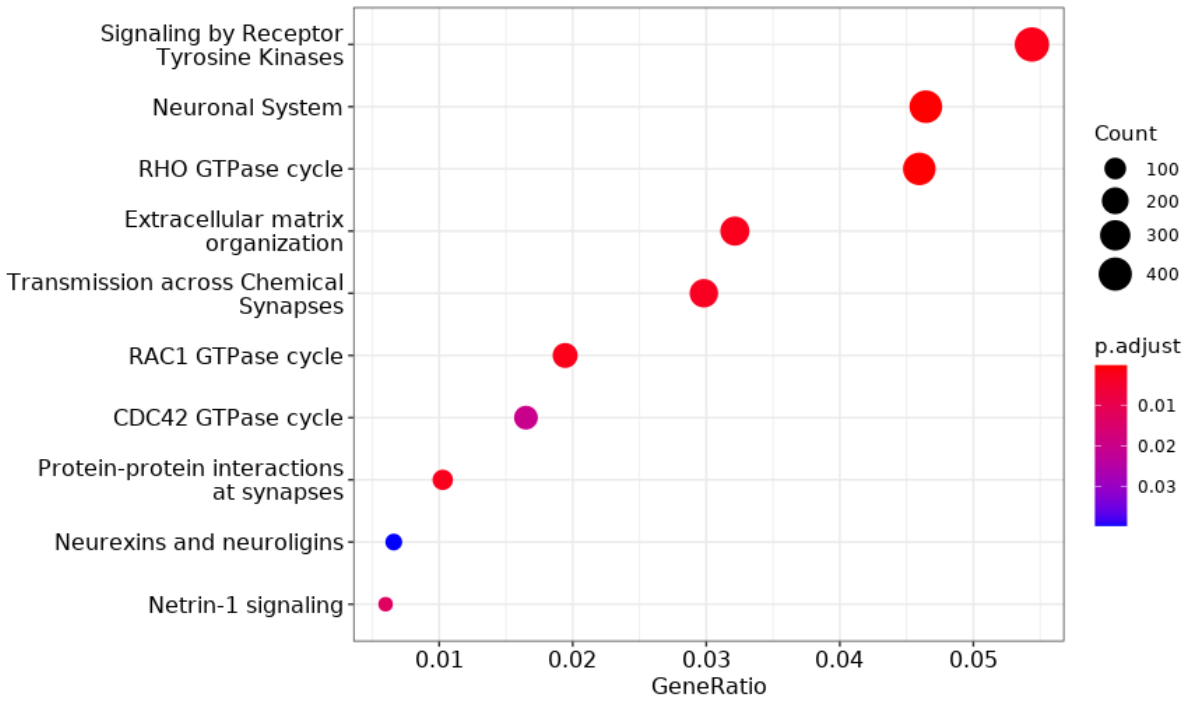


Figure 5.11: The most significantly enriched pathways of differentially methylated genes with a positive fold change at admission compared with 6 months post injury in the same patients. Shown is a dot plot containing are the pathway name, gene count, gene ratio and adjusted p value for the most significantly differentially methylated pathways in the same individuals at admission (n = 34) and 6 months post injury (n = 34) based on genes with a positive fold change.

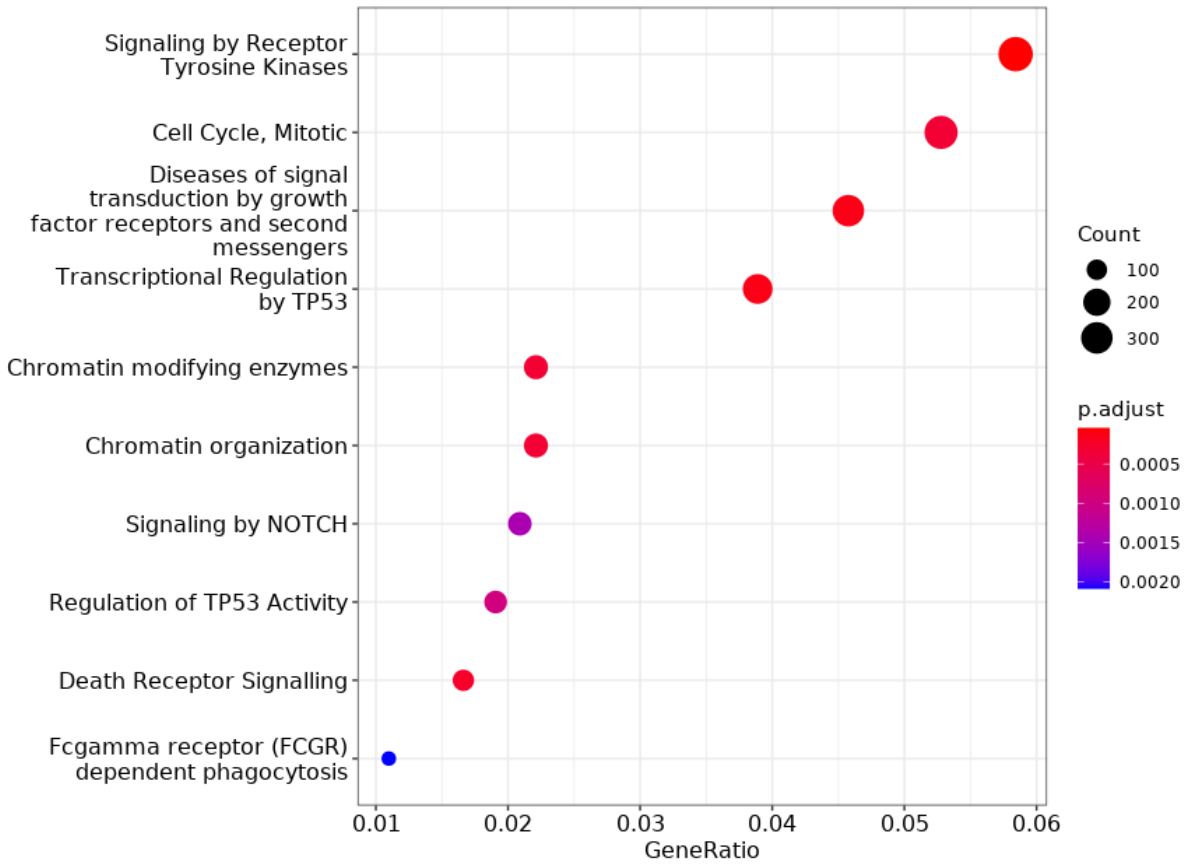


Figure 5.12: The most significantly enriched pathways of differentially methylated genes with a negative fold change at admission compared with 6 months post injury in the same patients. Shown is a dot plot containing are the pathway name, gene count, gene ratio and adjusted p value for the most significantly differentially methylated pathways in the same individuals at admission (n = 34) and 6 months post injury (n = 34) based on genes with a negative fold change.

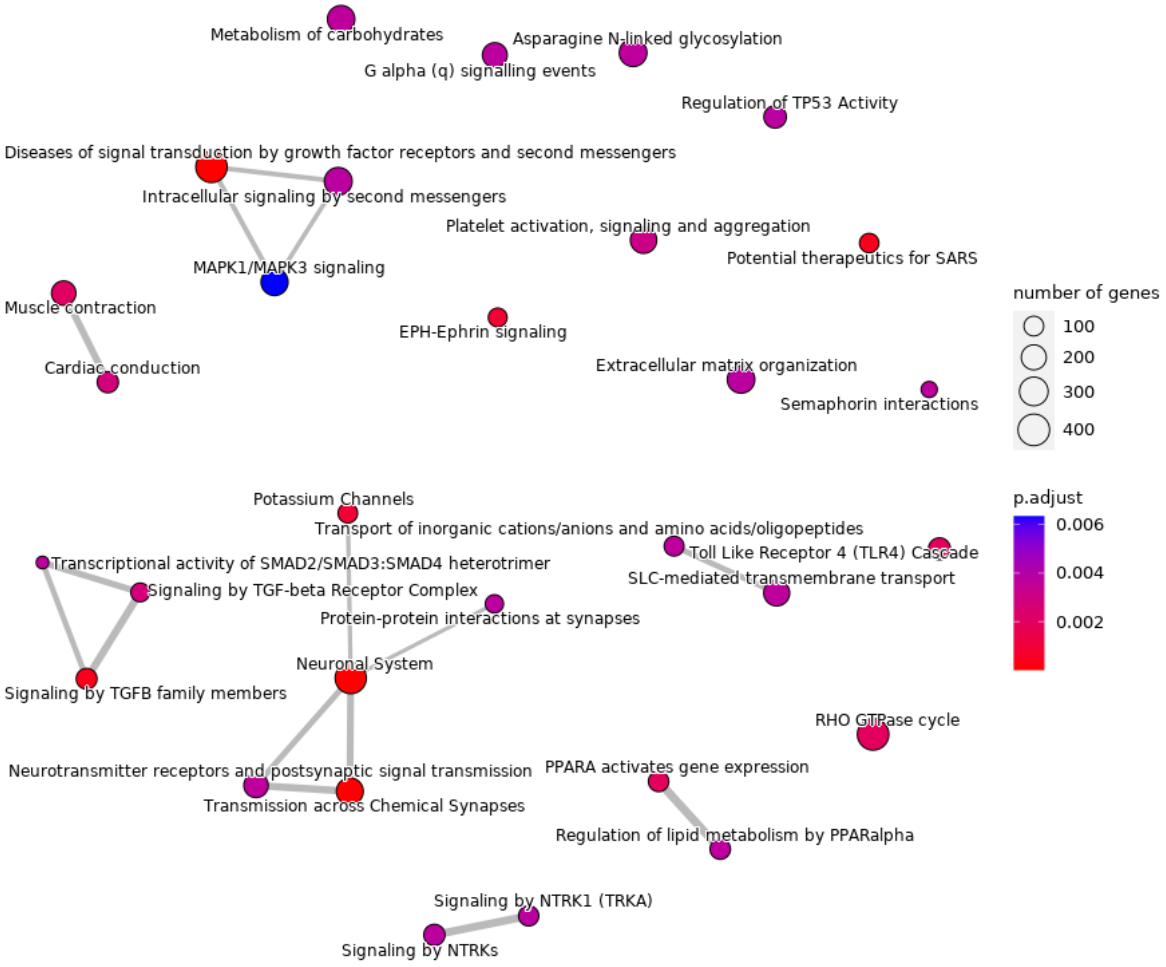


Figure 5.13: The most differentially methylated pathways between patients sampled at admission and again 6 months post injury. A map plot showing the relationships between the most significantly differentially methylated pathways between burn patients at admission and the same individuals 6 months post injury (n = 34). Node size denotes the number of genes associated with a specific pathway, with increasing size reflecting as greater number, colour can also be seen to reflect the adjusted p value.

5.2.1.2 DNA methylation analysis: Sepsis cohort

Acknowledgement: The raw data used in the in the analysis and comparison of septic and non-septic individuals was collected as part of the "Epigenetic Profiling in Severe Sepsis: A Pilot Study of DNA Methylation Profiles in Critical Illness" – Binnie et al., 2019. The raw data was provided by and used in collaboration with Dr Claudia dos Santo (Keenan Research Centre for Biomedical Science, St Michael's Hospital, Toronto, ON, Canada and the Institute of Medical Sciences and Department of Medicine, University of Toronto, Toronto, ON, Canada.) and Dr Alexandra Binnie (Department of Critical Care, William Osler Health System, Brampton, ON, Canada.).

5.2.1.2.1 Sample type

Within the sepsis cohort DNA methylation analysis was performed on DNA isolated from whole blood or buffy coat.

5.2.1.2.2 Patient information

Patient samples were collected as part of the "Epigenetic Profiling in Severe Sepsis: A Pilot Study of DNA Methylation Profiles in Critical Illness" (Binnie et al., 2019).

Septic patients were recruited to the study if they had a confirmed or suspected infection at the time of screening as well as at least one dysfunctional organ system and a minimum of 3 signs of systemic inflammatory response syndrome (SIRS) and were expected to be in the ICU for ≥ 72 hours. The non-septic patients were matched for age, illness severity (MODS scores) and number of survivors, though the proportion of males was higher in the non-septic cohort. The study protocol was approved by the research ethics boards of the participating institutions. Full inclusion/exclusion criteria and study information can be found in the methods chapter.

Shown in Table 5.4 are patient group numbers (n), 66 patients are in the septic cohort and 68 in the non-septic cohort. Also shown are the mean patient ages, multi-organ dysfunction scores (MODS) as well as ranges where appropriate. Also shown are the patient's sex at birth (M = male, F = female), the

numbers of patients who died and survived, as well the percentage of patients with a given co-morbidity. Shown also is the median length of stay (LOS) and interquartile range. The co-morbidity and LOS data were only available for the two patient cohorts as a group, not for each individual patient.

Septic ICU patients

n	Age	F	M	Died	Survived
66	65.03 (21 - 89)	30	36	25	41
				Comorbidities	
MODS < 9	MODS > 9	MODS	LOS	Cancer %	Immuno supression %
34	32	7.94 (0 - 17)	29 (26)	12.1	9.1

Non-septic ICU patients

n	Age	F	M	Died	Survived
68	64.93 (27 - 88)	21	47	25	43
				Comorbidities	
MODS < 9	MODS > 9	MODS	LOS	Cancer %	Immuno supression %
36	32	7.47 (1 - 14)	22 (20.5)	13.2	10.2

Table 5.4: Table containing septic and non-septic ICU patient cohort information. Listed are the number of patients in each group (n), the mean chronological age, the mean MODS score and the minimum and maximum values for each parameter are also included. Also included is the number of patients with a MODS less than or greater than 9, how many died following admission as well as how many survived. Also recorded is the sex at birth of the patients in each group "F" for female and "M" for male. Also included is the median length of stay and interquartile range as well as the percentage of patients with a given comorbidities. MODS = Multi Organ Disfunction Score; LOS = Length of stay.

5.2.1.2.3 Sepsis in the critical care environment: epigenetic age and chronological age

For the following analysis, a minfi RGChanellSet was provided in lieu of the raw IDAT files. The epigenetic ages of septic and non-septic ICU patients were calculated and then compared to parameters of interest. The correlation between epigenetic and chronological age was determined, as well as the difference between epigenetic and chronological age.

All epigenetic age estimates showed a significant strong positive correlation with chronological age in septic ICU patients; DNAm PhenoAge (R = 0.73, p = 7.9e-12, Spearman), Hannum (R = 0.73, p = 2.8e-12, Spearman) and Horvath (R = 0.69, p = 1.5e-10, Spearman) (Figure 5.14 **A**). Patients who were admitted to ICU without sepsis had a DNAm PhenoAge epigenetic age (R = 0.75, p = 1.2e-13, Spearman) which showed strong positive correlation with chronological age (Figure 5.14 **B**). The Hannum (R = 0.87, p = <2.2e-16, Spearman) and Horvath (R = 0.8, p = 3.8e-16, Spearman) epigenetic ages showed a very strong positive correlation with chronological age (Figure 5.14 **B**).

Both the DNAm PhenoAge and Hannum epigenetic ages were accelerated in septic ICU patients with a reduction in Horvath epigenetic age (Figure 5.14 **C**). There was a significant increase in DNAm PhenoAge epigenetic age of 6.37 years (p = 0.00011, Paired Wilcoxon) and Hannum epigenetic age of 6.91 years (p = 5.7e-07, Paired Wilcoxon) compared to chronological age. However, there was a modest but significant decrease in the Horvath epigenetic age of 2.5 years (p = 0.044, Paired Wilcoxon). In non-septic ICU patients, there was a significant increase in DNAm PhenoAge epigenetic age of 2.25 years (p = 0.047, Paired Wilcoxon) and Hannum epigenetic age of +4.68 years (p = 1.5e-06, Paired Wilcoxon) compared to chronological age. There was a significant decrease in the Horvath epigenetic age of -3.57 years compared to chronological age (p = 0.0013, Paired Wilcoxon) (Figure 5.14 **D**).

The epigenetic age residuals, meaning the difference between epigenetic and chronological age, were analysed for septic and non-septic ICU patients. There was a weak but significant negative correlation between epigenetic age residuals for Hannum (R = -0.25., p = 0.047, Spearman) and a stronger correlation for the Horvath clock (R = -0.32, p = 0.0087, Spearman). There was a greater amount of epigenetic age acceleration in the younger septic patients by both clocks. There was no significant correlation between the DNAm PhenoAge epigenetic age residual and chronological age (R = 0.059., p = 0.64, Spearman) (Figure 5.14 **E**). There was a significant weak negative correlation between the Horvath (R = -0.38., p = 0.0016, Spearman) epigenetic age residual and chronological age. There was a weak correlation between the DNAm PhenoAge epigenetic age and Hannum age residuals and chronological age nearing significance (R = 0.22., p = 0.072, Spearman and R = 0.22, p = 0.071, Spearman respectively) (Figure 5.14 **F**).

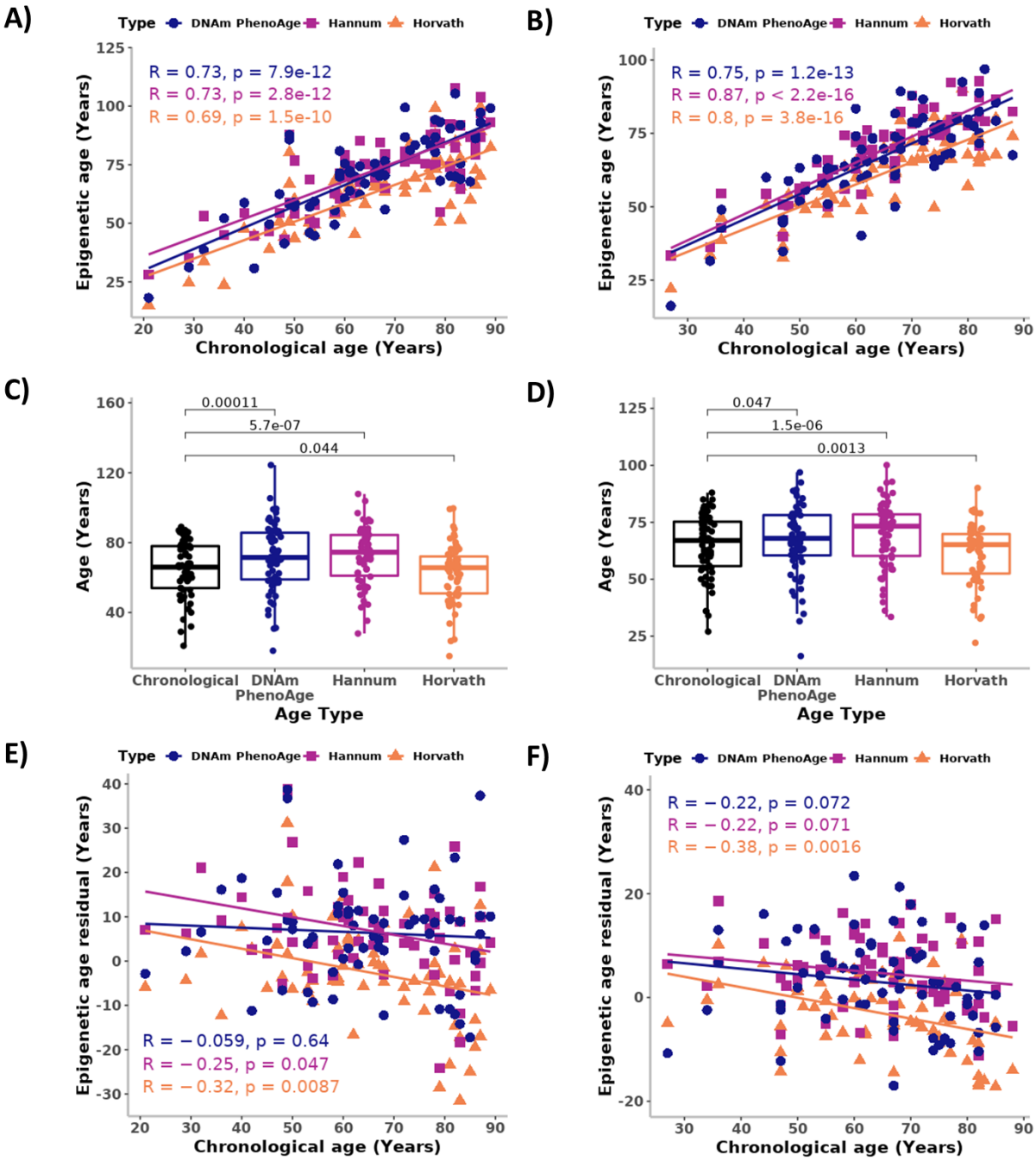


Figure 5.14: Epigenetic age analysis in septic and non-septic ICU patients – This figure shows epigenetic age data following admission to ICU both with sepsis (n = 66) and without sepsis (n = 68). **A** (septic) and **B** (non-septic) show the correlation between chronological age and DNAm PhenoAge as well as Hannum and Horvath epigenetic ages, **C** (septic) and **D** (non-septic) show the difference between chronological and calculated epigenetic age. **E** (septic) and **F** (non-septic) show the correlation between the epigenetic age residual (epigenetic age – chronological age) and chronological age. For each box plot the central line is median, the bottom line is the 1st quartile (Q1), the upper the 3rd quartile (Q3). The whiskers represent calculated minimum and maximum values using the interquartile range (IQR). Whiskers are calculated using the formula Q1 + 1.5 x IQR or Q3 + 1.5 x IQR.

There was a difference of 4.2 years between the mean DNAm PhenoAge epigenetic age acceleration between the septic (+6.3 years) and non-septic (+2.59 years) patients, (p=0.034, Wilcoxon). There was a non-significant difference of 2.33 years in the mean Hannum epigenetic age acceleration of septic (+6.91 years) patients compared to non-septic (+4.68 years) patients (p=0.156, Wilcoxon). There was also a non-significant difference of 1.15 years between the Horvath age deceleration present in septic (-2.52 years) compared with non-septic (-3.57 years) patients, (p=0.592, Wilcoxon) (Figure 5.15).

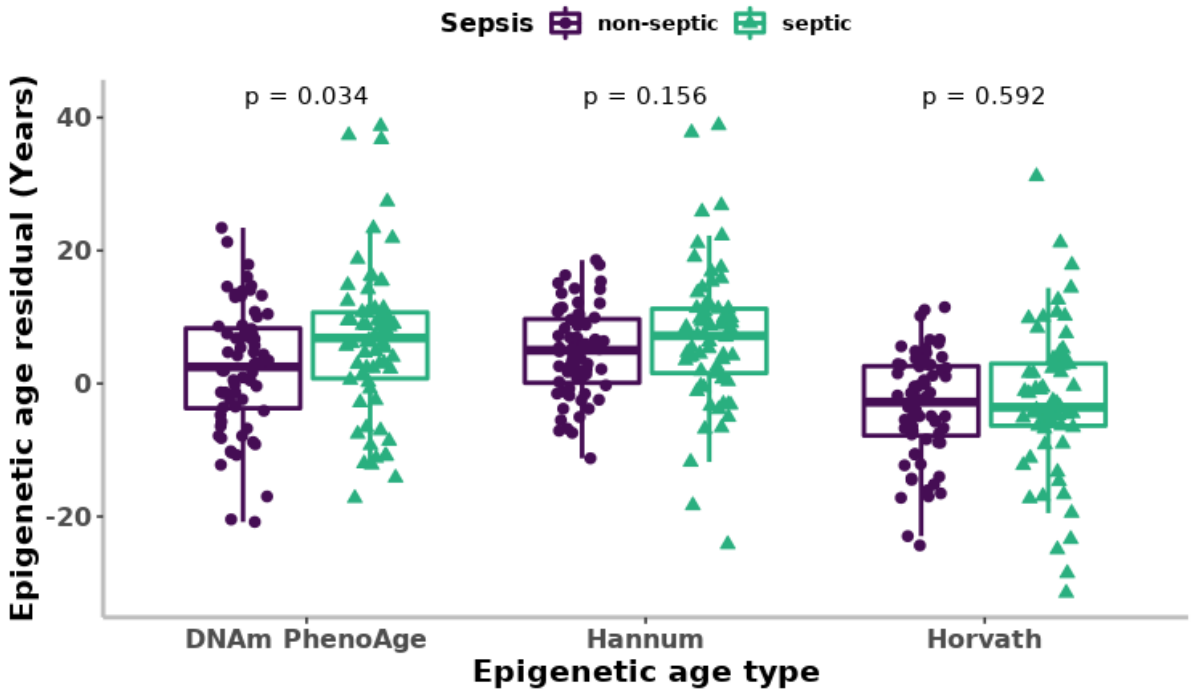


Figure 5.15: Comparison of difference in epigenetic age residuals between non-septic and septic ICU patients. A boxplot showing a comparison of the epigenetic age residuals (epigenetic age – chronological age) of septic (n = 66) and non-septic (n = 68) patients according the DNAm PhenoAge, Hannum and Horvath epigenetic clocks. For each box plot the central line is median, the bottom line is the 1st quartile (Q1), the upper the 3rd quartile (Q3). The whiskers represent calculated minimum and maximum values using the interquartile range (IQR). Whiskers are calculated using the formula Q1 + 1.5 x IQR or Q3 + 1.5 x IQR.

The epigenetic age acceleration of survivors and patients who died following and ICU admission with sepsis was examined (Figure 5.16). The demographic information for the septic patients who died and those who survived is shown in Table 5.5. Septic patients who died had age acceleration equal to +11.95 years according to the DNAm PhenoAge clock, compared with 2.96 years in those who survived meaning patients who died had a significant 8.9-year greater age acceleration (p = 0.00026, Wilcoxon). This observation also held for the Hannum clock, with patients who died having 10.9 years of age acceleration compared to 4.9 years in those who survived, a significant difference of 6 years (p = 0.03375, Wilcoxon). However, this difference was not seen with the Horvath clock (p = 0.136, Wilcoxon) (Figure 5.16).

Septic ICU patients who died

n	Age	F	M	MODS < 9	MODS > 9	MODS
25	66.56 (36 - 89)	12	13	12	13	8.88 (2 - 17)

Septic ICU patients who survived

n	Age	F	M	MODS < 9	MODS > 9	MODS
41	64.09 (21 - 87)	18	23	23	18	7.36 (0 - 12)

Non-septic ICU patients who died

n	Age	F	M	MODS < 9	MODS > 9	MODS
43	63.00 (27 - 88)	13	30	21	22	7.62 (1 - 14)

Non-septic ICU patients who survived

n	Age	F	M	MODS < 9	MODS > 9	MODS
25	68.24 (44 - 85)	8	17	16	9	7.2 (2 - 13)

Table 5.5: Cohort information of ICU patients who died and those who survived grouped by sepsis status. Listed are the number of patients in each group "n" as well as the mean chronological age as well as the mean MODS the minimum and maximum values for each parameter are also included. Also included is the number of patients with a MODS less than or greater than 9, how many died following admission as well as how many survived. Also recorded is the sex at birth of the patients in each group "F" for female and "M" for male. MODS = Multi Organ Disfunction Score.

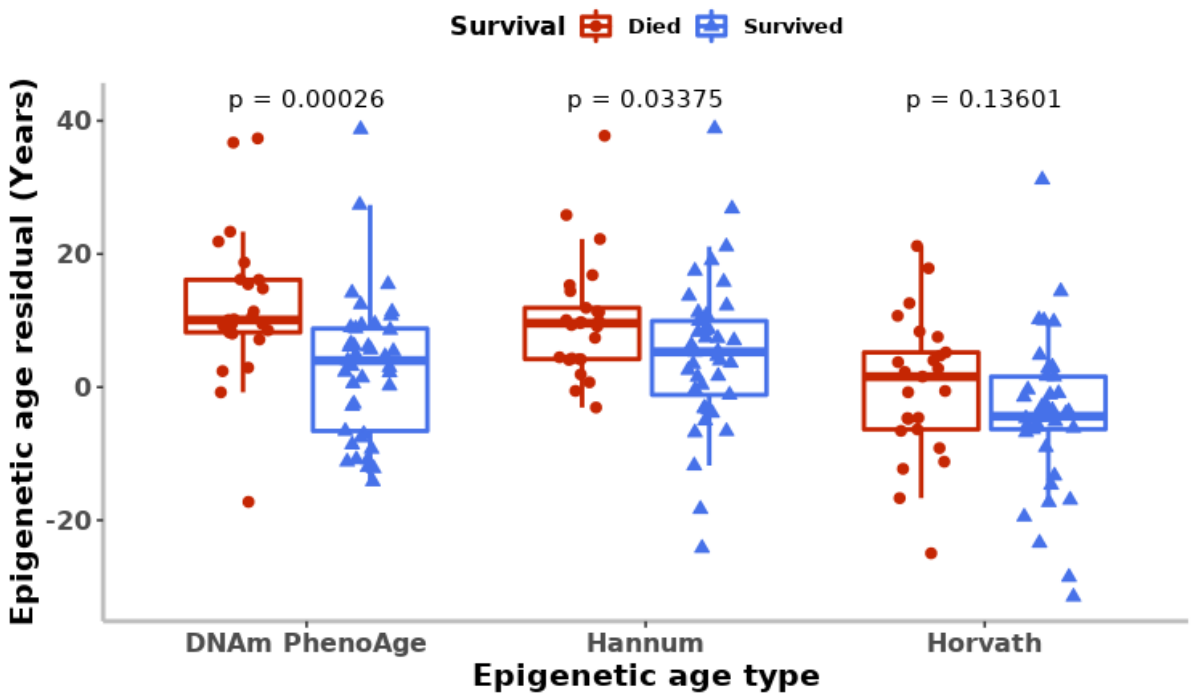


Figure 5.16: Comparison of difference in epigenetic age residuals between septic ICU patients who died and those who survived. A boxplot showing a comparison of the epigenetic age residuals (epigenetic age – chronological age) of septic ICU patients who died (n = 25) and those who survived (n = 41) according the DNAm PhenoAge, Hannum and Horvath epigenetic clocks. For each box plot the central line is median, the bottom line is the 1st quartile (Q1), the upper the 3rd quartile (Q3). The whiskers represent calculated minimum and maximum values using the interquartile range (IQR). Whiskers are calculated using the formula Q1 + 1.5 x IQR or Q3 + 1.5 x IQR.

Within the non-septic ICU patient cohort (patient demographics shown in Table 5.5), patients who died had age acceleration equal to 5.83 years according to the DNAm PhenoAge clock compared with 0.18 in those who survived meaning patients who died had a significant 5.65-year greater age acceleration (p = 0.017, Wilcoxon). This observation was not confirmed for the Hannum (p = 0.124, Wilcoxon) or Horvath (p = 0.081, Wilcoxon) clock, though the latter was close to significance (Figure 5.17).

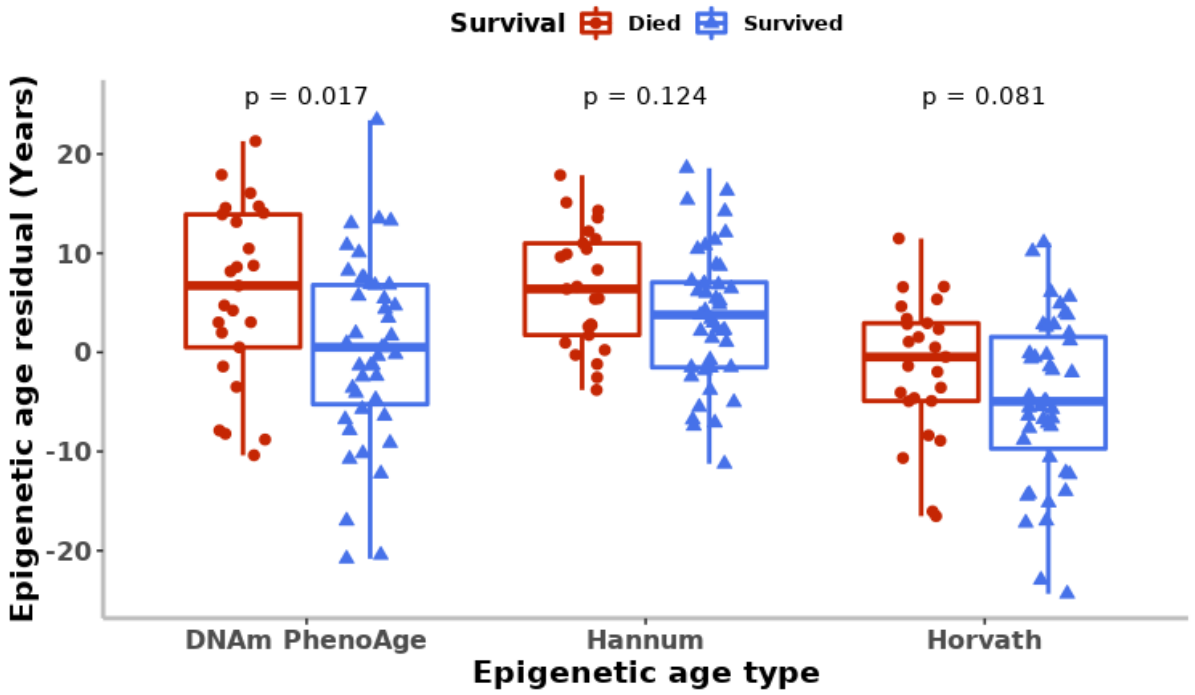


Figure 5.17: Comparison of difference in epigenetic age residuals between non-septic ICU patients who died and those who survived. A boxplot showing a comparison of the epigenetic age residuals (epigenetic age - chronological) of non-septic ICU patients who died (n = 25) and those who survived (n = 43) according the DNAm PhenoAge, Hannum and Horvath epigenetic clocks. For each box plot the central line is median, the bottom line is the 1st quartile (Q1), the upper the 3rd quartile (Q3). The whiskers represent calculated minimum and maximum values using the interquartile range (IQR). Whiskers are calculated using the formula Q1 + 1.5 x IQR or Q3 + 1.5 x IQR.

When comparing all patients admitted to ICU combined, patients who died had greater age acceleration than those who survived according to all epigenetic clocks (Figure 5.18), the cohort information for the patients who survived and those who died is shown in Table 5.6. Age acceleration equal to 8.89 years was seen in those who died according to the DNAm PhenoAge clock compared with 1.45 in those who survived, meaning patients who died had a significant 7.35-year greater age acceleration (p = 2.2e-05, Wilcoxon). This observation was also confirmed with the Hannum clock, with patients who died having 8.26 years of age acceleration compared to 4.3 in those who survived, a significant difference of 3.96 years (p = 0.0086, Wilcoxon). This observation also held according to the Horvath clock, with patients who died having 0.74 years lower epigenetic age compared to 4.44 years in those who survived, a significant difference of 3.7 years (p = 0.0177, Wilcoxon) (Figure 5.18).

ICU Patients who died

n	Age	F	M	Septic	Non-septic	MODS < 9	MODS > 9	MODS
50	67.40 (36 - 89)	20	30	25	25	28	22	8.04 (2 - 17)

ICU Patients who survived

n	Age	F	M	Septic	Non-septic	MODS < 9	MODS > 9	MODS
84	63.53 (21 - 88)	31	53	41	43	43	41	7.5 (1 - 14)

Table 5.6: Table containing cohort information of ICU patients who died and those who survived. Listed are the number of patients in each group "n" as well as the mean chronological age as well as the mean MODS the minimum and maximum values for each parameter are also included. Also included is the number of patients with a MODS less than or greater than 9, how many died following admission as well as how many survived. Also recorded is the sex at birth of the patients in each group "F" for female and "M" for male. MODS = Multi Organ Disfunction Score.

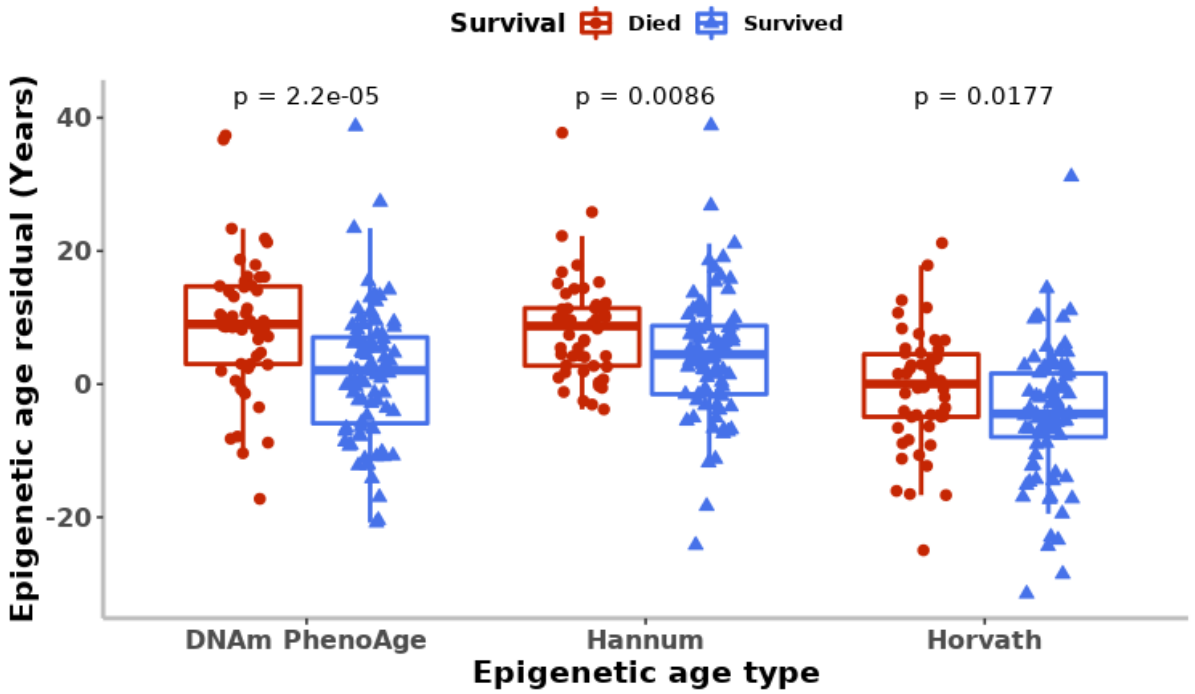


Figure 5.18: Comparison of difference in epigenetic age residuals between all ICU patients who died and those who survived. A boxplot showing a comparison of the epigenetic age residuals (epigenetic age - chronological) of all ICU patients who died (n = 50) and all of those who survived (n = 84) according the DNAm PhenoAge, Hannum and Horvath epigenetic clocks. For each box plot the central line is median, the bottom line is the 1st quartile (Q1), the upper the 3rd quartile (Q3). The whiskers represent calculated minimum and maximum values using the interquartile range (IQR). Whiskers are calculated using the formula Q1 + 1.5 x IQR or Q3 + 1.5 x IQR.

There was some significant difference between the age acceleration (epigenetic age – chronological age) as measured by the DNAm PhenoAge and Hannum epigenetic clocks in septic and non-septic patients when they were grouped based on their sepsis status combined with their multi-organ dysfunction scores (MODS), e.g., septic with a MODS < 9 or non-septic with a MODS > 9 (Figure 5.19).

There was greater age acceleration in the septic > 9 group (p = 0.024, Wilcoxon) and septic < 9 group (p = 0.033, Wilcoxon) compared to the non-septic < 9 group according to the DNAm PhenoAge clock (Figure 5.19 **A**). There was greater age acceleration in the septic < 9 group (p = 0.044, Wilcoxon) and non-septic < 9 group (p = 0.05, Wilcoxon) compared to the non-septic < 9 group according to the

Hannum clock (Figure 5.19 **B**). There were no significant differences according to the Horvath clock (Figure 5.19 **C**).

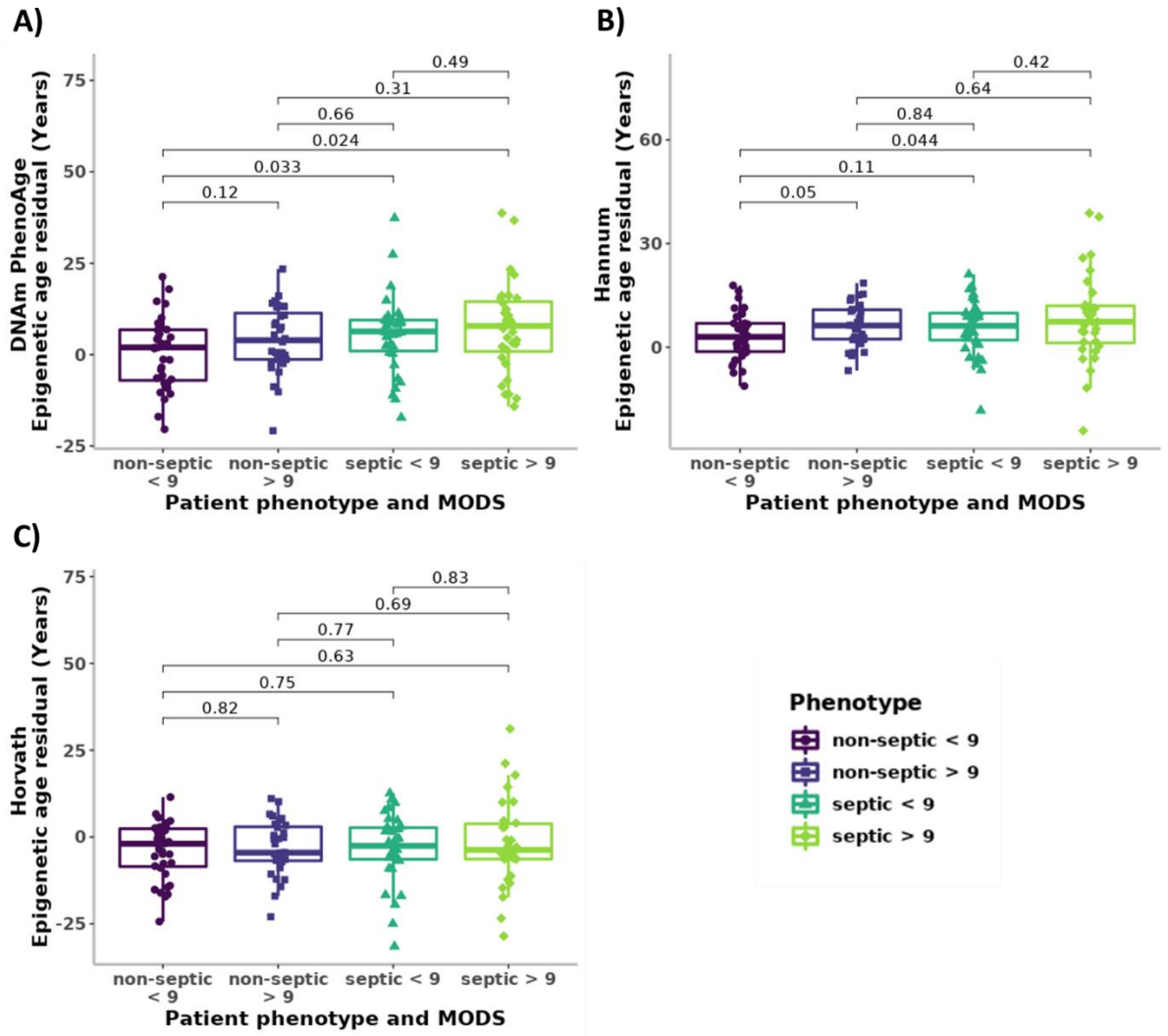


Figure 5.19: Comparison of difference in epigenetic age residuals between non-septic and septic ICU patients grouped by their MODS of > or < 9. A figure composed of 3 plots comparing the epigenetic age residuals (epigenetic age - chronological) of septic and non-septic patients grouped by their multi-organ dysfunction scores (MODS). The patient groups are non-septic with MODS < 9 (n = 36) or MODS > 9 (n = 32) as well as septic with MODS < 9 (n = 34) or MODS > 9 (n = 32). Plot **A** shows the DNAm PhenoAge epigenetic age residual information, plot **B** shows the Hannum data, and plot **C** shows the Horvath data. Also shown is the figure legend. For each box plot the central line is median, the bottom line is the 1st quartile (Q1), the upper the 3rd quartile (Q3). The whiskers represent calculated minimum and maximum values using the interquartile range (IQR). Whiskers are calculated using the formula Q1 + 1.5 x IQR or Q3 + 1.5 x IQR.

There was no significant correlation between MODS and the amount of epigenetic age acceleration present in septic patients (epigenetic age – chronological) (Spearman, Figure 5.20 **A**), or within the non-septic group of patients for the Horvath clock (Spearman, Figure 5.20 **B**). There was a significant but weak correlation between MODS and epigenetic age acceleration in non-septic patients according to the DNAm PhenoAge clock, (Figure 5.20 **B**: R = 0.31, p = 0.013, Spearman). There was a trend towards a positive correlation between epigenetic age acceleration and MODS according to the Hannum clock, (R = 0.23, p = 0.062, Spearman).

When patients were grouped by both sex and sepsis status (Figure 5.21), only male septic patients showed an age acceleration according to the DNAm PhenoAge (p = 0.031, Wilcoxon, Figure 5.21 **A**) and by the Hannum epigenetic clock the male septic patients only had a higher epigenetic age when compared to the female non-septic patients (p = 0.047, Wilcoxon, Figure 5.21 **B**). The DNAm PhenoAge clock showed that male septic patients had greater age acceleration than male non-septic and female non-septic patients, (Figure 5.21 **A**). The Hannum clock shoed that male septic patients had greater age acceleration than female non-septic patients (Figure 5.21 **B**). There was no significant difference between any group according to the Horvath clock (Figure 5.21 **C**).

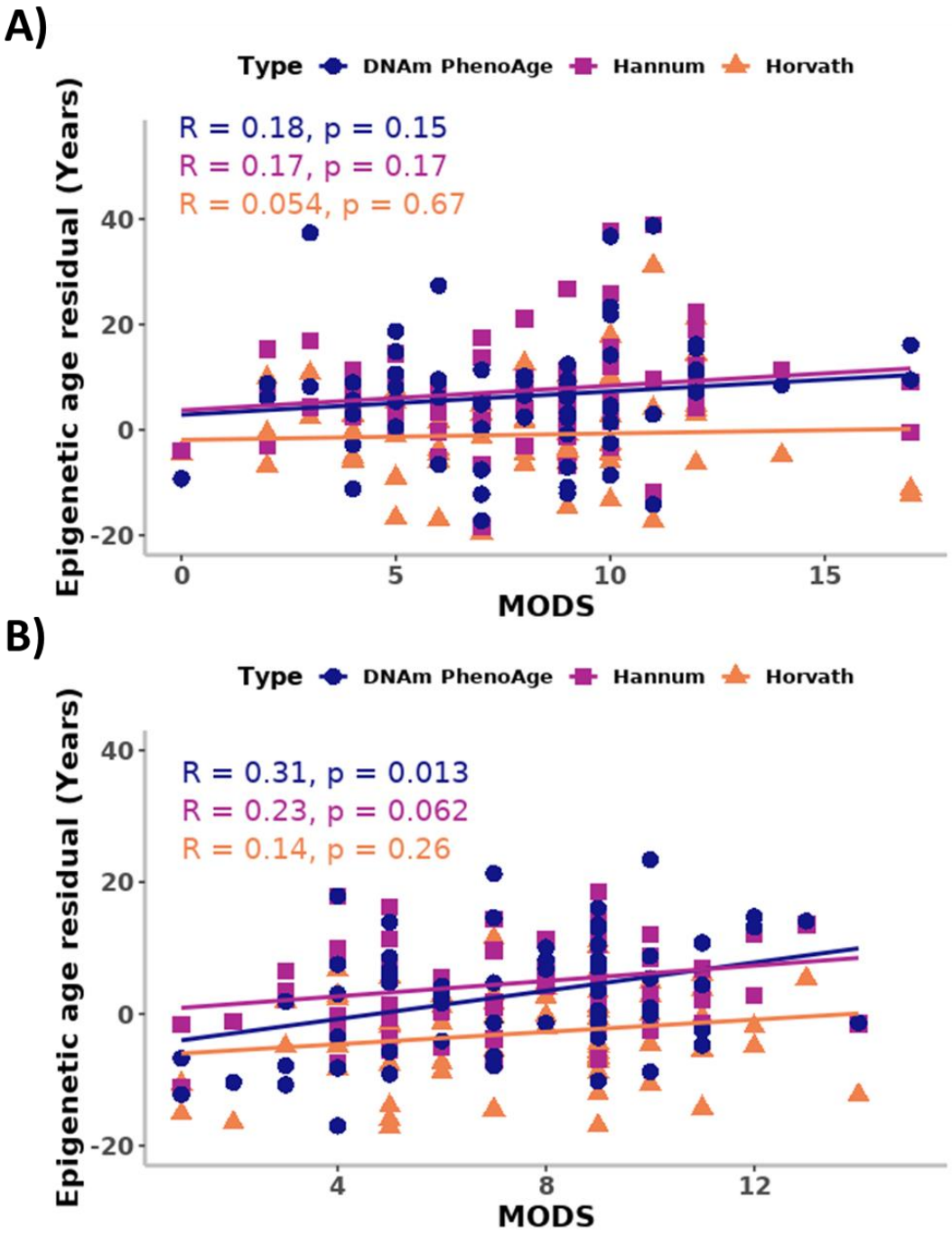


Figure 5.20: Epigenetic age residual and MODS in septic and non-septic ICU patients. A figure showing the relationship between the epigenetic residuals (epigenetic age – chronological age) and multi organ disfunction scores (MODS) of septic (**A**) and non-septic (**B**) ICU patients, correlation (Spearman) and significance are shown. Figure legend shows the colour and shapes used for each epigenetic clock data.

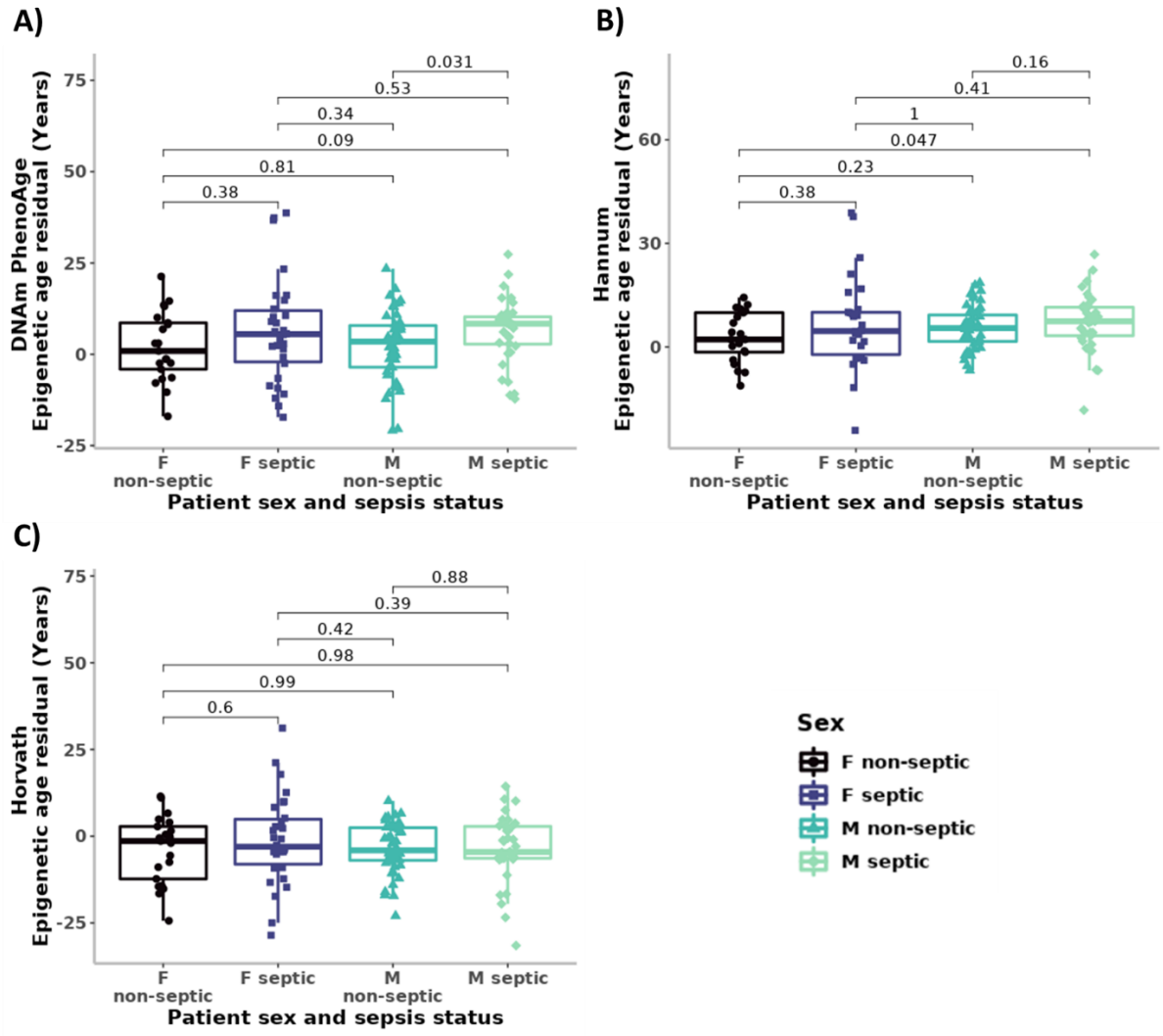


Figure 5.21: Epigenetic age residual in ICU patients grouped by sex and sepsis status. A figure composed of 3 plots comparing the different epigenetic age residuals (epigenetic age – chronological age) of septic and non-septic patients grouped by their sex (M = male, F = Female) and sepsis status. The patient groups are female non-septic (n = 21) or septic (n = 30) as well as male non-septic (n = 47) or septic (n = 36). Plot **A** shows the DNAm PhenoAge epigenetic age residual information, plot **B** shows the Hannum data, and plot **C** shows the Horvath data. Also shown is the figure legend. For each box plot the central line is median, the bottom line is the 1st quartile (Q1), the upper the 3rd quartile (Q3). The whiskers represent calculated minimum and maximum values using the interquartile range (IQR). Whiskers are calculated using the formula Q1 + 1.5 x IQR or Q3 + 1.5 x IQR.

For the following analysis, a minfi RGChanellSet was provided in leu of the raw IDAT files meaning that the data came pre-processed. The methylomes of patients at admission to ICU with sepsis and without were compared. While there were a large number of differentially methylated probes, once the P values were adjusted it was found that there was only one significantly differentiated probe (p value cut off = <0.5), corresponding to a single gene, ITGB2 (The genes with the next lowest p values can be seen in Figure A.5.2, in the appendix). Subsequent pathway enrichment analysis revealed the 10 most significantly differentially methylated pathways between groups based on this gene (Figure A.5.2 (appendix), and Figure 5.22). There was only one significantly differentially methylated gene, due to this, all enriched pathways shown have a GeneRatio of 1. This is because the GeneRatio can be understood as “genes associated with a pathway/the total number of genes of interest”. As the genes of interest here are any which are differentially methylated, only 1 gene in this case, any associated pathway will contain 100% of the genes of interest, returning a ratio of 1.

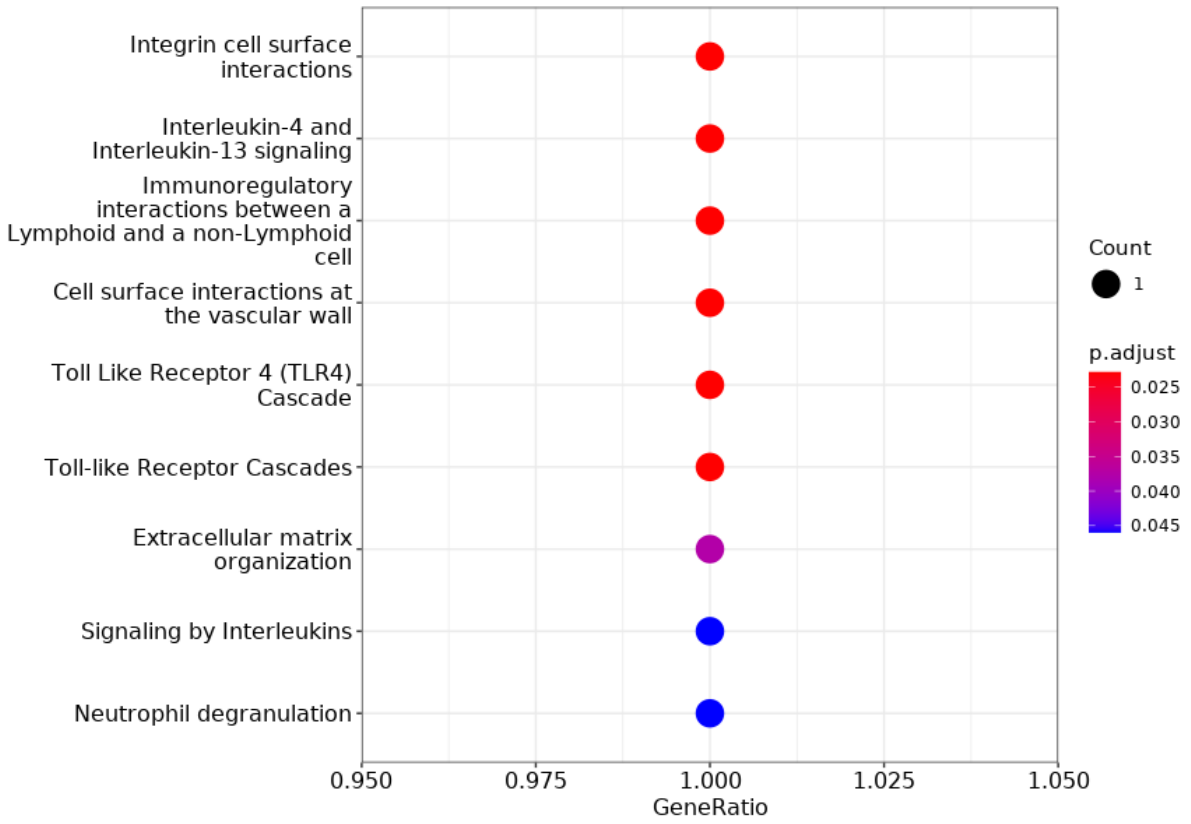


Figure 5.22: The most significantly enriched pathways of differentially methylated genes when comparing septic and non-septic ICU patients. Shown is a dot plot containing are the pathway name, gene count, gene ratio and adjusted p value for the 10 most significantly differentially methylated pathways between septic (n = 66) and non-septic ICU patients (n = 68).

5.2.1.3 DNA methylation analysis: COVID-19 cohort

Patients who were admitted to hospital with PCR-confirmed SARS CoV-2 infection were classified as moderate or severe based on their "fraction of inspired oxygen" or "FiO2" levels as well as their need for ventilation. Patients who required between 28-60% FiO2 were classified as having "moderate" COVID-19, those requiring above 60% FiO2 or who were admitted to intensive care were classified as severe.

Blood was taken at a "long-term" follow up appointment as part of one of the UK wide PHOSP-COVID studies (Evans et al., 2022). This meant that the epigenetic ages of patients were generated using blood samples taken between 2 and 7.5 months post-discharge. This allowed us to see the long-lasting impact of a moderate or severe covid-19 infection has on the ageing process.

The COVID-19 patients classified as severe were recruited in Birmingham, as part of the Coronavirus Immunological Analysis study. This study was approved by the North West Preston Research Ethics Committee (20/NW/0240). The patients classified as moderate were recruited as part of the Post-hospitalisation COVID-19 study, which was approved by Leeds West Research Ethics Committee (20/YH/0225).

5.2.1.3.1 Sample type

Within the COVID-19 Cohort DNA methylation analysis was performed on DNA from PBMCs isolated from whole blood.

5.2.1.3.2 Patient information

Shown in Table 5.7 are the clinical and demographic details of the 63 COVID-19 patients who were recruited to the study. Within the severe COVID-19 cohort some clinical information was not available. The missing information is as follows, **SEX**: 25 missing, **BMI**: 1 missing. However, the missing sex data for 25 patients was deduced for each using their epigenetic profiling data using the "getSex" function

of the R package "minfi". The sex estimation is based on the median values of measurements present on the sex chromosomes. Time spent on O_2 was not recorded for the severe cohort, although due to the severity of their illness it is likely that they were receiving oxygen supplementation for most of their hospital admission. Within the moderate COVID-19 cohort some clinical information was also not available. The missing information is as follows, **BMI**: 11 missing. The groups were matched for age, but the proportion of males was higher in the severe COVID group, 81.5% male compared to 68% in the moderate group. The moderate group also had a higher mean BMI though both groups were classed as obese.

Severe covid-19 patients

n	Age	F	M	BMI	LOS (Days)	Time on O_2 (Days)
38	53.74 (22 - 73)	7*	31*	31.60 (22.16 - 52.69)	32.54 (4 - 62)	N/A

Moderate covid-19 patients

n	Age	F	M	BMI	LOS (Days)	Time on O_2 (Days)
25	56.64 (26 - 70)	8	17	33.87 (27.6 - 44.1)	5.68 (0 - 45)	5.72 (1 - 43)

Table 5.7: Table containing COVID-19 patient cohort information. Listed are the number of patients in each group (n) as well as the mean chronological age, mean BMI, mean length of stay (LOS) and mean time spent on O_2. Also included are the minimum and maximum values for each parameter. Sex at birth of the patients in each group "F" for female and "M" for male is also shown. BMI = Body mass index; LOS = Length of stay.

5.2.1.3.3 COVID-19: Epigenetic age and chronological age

There was a strong positive correlation between all epigenetic ages and chronological age within the moderate COVID-19 cohort (Figure 5.23 **A**), DNAm PhenoAge (R = 0.55, p = 0.0041, Spearman) and Hannum (R = 0.4, p = 0.046, Spearman) epigenetic ages showed a moderate correlation with chronological age. Horvath (R = 0.69, p = 0.00012, Spearman) epigenetic age showed a strong positive

correlation with age at long-term follow up. Surprisingly, there was no significant correlation between epigenetic age at long-term follow up after severe COVID-19 infection and chronological age (Spearman) shown in Figure 5.23 **B**. Caution is therefore required when interpreting the data.

There was a significant difference between the chronological age and each epigenetic age within the moderate cohort (Figure 5.23 **C**). There was a significantly lower DNAm PhenoAge epigenetic age of (-25.29 years, p = 6e-08, Paired Wilcoxon), a significantly decreased Hannum epigenetic age (-6.08, p = 0.0023, Paired Wilcoxon) and a significant increase in Horvath epigenetic age (+6.25, p = 0.00014, Paired Wilcoxon) compared to chronological age. Within the severe cohort (Figure 5.23 **D**) there was a significant decrease in DNAm PhenoAge epigenetic age (-7.11, p = 0.083, Paired Wilcoxon), but no significant difference in Hannum epigenetic age (+2.6 1, p = 0.24, Paired Wilcoxon) compared with chronological age. There was a significant increase in Horvath epigenetic age compared to chronological age (+11.58 years, p = 3.4e-05, Paired Wilcoxon).

Within the moderate cohort there was no significant correlation between the age acceleration present and the chronological age of the participant. The Hannum and Horvath epigenetic age residuals showed a weak negative correlation and were nearing significance (p = 0.067, p = 0.091 Spearman, respectively) Figure 5.23 **E**. There was a very strong negative correlation between DNAm PhenoAge (R = -0.8., p = 1.5e-09, Spearman), Hannum (R = -0.84, p = 2.6e-11, Spearman) and Horvath (R = -0.83, p = 9.4e-11) epigenetic age residuals and chronological age within the severe cohort Figure 5.23 **F**.

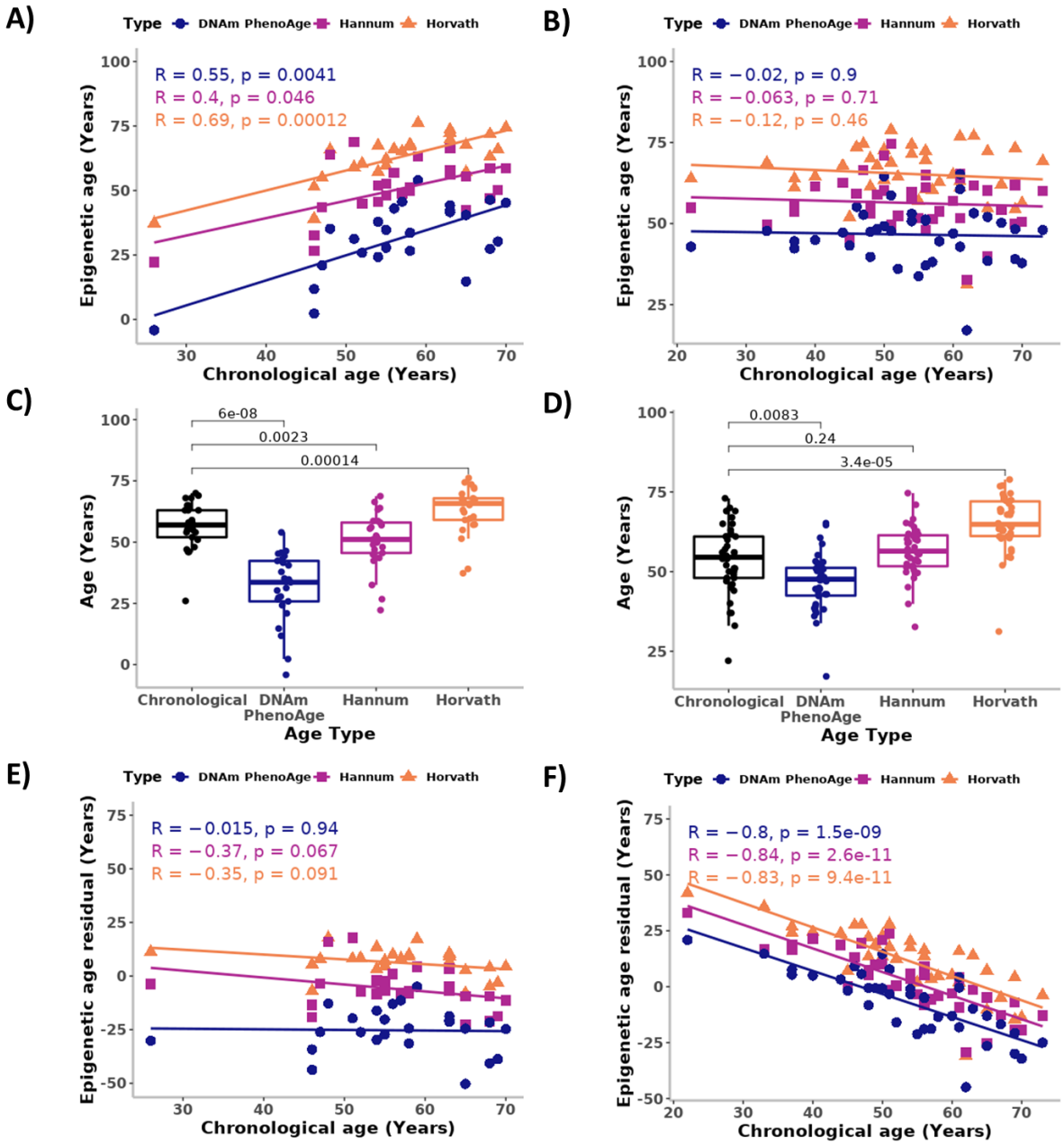


Figure 5.23: Epigenetic age analysis of moderate and severe COVID-19 patients: This figure shows epigenetic age data for patients with moderate (n = 25) and severe (n = 38) COVID-19. **A** (moderate) and **B** (severe) show the correlation between chronological age and DNAm PhenoAge as well as Hannum and Horvath epigenetic ages, **C** (moderate) and **D** (severe) show the difference between chronological and calculated epigenetic age. **E** (moderate) and **F** (severe) show the correlation between the epigenetic age residual (epigenetic age – chronological age) and chronological age. For each box plot the central line is median, the bottom line is the 1st quartile (Q1), the upper the 3rd quartile (Q3). The whiskers represent calculated minimum and maximum values using the interquartile range (IQR). Whiskers are calculated using the formula Q1 + 1.5 x IQR or Q3 + 1.5 x IQR.

5.2.1.3.4 COVID-19: Epigenetic age, disease severity and clinical parameters

There was a significant difference between the epigenetic age residuals (epigenetic age – chronological age) of the moderate and severe COVID-19 cohorts (Figure 5.24). There was greater epigenetic age residual in the severe cohort compared to the moderate cohort according to DNAm PhenoAge (18.18 years, p=1.4e-06, Wilcoxon) and Hannum (8.7 years, p=0.0036, Wilcoxon) clocks, though the difference in Horvath residual was just non-significant (5.32 years, p=0.0584, Wilcoxon).

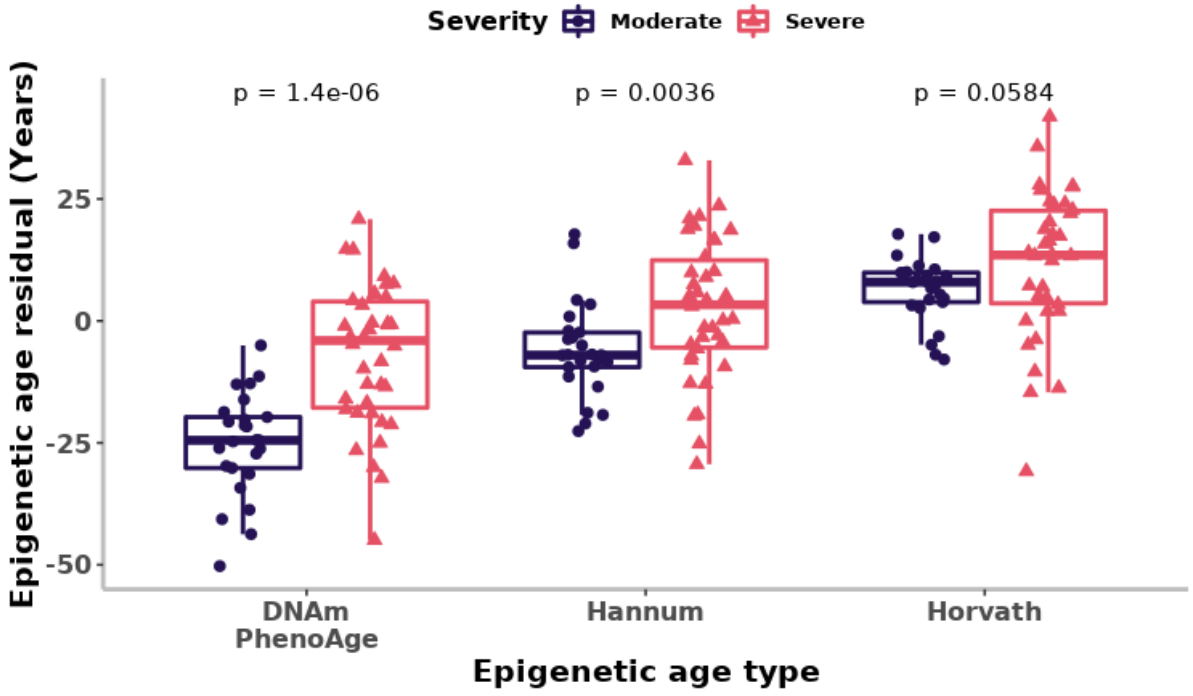


Figure 5.24: Comparison of difference in epigenetic age residuals between moderate and severe patient groups. A boxplot showing a comparison of the epigenetic age residuals (epigenetic age – chronological age) of moderate (n = 25) and severe (n = 38) COVID-19 patients according the DNAm PhenoAge, Hannum and Horvath epigenetic clocks. For each box plot the central line is median, the bottom line is the 1st quartile (Q1), the upper the 3rd quartile (Q3). The whiskers represent calculated minimum and maximum values using the interquartile range (IQR). Whiskers are calculated using the formula Q1 + 1.5 x IQR or Q3 + 1.5 x IQR.

When all the patients admitted to hospital with COVID-19 were combined to determine the influence of sex, there was no difference in epigenetic age acceleration according to all epigenetic clocks (Wilcoxon, Figure 5.25 **C**). This remained true when the patients were separated into the severe (Wilcoxon, Figure 5.25 **A**) or moderate (Wilcoxon, Figure 5.25 **B**) cohorts. There were however few female patients within the severe group which may impact the statistical power of these analyses.

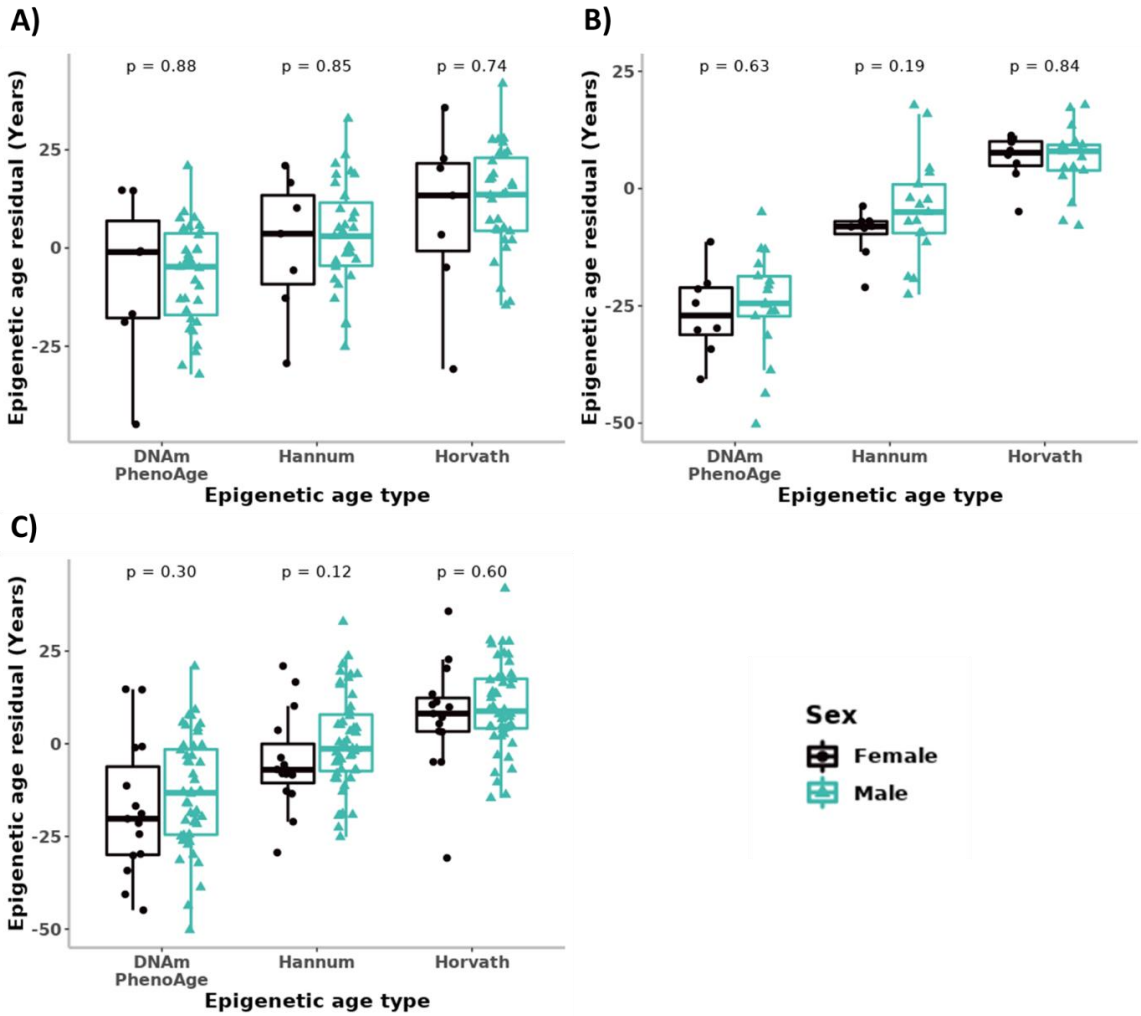


Figure 5.25: Epigenetic age residuals in ICU patients grouped by sex and sepsis status. A figure composed of 3 plots comparing the different epigenetic age residuals (epigenetic age – chronological age) of moderate and severe COVID-19 patients grouped by their sex (M = male, F = Female) and severity status. Plot **A** shows the epigenetic age residual comparison between male (n = 31) and female (n = 7) severe COVID-19 patients. Plot **B** shows the epigenetic age residual comparison between male (n = 17) and female (n = 8) moderate COVID-19 patients, plot **C** shows the comparison between all male (n = 48) and female (n = 15) patients. For each box plot the central line is median, the bottom line is the 1st quartile (Q1), the upper the 3rd quartile (Q3). The whiskers represent calculated minimum and maximum values using the interquartile range (IQR). Whiskers are calculated using the formula Q1 + 1.5 x IQR or Q3 + 1.5 x IQR.

There were no significant correlations (Spearman) between the different epigenetic age residuals and BMI in patients admitted to hospital with severe or moderate COVID-19 (Figure 5.26 **A**). The DNAm PhenoAge epigenetic age residuals of COVID-19 patients showed a positive significant correlation with their length of stay (R = 0.38, p = 0.0023, Spearman, Figure 5.26 **B**), the Hannum residual was nearing significance (R = 0.22, p = 0.089, Spearman).

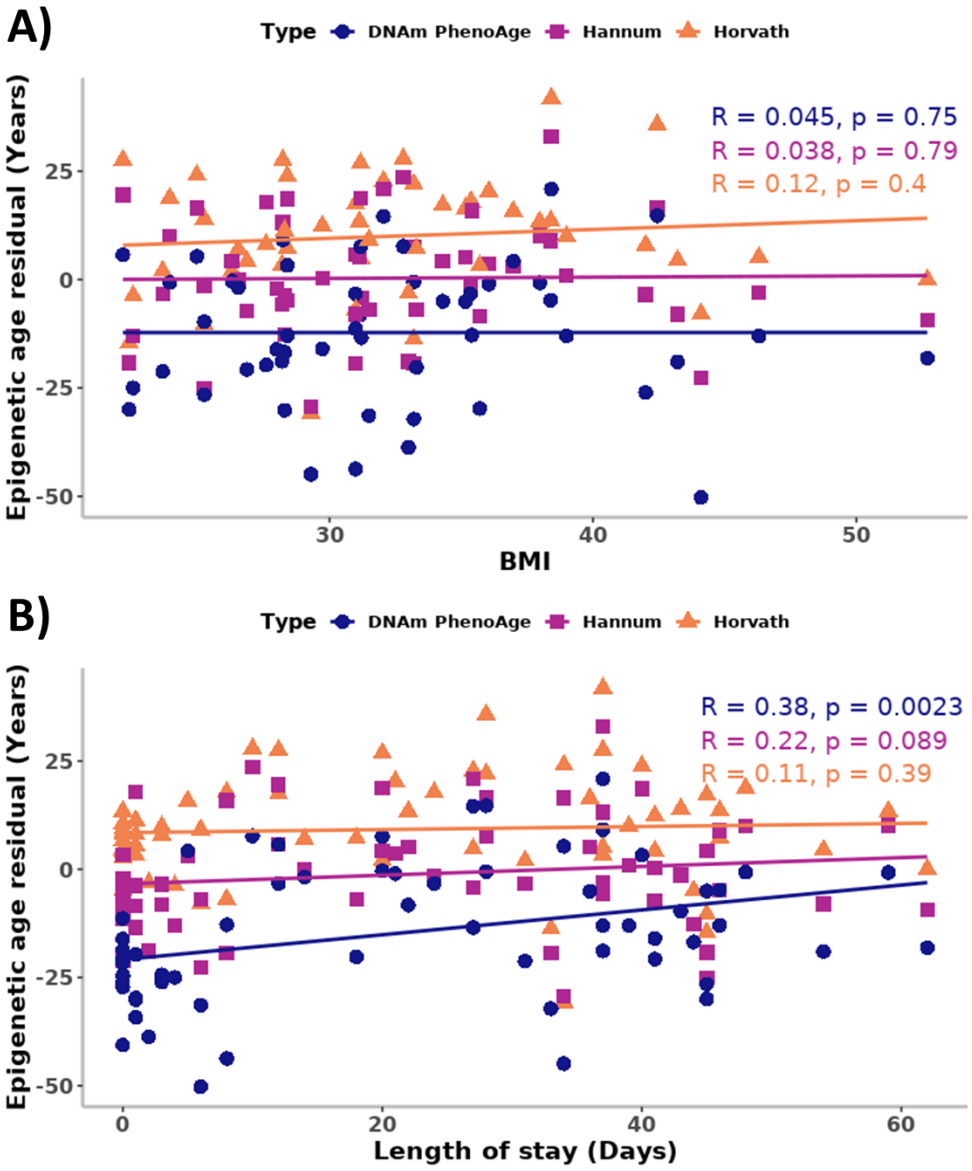


Figure 5.26: Epigenetic age residuals of patients admitted to hospital with COVID-19 compared with BMI. A figure containing a dot plot showing the correlation (Spearman) between the epigenetic age residuals (epigenetic age – chronological age) of individuals admitted to hospital with COVID-19 and their body mass index (BMI) **A** (n = 51). Also shown is a dot plot showing the correlation (Spearman) between the epigenetic age residuals of individuals admitted to hospital with COVID-19 and their length of stay (LOS) **B** (n = 62). LOS = Length of stay.

5.2.1.3.5 COVID-19: differential methylation analysis

A pathway enrichment analysis was performed on the differentially methylated genes detected between severe and moderate COVID-19 patients. While a large number of significantly differentially methylated genes were detected between the two groups, pathway enrichment analysis showed no significantly enriched pathways when not considering the log fold change of the levels of methylation present. Shown in Figure A.5.3 are the most significantly differentially methylated genes, as well as their log fold change and original and adjusted P values and their function. Figure 5.27 shows a map plot of the most significantly enriched pathways and their interactions, based on the most differentially methylated genes between moderate and severe COVID-19 infections. A subsection of these data is shown in Figure 5.28 which shows the 10 most significantly enriched pathways based on significantly differentially methylated genes, regardless of fold change. Neutrophil degranulation, Rho GTPase, general disease associated growth receptor signalling and neuronal system. Figure 5.29 shows the 10 most significantly enriched pathways based on genes with a positive fold change in methylation in severe COVID-19 compared with those who had a moderate infection. The dominant genes again are those associated with neutrophil degranulation, Rho GTPase, growth receptor signalling and neuronal system. Figure 5.30 shows the most enriched pathways based on genes with a negative fold change, with the greatest impact on cell cycle, Rho GTPase, antigen processing and DNA repair pathways.

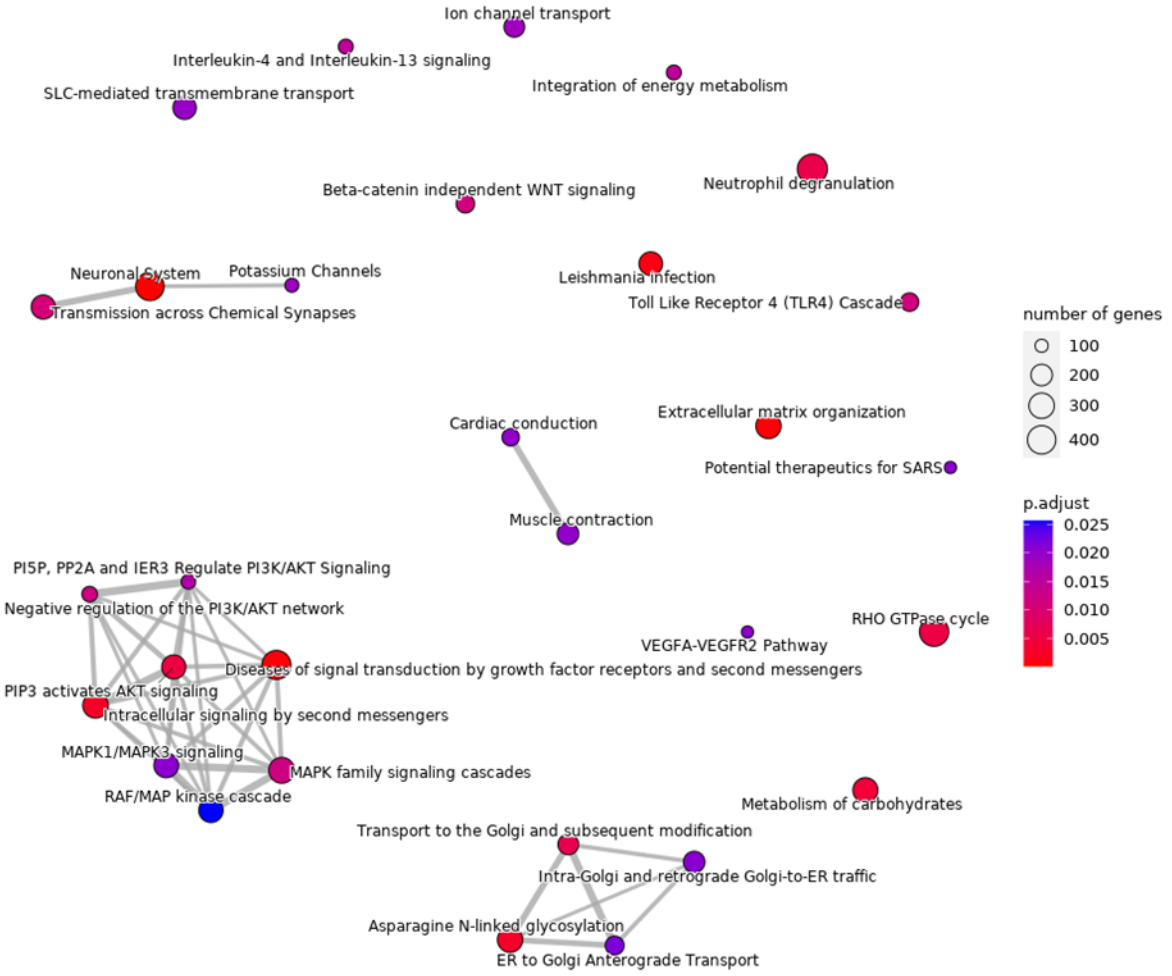


Figure 5.27: The most significantly enriched pathways of differentially methylated genes irrespective of fold change between moderate and severe COVID-19 patients. A map plot showing the relationships between the most significantly differentially methylated pathways between patients with moderate (n = 25) and severe (n = 38) COVID-19. Node size denotes the number of genes associated with a specific pathway, with increasing size reflecting as greater number, colour can also be seen to reflect the adjusted p value.

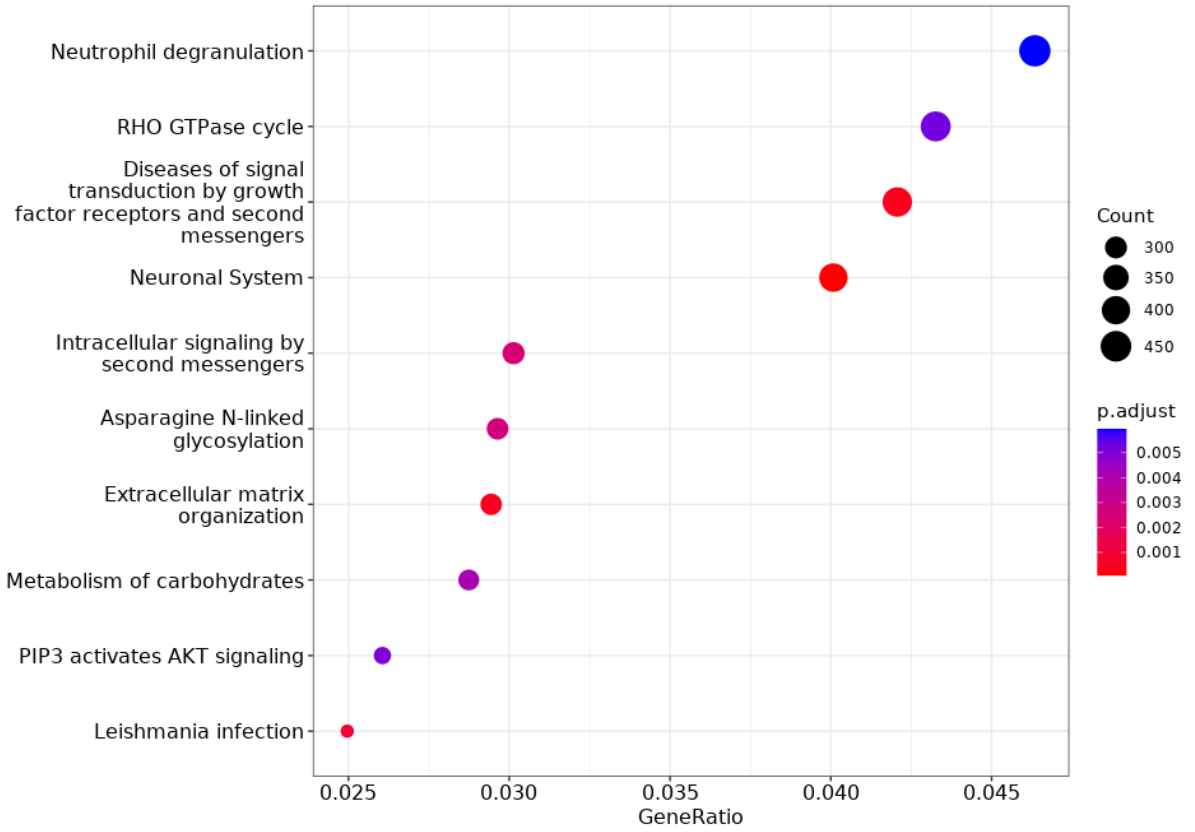


Figure 5.28: The most significantly enriched pathways of differentially methylated genes irrespective of fold change when comparing moderate and severe COVID-19 patients. Shown is a dot plot containing are the pathway name, gene count, gene ratio and adjusted p value for the 10 most significantly differentially methylated pathways between moderate (n = 25) and severe (n = 38) COVID-19 patients.

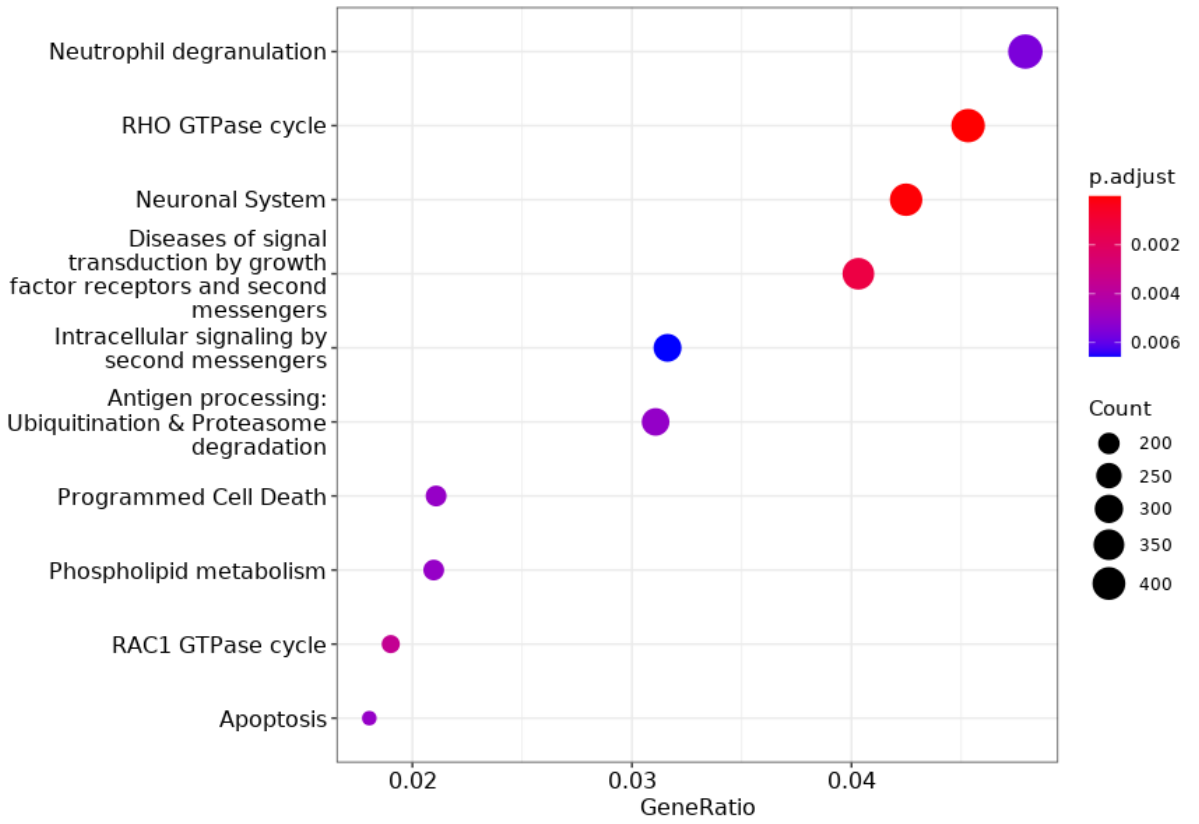


Figure 5.29: The most significantly enriched pathways of differentially methylated genes showing a positive fold change when comparing moderate and severe COVID-19 patients. Shown is a dot plot containing are the pathway name, gene count, gene ratio and adjusted p value for the 10 most significantly differentially methylated pathways based on genes showing a positive fold change between moderate (n = 25) and severe (n = 38) COVID-19 patients.

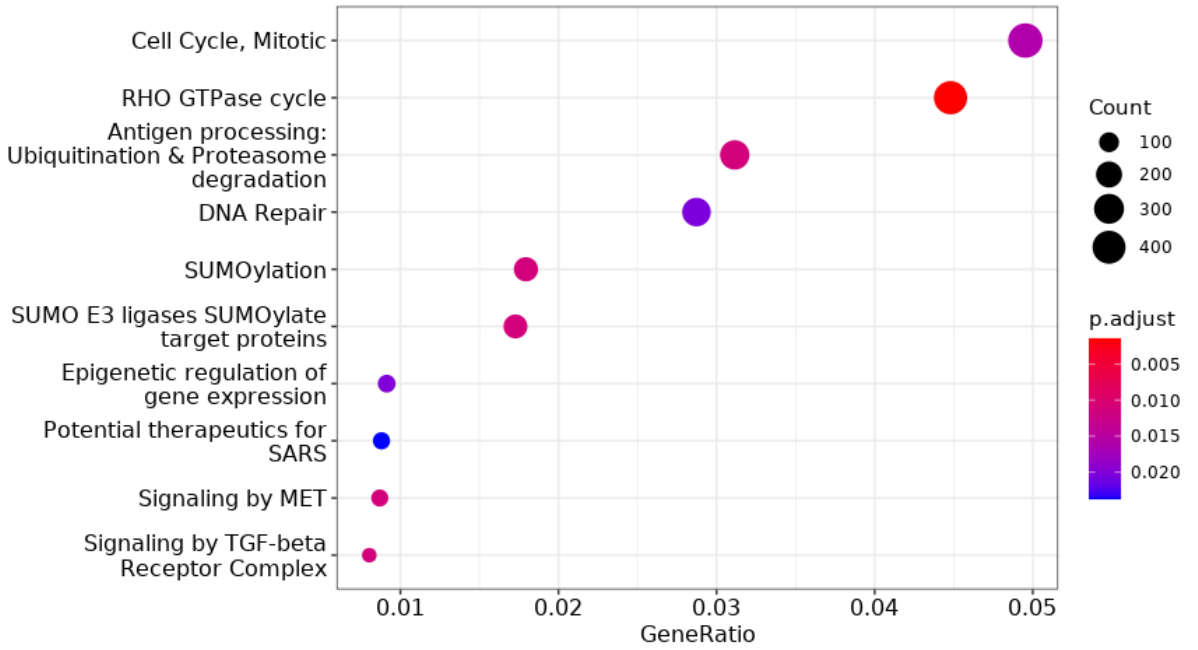


Figure 5.30: The most significantly enriched pathways of differentially methylated genes showing a negative fold change when comparing moderate and severe COVID-19 patients. Shown is a dot plot containing are the pathway name, gene count, gene ratio and adjusted p value for the 10 most significantly differentially methylated pathways based on genes showing a negative fold change between moderate (n = 25) and severe (n = 38) COVID-19 patients.

5.3 Discussion

5.3.1 Burns

The first observation that was made when looking at the epigenetic ages of the burn patients at two time points; was that there was a greater correlation between epigenetic age and chronological age at the 6-month time point compared with at admission. This suggests that there were large changes occurring to the methylome by 6 months, impacting regions which usually change reliably with age.

Surprisingly, the changes in epigenetic age were not consistent between the three epigenetic clocks. Horvath's algorithm suggested an acceleration of epigenetic age, Hannum showed no change and PhenoAge gave a reduction in epigenetic age. Such disagreements between the clocks has been reported by others (Franzen et al., 2021) and may reflect the tissues they were developed using and whether they were tested against mortality as an outcome or disease. The Horvath clock has a very high correlation with chronological age, Pearson correlation coefficient of 0.98 (Horvath, 2013) and was trained on mortality as an outcome. It was also developed from datasets from a wide variety of tissues and so is less affected by tissue composition changes than might be seen for the Hannum or DNAm PhenoAge clocks which were both developed on blood. The increased epigenetic age seen with the Horvath clock in the burns cohort may therefore explain the increased mortality risk in burns patients (Duke et al., 2015c). In comparison the DNAm PhenoAge clock, developed by Morgan Levine, was based on data from blood cells but trained on indicators of the aged phenotype, such as kidney and liver function and thus predicts age-related ill health well (Levine et al., 2018). The lack of acceleration observed according to the DNAm PhenoAge clock might suggest that burns patients do not have an increased risk of age-related disease. However this is not supported by the increased cardiovascular risk in this patient group (Duke et al., 2017). More recently the same group has compared 11 different epigenetic clocks and concluded that although the CpG islands used in their algorithms may differ, many still related to key hallmarks in the biological ageing process, including

autophagy, mitochondrial function, senescence (Z. Liu et al., 2020). What may be required of our data is to drill down further to see if amongst the PhenoAge and Horvath data specified nodes may be common and affected in the same direction.

The epigenetic age acceleration, seen with the Horvath clock is greater in the younger patients at both time points, as shown by the negative correlation with age. It may seem slightly counter intuitive that younger people are showing the most ageing. It must be remembered however that there is only so much biological ageing that a person can experience, an increase of 30 years in biological age is readily possible at 20 years of age but would be less likely at 70 when it could be fatal. Currently there is no literature supporting this idea and in fact this is counter to what is observed within healthy populations, where more variation in epigenetic age is seen later in life as the epigenetic age altering lifestyle, genetic and environmental factors have accumulated over time (Talens et al., 2012). However, the insult to the body may be sufficient in this case to deliver significant epigenetic changes even in the young. At the time of writing there are no other studies of the impact of traumatic injury on epigenetic age across a broad age spectra, the only report in the literature is of young male war veterans who showed an acceleration of approximately 2 years by 6 months after their injury (Boks et al., 2015).

Another novel aspect of the investigation into epigenetic ageing in burns patients is undoubtedly the paired analysis performed looking at how in the same patients epigenetic age changed from admission to 6 months later. The literature to date on trauma and epigenetic age is limited, and the studies that do exist focus mainly on psychological trauma and are cross-sectional in design (Jovanovic et al., 2017; Mehta et al., 2018; E J. Wolf et al., 2017). If burn injury was to have no long-lasting effect on epigenetic ageing, the expected result would have been a 0.5-year increase in epigenetic age between the two time points, as the person's chronological age increased by 6 months. This, however, was not the case. Instead, the Horvath epigenetic age at admission was significantly greater than at 6 months post injury within the same patient. This change was observed in virtually every patient and represents clear

evidence that burn injury is sufficient to elevate an individual's epigenetic age, at least for 6 months post injury and using the Horvath clock. This trend was also observed and was significant according to every epigenetic clock employed here, which was somewhat surprising given that each clock varies in how the age estimation is generated. The Horvath clock was developed on multiple tissue types, the Hannum and DNAm PhenoAge clocks were developed on blood data. The fact that these clocks all of which were developed using different criteria agree on the general trend in epigenetic age lends strength to the observations, making it likely that these are genuine changes in epigenetic age and less likely to be a confounding factor such as changes in cell composition.

What isn't clear however is how long the epigenetic age changes persist beyond 6 months, neither is it clear if epigenetic age at 6 months post-injury is back to a pre-injury level or remains elevated/reduced compared to what it was pre-injury. Comparing the epigenetic ages of the 6-month post burn injury patient group and those of an age and sex matched control group was done to address these questions. Analysis revealed no significant difference between the epigenetic ages of the two groups. This suggests that the higher epigenetic age observed at admission is a result of the burn injury. The burn injured patients epigenetic age then decreases over time as they recover from their injury, eventually returning to that observed within a healthy population, this can be assumed to be their "pre-injury level". More long-term and medium-term samples from the burn group would need to be analysed (1-5 years post injury) to see at what rate the epigenetic ages of burn injured individuals decreases over time. This could be considered work for the future.

A surprising finding was that there was no significant positive correlation between the amount of epigenetic age acceleration and any of the clinical markers considered at admission or in the long-term, apart from the rBaux score which incorporates patient chronological age and TBSA% which was seen to be less correlated with epigenetic age acceleration than chronological age alone. This suggests that injury severity, at least as currently assessed for burn injury, is not an influence on how much age acceleration or reduction a patient is likely to experience.

Recently, large scale epigenome-wide “Mendelian Randomization” has been used to identify a collection of CpG sites causal to ageing-related traits, both positive and negative (Ying et al., 2022). Ying et al., state that none of the CpGs identified feature within any widely used epigenetic clock, limiting the interpretability of epigenetic ageing data generated using the current generation of epigenetic clocks. Another reason for the lack of relationship between epigenetic age and injury scoring methods could be that all the patients included were very severely injured, meaning that there was not a great enough range in injury severity to determine an influence. However, with patient TBSA% ranging from 4-95% and length of stay ranging from 1 to 215 days it is clear that a variety of burn severity is present within the cohort. Other measures of patient response to injury such as inflammatory or metabolic markers may share more of a relationship with epigenetic age, and again this should be considered for future study design.

Those patients who died following admission showed no difference in the levels of epigenetic age acceleration compared with those who survived. There are two possible explanations. One, there simply is no difference, which is possible, although this finding would be contradicted by what was observed within the septic cohort. Or two, the number of patients who died (n=14) is too low and contains too wide a spread of epigenetic age residual to be of statistical worth. It is likely that both explanations apply. Also, it is likely that the difference may be small and difficult to detect. This was surprising as all of the epigenetic clocks used, purport to strongly relate to mortality risk in “normal” ageing (Fransquet et al., 2019), which is not supported by what was observed within the burns cohort here. This may suggest that burn injury causes epigenetic changes dissimilar to those used in calibrating the epigenetic clocks relationship to mortality.

The epigenetic ages of patients were not the only difference between patients at admission and 6 months post injury. There were also large changes to the methylation at sites within genes relating to specific pathways. There was one pathway which was differentially methylated when comparing all admission samples and month 6 samples, as well as the paired admission and 6-month samples. The

"neuronal system pathway" showed differential methylation 300-375 pathway-associated genes at admission compared with 6 months post injury. This pathway, discussed below is involved in the regulation of activity within the brain (Purves and Williams, 2001). The presence of increased methylation activity in genes affecting neuronal activity has so far received no attention within the literature. While there is no supporting literature it is possible that the increased regulatory neuronal activity may be in response to the trauma and severe pain and itch which accompanies burn injury (Summer et al., 2007) and is often resistant to traditional pharmacological intervention (Chang and Waxman, 2010). This is surprising given that the DNA examined was extracted from PBMCs and not a tissue containing neurons. One explanation for this is that many of the 300+ differentially methylated genes have a different function within the PBMCs, but their gene ontology currently has them predominantly associated with the "neuronal systems pathway".

Within the paired analysis it was interesting to observe the variety of differentially methylated pathways. Ranging from cardiac conduction to cell signalling, metabolism, chromatin modification and cell death. "RHO GTPase cycle" and "RAC1 GTPase cycle" are related members of the GTPase family of proteins which both play key roles in the maintenance of vascular integrity and cellular structure, as well as regulating proinflammatory NFκB, immune cell migration, neutrophil function and activity and NADPH induced oxidative stress (Q. Lu et al., 2009). This family of proteins therefore plays an important role in inflammation and ion signalling within multiple cardiac tissues as well as cell remodelling and cellular survival more generally (Bosco et al., 2009; Q. Lu et al., 2009).

The "cardiac conduction" pathway was significantly differentially methylated between admission and month six. Cardiac conduction is clearly vital for life and essential for the proper maintenance of cardiac function (Park and Fishman, 2011). Its presence within the most enriched pathways may be explained by the unique effects burn injury has on the heart. Following burn injury patients usually enter tachycardia, a resting heart rate exceeding 100 beats per minute (Awtry et al., 2006), this can result in increased cardiac stress and output. A patient's heart rate and output can remain significantly

elevated for over two years (Williams et al., 2011) which may explain the poor long term cardiac health of burn patients (Duke et al., 2017), as well as this pathways presence in the list of most enriched pathways. The differential methylation of multiple pathway's related to cardiac function may explain or be reflective of the poor cardiovascular outcomes associated with burn injury. One obvious question remains, why are PBMCs showing differential methylation related to cardiac signalling. It is possible that the 200+ differentially methylated genes which are associated with the cardiac conduction pathway have alternative functions within PBMCs but predominantly have their gene ontology linked to their functions within the heart. One other hypothesis, although not discussed within the literature, is that PBMCs are being stimulated by a cardiac specific protein. As mentioned tachycardia is common during the acute burn injury phase, and can cause damage to the heart (Awtry et al., 2006), poor cardiac outcomes following burn injury are widely recognised and are suggestive of cardiac injury (Duke et al., 2017). Cardiac tissue specific proteins such as troponin I are released from cardiac tissues into the blood following cardiac injury (Santoso et al., 2021). These proteins are also present at elevated levels following burn injury (Alexander et al., 2018). Given that burn injury can cause damage to the heart, it is possible that these proteins are interacting with PBMCS and influencing pathways usually associated with the cardiac tissue itself.

When looking at the pathways which showed an increase or decrease in methylation it is easy to assume that those genes with an increase in methylation would experience decreased expression and vice versa. It is worth bearing in mind however, that this analysis does not show which region within the gene is experiencing methylation changes, therefore it is better to view these pathways as experiencing increased regulatory activity which could be positive or negative, rather than assuming expression is increasing or decreasing. "Signalling by receptor tyrosine kinases" was the pathway which showed both the greatest increase and decrease in methylation between admission and month 6. Receptor tyrosine kinases (RTK) are multi-purpose receptor proteins located on the cell surface which serve as diverse regulators of cellular processes ranging from cell division to apoptosis to immune cell signalling as well as multiple metabolic processes (Sudhesh Dev et al., 2021). Given the

massive inflammatory cascade that follows a burn injury (Guillory et al., 2016), seeing changes in the methylation of signalling pathways such as this and others is to be expected.

Transcriptional regulation by TP53 as well as chromatin organisation and chromatin modifying enzyme pathways were observed to be significantly differentially methylated. Likewise, Genes controlling another regulatory mechanism, chromatin organisation (as well as chromatin modifying enzymes) were also differentially methylated between the two time points. This is to be expected as these pathways play a key role in regulating gene expression, something which changes dramatically following any injury, especially burns, as was outlined in the "Genomic storm" paper by Xiao et al., (2011). The "Genomic storm" paper describes the massive reprioritisation in transcription following a major trauma. Xiao et al., (2011) showed that >80% of cellular functions and pathways change in response to trauma. Given this finding that the vast majority of biological processes change in response to injury, it seems unsurprising that so many cell signalling and regulatory processes appear to be differentially methylated at admission compared with 6 months post injury.

The presence of the "cell cycle, mitotic" pathway in the list of differentially methylated pathways is also informative. Following injury, mitotic cellular proliferation occurs not only as damaged cells local to the injury site begin to be replaced (Jun and Lau, 2010), but also among the cells of the immune system. For example as naive T cells begin to divide following exposure to an antigens such as DAMPs (Oliaro et al., 2010), something which is likely to occur following burn injury and is supported by the increase in white blood cell percentage in the days that follow (Murray et al., 2007). The pathways relating to phagocytosis such as "FCGR dependent phagocytosis" are likely enriched due to the increased immune activation of, neutrophils, monocytes and macrophages which follows immediately following burn injury and any subsequent infection (Xiu and Jeschke, 2013).

The last pathway of note is "Diseases of signal transduction by growth factor receptors and second messengers". This is a non-disease specific pathway which has been broadly associated with multiple diseases, rather than being specific to one disease. Increased dysregulation of the genes associated

with this pathway appear to be a general indication of serious disease (Pires-daSilva and Sommer, 2003), which makes sense within the context of a major traumatic injury, where the body is responding much in the way it might to a serious disease challenge.

5.3.2 Sepsis

The methylation data used in the comparisons between septic and non-septic individuals presenting to ICU was collected as part of the study "Epigenetic profiling in severe sepsis: a pilot study of DNA methylation profiles in critical illness" - Binnie et al., 2019. The original study focused on investigating the differences in methylomes of septic and non-septic ICU patients and did not investigate how these changes related to epigenetic ageing. Both septic and non-septic patients showed accelerated ageing, according to the DNAm PhenoAge and Hannum epigenetic clocks. It is perhaps unsurprising to see that the non-septic patients also showed some degree of epigenetic age acceleration as they were still critically ill enough to warrant admission to ICU.

Non-septic patients on average showed a stronger and more significant correlation between epigenetic age and chronological age than was observed in the septic group. This is perhaps an indication that while both groups are showing signs of epigenetic ageing, the changes present within the septic group suggests that sepsis is having a more disruptive effect on the methylome than ICU admission alone. As with the burns cohort there was a greater degree of age acceleration in younger patients than in older patients. This suggests this may be a feature of critical illness in young adults that in the future may lead to targeting this group with interventions to reduce epigenetic age.

While there was no difference in epigenetic age acceleration based on sepsis status, there was a significantly greater increase in epigenetic age in septic patients who died compared to those who survived (difference of +7.18 years, DNAm PhenoAge). This result may have 3 explanations. Firstly, if increased metabolic and physical stress results in an increase in epigenetic age, then it follows that those patients who died had the greatest biological stress and therefore the greatest increase in epigenetic age, although this was not observed within the burns cohort. Secondly, age is a primary risk

factor for almost every major disease (Harman, 1991) and is also predictive of worse outcomes not only in the trauma environment such as following burn or TBI (Hukkelhoven et al., 2003; Pham et al., 2009) but also specifically with sepsis (Martin et al., 2006). Therefore, someone who has a higher biological age before their critical illness is more likely to have poorer outcomes. Thirdly, the DNAm PhenoAge is an effective predictor of mortality (Levine et al., 2018), therefore those patients most likely to die are also the most likely to return an accelerated DNAm PhenoAge epigenetic age.

The finding that there was a significant difference in age acceleration between ICU patients who died compared to those who survived was in contrast to what was observed in the burns cohort. In the burns cohort there was no difference in age acceleration between survivors and non-survivors. This may be because there was a low number of deaths within the burns cohort. There were only 13 burns patients who died compared with 50 ICU patients who died. This low number of burns patients who died may mean that the burns analysis does not have adequate statistical power to detect any relationship between death following burn injury and epigenetic age, rather than directly contradicting the findings within the ICU group.

Analysing the patient groups by illness severity surprisingly revealed no significant differences, although the two comparisons which were near significance suggested that septic patients with a MODS both above or below 9 had more age acceleration than non-septic patients with MODS <9. This was reflected in the fact that MODS showed no correlation with epigenetic age acceleration in the septic patient group according to any clock. Illness severity then, at least as measured by the MODS system, has no impact on how much age acceleration a person with sepsis experiences, which is surprising considering that survivability is shown to have an impact on epigenetic age. This may indicate that while the MODS is a measure of illness severity, it has little relationship with epigenetic age in sepsis. This suggests that the way in which epigenetic ageing is influencing sepsis and mortality is not related to organ dysfunction. There appears to be no literature so far linking MODS with

epigenetic age but based on the evidence here is suggests that MODS is not a reliable way to predict epigenetic ageing.

Grouping the patients by sepsis status and sex further illustrated the impact that sepsis and sex has on epigenetic ageing. It has been observed that the males of many animal species age at an accelerated rate compared to females (Austad and Fischer, 2016; Constantinou et al., 2019). The reason for this phenomenon in humans is not clear, with some people suggesting that testosterone is involved, studies of historic cohorts (1392-1910) of men missing testosterone due to castration at a young age showed they lived up to 20 years longer than their contemporaries, even longer than the most wealthy members of their society (Min et al., 2012). Men having greater epigenetic age acceleration in a condition such as sepsis, which has an inflammatory pathology, is not surprising when the sexual dimorphism of the immune response is examined. Epidemiological analysis has shown that women have both a lower incidence of morbidity and mortality following sepsis (Kondo et al., 2021). This may be due to the fact that in multiple species, ranging from mice to humans, males have a greater pro-inflammatory response to insults than is seen in females (Klein and Flanagan, 2016). For example, male mice have greater TLR4 expression than females. This greater TLR4 expression results in greater pro-inflammatory cytokine production following immune stimulation in males than in females (Rettew et al., 2008). This male pro-inflammatory phenotype was showed to be mediated by the presence of male sex hormones (Rettew et al., 2008). Males also have higher percentages of NK cells than females (Abdullah et al., 2012), and the other immune cells such as neutrophils and macrophages and lymphocytes appear to have reduced function in males compared to females (Spitzer, 1999; Weinstein et al., 1984). This less “fine-tuned” immune response observed in men clearly plays a decisive role in the different sex based outcomes observed in multiple diseases as has been seen in COVID-19 (Takahashi et al., 2020).

This more pro-inflammatory immune response present in males may explain why they were observed to have greater epigenetic age acceleration than female patients within this study. Septic and non-

septic men both showed greater epigenetic age acceleration than women, with septic men the highest of any group, sepsis again showing to be a contributing factor to an accelerated epigenetic age.

The original publication of the ICU data (septic and non-septic) analysed in this chapter (Binnie et al., 2019) showed a large difference in the methylomes of septic and non-septic patients, an observation not seen following pathway enrichment analysis here. This is likely due in large part to the method of analysis, identifying differentially methylated regions as opposed to individual probes and adjusting for enrichment. This may have been confounded further by the fact that for the analysis performed here I did not have access to the raw IDAT files, but instead a pre-processed methylation object.

Sepsis status appears to have significant impact on a person's epigenetic age in some cases increasing it by several years, with individuals who show the greatest epigenetic ages being at the greatest risk of death. How long these changes persist in the survivors remain unknown, as do their long-term health implications.

5.3.3 COVID-19

Since epigenetic analysis began on the samples from COVID-19-infected individuals outlined in this chapter, other groups have begun to publish similar work investigating the impact COVID-19 has on the ageing process. Initial reports within the literature have been contradictory, despite samples being run on the same array platform (Illumina EPIC) and using the same sample type (blood). Franzen et al., (2021) saw no accelerated ageing according to Horvath and Hannum clocks whereas Cao et al., (2022) observed accelerated ageing using the Horvath, Hannum and DNAm PhenoAge clocks.

The data presented here suggests that there is likely to be a long-term impact on epigenetic age following COVID-19 infection, with some clocks showing age acceleration, though caution is required as one shows a deceleration. The amount of age acceleration present was related to disease severity; this is shown by the most severe disease resulting in a significantly greater epigenetic age compared with moderate infections. This relationship between severity and age acceleration is also reflected in

the correlation between patient length of stay and age acceleration. With a patient's length of stay often being used as an indication of how ill they are, with illness severity correlating positively with length of stay (Setareh et al., 2021). Although those with severe COVID-19 and longer stays in hospital had the greatest epigenetic age residuals, it isn't yet known if what was observed was a result of COVID-19 infection severity, or, if those with severe COVID-19 were already the oldest biologically prior to infection, so developed the worst symptoms, something reported by Kuo et al., (2020). These findings are in line with what Cao et al., (2022) observed and also seems to agree with the findings observed within the septic cohort, another infection-driven disease state, that more severe biological stress seems to correlate with an increased epigenetic age. This was seen in patients who died or were septic having higher epigenetic ages than those who survived.

One finding which was surprising was the lack of relationship between epigenetic age and chronological age within the severe COVID-19 cohort. It has been established in the literature that even in ill individuals chronological age will have significant positive correlation with epigenetic age, something shown previously in HIV, hepatitis B and C as well as in the COVID-19 epigenetic ageing research previously mentioned (Cao et al., 2022; Fransquet et al., 2019; Gindin et al., 2020; Horvath and Levine, 2015). This positive relationship between epigenetic and chronological age was something observed in the moderate COVID-19 infection group. The lack of correlation in the severe group suggests that severe disease had a long-term impact on the methylome sufficient to disrupt the usually robust predictive abilities of all 3 epigenetic clocks used here. The long-term impacts of COVID-19 have been recognised in the form of "long covid". Long covid is a broad collection of symptoms persisting for several months post covid infection, these conditions range from cardio-respiratory syndrome to neuro-psychiatric syndrome (Raveendran et al., 2021). This long-term disruption may result from epigenetic reprogramming associated with long covid. However, this could not be tested since the long covid status of these patients was unavailable.

There were many differentially methylated pathways between the severe and moderate COVID-19 groups post discharge which again points to this long-term phenotypic change following critical illness.

The differentially methylated pathways when looking at the severe and moderate patients showed a positive fold change in methylation in the severe group compared with the moderate group contained the “neuronal system” pathway. This pathway, as described earlier, is associated with the regulation of the 100 billion neurons within the human brain (Purves and Williams, 2001). The presence of this enriched pathway long-term post illness could well be an epigenetic sign of the now infamous “brain fog” experienced by many people with even mild COVID-19 (Asadi-Pooya et al., 2022). As discussed previously though, it is somewhat surprising to see this pathway enriched given that the DNA examined was not extracted from neuron containing tissues. The individual genes which were associated with this pathway may be serving an alternate function within the cells of the blood.

Following a viral infection, it is perhaps unsurprising to see the enrichment of pathways such as “antigen processing: ubiquitination & proteasome degradation” and “neutrophil degranulation”. The neutrophil degranulation has already been shown to be up-regulated following COVID-19 (Rosa et al., 2021) thought to represent innate immune response to localised infections within the lungs. Infection can occur in around 30% of hospitalised patients requiring respiratory ventilation for any reason (Koenig and Truwit, 2006). Ventilation is a common part of treating patients with severe COVID-19 which may explain why this pathway showed a particular difference between the moderate and severe patients, with severe COVID-19 patients usually requiring ventilation. Enrichment of antigen processing pathways makes sense within the context of both the bacterial and viral pathogenic response, both of which are at play during COVID-19. This is due to this pathway being involved in the degradation of both foreign and malformed host proteins both of which are likely to be present following any infection (Princiotta et al., 2003; Kloetzel and Ossendorp, 2004).

With SARS-CoV and SARS-CoV2 being closely related it makes sense that the “Potential therapeutics for SARS” pathway was enriched. It contains genes which were identified as potential targets for

clinical trials pertaining to novel or repurposed drug treatments in the treatment of SARS-CoV and SARS-CoV2 infections (Harrison, 2020; Rosa and Santos, 2020).

DNA repair in the form of “DNA repair” and the “SUMO” pathways at first seems a somewhat unusual appearance within the list of enriched pathways. COVID-19 however has been suggested as being a direct cause of DNA damage (Pánico et al., 2022). Especially as COVID-19 can trigger severe inflammatory illness. Increasing inflammation, as well as being associated with the ageing process (Bartlett et al., 2012), is known to increase DNA damage (Meira et al., 2008), and is a key feature of severe COVID-19, termed the cytokine storm (McElvaney et al., 2020). This when paired with the organ damage experienced by some patients may explain why DNA repair protein pathways may have been particularly active following infection resulting in the observed enrichment of the DNA repair pathway.

Chronological age and BMI are well established risk factors for patient outcomes for most diseases, with COVID-19 being no exception (Sawadogo et al., 2022; Starke et al., 2021). Despite this, BMI did not show any correlation with the epigenetic age acceleration of the patient groups. This indicates that while BMI may pre-dispose patients to worse outcomes, it is not seen to have a direct relationship with epigenetic age acceleration, at least within the acute hospital environment.

It appears that COVID-19 infection, especially severe infection, has a definite long-term effect not only on epigenetic age, which appears increased when compared to moderate disease, but on the methylome as a whole.

5.4 Conclusion

Does accelerated ageing occur in the hospital environment? The conclusion is yes it can, but the data vary with which clock was considered and the illness the patient experienced. Does insult severity impact the amount of epigenetic ageing? It appears that patients with the most severe infections, or who sustained life ending infections had greater epigenetic ages. This could reflect injury severity

influencing epigenetic age acceleration, or that these patients were biologically older prior to their infection or injury.

Epigenetic changes and age acceleration appeared to be present long-term following COVID-19, though the burn data suggested that epigenetic age does change over time post injury returning closer to that of controls. Changes in methylation observed in pathways linked to long term health outcomes such as long covid and cardiac function in burns suggests that long term epigenetic reprogramming may be influencing health outcomes. More longitudinal investigations are needed to establish the true long-term impact of injury and disease on the methylome and epigenetic ageing. The evidence presented here suggests that critical illness can have long term effects on the methylome, revealing differentially methylated pathways and epigenetic ageing months after initial recovery.

One question that remains largely unanswered is; whether an injury or infection of sufficient severity to require hospitalisation causes accelerated ageing, or are patients with accelerated ageing particularly susceptible to insults of various types? For both sepsis and severe COVID-19 it seems likely that both are true. Age, BMI, and co-morbidity are all risk factors for COVID-19 and sepsis outcomes, and all are factors which accelerate epigenetic age. Indeed, one study used UKBiobank data to estimate biological age using the PhenoAge based on clinical biochemistry data and found that those adults who developed severe COVID-19 were biologically 10-14 years older than their chronological age prior to infection (Kuo et al., 2020).

Injury, however, is a different story. While many individuals who are admitted to hospital with burn injury also have comorbidities, what has been shown in this investigation is that within a single individual their epigenetic age was higher immediately following admission to hospital with a burn injury than at 6 months later. This is direct and compelling evidence that injury alone is sufficient to cause an acceleration in epigenetic age, an acceleration which while it decreases in size over time appears to persist up to 6 months post injury. This initially higher epigenetic age, as well as the long-term methylation changes of genes and pathways associated with the known negative outcomes may

go some way to explaining the well-known long term health impact burn, general injury and to some extent all trauma has on the individual.

5.5 Appendix

5.5.1 Differentially methylated genes

Log FC	P Value	Adj P Val	Gene	Gene function
-0.35	6.85E-29	1.38E-23	KCTD11	As well as playing a role in neurogenic signalling this protein also Induces apoptosis, growth arrest and the expression of cyclin-dependent kinase inhibitors (NCBI - Gene, 2022a).
-0.23	1.56E-28	2.09E-23	NXNL1	Has been shown to play a role in promoting aerobic glycolysis and accelerate the entry of glucose into cells within the eye, promoting survival (Aït-Ali et al., 2015).
-0.18	6.83E-27	6.63E-22	PCDHGA4	May code for a calcium ion binding protein as well potentially playing a role in cell-cell communications within the brain (NCBI - Gene, 2022b).
-0.12	8.25E-27	6.63E-22	NMBR	May play a role in cell growth regulation as well as being involved with smooth muscle contraction and neuronal responses (PubChem, 2022a).
-0.14	9.96E-27	6.68E-22	KPNA2	May play a role in the nuclear transportation of proteins and may also be involved in the somatic recombination found in developing T and B cells (NCBI - Gene, 2022c).
0.06	5.56E-24	3.19E-19	ANKRD11	Ankyrin Repeat Domain Containing 11 inhibits ligand-dependent activation of transcription (NCBI - Gene, 2022d).
-0.57	1.14E-23	5.73E-19	DAZAP1	Coded on the Y chromosome (19), is an RNA binding protein which may play a role in spermatogenesis (NCBI - Gene, 2022e).
-0.54	1.35E-23	6.02E-19	TAF4	A member of an evolutionarily conserved protein family involved in the initiation of transcription (NCBI - Gene, 2022f).
-0.07	6.55E-23	2.63E-18	TMEM123	Proposed to function as a cell surface receptor which mediated cell death through oncosis (NCBI - Gene, 2022g).
0.03	2.13E-22	7.78E-18	SEC24A	Forms a subunit of the COPII vesicle coat, which is required for the selective transport of vesicles from the endoplasmic reticulum (Bonnon et al., 2010).

Figure A.5.1: The most differentially methylated individual genes between all Burns admission and month 6 samples. Listed are the log fold change, P value, BH Adjusted P value, and function of the most differentially methylated genes between all admission and month 6 burns samples. FC – Fold change.

Log FC	P value	Adj P value	Gene	Gene function
-0.1	1.00E-07	0.0432	ITGB2	A cell surface signalling and cell surface adhesion protein which plays an important role in the immune response (PubChem, 2022b).
-0.03	8.36E-07	0.1718	SLC25A20	A mitochondrial membrane carrier protein which shuttles different substrates to the intramitochondrial matrix space (NCBI - Gene, 2022h).
0.12	2.46E-06	0.2655	LIPC	Associated with the pathway "Plasma lipoprotein assembly, remodelling, and clearance", LIPC encodes hepatic triglyceride lipase, which is expressed in liver. LIPC is a triglyceride hydrolase and ligand/bridging factor for receptor-mediated lipoprotein uptake (PubChem, 2022c).
0.12	6.62E-06	0.5715	AIM2	Is involved in tumorigenic reversion and may also play a role in cellular proliferation. Expression of AIM2 is induced by interferon-gamma (PubChem, 2022d).
0.02	1.40E-05	0.7222	RERGL	The exact function of the "Ras-Related and Oestrogen-Regulated Growth Inhibitor-Like Protein" is not known, it is however predicted to enable G protein activity and GTP binding activity (NCBI - Gene, 2022i).
0.15	1.68E-05	0.7222	ZEB2	A DNA transcription inhibitor (UniProt, 2022a).
0.02	1.68E-05	0.7222	TMEM18	Predicted to be involved in cell migration as well as playing a role in DNA blinding activity (NCBI - Gene, 2022g).
-0.02	1.72E-05	0.7222	ANO10	A transmembrane calcium activated chloride channel protein (NCBI - Gene, 2022j).
0	1.77E-05	0.7222	SNTA1	May link various receptors and membrane proteins to the cellular cytoskeleton and the extracellular matrix (UniProt, 2022b).

Figure A.5.2: The most differentially methylated individual genes between septic and non-septic ICU patients. Listed are the log fold change, P value, BH Adjusted P value, and function of the most differentially methylated genes between all septic and non-septic patients. FC – Fold change.

Log FC	P value	Adj P Val	Gene	Gene function
-0.41	1.87E-32	1.33E-26	CEBPE	A protein which may be involved in granulocyte differentiation and maturation and is pro-apoptotic (Nakajima et al., 2006).
-0.16	5.04E-31	1.33E-25	FNDC3B	Enables RNA binding and is predicted to be in the endoplasmic reticulum and may be a positive regulator of adipogenesis (NCBI - Gene, 2022k).
-0.32	2.38E-30	4.31E-25	HDLBP	Binds to RNA and is able to induce heterochromatin formation as well as binding to high density lipoprotein (NCBI - Gene, 2022l).
-0.43	7.34E-30	9.71E-25	BAZ1B	A member of the bromodomain family, involved in chromatin-dependent transcription regulation (PubChem, 2022e).
-0.33	1.14E-29	1.13E-24	CAMK1D	Associated with granulocyte function, CREB-dependent gene transcription, neutrophil activation and B Cell receptor signalling pathways (GeneCards, 2022).
-0.32	1.39E-29	1.23E-24	CRTAP	A cartilage associated scaffolding protein which may regulate cytosine/ARNO activity (PubChem, 2022f).
-0.30	1.70E-29	1.35E-24	P4HB	Enhances helper T cell migration and is involved in the VEGFA vascularisation pathways (NCBI - Gene, 2022m).
-0.25	2.10E-29	1.51E-24	PML	Regulates the P53 response to oncogenic signals, it functions as a transcription factor and tumour suppressor (PubChem, 2022g).
-0.39	2.32E-29	1.54E-24	DAZAP1	Coded on the Y chromosome (19), is an RNA binding protein which may play a role in spermatogenesis (NCBI - Gene, 2022e).
-0.29	2.83E-29	1.73E-24	CSNK1D	Regulates cell growth and cell survival mechanisms such as DNA repair (Greer and Rubin, 2011).

Figure A.5.3: The most differentially methylated individual genes between moderate and severe COVID-19 patients. Listed are the log fold change, P value, BH Adjusted P value, and function of the most differentially methylated genes between all admission and month 6 burns samples. FC – Fold change.

6. Unexpected survivors of traumatic injury

6.1 Introduction

6.1.1 What is an unexpected survivor?

The primary aim of any clinical care practitioner within the trauma environment is to ensure the survival of their patients. Some patients, despite the best efforts of those around them may have been injured to such a degree that they die during treatment. The patients who die following admission generally fall into two categories, those who die despite medical care, perhaps having developed sepsis, having had an underlying health condition, or not being administered sufficient fluids. The other category contains patients whose wounds are so severe, that they are considered "un-survivable". Occasionally, a patient in this second group, who presents with what are considered to be "un-survivable" injuries manages to beat the odds and survive. What allows these patients to survive is poorly understood and receives little research attention, despite the potential to identify processes that could be mimicked to improve emergency medicine further.

During the DNA methylation profiling element of this thesis, we noticed that there was a small number of burns patients who survived to outpatient status despite having "un-survivable" injuries as measured by the rBaux scoring system, the standard injury severity score for burn injury. The rBaux score is used for predicting mortality in burn injured individuals and is generated by combining age in years, total burn surface area as a percentage (TBSA%) and awarding an additional 17 "points" if there was an inhalation injury (Lam et al., 2021). An rBaux score approaching 130 is generally thought to be un-survivable in developed nations with specialised burn care. A lower score can be just as fatal should adequate burn care not be available.

In our burns cohort there were 6 "unexpected survivor" patients who survived to outpatient status despite having a mean rBaux score of 138.5. This is compared to 14 patients who died following

admission having a mean rBaux score of 109.7 (Table 6.1). This chapter aims to try and understand the response to injury in these patients that allowed them to survive despite having severe injuries.

6.1.2 The response to injury

To understand what influences survival following injury, one must first understand what occurs in the body following injury. The body's first and in some cases, most powerful response to an injury is inflammation. Under normal circumstances, for example a laceration, localised inflammation recruits immune cells to the sight of injury, to fight off infection, remove dead cells and promote cell proliferation and tissue repair (Koh and DiPietro, 2011). Following a major injury, such as a large burn, rather than inflammation local to the site of injury, patients experience a disseminated systemic inflammatory response syndrome (SIRS). This is the inappropriate maintenance of the pro and anti-inflammatory axis that can lead to multi-organ failure and dysfunction due to a heightened cytokine cascade (Chakraborty and Burns, 2022), where the body rapidly releases more cytokines than are required to return homeostasis (Fajgenbaum and June, 2020). The pathology of burn injury has a large pro-inflammatory component, with SIRS and MODS, the intrinsically linked conditions affecting most people who sustain a severe burn, regardless of sepsis status (Dahiya, 2009). Given that MODS is the largest cause of death in burn patients who survive the initial shock associated with burn injury (Greenhalgh, 2017), it seems likely that patients who are resistant to MODS, or the associated SIRS, may have an increased chance of survival.

Inflammation however is just one part of the response to injury. Burn injury is characterised not only by its pro-inflammatory pathology but also features metabolic changes resulting in hypermetabolism and hypercatabolism with the significant reduction of skeletal muscle (Williams et al., 2009). Burn injury also causes rapid and long-lasting changes to the endocrine system. In a study of 970 severely burned paediatric patients all endocrine markers examined, which included inflammatory cytokines, human growth hormone, oestrogen and testosterone, remained significantly disrupted in the long-term following burn injury (Jeschke et al., 2011). This is to say nothing of the metabolic and

physiological changes which occur during wound healing, a vital long term-process for survival (Tiwari, 2012).

It follows then that how a person responds to injury with regard to inflammation, and a host of other metabolic and endocrine processes may be what determines a patient's survival potential.

6.1.3 Possible factors influencing survival

Age is the greatest risk factor for mortality during normal life and this does not change within the injury context. Burn, traumatic brain injury (TBI) or injury from traffic collisions all show an increased risk of mortality and morbidity with age (Bauzá et al., 2008; Rani and Schwacha, 2011; Tokutomi et al., 2008). Comorbidity, which increases with age, also has a negative impact on survival following injury (Rochon et al., 1996; Scheetz, 2005).

Sex is another important factor when it comes to surviving injury. Females are, generally speaking, longer lived than males, this is true across the animal kingdom (Austad and Fischer, 2016), from humans (Ginter and Simko, 2013) to the planktonic crustaceans known as daphnia (Constantinou et al., 2019). This longevity however does not appear to translate to resilience to injury. Women appear to suffer from significantly higher rates of mortality from injury such as burn (George et al., 2005; Kerby et al., 2006) and TBI (Gupte et al., 2019). One proposed explanation is the conferred survival benefits of testosterone. Low testosterone and precursor hormones such as DHEA are associated with reduced rates of survival in diabetes cohorts (Muraleedharan et al., 2013), as well as adverse outcomes from injury following battlefield injuries (Phillips et al., 2010) and more common injuries such as hip fracture (Butcher et al., 2005; Ohlsson et al., 2017). Administration of testosterone has been shown to reduce rates of mortality following cardiovascular events in men (Wallis et al., 2016). Clinical trials have also shown that treatment with the testosterone analogue oxandrolone results in the retardation of the muscular catabolism usually observed in burn injury, as well as increasing the rate of wound healing (Napolitano, 2001).

6.1.4 Study aims

Each aspect of a person's response to injury can be examined individually to try to distinguish what makes a person an unexpected survivor. Hormone and cytokine levels can be measured in serum or immune cell populations can be examined using flow cytometry. Genomic profiling however allows one to see the dynamic changes occurring within individual cells and to use that information to build a complete picture of how a person is responding to an insult of any kind. By examining the methylation and expression profiles of unexpected survivors it is hoped that the mechanisms of their survival may be better understood. In this chapter, the aim was to examine the transcriptomic profile of blood cells and their DNA methylation status between survivors and non-survivors of a critical burn injury.

6.2 Results

The study of the transcriptomic and DNA methylation response to burn injury in survivors and non-survivors arose from an initial study by Dr Jon Hazeldine. This first study focussed on the inflammatory response to injury and compared a cohort of unexpected non-survivors, with a high but normally survivable rBaux score (ca 85), with a cohort of unexpected survivors with a higher rBaux score deemed un-survivable (> 100). Subsequently, the patients included in the RNA sequencing and DNA methylation analysis were considered to be either "expected deaths" or unexpected survivors with similar rBaux scores. The decision to move from expected to unexpected deaths for genomic analysis was due to the many confounding factors which contribute to an "unexpected" death. For example, Inappropriate or insufficient patient care may lead to an unexpected death, if we are interested in seeing if innate differences in gene expression determine survival or death then these patients are not suitable for inclusion. For this reason, patients with similar levels of injury all broadly deemed "un-survivable" were selected for comparison. The cohort information for cytokine, DNA methylation and RNA analysis can be seen in the relevant sections below.

6.2.1 Cytokine differences in patients who unexpectedly died compared with unexpected survivors.

Acknowledgement: The raw cytokine and Sysmex data used in the figures below were generated by Dr Jon Hazeldine. Cytokine data was generated using a custom 9-plex Bio-Rad bio-plex luminex. It is included as this cytokine data was generated using samples from patients included in the DNA methylation and RNA sequencing analysis performed and these data informed the selection of patients used in this chapter.

After the identification of “unexpected survivors” within the burns cohort it was decided that looking at if the cytokine response of these patients differed from their peers who unexpectedly succumbed to their injuries.

6.2.1.1 Cytokine cohort information

As previously described unexpected survivors and unexpected deaths were compared, paired analysis of patients based on age was performed, the patient information for the illustrative figures below is shown in Table 6.1.

	Unexpected survivors	Died
n	1	1
Age	35.00	32
F	0	0
M	1	1
TBSA%	46.00	30.00
rBaux	123.00	79.00
APACHE	34	23.00
SOFA	12.00	12
LOS	45.00	8.00
Time from injury to death	n/a	8.47

Table 6.1: Cytokine analysis cohort information. Shown are the patient information for each group, a patient who died following survivable injuries and one who unexpectedly survived. Listed are the sex at birth, age, TBSA% (total burn surface area), rBaux score (revised Baux), APACHE (Acute Physiology and Chronic Health Evaluation) score, SOFA (sequential organ failure assessment) score, LOS (length of stay) and time from injury to death for these exemplar patients.

6.2.1.2 Cytokine and neutrophil analysis comparing unexpected survivors and unexpected deaths

What can be observed in the figures 6.1 to 6.3 is a less pro-inflammatory or more “dampened” immune response to burn injury in the unexpected survivors. IL-6, IL-10 and neutrophil numbers were all present at higher levels in those patients who died compared with those who survived. Each figure shows a comparison between an unexpected survivor and an unexpected death. Additional analysis of G-CSF, MCP-1, IL-8 and IL-1Ra all showed a similar relationship, in this matched analysis and in additional paired patients.

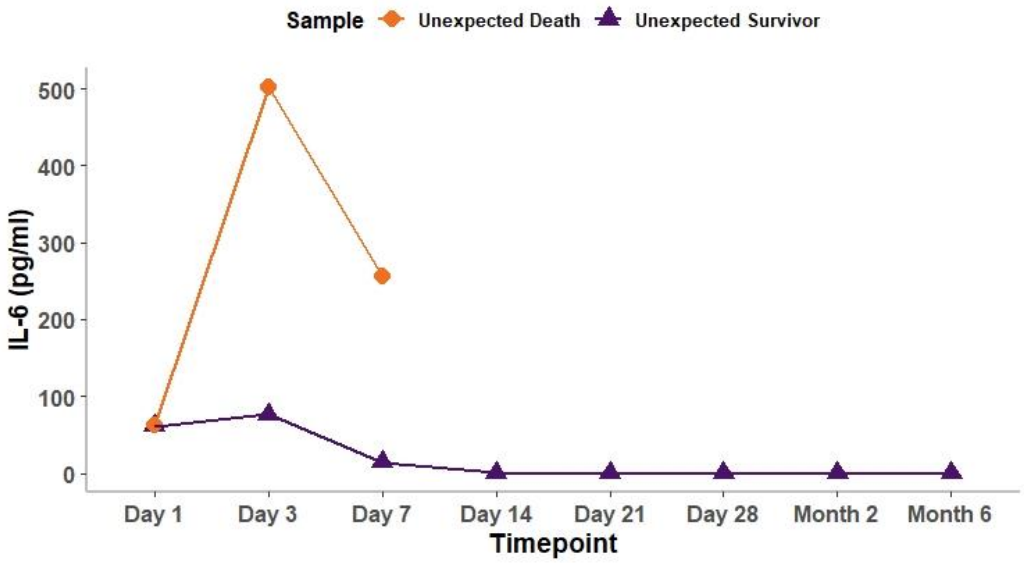


Figure 6.1: IL-6 Cytokine levels following trauma. Shown are the IL-6 levels of one unexpected survivor paired with one unexpected death. There is a clear difference in the levels of IL-6 observed, with notably higher levels in the unexpected death.

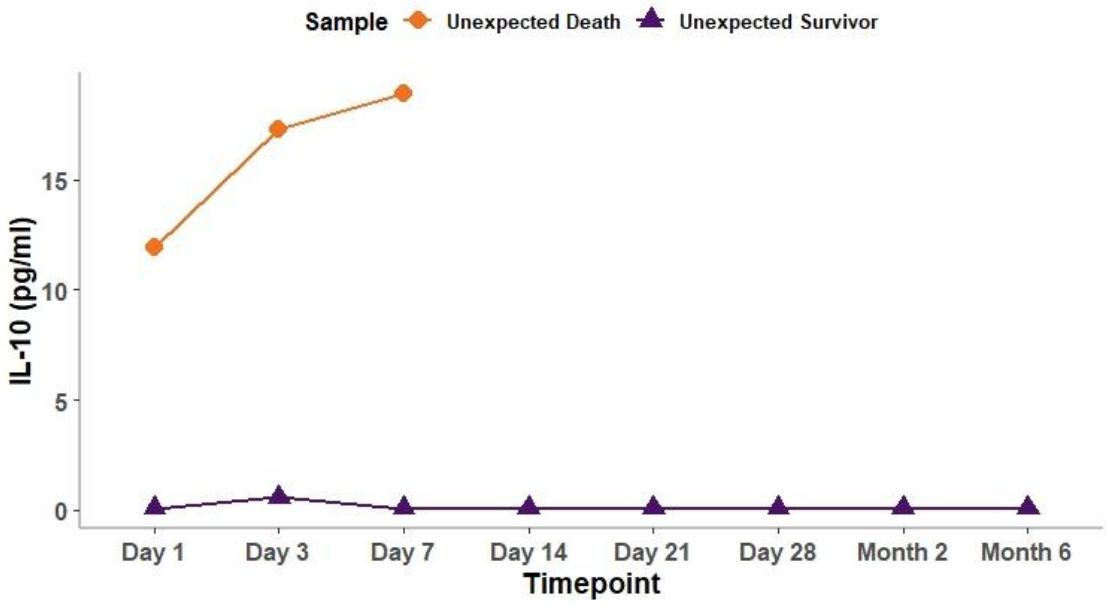


Figure 6.2: IL-10 Cytokine levels following trauma. Shown are the IL-10 levels of one unexpected survivor paired with one unexpected death. There is a clear difference in the levels of IL-10 observed, with notably higher levels in the unexpected death.

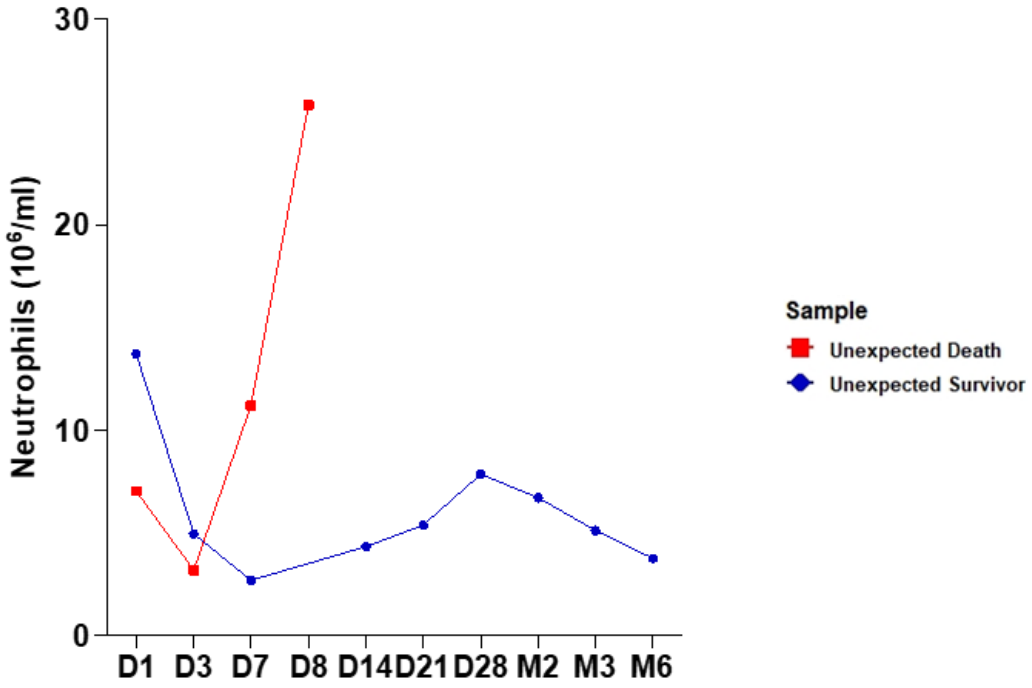


Figure 6.3: Neutrophil levels following burn trauma. Shown are the neutrophil numbers of one unexpected survivor paired with one unexpected death. There is a clear difference in the number of neutrophils after day 3, with notably higher numbers in the unexpected death.

6.2.2 Differential methylation between patients who died vs unexpected survivors

Following the discovery of these differential cytokine responses, the decision was made to investigate the "unexpected survivor" cohort from a genomic perspective. Considering that all these patients had their methylomes profiled following admission to hospital, the initial course of investigation was to see if there were any differentially methylated probes between patients who died and those who "unexpectedly" survived.

6.2.2.1 Differential methylation cohort information

The cohort consisted of the "unexpected survivors" and a group of patients who died following admission to hospital with what would be generally regarded as un-survivable injuries (Table 6.2).

	Unexpected survivors	Died
n	6	14
Age	49.78 (35.59 - 69.81)	55 (25.14-85.76)
F	0	4
M	6	10
TBSA%	79.00 (71- 95)	40.96 (14 - 79)
rBaux	139.13 (124 - 154)	109.79 (79.49 - 155)
APACHE	26 (18- 34)	30.08 (4 - 42)
SOFA	11.50 (11- 12)	11 (4 - 15)
LOS	83.50 (82 - 85)	12.71 (1 - 31)
Time from injury to death	n/a	12.95 (0.9 - 31.8)

Table 6.2: DNA methylation cohort information. Shown is the cohort information for each group, patients who died following un-survivable injuries and those who unexpectedly survived. Listed are the number of participants (n), sex at birth, mean; age, TBSA% (total burn surface area), rBaux score (revised Baux), APACHE (Acute Physiology and Chronic Health Evaluation) score, SOFA (sequential organ failure assessment) score, LOS (length of stay) and time from injury to death. Ranges are provided where appropriate.

6.2.2.2 Differential methylation analysis

Following p value adjustment to account for the false discovery rate, there were no differentially methylated genes or associated pathways between the groups (Figure 6.4).

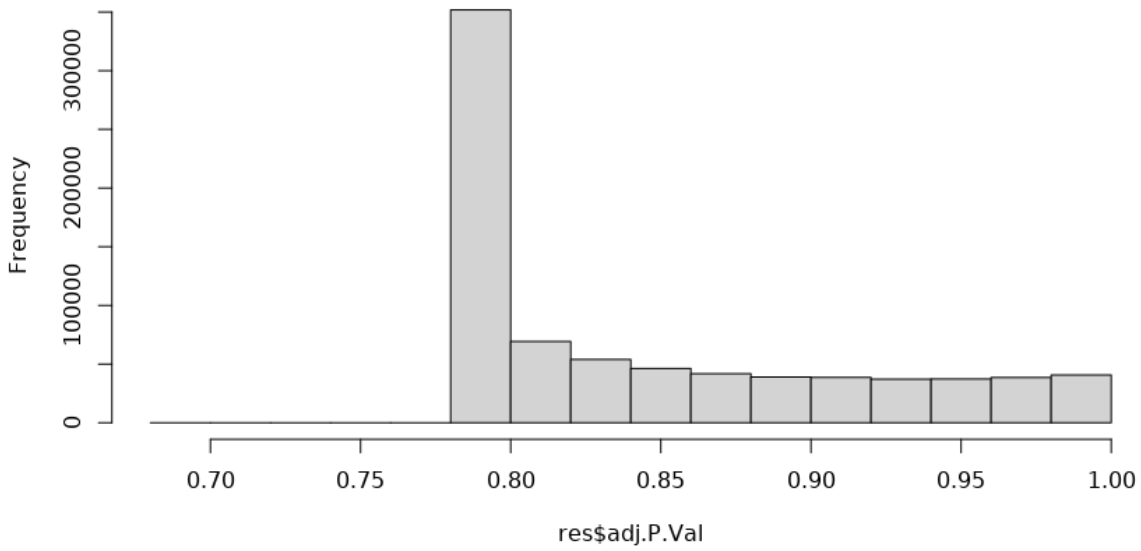


Figure 6.4: Differential methylation p value bar-plot. Shown in this figure are the BH adjusted p values and the frequency of these p values when looking at the differentially methylated probes when comparing unexpected survivors with patients who died following admission to hospital with burn injury. There are no adjusted p values below 0.775.

There was no significant difference in the epigenetic age acceleration observed in the unexpected survivors compared with the patients who died following admission (Figure 6.5).

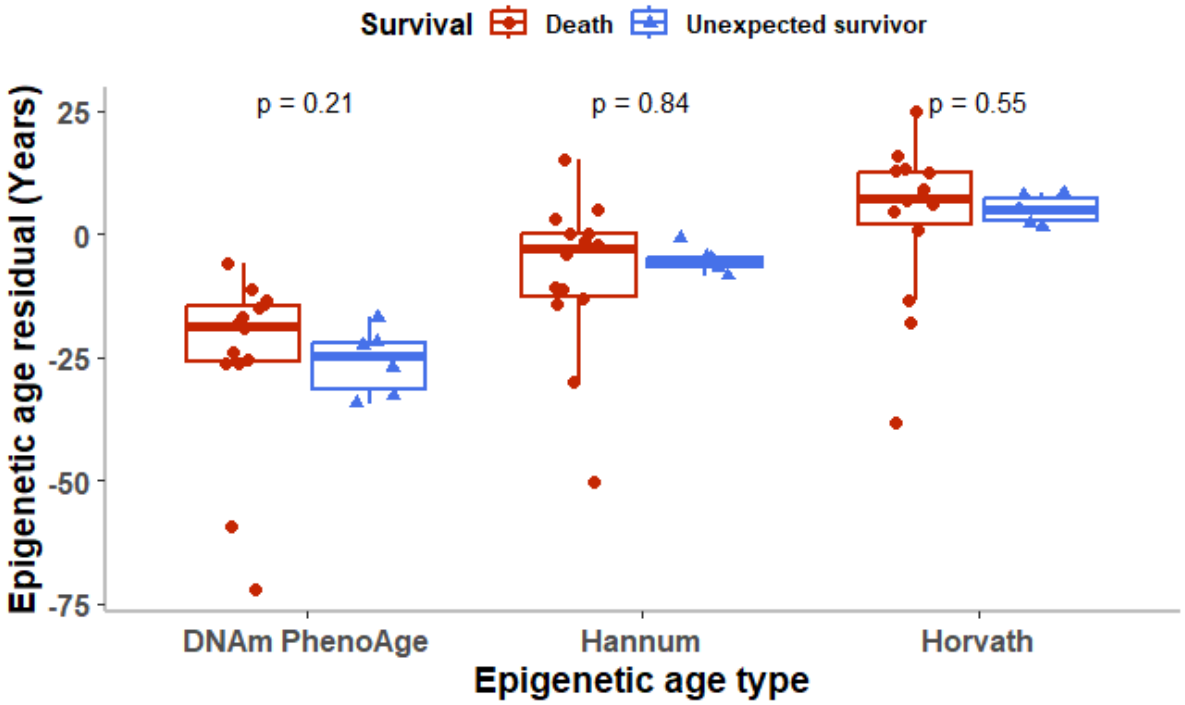


Figure 6.5: Epigenetic age acceleration in burn injured patients who died vs unexpected survivors. Shown in this figure are the epigenetic age residuals for the unexpected survivors compared with those patients who died. There was no significant difference between the groups according to any epigenetic clock.

6.2.3 RNA Sequencing analysis

RNA was extracted from PBMCs. The initial quality of this RNA was measured using the "RNA integrity number" or "RIN" feature present on the micro-gel electrophoresis platform the "Agilent 2200 TapeStation" (Schroeder et al., 2006). The RIN is generated independent of user interpretation reducing the risk of error and measures not only the ratio of the ribosomal bands (28S:18S) but using the entire electrophoretic trace of the RNA within the micro-gel, including any degraded sample.

Initial analysis revealed the extracted RNA to be low quality, this is reflected in the low RIN scores shown in Figure 6.6. Despite the low RIN the sequencing service advised that the samples were sufficient to use for RNA sequencing. RNA was run on the illumina HiSeq Xten platform following library construction with Lexogen modules. which perform well on samples of diminished quality, the exact modules used are listed in the methods chapter. The same cohort included above in the DNA methylation analysis were also used for RNA analysis.

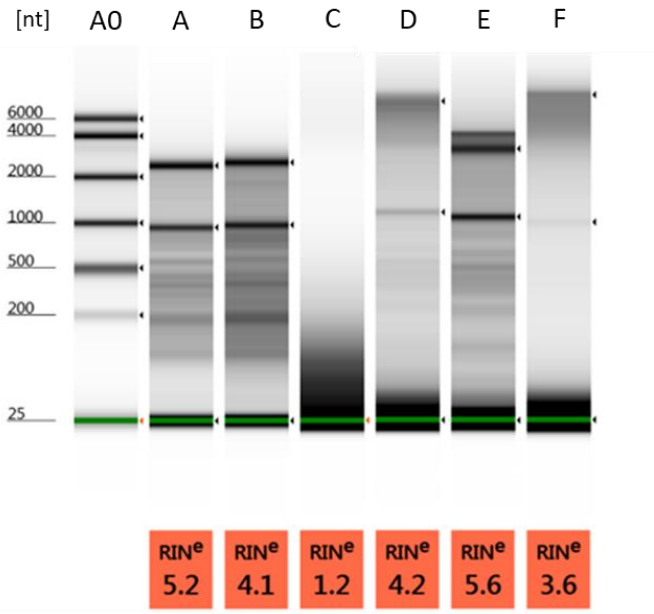


Figure 6.6: RNA microgel electrophoresis result from the Agilent 2200 TapeStation. RNA samples were loaded into lanes A1 and B1 and the RNA ladder was loaded into lane A0(L). There are multiple thick bands as well as a high level or smudging within the sample lanes indicating a high degree of sample degradation. This fragmentation is reflected in low RNA integrity numbers (RIN). RNA integrity numbers range from 0-10, 0 being the lowest.

6.2.3.1 RNA Sequencing cohort information

Although the same samples selected for RNA analysis were used for DNA methylation analysis, as listed in the previous section, 2 samples were excluded from analysis. This was due to issues de-multiplexing resulting in a high number of unassigned reads. The revised cohort information is listed below (Table 6.3).

	Unexpected survivors	Died
n	6	12
Age	49.78 (35.59 - 69.81)	50.18 (25.14 - 77.16)
F	0	4
M	6	8
TBSA%	79 (71 - 95)	45.77 (21 - 79)
rBaux	139.13 (124 - 154)	111.70 (79.49 - 155)
APACHE	26 (18- 34)	32 (23 - 42)
SOFA	11.50 (11 - 12)	11.30 (7 - 14)
LOS	83.50 (82 - 85)	14.08 (1 - 31)
Time from injury to death	n/a	14.29 (0.9 - 31.8)

Table 6.3: RNA sequencing cohort information. Shown is the cohort information for each group, patients who died following un-survivable injuries and those who unexpectedly survived. Listed are the number of participants (n), sex at birth, mean; age, TBSA% (total burn surface area), rBaux score (revised Baux), APACHE (Acute Physiology and Chronic Health Evaluation) score, SOFA (sequential organ failure assessment) score, LOS (length of stay) and time from injury to death. Ranges are provided where appropriate.

6.2.3.2 RNA sequencing analysis

"Trim Galore", a wrapper which contains "Cutadapt" and "FastQC" was used to assess sample quality and trim unwanted sequences from the data. The improved sample quality and reduced adapter content can be seen illustrated in Figure 6.7. Alignment was performed using the Rsubread package for R Studio and the GENCODE comprehensive Human genome annotation (Release 40).

A heatmap comparisons of the 100 most expressed genes showed, a somewhat unique expression profile in some of the unexpected survivors, however there appeared to be no specific genes for which expression levels appeared completely different between groups. Suggesting that the expression profiles of the patients were not drastically different (Figure 6.8).

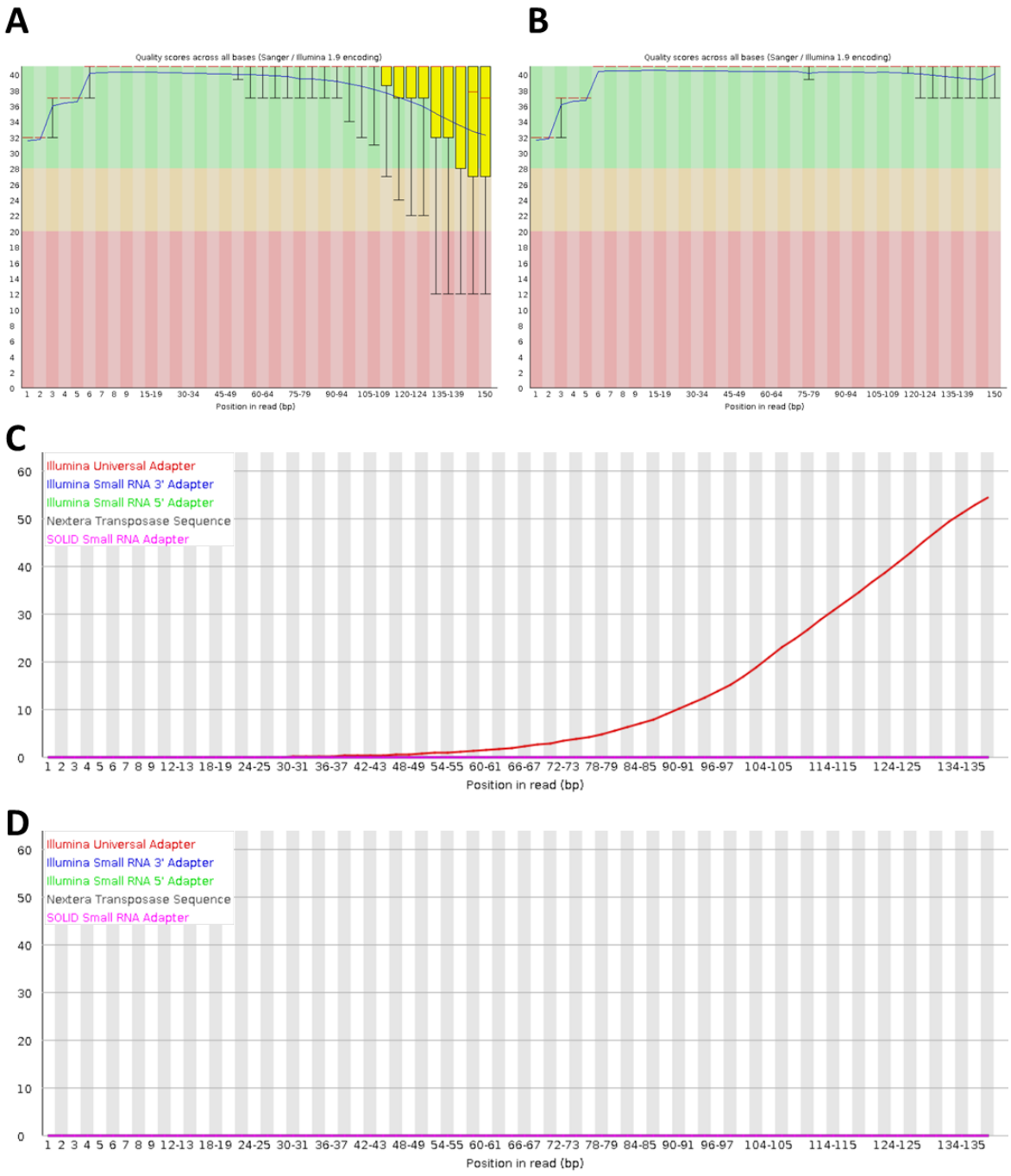


Figure 6.7: RNA Sequencing QC and trimming. Shown are the FastQC per base sequence quality sore graphs before (**A**) and after (**B**) processing with Trim Galore. Also shown are the adapter content graphs before (**C**) and after (**D**) processing.

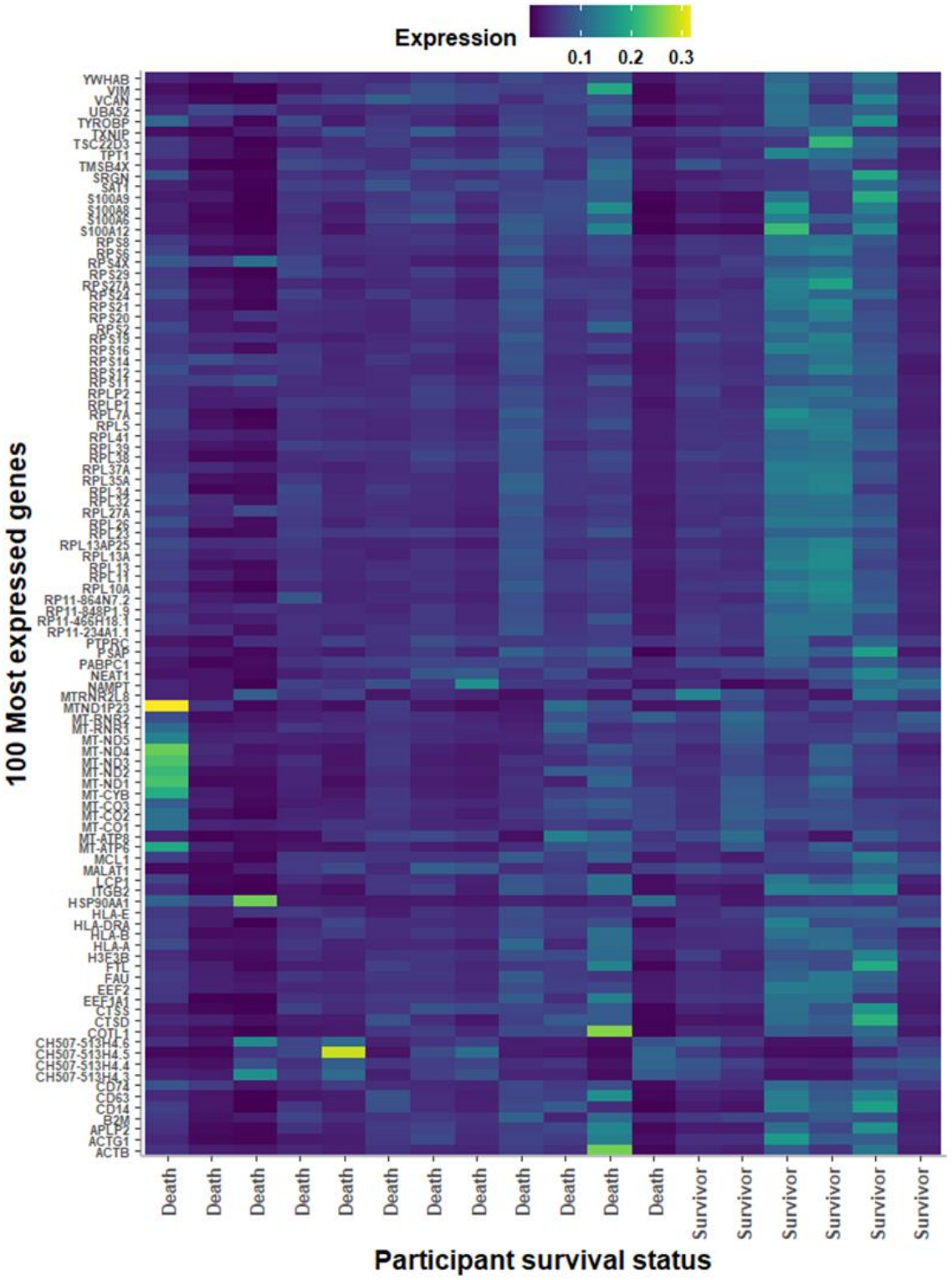


Figure 6.8: A heatmap of the top 100 most highly expressed genes for each patient. Shown are the top 100 most highly expressed genes for each patient labelled along the x axis according to survival status.

A PCA analysis also shows no clear distinction between patients based on survival status (Figure 6.9).

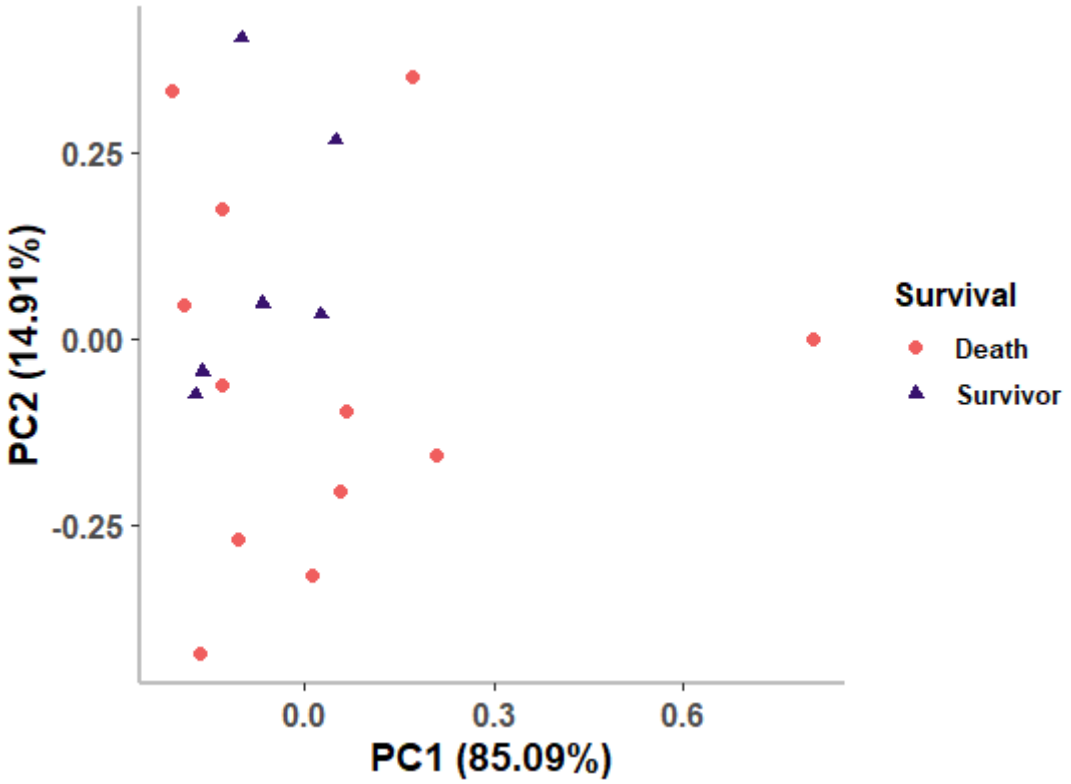


Figure 6.9: Transcriptional similarity between unexpected survivors and patients who died following burn injury. This PCA plot shows the Euclidian similarity of the samples according to their survival status.

When looking at all annotated genes, there were a large number of transcripts differentially expressed between the unexpected survivors and those patients who died. However, when adjusting for the false discovery rate, none were significant (Table 6.4). Seven sequences which did not map to a specific gene were excluded from this table, none of these sequences had a significant adjusted p value.

Gene	logFC	P.Value	adj.P.Val	Gene function
ADRA1B	-2.35	3.1E-05	0.2290	G Protein-coupled receptor involved in the activation of mitogenic response, growth and proliferation in multiple cell types (PubChem, 2022h).
MT1M	-2.17	0.00018	0.2290	Codes a metallothionein superfamily member. It is transcriptionally regulated by both glucocorticoids and heavy metals (NCBI - Gene, 2022n).
FDX1L	-1.56	0.00032	0.2290	A member of the ferredoxin family, it is Involved in heme-protein biosynthesis (Spiegel et al., 2014).
LRRTM1	-2.05	0.00024	0.2290	A transmembrane protein found in neurons (NCBI - Gene, 2022o).
OR52P1P	-2.38	0.00026	0.2290	An olfactory G Protein-coupled receptor (NCBI - Gene, 2021).
EFNA2	-2.70	0.00032	0.2290	A member of the ephrin family, a protein-tyrosine kinase implicated in nervous system developments and ephrin receptor binding (NCBI - Gene, 2022p).
PDE11A	-1.40	0.00041	0.2290	Involved in a variety of signal transduction pathways(PubChem, 2022i).
ELAVL2	-1.44	0.00042	0.2290	RNA binding protein which regulates gene expression post-transcriptionally (PubChem, 2023).
GCSAML	2.84	0.00013	0.2290	Associated with mature B cell proliferation (NCBI - Gene, 2022q).
FREM3	-2.07	0.00048	0.2290	Extracellular matrix protein which may be involved in cell adhesion (NCBI - Gene, 2022r).

Table 6.4: Top 10 differentially expressed genes between survivors and deaths. A table showing the 10 most differentially expressed genes between unexpected survivors and those patients who died following admission. Shown is gene name, fold change, p value, adjusted p value and gene ontology. Differentially expressed sequences which did not map to a specific gene have been excluded from this table. Following BH p value adjustment to account for the false discovery rate there were no significantly differentially expressed genes detected. logFC = log fold change; adj.P.Val = BH (Benjamini-Hochberg) P value adjusted for false discovery rate.

6.3 Discussion

6.3.1 Cytokine analysis

Data provided by Dr Hazeldine showed that all cytokines analysed, both pro- and anti-inflammatory appeared to be at lower levels in the patient who survived unexpectedly compared with the expected fatality. The unexpected survivor appeared to have an incredibly limited cytokine response given the degree of injury they sustained. It is reasonable to propose that these lower levels of cytokines and reduced neutrophilia would support the patient's unexpected survival. Multiple organ dysfunction syndrome (MODS) is a serious but common complication resulting from burn injury, with one study finding that it was present in 45.3% of burn patients, with MODS risk being increased in those over 40 years of age (Nguyen and Nguyen, 2009). This can often result in respiratory failure and anoxic brain injury (Silva et al., 2016), which one study showed to be the second and third largest causes of death in burn injury after sepsis (Williams et al., 2009). All of these post-burn morbidity risk factors have a commonality, they all cause death through, or as a result of, systemic inflammatory response syndrome (SIRS) (Fry, 2012).

Given the inflammatory pathology of burn-related mortality, it seems likely that an individual's inflammatory response would at least in part dictate their outcome. Patients with more muted inflammatory responses are likely to avoid SIRS and its associated cytokine storm (Fajgenbaum and June, 2020). The link between elevated inflammatory markers and patient outcomes has been demonstrated before. One study showed that in an ischaemic stroke cohort of 203 patients, a one unit increase in IL-6 gave an 18% increase in the risk of patients dying during admission. The same relationship to a slightly lower degree was observed with CRP and SAA (Rallidis et al., 2006). This relationship between increased inflammatory markers and increased mortality has also been shown in patients with COVID-19 where increased levels of IL-6 and CRP both showed a significant level of correlation with mortality and disease severity (Sakthidavel et al., 2021).

6.3.2 DNA methylation and transcriptome analysis

There were no observable differences in the methylomes of those patients who survived the un-survivable burn injury and those who succumbed to their injuries. We know that there are enormous changes in gene expression following critical illness (Xiao et al., 2011) and that DNA methylation plays a key role in regulating expression, so comparing a group of patients who survived with those who died, one might expect there to be differences in their DNA methylation profiles. This is especially true given that changes in methylation have been shown to occur quickly following injury (Verlinden et al., 2020) and vary based on insult type (Binnie et al., 2019).

DNA methylation arrays, as they currently perform, may be insufficiently sensitive to detect any differences between the groups examined in this study. Given the relatively small number of patients in each group, the large degree of variation observed between individuals, and the large changes that happen within the methylome following injury, regardless of survival, it may have been optimistic to expect to see any significant differences. It may also be true that while DNA methylation profiling can detect changes between groups such as severe and non-severe COVID-19, as demonstrated in this thesis, the distinction between sub-groups of patients who all have severe burns may be too subtle to detect. Since there were no differences detectable here the question still remained whether differences in gene expression may help to explain unexpected survival and the cytokine response.

The patients who died had a mean time to death of 14.29 days, but the range was broad from under 24 hours to close to 1 month. This would indicate that the factors influencing a patient's survival are at work early on following injury, perhaps even pre-dating the acquisition of the injury itself. We know that some people have a genetic pre-disposition which can make them immune to certain diseases. It has been observed for example that while sickle cell anaemia is detrimental to human health, and can often be fatal (Rees et al., 2010), however a polymorphism of this disease resulting in a less severe condition known as sickle cell trait can impart significant protection from malaria (Gong et al., 2013). Similarly, around 10% of northern Europeans are naturally immune to some strains of HIV due to an

imparted resistance from a CCR5-Δ32 allele passed down from ancestors who survived the bubonic plague (Galvani and Novembre, 2005). It is possible that there is a similar as yet unknown set of genes and variations which impart physical resilience and survival benefits with regards to injury?

However, the RNA analysis here suggested that there is no detectable difference in expression at admission between those patients who died and those who survived. This is again somewhat surprising given the difference observed in the cytokine levels in the preceding analysis. It is worth reiterating that the patients who died in the cytokine analysis were unexpected deaths occurring at an rBaux score deemed survivable, whereas the two groups used in the RNA analysis both had degrees of injury considered un-survivable. It will be important to go back and analyse the cytokine response in the non-survivors to determine whether they too had a higher cytokine response than the unexpected survivors. It was not possible to compare the expression of the genes associated with inflammation or different cytokines between the survivors and non-survivors due to there being no significant differences in the expression of any genes between the groups following false discovery correction. We are currently also collaborating up with Prof Marc Jeshcke in Canada to gain access to another 30 unexpected survivors in his buns clinic to determine if increasing the sample size reveals differences between survivors and non-survivors.

A second limitation is that quality of the starting material can greatly affect gene expression analysis. The PBMCs used for RNA extraction were in some cases approaching a decade in cold storage before use, this advanced sample age, paired with the non-RNA specific storage medium may go some way to explaining the relatively poor RNA quality obtained. The RNA integrity scores of samples examined ranged from 1.2-5.6, suggesting a high degree of fragmentation. Due to a lack of viable alternatives and the fact that these samples had already been obtained, this preliminary examination was undertaken. Two patients whose samples were unable to be de-multiplex were excluded from analysis. The number of reads per sample ranged from 14 to 34 million reads, with even the lowest number of reads sufficient to detect differentially expressed genes (Liu et al., 2014).

This lack of distinction between groups may also be explained somewhat by initial sample quality. During feature mapping there was a high degree of variability in the number of genomic features assigned to the sequencing data from each patient, ranging from as low as ~40% to as high as ~75%. This can be caused by the "multimapping" of short fragments of RNA mapping to multiple possible genes (Gallego Romero et al., 2014). Given the low starting quality it may be that much of the RNA has degraded, or that the presence of degraded RNA is masking the true differences in expression.

6.4 Conclusion

It is not yet clear based on this investigation whether unexpected survivors have a unique response to injury that relates to gene expression, or whether their response is purely related to a muted cytokine response. However, the cytokine response remained suppressed for an extended period it is hard to see how altered gene expression was not involved. Given what we know about the human genomic response to traumatic injury it seems likely that how a person's body responds is likely to determine their chances of survival. There are large changes in expression following a traumatic injury (Xiao et al., 2011), damaged tissues show expression profiles distinctly different from undamaged tissue (Michael et al., 2005), with different forms of injury causing different expression profiles (Lederer et al., 2008). Given that all the patients examined had, in broad terms, the same injury any subtle changes in expression which confer survival may be simply drowned out amongst the common, substantial changes in gene expression. It is also worth considering however that any differences in expression which help these unexpected survivors may not be detectable upon admission and in fact occur later. Alternatively, that there are no differences in expression in PBMCs, and that any advantages these patients possess is in fact not mediated through PBMCs and may relate to other systemic factors such as stress hormone responses.

To fully confirm or refute the hypothesis that differential gene expression is responsible for survival a dedicated and more specific study would need to be designed. The primary change would be to isolate

RNA immediately upon sample collection to prevent the RNA degradation observed in this study. While read depth does give diminishing returns after a certain point (Liu et al., 2014), it may still be beneficial to increase the read depth to increase the chances of detecting any small and subtle differences. Single cell RNA sequencing would further reduce the number of confounding factors and given that the inflammatory response seems to be altered in the unexpected survivors, the profiling of a single immune cell type may be a suitable place to start.

7. General discussion

The topics of trauma, disease and gerontology are widely researched. While our understanding of how age affects injury and disease outcome is fairly well established how injury specifically affects ageing is not. As has been discussed throughout this thesis, injury and disease have been shown to increase mortality and the rate at which individuals acquire many age associated diseases (Casey and Ballantyne, 2017; Duke et al., 2016, 2015b, 2015c). Despite this, information pertaining to the impact injury has on specific biomarkers used to quantify biological ageing is limited. The overall aim of this thesis was therefore to determine if there was an acceleration of the ageing process within the critical care environment, and whether illness was related to a traumatic injury, surgery, or infection (COVID-19). Overall biological age as well as ageing of the immune system were considered and whether severity of illness was associated with the degree of age acceleration was also considered. As a result of the COVID-19 pandemic an additional study was conducted looking at whether cell senescence, one of the hallmarks of ageing, could be reversed using epigenetic modifiers.

7.1 Key findings and interpretation

Telomere length: replicative senescence was perhaps the first biomarker of ageing to be described (Hayflick and Moorhead, 1961), and is now known to be caused by telomere attrition. Telomere length has been shown to decrease as chronological age increases (Rizvi et al., 2014). Leukocyte telomeres have been shown to be shorter in those who have experienced psychological injury such as childhood trauma or in combat exposed veterans (Behravan et al., 2018; Z. Li et al., 2017). Evidence showing physical injury is sufficient to cause leukocyte telomere attrition is less conclusive, but with near-significant trends being reported (Monroe et al., 2019). However, in this thesis I did not find a significant difference in telomere length in PBMCs between patients at admission and month 6 post injury or at either time point when compared with a healthy control group, nor was there any observed correlation between telomere length and chronological age, although the negative relationship was

approaching significance in the control group. This may be in part due to the high degree of interpersonal variation in telomere length. The evidence presented within the literature may explain why telomere length as a reliable marker of ageing is now more in doubt (Sanders and Newman, 2013; Shiels, 2010).

Immune phenotype: In this thesis, some aspects of immune senescence were observed within the burns cohort 6 months post injury relative to a healthy control population, including a reduction in naïve CD4+ T cells and recent thymic emigrants, and a general increase or remodelling of the memory compartments of cell populations towards the more differentiated EM cells. It has previously been reported in a paediatric cohort that even a minor burn injury (~10% TBSA%) was sufficient to cause a long-term change in the immune profiles of patients. This was seen via an increase in CD4+ central memory cells, as well as B cell remodelling when compared to healthy controls (Johnson et al., 2020). This is broadly in alignment with the data presented here. A further study also suggests that a spinal cord injury, is sufficient to cause immune senescence (Pavlicek et al., 2017). With injury mediated changes to the immune system occurring in under an hour (Hazeldine et al., 2017), characterised by a reduction in naïve T cell populations, and an increase in memory populations. This again lends support to the data presented in this thesis showing that burn injury is sufficient to cause long term remodelling of the immune system. In support of this proposal, there was a lower proportion of CD4+ naïve T cells as well as recent thymic emigrants in burns patients, and a greater proportion of specific CD8+ and CD4+ memory T cell subsets. As inflammatory cytokines such as TNFα are raised for many months after burn injury (Mulder et al., 2021), and are known to promote thymic atrophy (Luo et al., 2021), raised systemic inflammation may be a cause of this immune system ageing. A lower proportion of naïve B cells were also present in the burn group compared to the control group, again suggesting a shift towards an aged immune phenotype following injury. Many of these changes, such as reducing naïve and increasing memory populations correlated with chronological age, emphasising that these often age-associated changes are exacerbated in the burn group. Despite these changes to naïve cell and memory populations there was no significant difference in the number of senescent (CD57+,

CD28-) CD8+ and CD4+ T cells between groups, a finding which agrees with the telomere data and suggesting that the main effect of trauma was on thymic output.

Senescent cells in burn injured skin: The situation in tissue is quite different though. In vivo models have shown that following injury, such as cardiac ischemia-reperfusion, there is an increase in senescent cells at and around the site of injury (Dookun et al., 2020). Other in vitro investigations have shown that heat exposure was sufficient to induce senescence in BJ fibroblasts at the site of exposure, and that subsequent SASP release caused senescence to occur in non-senescent cells via the bystander effect (Kerschbaum et al., 2021b). It is also widely understood that senescent cells play a vital role in wound healing, with mice in which senescent cells are deleted having slower wound healing (Demaria et al., 2014). Given this, it was unsurprising to see that senescent cell frequency became elevated over time in tissue taken from burn injured sites, a finding supported by the literature and suggests that these cells are also important in human wound healing. What was somewhat surprising was that in some patients the senescent cell load remained elevated in the long-term, it is possible that these cells through their MMP-containing SASP may still be involved in scar tissue remodelling even 6 months after injury. However, there is not a great deal of literature discussing how injury affects senescent cell load in the long term in animal models or humans.

Modulation of senescence: If the studies reported here indicate a beneficial role for senescent cells, then future trials could use elements of the SASP shown to be important for wound healing, notably PDGFaa (Demaria et al., 2014), in topical applications for burns patients and in other patients with poor wound healing (e.g., type 2 diabetes). In other cases, it may be beneficial to slow or reverse cell senescence and here the data showed that (from an epigenetic compound library provided by Dr Annette von Delft), several compounds were identified which showed a senescence modulating effect. These compounds were observed to promote senescent fibroblast survival and reduce the percentage of β-galactosidase positive cells present. These represent potential therapeutic agents to use in situations where killing senescent cells could remove cells that are valuable and hard to replace, such

as cells such as in the brain and nervous system. As the drug library contained relatively new epigenetic research compounds, there is no literature pertaining to their effectiveness at modulating the senescent fibroblast phenotype. There are however other studies with similar aims which have identified compounds which behave in a similar way, reversing some aspects of cellular senescence (Latorre et al., 2017). This may therefore be a productive area for future drug discovery with the next step being potentially to pharmacologically modulate the senescent cell load in an animal model of injury to see how this impacts the ageing process.

Epigenetic age changes with critical illness: The field of epigenetics is perhaps the best suited to answering if age acceleration is occurring systemically, rather than in one particular tissue or cell type, encapsulating the totality of biological ageing. Epigenetic age acceleration has been shown to occur in a whole host of diseases and conditions (Boks et al., 2015; Horvath and Levine, 2015; Lawn et al., 2018; Verhoeven et al., 2018). Literature regarding epigenetic age acceleration because of physical injury however is much more limited. In this thesis DNA methylation analysis showed epigenetic age acceleration in all critical illness groups examined, though some clocks, notably DNAm PhenoAge also showed a reduced epigenetic age. Within burns patients their epigenetic ages were greater at admission compared with 6 months post injury with paired analysis showing a decline in epigenetic age over time. This suggests that burn injury caused acute epigenetic age acceleration which could be resolved partially over time. Septic and non-septic ICU patients also showed epigenetic age acceleration according to some epigenetic clocks, notably the Hannum clock. Septic patients showed a greater epigenetic age acceleration compared to non-septic patients and ICU patients who died showed greater epigenetic age residuals than those who survived. Increased MODS score also resulted in increased epigenetic age residuals when comparing septic and non-septic patients.

One interpretation of these data is that an insult sufficient to result in ICU admission causes epigenetic age acceleration, with sepsis and fatal insults further increasing the age acceleration experienced. An alternative interpretation is that these patients entering ICU with a higher epigenetic age were more

susceptible to sepsis and MODS. That the admission burns epigenetic age resolved partially by 6 months suggest that injury can accelerate ageing temporarily, though whether it returns to pre-injury levels is unknown. As tissue repair after a burn, or major surgery, involves substantial tissue regeneration and immune cell activation, it could result in aged tissue and immune cells. As we do not have pre-illness data, we cannot currently resolve this question. As already stated, there is limited literature looking at how physical injury impacts epigenetic ageing. What has been studied more widely is psychological injury such as PTSD, which has been shown to significantly increase epigenetic age (E. J. Wolf et al., 2017). Given the high degree of physiological stress incurred by a severe injury such as a large burn, it seems likely that a major injury too may cause epigenetic ageing, as is suggested by the epigenetic data presented here. While there is literature discussing epigenetic ageing following the development of sepsis it was focused on how age affects sepsis risk rather than if sepsis causes age acceleration itself (Lang et al., 2022). Given that HIV (Horvath and Levine, 2015), cytomegalovirus (Kananen et al., 2015) and bacterial infections (Gao et al., 2017) have been shown to cause age acceleration it follows that a diagnosis of sepsis is also likely to be associated with epigenetic age acceleration, as was suggested by the data in this thesis.

Whether COVID-19 causes epigenetic ageing is still debated in the literature. Two early publications had contradictory findings, with one finding no signs of epigenetic age acceleration (Franzen et al., 2021) and another finding there was epigenetic age acceleration acutely in COVID-19 (Cao et al., 2022). While there is no current consensus within the literature, at least some of it agrees with the findings presented within this thesis, that epigenetic ageing does occur following COVID-19, with disease leading to acceleration. Here both moderate and severe COVID-19 infection was associated with age acceleration according to some clocks though a reduced epigenetic age was suggested by PhenoAge. Differences in epigenetic clock data with COVID-19 were also reported by others (Cao et al., 2022) and may reflect the tissue they were developed from, with for example Hannum being more reliable for PBMCs. By Hannum and Horvath clocks, patients with severe infections showed a greater epigenetic age than those with moderate infections, which again could be interpreted as an effect of

infection on age acceleration. As infection involves sustained activation and proliferation of immune cells this is not surprising. However, it is also possible that these patients were more susceptible to infection due to their higher biological age. Most of our patients were obese and it is known that this will accelerate the DNAm age (reviewed by Hazeldine and Lord, 2020). Analysis of UKBiobank data revealed that those participants who succumbed to serious COVID-19 had 10-14 years higher PhenoAge (Kuo et al., 2020). Therefore, there are likely to be at least 2 explanations for the higher epigenetic and immune age in the COVID-19 patients with severe disease: Patients with severe disease symptoms experienced the most biological stress, accelerating their biological age, and those who already had an accelerated biological age were most likely to have severe symptoms.

Differential methylation analysis: Differential methylation analysis revealed changes to the methylation of genes associated with many pathways within the burns cohort, including pathways related to cell signalling, neuronal activity, the cardiovascular system, and general disease. The differential methylation of genes related to the cardiovascular system would suggest an impact upon this system which is known to be negatively impacted in the long term in burns patients (Duke et al., 2017; Guillory et al., 2016). In contrast, there was a noticeable lack of differentially methylated genes present within the ICU sepsis cohort which may have been a result of the format of the data provided by our collaborators for this thesis, being a pre-processed file rather than the raw data, allowing for a less thorough interrogation of the data. Within the COVID-19 cohort there were a wide range of differentially methylated genes and associated pathways. As the data were derived from patients 5 months after discharge, with many of them experiencing “long COVID" (Evans et al., 2021), it is interesting to note that the pathways which showed differential methylation appeared consistent with some of the clinical features of this syndrome. Thus, there were differentially methylated pathways which could be linked to “long covid” such as neuronal system pathways, with mental health issues such as brain fog being common in this cohort of patients (Evans et al., 2021). This link between epigenetic reprogramming and post-covid syndromes was also discussed by Cao et al (Cao et al., 2022) and recent data has shown that host cell epigenetic regulation is modified by the SARS-CoV-2 virus via

histone mimicry, effecting the transcriptional response to infection (Kee et al., 2022). This supports the idea of epigenetic reprogramming being at least partly responsible for the long-term health outcomes of these patients.

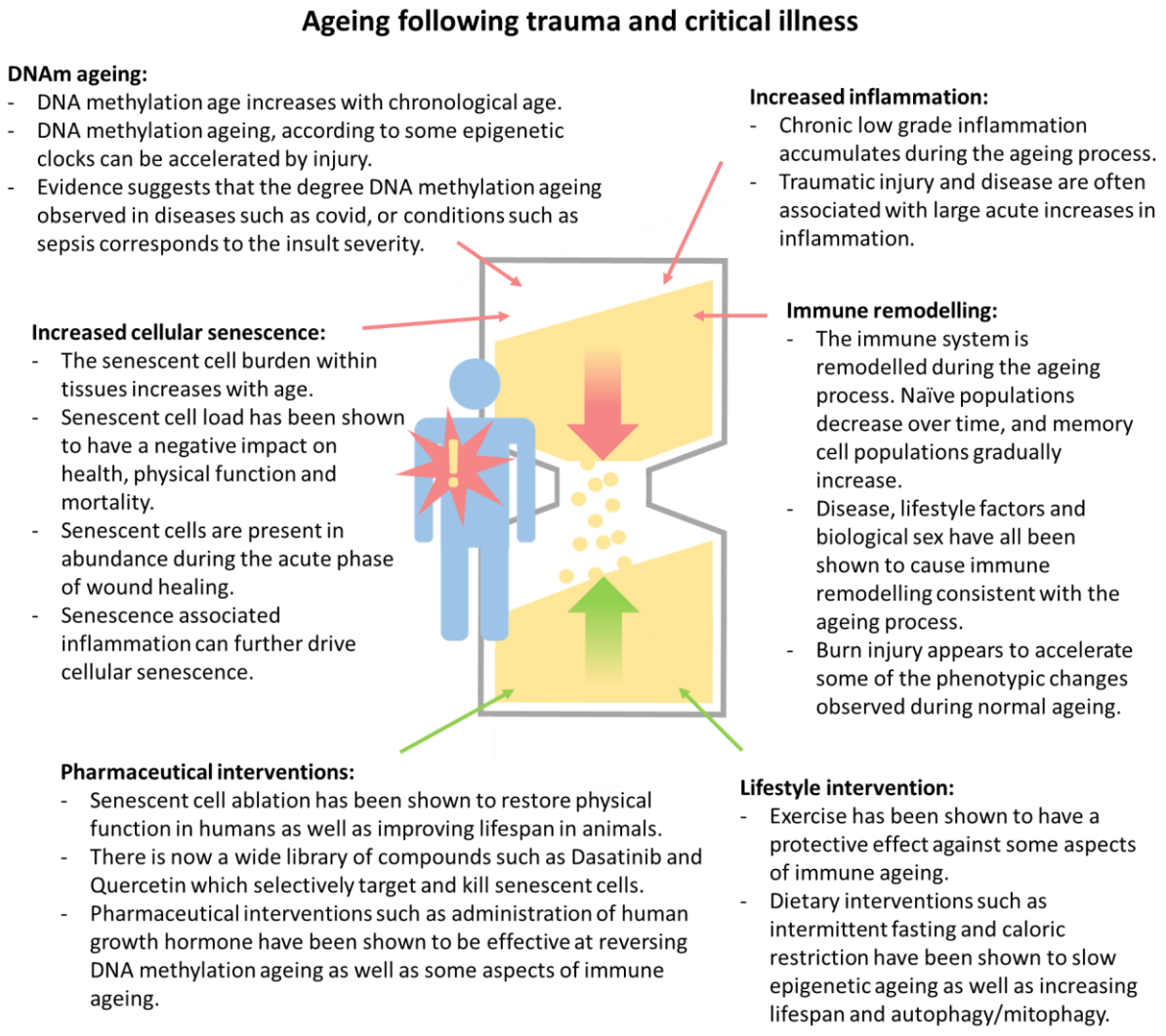


Figure 7.1: Ageing following trauma and critical illness - A figure showing several biological changes associated with the ageing process, how trauma and critical illness may mimic the ageing process by effecting these biological processes. Also shown are potential ways to combat the negative impact of the ageing process, and potentially improve patient outcomes following injury and illness.

7.2 Study limitations

Given the large amount of variation in telomere length between individuals this investigation may have been somewhat optimistic in its sample size. However, when working with samples taken at admission and at month 6 in burns patients there is going to be a fairly limited pool of patients to choose from as our unit generally sees less than 60 patients per year, many of whom do not agree to return for long term follow up. Increasing the relatively small sample size would be the major change suggested. Another change would be to look at more time points, seeing if the non-significant trend of telomere length increasing over time remained consistent.

With regards to the flow cytometry performed for immune phenotyping there were some limitations, some specific to this study, some more generally accepted limitations. Generating an IMM-AGE score to quantify the degree of immune ageing numerically rather than in cell subtype specific terms would have been a good addition to this work. As was discussed in the immune aging chapter, the modified IMM-AGE algorithm used did not appear sufficient to generate valid results. It would therefore have been preferable to use the original mass cytometry method of analysis. This wasn't possible for several reasons, the primary reason being that flow cytometry was chosen, rather than time of flight cytometry (CyTOF) as was used in the original generation of the IMM-AGE score (Alpert et al., 2019) due to cost. CyTOF, using metal isotopes, and much more specialised equipment makes it much more expensive and inaccessible than conventional flow cytometry. This also meant that a more limited number of cell subtypes could be examined as flow cytometry is limited in the amount of surface markers that can be used compared to CyTOF. With the flow cytometer available to me, only 10 colours could be used with 50 to 100 in CyTOF. This reduced number of markers however was still sufficient to profile all major cell types within the isolated PBMCs of patients, including those commonly used to describe immunosenescence.

When looking for cellular senescence it is preferable to confirm the presence of senescent cells using several markers. While $p16^{ink\ 4a}$ staining was successful, γH2AX staining was not optimised and was highly variable. Control tissues showed successful staining, but this could not be achieved in patient samples despite my best efforts. This was due in part to the "bubbled" working schedule used during parts of the COVID-19 pandemic which gave me only alternate days in the lab. The γH2AX staining protocol required an overnight incubation which was not possible during this time. Despite this reduction in data collection, the p16 staining proved fruitful and showed changes occurring within the tissue of burn injured patients which can form the basis of future investigations given that there are still plenty of tissue sections remaining meaning that other markers can be investigated.

The one aspect of the senescence reversal study which would have been improved upon would have been to try the compounds at different concentrations. However, given that samples were run in triplicate for cell viability and in triplicate for the β-galactosidase staining, and that there were many compounds to investigate, this was not feasible in the time frame of the thesis with the methods used. Despite only using the provided EC/50 values compounds with a senescence modulating effect were identified. Future studies should assess other aspects of senescence such as reversal of proliferative arrest and SASP output. It will also be important to evaluate the compounds with cells induced by different triggers such as oncogene-induced senescence or oxidative stress.

DNA methylation studies often benefit from high numbers of participants, here, additional injury cohorts were profiled, including military samples from veterans injured in Afghanistan. These were not included due to the small number of patients making up the cohort, but we have recently acquired another 150 samples which I will analyse going forward. The issues surrounding the RNA analysis of unexpected survivors of trauma were covered at length within the chapter, with poor sample quality likely to be the reason that no differences were detected between the examined groups. Despite this I believe that the investigation was still worthwhile, as there was no alternative sample available, and the potential novel results warranted taking a risk.

The overall limitation of all of the work performed here is that it was all done post critical illness. If cost were not a concern the most revealing method of measuring the impact of injury and disease on ageing would be to profile large swathes of the public over an extended period of time. This would include immune phenotyping, telomere analysis and DNAm profiling. This would allow a greater view of an individual's ageing trajectory up-to, during and post injury. Although the scale and cost of such a study is for now at least, out of the realms of possibility. Analysing patient samples before and after elective surgery offers one approach to gaining pre and post "injury" samples.

7.3 Recommendations for future work

There are often long-term health implications post injury and critical illness, regardless of recovery, and this study has outlined how accelerated ageing may be driving some of these poor outcomes. It remains to be seen how other aspects of the ageing process are altered in patients with injury or disease resulting in admission to the trauma and ICU environment. The physiological impact of injury and disease outlined in this study offer a potential way to improve the outcomes of patients if accelerated ageing is found, such as the testing of drugs able to modify ageing processes.

Given the long-term changes in cell senescence observed within the tissue, and the immunosenescence observed 6 months post burn injury, the use of senescence modulating compounds seems a logical step in developing a patient care pathway which could improve the long-term health outcomes of patients. The use of senolytic compounds to ablate senescent cells is already being assessed in clinical trials. Trials of compounds such as fisetin, dasatinib and quercetin all appear to be showing the ability to ameliorate many of the phenotypic changes associated with ageing (Wissler Gerdes et al., 2020). Other trials have also found success in reversing immune senescence by regenerating the thymic tissue of individuals following administration of human growth hormone, DHEA and metformin, this also had the effect of as well as reducing the trial subject's epigenetic age (Fahy et al., 2019). Caloric restriction and has been shown to slow the rate of epigenetic ageing and

increase lifespan in primates (Maegawa et al., 2017) as well as increasing autophagy (Bagherniya et al., 2018) and mitophagy (Mehrabani et al., 2020). While caloric restriction is perhaps the most robust and reproducible method of improving the rate of ageing (Lane et al., 2007), there are obvious issues regarding its practicability. There are however a growing group of compounds which mimic some of the effects of calorie restriction, known as CR-mimetics, many of which are currently in human trails with promising results (Hofer et al., 2022, 2021). Other compounds, such as alpha-ketoglutarate have been suggested as potential therapeutics for increasing health and lifespan due to their beneficial effects on immune and epigenetic regulation, as well as promoting positive outcomes in the treatments of many age associated diseases (Gyanwali et al., 2022). Alpha-ketoglutarate has also been demonstrated to improve wound healing in burn injury, further supporting its use in the trauma environment (De Bandt et al., 1998; Donati et al., 1999). Other compounds which are commonly prescribed also show positive modulatory effects on many aspects of the ageing process, including the diabetes drug metformin which has been associated with decrease in mortality (Novelle et al., 2016) and cholesterol reducing drugs known as statins which have been shown to have anti-inflammatory properties (Kim et al., 2019). The compounds mentioned modulate some aspect of the ageing process and represent a possible means of reversing or at least combating some the negative long-term impacts of traumatic injury, critical illness and infection. This, in the long term, may improve patient outcomes. In addition, further study into what enabled “unexpected survivors” to beat the odds and survive un-survivable injuries may reveal as yet unknown ways to help improve patient care.

7.4 Concluding remarks

It is widely known that regardless of how well a patient recovers from their initial critical illness, contracting a serious disease often does have a long-term negative impact on health. Despite this, little long-term care is available for patients beyond treating new ailments and conditions as and when they inevitably arise. Rather than being the result of some kind of apathy in the medical profession, I think the lack of action is due in large part to poor understanding of the longer-term consequences of

critical illness at the cell and molecular level. It is not possible to offer treatment for a condition before it occurs if its aetiology is not well understood. Given the research presented in this thesis, it may be that the common factor that predicts poor health and outcomes following injury and disease is an acceleration of the ageing process. Importantly the emerging field of geoscience is pointing the way to treating accelerated ageing by targeting core ageing hallmarks (Lopez-Otin et al., 2013), offering new hope for survivors of critical illness.

8. Glossary

Acronym, initialisation, or term	Definition and additional information
ACEs	Adverse childhood experiences.
APACHE	The APACHE II is a system for classifying disease severity and stands for "acute physiology and chronic health evaluation". It uses several lab and clinical parameters such as heart rate and white blood cell count (Knaus et al., 1985).
ARDS	Acute respiratory distress syndrome. Characterised by the rapid acute onset of inflammation in the lungs, effecting respiration (Matthay et al., 2019).
ATL	Absolute telomere length.
BMI	Body mass index. A weight index scoring system used clinically to establish if an individual is under, normal or overweight. BMI is calculated by dividing an individual's mass in kilograms by the square of their height in meters and multiplying by 703 (Keys et al., 1972).
Breg	Regulatory B cells
BSA	Bovine serum albumin.
Burn (Injury)	Burns or "burn injuries" are characterised by tissue damage arising from overexposure to heat for example from a flame or scald. Burns can also result from exposure to excessive amounts of radiation, electricity, or certain chemicals. They range from 1st degree burns which only effect the outer most layer of the skin (epidermis) to 3rd degree burns which penetrate through all the skin layers and reach the subdermal fat tissue. 4th degree burns may effect bone or muscle tissue (Jeschke et al., 2020).
CM	Central memory.
COPD	Chronic obstructive pulmonary disease.
CpG or CpG site	A site within the DNA structure where a cytosine nucleotide is followed by a guanine nucleotide.
CRP	C-Reactive protein.
CyTOF	Time of flight cytometry. A mass cytometry method of cell analysis which is able to detect upwards of 50 surface markers on a single cell.
DAMP(s)	Damage-associated molecular pattern(s).
DNA	Deoxyribonucleic acid.
DNAm	DNA Methylation.
EM	Effector memory.
Gy	Gray. The unit used to quantify absorbed radiation.
HIV	Human immunodeficiency virus.
ICU	Intensive care unit.
IHC	Immunohistochemistry. An immunostaining method used primarily to confirm the presence of proteins of interest.
IL	Interleukin, a family of cytokines. When used in the text it is usually followed by a number i.e., IL-1, to refer to a specific cytokine.
ISS	Injury severity score. An injury scoring system based on the most severe injury sustained to 6 regions of the body: the head and neck, face, chest, abdomen, extremity (including pelvis) and external (Baker and O'neill, 1976).
kb	Kilobase. A unit equal to 1000 bases.
LOS	Length of stay (referring to the amount of time a patient is admitted to the hospital for).
NAD	Nicotinamide adenine dinucleotide.
NADP/H	Nicotinamide adenine dinucleotide phosphate.
NK Cells	Natural killer cells
PBMC	Human peripheral blood mononuclear cells. Isolated from whole blood for use in this study. PBMCs are comprised of T cells, B cells, NK cells as well as monocytes and macrophages.

PBS	Phosphate-buffered saline.
PI	Propidium Iodide.
PTSD	Post-traumatic stress disorder.
qPCR	Quantitative polymerase chain reaction.
rBaux	Revised Baux score. A clinical scoring system specific to burn injury which incorporates total burn surface area percentage (TBSA%), chronological age and inhalation injury.
RNA	Ribonucleic acid.
RNS	Reactive nitrogen species.
ROS	Reactive oxygen species.
RTE	Recent thymic emigrants.
SASP	Senescence associated secretory phenotype.
SA-βGal	Senescence-associated beta-galactosidase. Widely considered to be a biomarker for cellular senescence.
SCI	Spinal cord injury.
SIFTI	A burn injury research study "**S**cientific **i**nvestigation of the Biological Pathways **F**ollowing **T**hermal **I**njury I & II".
SNP	Single-nucleotide polymorphism. A single nucleotide substitution at a specific point in the genome.
SOFA (Score)	The sequential organ failure assessment score. The SOFA score predicts ICU mortality based on a combination of clinical and lab data (Lambden et al., 2019).
TBI	Traumatic brain injury. The term describes injury to the brain resulting from sudden trauma. Examples of this would be a forceful blow to the head, or an object piercing the skull, causing injury to the brain tissue directly, secondary injury such as hypoxia and herniation (Ghajar, 2000).
TBSA (%)	Total burn surface area percentage. The area of the body effected by a burn injury expressed as a percentage of the total body surface area.
TCA cycle	The tricarboxylic acid, often referred to as the Krebs cycle.
TEMRA	Terminally differentiated effector memory T cells.
TNF(α)	Tumour necrosis factor (Alpha).
Treg	Regulatory T cells
UKB	United Kingdom Biobank.
US	United States (of America)
WBC	White blood cell.

9. Bibliography

Aas, M., Elvsåshagen, T., Westlye, L.T., Kaufmann, T., Athanasiu, L., Djurovic, S., Melle, I., van der Meer, D., Martin-Ruiz, C., Steen, N.E., Agartz, I., Andreassen, O.A., 2019. Telomere length is associated with childhood trauma in patients with severe mental disorders. Transl Psychiatry 9, 1–7. https://doi.org/10.1038/s41398-019-0432-7

Abbas, T., Dutta, A., 2009. p21 in cancer: intricate networks and multiple activities. Nat Rev Cancer 9, 400–414. https://doi.org/10.1038/nrc2657

Abdelrahman, Z., Li, M., Wang, X., 2020. Comparative Review of SARS-CoV-2, SARS-CoV, MERS-CoV, and Influenza A Respiratory Viruses. Frontiers in Immunology 11. https://doi.org/10.3389/fimmu.2020.552909

Abdullah, M., Chai, P.-S., Chong, M.-Y., Tohit, E.R.M., Ramasamy, R., Pei, C.P., Vidyadaran, S., 2012. Gender effect on in vitro lymphocyte subset levels of healthy individuals. Cell Immunol 272, 214–219. https://doi.org/10.1016/j.cellimm.2011.10.009

Ademokun, A., Wu, Y.-C., Dunn-Walters, D., 2010a. The ageing B cell population: Composition and function. Biogerontology 11, 125–137. https://doi.org/10.1007/s10522-009-9256-9

Ademokun, A., Wu, Y.-C., Dunn-Walters, D., 2010b. The ageing B cell population: composition and function. Biogerontology 11, 125–137. https://doi.org/10.1007/s10522-009-9256-9

Agarwal, P., Sandey, M., DeInnocentes, P., Bird, R.C., 2013. Tumor suppressor gene p16/INK4A/CDKN2A-dependent regulation into and out of the cell cycle in a spontaneous canine model of breast cancer. J Cell Biochem 114, 1355–1363. https://doi.org/10.1002/jcb.24476

Ahmadi, N., Hajsadeghi, F., Mirshkarlo, H.B., Budoff, M., Yehuda, R., Ebrahimi, R., 2011. Post-traumatic Stress Disorder, Coronary Atherosclerosis, and Mortality. The American Journal of Cardiology 108, 29–33. https://doi.org/10.1016/j.amjcard.2011.02.340

Aiello, A., Farzaneh, F., Candore, G., Caruso, C., Davinelli, S., Gambino, C.M., Ligotti, M.E., Zareian, N., Accardi, G., 2019. Immunosenescence and Its Hallmarks: How to Oppose Aging Strategically? A Review of Potential Options for Therapeutic Intervention. Front. Immunol. 10, 2247. https://doi.org/10.3389/fimmu.2019.02247

Aït-Ali, N., Fridlich, R., Millet-Puel, G., Clérin, E., Delalande, F., Jaillard, C., Blond, F., Perrocheau, L., Reichman, S., Byrne, L.C., Olivier-Bandini, A., Bellalou, J., Moyse, E., Bouillaud, F., Nicol, X., Dalkara, D., van Dorsselaer, A., Sahel, J.-A., Léveillard, T., 2015. Rod-derived cone viability factor promotes cone survival by stimulating aerobic glycolysis. Cell 161, 817–832. https://doi.org/10.1016/j.cell.2015.03.023

Akira, S., Hemmi, H., 2003. Recognition of pathogen-associated molecular patterns by TLR family. Immunology Letters 85, 85–95. https://doi.org/10.1016/S0165-2478(02)00228-6

Alexander, W., Schneider, H.-G., Smith, C., Cleland, H., 2018. The Incidence and Significance of Raised Troponin Levels in Acute Burns. J Burn Care Res 39, 729–735. https://doi.org/10.1093/jbcr/irx020

Allali-Hassani, A., Szewczyk, M.M., Ivanochko, D., Organ, S.L., Bok, J., Ho, J.S.Y., Gay, F.P.H., Li, F., Blazer, L., Eram, M.S., Halabelian, L., Dilworth, D., Luciani, G.M., Lima-Fernandes, E., Wu, Q., Loppnau, P., Palmer, N., Talib, S.Z.A., Brown, P.J., Schapira, M., Kaldis, P., O'Hagan, R.C., Guccione, E., Barsyte-Lovejoy, D., Arrowsmith, C.H., Sanders, J.M., Kattar, S.D., Bennett, D.J., Nicholson, B., Vedadi, M., 2019. Discovery of a chemical probe for PRDM9. Nat Commun 10, 5759. https://doi.org/10.1038/s41467-019-13652-x

Allen, J.C., Toapanta, F.R., Chen, W., Tennant, S.M., 2020. Understanding immunosenescence and its impact on vaccination of older adults. Vaccine 38, 8264–8272. https://doi.org/10.1016/j.vaccine.2020.11.002

Alpert, A., Pickman, Y., Leipold, M., Rosenberg-Hasson, Y., Ji, X., Gaujoux, R., Rabani, H., Starosvetsky, E., Kveler, K., Schaffert, S., Furman, D., Caspi, O., Rosenschein, U., Khatri, P., Dekker, C.L., Maecker, H.T., Davis, M.M., Shen-Orr, S.S., 2019. A clinically meaningful metric of immune age derived from high-dimensional longitudinal monitoring. Nat Med 25, 487–495. https://doi.org/10.1038/s41591-019-0381-y

Anand, R., Beach, A., Li, K., Haber, J., 2017. Rad51-mediated double-strand break repair and mismatch correction of divergent substrates. Nature 544, 377–380. https://doi.org/10.1038/nature22046

Antonangeli, F., Zingoni, A., Soriani, A., Santoni, A., 2019. Senescent cells: Living or dying is a matter of NK cells. Journal of Leukocyte Biology 105, 1275–1283. https://doi.org/10.1002/JLB.MR0718-299R

Araki, T., Nishino, M., Gao, W., Dupuis, J., Hunninghake, G.M., Murakami, T., Washko, G.R., O'Connor, G.T., Hatabu, H., 2016. Normal Thymus in Adults: Appearance on CT and Associations with Age, Sex, BMI and Smoking. Eur Radiol 26, 15–24. https://doi.org/10.1007/s00330-015-3796-y

Asadi-Pooya, A.A., Akbari, A., Emami, A., Lotfi, M., Rostamihosseinkhani, M., Nemati, H., Barzegar, Z., Kabiri, M., Zeraatpisheh, Z., Farjoud-Kouhanjani, M., Jafari, A., Sasannia, S., Ashrafi, S., Nazeri, M., Nasiri, S., Shahisavandi, M., 2022. Long COVID syndrome-associated brain fog. Journal of Medical Virology 94, 979–984. https://doi.org/10.1002/jmv.27404

Asito, A.S., Piriou, E., Jura, W.G., Ouma, C., Odada, P.S., Ogola, S., Fiore, N., Rochford, R., 2011. Suppression of circulating IgD+CD27+ memory B cells in infants living in a malaria-endemic region of Kenya. Malar J 10, 362. https://doi.org/10.1186/1475-2875-10-362

Austad, S.N., Fischer, K.E., 2016. Sex Differences in Lifespan. Cell Metab 23, 1022–1033. https://doi.org/10.1016/j.cmet.2016.05.019

Awtry, E., Jeon, C., Ware, M.G., 2006. Blueprints Cardiology. Lippincott Williams & Wilkins. ISBN: 9781405104647

Azcona-Sanjulian, M.C., 2021. Telomere Length and Pediatric Obesity: A Review. Genes 12, 946. https://doi.org/10.3390/genes12060946

Bagherniya, M., Butler, A.E., Barreto, G.E., Sahebkar, A., 2018. The effect of fasting or calorie restriction on autophagy induction: A review of the literature. Ageing Res Rev 47, 183–197. https://doi.org/10.1016/j.arr.2018.08.004

Baker, D.J., Wijshake, T., Tchkonia, T., LeBrasseur, N.K., Childs, B.G., van de Sluis, B., Kirkland, J.L., van Deursen, J.M., 2011. Clearance of p16Ink4a-positive senescent cells delays ageing-associated disorders. Nature 479, 232–236. https://doi.org/10.1038/nature10600

Baker, S.P., O'neill, B., 1976. THE INJURY SEVERITY SCORE: AN UPDATE. Journal of Trauma and Acute Care Surgery 16, 882. https://doi.org/10.1097/00005373-197611000-00006

Bano, G., Trevisan, C., Carraro, S., Solmi, M., Luchini, C., Stubbs, B., Manzato, E., Sergi, G., Veronese, N., 2017. Inflammation and sarcopenia: A systematic review and meta-analysis. Maturitas 96, 10–15. https://doi.org/10.1016/j.maturitas.2016.11.006

Barbé-Tuana, F., Funchal, G., Schmitz, C.R.R., Maurmann, R.M., Bauer, M.E., 2020. The interplay between immunosenescence and age-related diseases. Semin Immunopathol 42, 545–557. https://doi.org/10.1007/s00281-020-00806-z

Barnes, J., Duffy, A., Hamnett, N., McPhail, J., Seaton, C., Shokrollahi, K., James, M.I., McArthur, P., Jones, R.P., 2015. The Mersey Burns App: evolving a model of validation. Emerg Med J 32, 637–641. https://doi.org/10.1136/emermed-2013-203416

Bartlett, D.B., Firth, C.M., Phillips, A.C., Moss, P., Baylis, D., Syddall, H., Sayer, A.A., Cooper, C., Lord, J.M., 2012. The age-related increase in low-grade systemic inflammation (Inflammaging) is not driven by cytomegalovirus infection. Aging cell 11, 912–915. https://doi.org/10.1111/j.1474-9726.2012.00849.x

Basu, S., Dewangan, S., Shukla, R.C., Anupurva, S., Kumar, A., 2012. Thymic involution as a predictor of early-onset neonatal sepsis. Paediatrics and International Child Health 32, 147–151. https://doi.org/10.1179/2046905512Y.0000000018

Batista, I. de A.A., Helguero, L.A., 2018. Biological processes and signal transduction pathways regulated by the protein methyltransferase SETD7 and their significance in cancer. Sig Transduct Target Ther 3, 1–14. https://doi.org/10.1038/s41392-018-0017-6

Battaglia, A., Carey, J.C., South, S.T., 2015. Wolf–Hirschhorn syndrome: A review and update. American Journal of Medical Genetics Part C: Seminars in Medical Genetics 169, 216–223. https://doi.org/10.1002/ajmg.c.31449

Baumeister, D., Akhtar, R., Ciufolini, S., Pariante, C.M., Mondelli, V., 2016. Childhood trauma and adulthood inflammation: a meta-analysis of peripheral C-reactive protein, interleukin-6, and tumour necrosis factor-α. Molecular Psychiatry 21, 642–649. https://doi.org/10.1038/mp.2015.67

Bauzá, G., LaMorte, W.W., Burke, P.A., Hirsch, E.F., 2008. High Mortality in Elderly Drivers is Associated With Distinct Injury Patterns: Analysis of 187,869 Injured Drivers. Journal of Trauma and Acute Care Surgery 64, 304–310. https://doi.org/10.1097/TA.0b013e3181634893

Baylis, D., Ntani, G., Edwards, M.H., Syddall, H.E., Bartlett, D.B., Dennison, E.M., Martin-Ruiz, C., Zglinicki, T. von, Kuh, D., Lord, J.M., Sayer, A.A., Cooper, C., 2014. Inflammation, telomere length, and grip strength: a 10-year longitudinal study. Calcified tissue international 95, 54–63. https://doi.org/10.1007/s00223-014-9862-7 [doi]

Behravan, E., Moallem, S.A., Kalalinia, F., Ahmadimanesh, M., Blain, P., Jowsey, P., Khateri, S., Forghanifard, M.M., BalaliMood, M., 2018. Telomere shortening associated with increased levels of oxidative stress in sulfur mustard-exposed Iranian veterans. Mutat Res Genet Toxicol Environ Mutagen 834, 1–5. https://doi.org/10.1016/j.mrgentox.2018.06.017

Benjamini, Y., Hochberg, Y., 1995. Controlling the False Discovery Rate: A Practical and Powerful Approach to Multiple Testing. Journal of the Royal Statistical Society. Series B (Methodological) 57, 289–300. https://doi.org/10.1111/j.2517-6161.1995.tb02031.x

Bernadotte, A., Mikhelson, V.M., Spivak, I.M., 2016. Markers of cellular senescence. Telomere shortening as a marker of cellular senescence. Aging (Albany NY) 8, 3–11. https://doi.org/10.18632/aging.100871

Bessel, van der K., 2014. The body keeps the score. Viking Press. ISBN: 978-0143127741

Bhadricha, H., Patel, V., Singh, A.K., Savardekar, L., Patil, A., Surve, S., Desai, M., 2021. Increased frequency of Th17 cells and IL-17 levels are associated with low bone mineral density in postmenopausal women. Sci Rep 11, 16155. https://doi.org/10.1038/s41598-021-95640-0

Bhat, R., Crowe, E.P., Bitto, A., Moh, M., Katsetos, C.D., Garcia, F.U., Johnson, F.B., Trojanowski, J.Q., Sell, C., Torres, C., 2012. Astrocyte Senescence as a Component of Alzheimer's Disease. PLOS ONE 7, e45069. https://doi.org/10.1371/journal.pone.0045069

Binnie, A., Walsh, C., Hu, P., Dwivedi, D., Fox-Robichaud, A., Liaw, P., Tsang, J., Batt, J., Carrasqueiro, G., Gupta, S., Marshall, J., Castelo-Branco, P., Santos, C., 2019. Epigenetic Profiling in Severe Sepsis: A Pilot Study of DNA Methylation Profiles in Critical Illness. Critical care medicine 48. https://doi.org/10.1097/CCM.0000000000004097

Biran, A., Zada, L., Abou Karam, P., Vadai, E., Roitman, L., Ovadya, Y., Porat, Z., Krizhanovsky, V., 2017. Quantitative identification of senescent cells in aging and disease. Aging Cell 16, 661–671. https://doi.org/10.1111/acel.12592

Birch, J., Gil, J., 2020. Senescence and the SASP: many therapeutic avenues. Genes Dev. 34, 1565–1576. https://doi.org/10.1101/gad.343129.120

Björkström, N.K., Riese, P., Heuts, F., Andersson, S., Fauriat, C., Ivarsson, M.A., Björklund, A.T., Flodström-Tullberg, M., Michaëlsson, J., Rottenberg, M.E., Guzmán, C.A., Ljunggren, H.-G., Malmberg, K.-J., 2010. Expression patterns of NKG2A, KIR, and CD57 define a process of CD56dim NK-cell differentiation uncoupled from NK-cell education. Blood 116, 3853–3864. https://doi.org/10.1182/blood-2010-04-281675

Blackburn, E.H., Epel, E.S., Lin, J., 2015. Human telomere biology: A contributory and interactive factor in aging, disease risks, and protection. Science 350, 1193–1198. https://doi.org/10.1126/science.aab3389

Blagosklonny, M.V., 2010. Calorie restriction: Decelerating mTOR-driven aging from cells to organisms (including humans). Cell Cycle 9, 683–688. https://doi.org/10.4161/cc.9.4.10766

Blanchard, N., Salvioni, A., Robey, E.A., 2020. Chapter 26 - Adaptive immunity, in: Weiss, L.M., Kim, K. (Eds.), Toxoplasma Gondii (Third Edition). Academic Press, pp. 1107–1146. https://doi.org/10.1016/B978-0-12-815041-2.00026-8

Boccardi, V., Pelini, L., Ercolani, S., Ruggiero, C., Mecocci, P., 2015. From cellular senescence to Alzheimer's disease: The role of telomere shortening. Ageing Research Reviews 22, 1–8. https://doi.org/10.1016/j.arr.2015.04.003

Boks, M.P., Mierlo, H.C. van, Rutten, B.P.F., Radstake, T.R.D.J., Witte, L.D., Geuze, E., Horvath, S., Schalkwyk, L.C., Vinkers, C.H., Broen, J.C.A., Vermetten, E., 2015. Longitudinal changes of telomere length and epigenetic age related to traumatic stress and post-traumatic stress disorder. https://doi.org/10.1016/j.psyneuen.2014.07.011

Bonnon, C., Wendeler, M.W., Paccaud, J.-P., Hauri, H.-P., 2010. Selective export of human GPI-anchored proteins from the endoplasmic reticulum. J Cell Sci 123, 1705–1715. https://doi.org/10.1242/jcs.062950

Bosco, E.E., Mulloy, J.C., Zheng, Y., 2009. Rac1 GTPase: A "Rac" of All Trades. Cell Mol Life Sci 66, 370–374. https://doi.org/10.1007/s00018-008-8552-x

Brooks, J.C., Strauss, D.J., Shavelle, R.M., Paculdo, D.R., Hammond, F.M., Harrison-Felix, C.L., 2013. Long-term disability and survival in traumatic brain injury: results from the National Institute on Disability and Rehabilitation Research Model Systems. Archives of Physical Medicine and Rehabilitation 94, 2203–2209. https://doi.org/10.1016/j.apmr.2013.07.005

Brown, A.W., Leibson, C.L., Malec, J.F., Perkins, P.K., Diehl, N.N., Larson, D.R., 2004. Long-term survival after traumatic brain injury: a population-based analysis. NeuroRehabilitation 19, 37–43. PMID: 14988586

Brown, D.W., Anda, R.F., Tiemeier, H., Felitti, V.J., Edwards, V.J., Croft, J.B., Giles, W.H., 2009. Adverse childhood experiences and the risk of premature mortality. American Journal of Preventive Medicine 37, 389–396. https://doi.org/10.1016/j.amepre.2009.06.021

Brubaker, A.L., Rendon, J.L., Ramirez, L., Choudhry, M.A., Kovacs, E.J., 2013. Reduced neutrophil chemotaxis and infiltration contributes to delayed resolution of cutaneous wound infection with advanced age. J Immunol 190, 1746–1757. https://doi.org/10.4049/jimmunol.1201213

Bruno, S., Herrera Sanchez, M.B., Pasquino, C., Tapparo, M., Cedrino, M., Tetta, C., Camussi, G., 2019. Human Liver-Derived Stem Cells Improve Fibrosis and Inflammation Associated with Nonalcoholic Steatohepatitis. Stem Cells International 2019, e6351091. https://doi.org/10.1155/2019/6351091

Bueno, V., Lord, J.M., Jackson, T.A., 2016. The Ageing Immune System and Health. Springer. ISBN: 978-3-319-43363-9

Burini, R.C., Anderson, E., Durstine, J.L., Carson, J.A., 2020. Inflammation, physical activity, and chronic disease: An evolutionary perspective. Sports Medicine and Health Science 2, 1–6. https://doi.org/10.1016/j.smhs.2020.03.004

Burton, D.G.A., 2009. Cellular senescence, ageing and disease. AGE 31, 1–9. https://doi.org/10.1007/s11357-008-9075-y

Butcher, S.K., Chahal, H., Nayak, L., Sinclair, A., Henriquez, N.V., Sapey, E., O'Mahony, D., Lord, J.M., 2001. Senescence in innate immune responses: reduced neutrophil phagocytic capacity and CD16 expression in elderly humans. J. Leukoc. Biol. 70, 881–886. https://doi.org/10.1189/jlb.70.6.881

Butcher, S.K., Killampalli, V., Lascelles, D., Wang, K., Alpar, E.K., Lord, J.M., 2005. Raised cortisol:DHEAS ratios in the elderly after injury: potential impact upon neutrophil function and immunity. Aging Cell 4, 319–324. https://doi.org/10.1111/j.1474-9726.2005.00178.x

Cai, Y., Zhou, H., Zhu, Y., Sun, Q., Ji, Y., Xue, A., Wang, Y., Chen, W., Yu, X., Wang, L., Chen, H., Li, C., Luo, T., Deng, H., 2020. Elimination of senescent cells by β-galactosidase-targeted prodrug attenuates inflammation and restores physical function in aged mice. Cell Res. https://doi.org/10.1038/s41422-020-0314-9

Callender, L.A., Carroll, E.C., Beal, R.W.J., Chambers, E.S., Nourshargh, S., Akbar, A.N., Henson, S.M., 2018a. Human CD8+ EMRA T cells display a senescence-associated secretory phenotype regulated by p38 MAPK. Aging Cell 17, e12675. https://doi.org/10.1111/acel.12675

Campisi, J., 2005. Senescent Cells, Tumor Suppression, and Organismal Aging: Good Citizens, Bad Neighbors. https://doi.org/10.1016/j.cell.2005.02.003

Campisi, J., d'Adda di Fagagna, F., 2007. Cellular senescence: when bad things happen to good cells. Nat Rev Mol Cell Biol 8, 729–740. https://doi.org/10.1038/nrm2233

Cao, X., Li, W., Wang, T., Ran, D., Davalos, V., Planas-Serra, L., Pujol, A., Esteller, M., Wang, X., Yu, H., 2022. Accelerated biological aging in COVID-19 patients. Nat Commun 13, 2135. https://doi.org/10.1038/s41467-022-29801-8

Carrero, D., Soria-Valles, C., López-Otín, C., 2016. Hallmarks of progeroid syndromes: lessons from mice and reprogrammed cells. Dis Model Mech 9, 719–735. https://doi.org/10.1242/dmm.024711

Casey, R., Ballantyne, P.J., 2017. Diagnosed Chronic Health Conditions Among Injured Workers With Permanent Impairments and the General Population. Journal of occupational and environmental medicine 59, 486–496. https://doi.org/10.1097/JOM.0000000000000998

Cawthon, R.M., Smith, K.R., O'Brien, E., Sivatchenko, A., Kerber, R.A., 2003. Association between telomere length in blood and mortality in people aged 60 years or older. The Lancet 361, 393–395. https://doi.org/10.1016/S0140-6736(03)12384-7

Chakraborty, R.K., Burns, B., 2023. Systemic Inflammatory Response Syndrome, in: StatPearls. StatPearls Publishing, Treasure Island (FL). StatPearls Publishing; 2023 Jan–. PMID: 31613449.

Chandra, T., Ewels, P.A., Schoenfelder, S., Furlan-Magaril, M., Wingett, S.W., Kirschner, K., Thuret, J.-Y., Andrews, S., Fraser, P., Reik, W., 2015. Global Reorganization of the Nuclear Landscape in Senescent Cells. Cell Rep 10, 471–483. https://doi.org/10.1016/j.celrep.2014.12.055

Chang, Y.-W., Waxman, S.G., 2010. Minocycline Attenuates Mechanical Allodynia and Central Sensitization Following Peripheral Second-Degree Burn Injury. The Journal of Pain 11, 1146–1154. https://doi.org/10.1016/j.jpain.2010.02.010

Chen, B.H., Marioni, R.E., Colicino, E., Peters, M.J., Ward-Caviness, C.K., Tsai, P.-C., Roetker, N.S., Just, A.C., Demerath, E.W., Guan, W., Bressler, J., Fornage, M., Studenski, S., Vandiver, A.R., Moore, A.Z., Tanaka, T., Kiel, D.P., Liang, L., Vokonas, P., Schwartz, J., Lunetta, K.L., Murabito, J.M., Bandinelli, S., Hernandez, D.G., Melzer, D., Nalls, M., Pilling, L.C., Price, T.R., Singleton, A.B., Gieger, C., Holle, R., Kretschmer, A., Kronenberg, F., Kunze, S., Linseisen, J., Meisinger, C.,

Rathmann, W., Waldenberger, M., Visscher, P.M., Shah, S., Wray, N.R., McRae, A.F., Franco, O.H., Hofman, A., Uitterlinden, A.G., Absher, D., Assimes, T., Levine, M.E., Lu, A.T., Tsao, P.S., Hou, L., Manson, J.E., Carty, C.L., LaCroix, A.Z., Reiner, A.P., Spector, T.D., Feinberg, A.P., Levy, D., Baccarelli, A., van Meurs, J., Bell, J.T., Peters, A., Deary, I.J., Pankow, J.S., Ferrucci, L., Horvath, S., 2016. DNA methylation-based measures of biological age: meta-analysis predicting time to death. Aging (Albany NY) 8, 1844–1865. https://doi.org/10.18632/aging.101020

Chen, C.-L., Mo, H.-Q., Jiang, Y.-H., Zhao, X.-H., Ma, S., You, K.-Y., Pan, Y., Liu, Y.-M., 2021. BRD7 inhibits tumor progression by positively regulating the p53 pathway in hepatocellular carcinoma. J Cancer 12, 1507–1519. https://doi.org/10.7150/jca.50293

Chen, L.-B., Xu, J.-Y., Yang, Z., Wang, G.-B., 2007. Silencing SMYD3 in hepatoma demethylates RIZI promoter induces apoptosis and inhibits cell proliferation and migration. World J Gastroenterol 13, 5718–5724. https://doi.org/10.3748/wjg.v13.i43.5718

Chen, X., Li, M., Yan, J., Liu, T., Pan, G., Yang, H., Pei, M., He, F., 2017. Alcohol Induces Cellular Senescence and Impairs Osteogenic Potential in Bone Marrow-Derived Mesenchymal Stem Cells. Alcohol and Alcoholism 52, 289–297. https://doi.org/10.1093/alcalc/agx006

Chen, Y., Yang, S., Hu, J., Yu, C., He, M., Cai, Z., 2016. Increased Expression of SETD7 Promotes Cell Proliferation by Regulating Cell Cycle and Indicates Poor Prognosis in Hepatocellular Carcinoma. PLOS ONE 11, e0154939. https://doi.org/10.1371/journal.pone.0154939

Chen, Z., Cao, K., Xia, Y., Li, Y., Hou, Y., Wang, L., Li, L., Chang, L., Li, W., 2019. Cellular senescence in ionizing radiation (Review). Oncology Reports 42, 883–894. https://doi.org/10.3892/or.2019.7209

Cheng, C.L.-H., Tsang, F.H.-C., Wei, L., Chen, M., Chin, D.W.-C., Shen, J., Law, C.-T., Lee, D., Wong, C.C.-L., Ng, I.O.-L., Wong, C.-M., 2021. Bromodomain-containing protein BRPF1 is a therapeutic target for liver cancer. Commun Biol 4, 1–14. https://doi.org/10.1038/s42003-021-02405-6

Childs, B.G., Durik, M., Baker, D.J., Deursen, J.M. van, 2015. Cellular senescence in aging and age-related disease: from mechanisms to therapy. Nature medicine 21, 1424–1435. https://doi.org/10.1038/nm.4000

Childs, B.G., Li, H., Deursen, J.M. van, 2018. Senescent cells: a therapeutic target for cardiovascular disease. J Clin Invest 128, 1217–1228. https://doi.org/10.1172/JCI95146

Chung, H.Y., Cesari, M., Anton, S., Marzetti, E., Giovannini, S., Seo, A.Y., Carter, C., Yu, B.P., Leeuwenburgh, C., 2009. Molecular inflammation: underpinnings of aging and age-related diseases. Ageing research reviews 8, 18–30. https://doi.org/10.1016/j.arr.2008.07.002

Chung, M., Ruan, M., Zhao, N., Koestler, D.C., Vivo, I.D., Kelsey, K.T., Michaud, D.S., 2020. DNA methylation aging clocks and pancreatic cancer risk: Pooled analysis of three prospective nested case-control studies. https://doi.org/10.1101/2020.01.30.20019174

Colman, R.J., Anderson, R.M., Johnson, S.C., Kastman, E.K., Kosmatka, K.J., Beasley, T.M., Allison, D.B., Cruzen, C., Simmons, H.A., Kemnitz, J.W., Weindruch, R., 2009. Caloric restriction delays disease onset and mortality in rhesus monkeys. Science 325, 201–204. https://doi.org/10.1126/science.1173635

Conley, S.M., Hickson, L.J., Kellogg, T.A., McKenzie, T., Heimbach, J.K., Taner, T., Tang, H., Jordan, K.L., Saadiq, I.M., Woollard, J.R., Isik, B., Afarideh, M., Tchkonia, T., Kirkland, J.L., Lerman, L.O., 2020. Human Obesity Induces Dysfunction and Early Senescence in Adipose Tissue-Derived Mesenchymal Stromal/Stem Cells. Frontiers in Cell and Developmental Biology 8. https://doi.org/10.3389/fcell.2020.00197

Constantinou, J., Sullivan, J., Mirbahai, L., 2019. Ageing differently: Sex-dependent ageing rates in Daphnia magna. Experimental Gerontology 121, 33–45. https://doi.org/10.1016/j.exger.2019.03.008

Contoyannis, P., Jones, A.M., 2004. Socio-economic status, health and lifestyle. Journal of Health Economics 23, 965–995. https://doi.org/10.1016/j.jhealeco.2004.02.001

Coppé, J.-P., Desprez, P.-Y., Krtolica, A., Campisi, J., 2010. The Senescence-Associated Secretory Phenotype: The Dark Side of Tumor Suppression. Annu Rev Pathol 5, 99–118. https://doi.org/10.1146/annurev-pathol-121808-102144

Coppe, J.P., Patil, C.K., Rodier, F., Sun, Y., Munoz, D.P., Goldstein, J., Nelson, P.S., Desprez, P.Y., Campisi, J., 2008. Senescence-associated secretory phenotypes reveal cell-nonautonomous functions of oncogenic RAS and the p53 tumor suppressor. PLoS biology 6, 2853–2868. https://doi.org/10.1371/journal.pbio.0060301

Correia-Melo, C., Hewitt, G., Passos, J.F., 2014. Telomeres, oxidative stress and inflammatory factors: partners in cellular senescence? Longev Healthspan 3, 1. https://doi.org/10.1186/2046-2395-3-1

Cox, L., Boubriak, I., 2016. DNA Instability in premature aging. Nova Science Publishers, Inc., pp. 1–34. ISBN 978-1-61324-305-3

Cox, L.S., Bellantuono, I., Lord, J.M., Sapey, E., Mannick, J.B., Partridge, L., Gordon, A.L., Steves, C.J., Witham, M.D., 2020. Tackling immunosenescence to improve COVID-19 outcomes and vaccine response in older adults. The Lancet Healthy Longevity 1, e55–e57. https://doi.org/10.1016/S2666-7568(20)30011-8

Cuervo, A.M., Bergamini, E., Brunk, U.T., Dröge, W., Ffrench, M., Terman, A., 2005. Autophagy and Aging: The Importance of Maintaining "Clean" Cells. Autophagy 1, 131–140. https://doi.org/10.4161/auto.1.3.2017

da Silva, P.F.L., Ogrodnik, M., Kucheryavenko, O., Glibert, J., Miwa, S., Cameron, K., Ishaq, A., Saretzki, G., Nagaraja-Grellscheid, S., Nelson, G., von Zglinicki, T., 2019. The bystander effect contributes to the accumulation of senescent cells in vivo. Aging Cell 18, e12848. https://doi.org/10.1111/acel.12848

Dahiya, P., 2009. Burns as a model of SIRS. Front Biosci 14, 4962. https://doi.org/10.2741/3580

D'Aiuto, F., Nibali, L., Parkar, M., Patel, K., Suvan, J., Donos, N., 2010. Oxidative stress, systemic inflammation, and severe periodontitis. Journal of dental research 89, 1241–1246. https://doi.org/10.1177/0022034510375830

Das, A., Ranganathan, V., Umar, D., Thukral, S., George, A., Rath, S., Bal, V., 2017. Effector/memory CD4 T cells making either Th1 or Th2 cytokines commonly co-express T-bet and GATA-3. PLOS ONE 12, e0185932. https://doi.org/10.1371/journal.pone.0185932

Davidson, G.H., Hamlat, C.A., Rivara, F.P., Koepsell, T.D., Jurkovich, G.J., Arbabi, S., 2011. Long-term survival of adult trauma patients. JAMA 305, 1001–1007. https://doi.org/10.1001/jama.2011.259

De Bandt, J.-P., Coudray-Lucas, C., Lioret, N., Lim, S.K., Saizy, R., Giboudeau, J., Cynober, L., 1998. A Randomized Controlled Trial of the Influence of the Mode of Enteral Ornithine α-Ketoglutarate Administration in Burn Patients , ,. The Journal of Nutrition 128, 563–569. https://doi.org/10.1093/jn/128.3.563

De Bellis, M.D., 2002. Developmental traumatology: a contributory mechanism for alcohol and substance use disorders. Psychoneuroendocrinology 27, 155–170. https://doi.org/10.1016/S0306-4530(01)00042-7

De Biasi, S., Meschiari, M., Gibellini, L., Bellinazzi, C., Borella, R., Fidanza, L., Gozzi, L., Iannone, A., Lo Tartaro, D., Mattioli, M., Paolini, A., Menozzi, M., Milić, J., Franceschi, G., Fantini, R., Tonelli, R., Sita, M., Sarti, M., Trenti, T., Brugioni, L., Cicchetti, L., Facchinetti, F., Pietrangelo, A., Clini, E., Girardis, M., Guaraldi, G., Mussini, C., Cossarizza, A., 2020. Marked T cell activation, senescence, exhaustion and skewing towards TH17 in patients with COVID-19 pneumonia. Nat Commun 11, 3434. https://doi.org/10.1038/s41467-020-17292-4

Debacq-Chainiaux, F., Leduc, C., Verbeke, A., Toussaint, O., 2012. UV, stress and aging. Dermatoendocrinol 4, 236–240. https://doi.org/10.4161/derm.23652

DeBoer, M.D., 2013. Obesity, systemic inflammation, and increased risk for cardiovascular disease and diabetes among adolescents: a need for screening tools to target interventions. Nutrition 29, 379–386. https://doi.org/10.1016/j.nut.2012.07.003

Dedert, E.A., Calhoun, P.S., Watkins, L.L., Sherwood, A., Beckham, J.C., 2010. Posttraumatic stress disorder, cardiovascular, and metabolic disease: a review of the evidence. Annals of Behavioral Medicine : A Publication of the Society of Behavioral Medicine 39, 61–78. https://doi.org/10.1007/s12160-010-9165-9

Demaria, M., Ohtani, N., Youssef, S.A., Rodier, F., Toussaint, W., Mitchell, J.R., Laberge, R.M., Vijg, J., Steeg, H.V., Dolle, M.E., Hoeijmakers, J.H., Bruin, A. de, Hara, E., Campisi, J., 2014. An essential role for senescent cells in optimal wound healing through secretion of PDGF-AA. Developmental cell 31, 722–733. https://doi.org/10.1016/j.devcel.2014.11.012

Deng, M., Li, D., Zhang, Y., Zhou, G., Liu, W., Cao, Y., Zhang, W., 2018. Protective effect of crocin on ultraviolet B-induced dermal fibroblast photoaging. Molecular Medicine Reports 18, 1439–1446. https://doi.org/10.3892/mmr.2018.9150

Desdín-Micó, G., Soto-Heredero, G., Aranda, J.F., Oller, J., Carrasco, E., Gabandé-Rodríguez, E., Blanco, E.M., Alfranca, A., Cussó, L., Desco, M., Ibañez, B., Gortazar, A.R., Fernández-Marcos, P., Navarro, M.N., Hernaez, B., Alcamí, A., Baixauli, F., Mittelbrunn, M., 2020. T cells with dysfunctional mitochondria induce multimorbidity and premature senescence. Science 368, 1371–1376. https://doi.org/10.1126/science.aax0860

Deursen, J.M. van, 2014. The role of senescent cells in ageing. Nature 509, 439–446. https://doi.org/10.1038/nature13193

Dickey, J.S., Redon, C.E., Nakamura, A.J., Baird, B.J., Sedelnikova, O.A., Bonner, W.M., 2009. H2AX: functional roles and potential applications. Chromosoma 118, 683–692. https://doi.org/10.1007/s00412-009-0234-4

Dimitrov, L., Hong, C.S., Yang, C., Zhuang, Z., Heiss, J.D., 2015. New Developments in the Pathogenesis and Therapeutic Targeting of the IDH1 Mutation in Glioma. Int J Med Sci 12, 201–213. https://doi.org/10.7150/ijms.11047

Diniz, B.S., Reynolds III, C.F., Sibille, E., Bot, M., Penninx, B.W.J.H., 2019. Major depression and enhanced molecular senescence abnormalities in young and middle-aged adults. Transl Psychiatry 9, 198. https://doi.org/10.1038/s41398-019-0541-3

Dixit, V.D., 2010. Thymic Fatness and Approaches to Enhance Thymopoietic Fitness in Aging. Current opinion in immunology 22, 521. https://doi.org/10.1016/j.coi.2010.06.010

Domaszewska-Szostek, A., Puzianowska-Kuźnicka, M., Kuryłowicz, A., 2021. Flavonoids in Skin Senescence Prevention and Treatment. IJMS 22, 6814. https://doi.org/10.3390/ijms22136814

Donati, L., Ziegler, F., Pongelli, G., Signorini, M.S., 1999. Nutritional and clinical efficacy of ornithine alpha-ketoglutarate in severe burn patients. Clin Nutr 18, 307–311. https://doi.org/10.1054/clnu.1999.0040

Dookun, E., Walaszczyk, A., Redgrave, R., Palmowski, P., Tual-Chalot, S., Suwana, A., Chapman, J., Jirkovsky, E., Donastorg Sosa, L., Gill, E., Yausep, O.E., Santin, Y., Mialet-Perez, J., Andrew Owens, W., Grieve, D., Spyridopoulos, I., Taggart, M., Arthur, H.M., Passos, J.F., Richardson, G.D., 2020. Clearance of senescent cells during cardiac ischemia–reperfusion injury improves recovery. Aging Cell 19, e13249. https://doi.org/10.1111/acel.13249

Dorshkind, K., Montecino-Rodriguez, E., Signer, R.A.J., 2009. The ageing immune system: is it ever too old to become young again? Nature Reviews Immunology 9, 57–62. https://doi.org/10.1038/nri2471

Drost, J., Mantovani, F., Tocco, F., Elkon, R., Comel, A., Holstege, H., Kerkhoven, R., Jonkers, J., Voorhoeve, P.M., Agami, R., Del Sal, G., 2010. BRD7 is a candidate tumour suppressor gene required for p53 function. Nat Cell Biol 12, 380–389. https://doi.org/10.1038/ncb2038

Du, H., Zhang, L., 2022. DOT1L Epigenetically Induces the Expression Level of FoxM1 through H3K79me2 and Affects the Malignant Behaviors of Head and Neck Squamous Cell Carcinoma Cells. Journal of Hard Tissue Biology 31, 101–108. https://doi.org/10.2485/jhtb.31.101

Duah, M., Li, L., Shen, J., Lan, Q., Pan, B., Xu, K., 2021. Thymus Degeneration and Regeneration. Front Immunol 12, 706244. https://doi.org/10.3389/fimmu.2021.706244

Duggal, N.A., 2018. Reversing the immune ageing clock: lifestyle modifications and pharmacological interventions. Biogerontology 19, 481–496. https://doi.org/10.1007/s10522-018-9771-7

Duggal, N.A., Pollock, R.D., Lazarus, N.R., Harridge, S., Lord, J.M., 2018a. Major features of immunesenescence, including reduced thymic output, are ameliorated by high levels of physical activity in adulthood. Aging Cell 17. https://doi.org/10.1111/acel.12750

Duggal, N.A., Snelson, C., Shaheen, U., Pearce, V., Lord, J.M., 2018c. Innate and adaptive immune dysregulation in critically ill ICU patients. Sci Rep 8, 10186. https://doi.org/10.1038/s41598-018-28409-7

Duggal, N.A., Upton, J., Phillips, A.C., Hampson, P., Lord, J.M., 2014. Depressive symptoms post hip fracture in older adults are associated with phenotypic and functional alterations in T cells. Immun Ageing 11, 25. https://doi.org/10.1186/s12979-014-0025-5

Duggal, Niharika A., Upton, J., Phillips, A.C., Sapey, E., Lord, J.M., 2013. An age-related numerical and functional deficit in CD19+CD24hiCD38hi B cells is associated with an increase in systemic autoimmunity. Aging Cell 12, 873–881. https://doi.org/10.1111/acel.12114

Duggal, Niharika A, Upton, J., Phillips, A.C., Sapey, E., Lord, J.M., 2013. An age-related numerical and functional deficit in CD19+CD24hiCD38hi B cells is associated with an increase in systemic autoimmunity. Aging Cell 12, 873–881. https://doi.org/10.1111/acel.12114

Duke, J.M., Boyd, J.H., Rea, S., Randall, S.M., Wood, F.M., 2015a. Long-term mortality among older adults with burn injury: a population-based study in Australia. Bulletin of the World Health Organization 93, 400–406. https://doi.org/10.2471/BLT.14.149146

Duke, J.M., Randall, S.M., Fear, M.W., Boyd, J.H., O'Halloran, E., Rea, S., Wood, F.M., 2016. Increased admissions for diabetes mellitus after burn. Burns 42, 1734–1739. https://doi.org/10.1016/j.burns.2016.06.005

Duke, J.M., Randall, S.M., Fear, M.W., O'Halloran, E., Boyd, J.H., Rea, S., Wood, F.M., 2017. Long term cardiovascular impacts after burn and non-burn trauma: A comparative population-based study. Burns 43, 1662–1672. https://doi.org/10.1016/j.burns.2017.08.001

Duke, J.M., Rea, S., Boyd, J.H., Randall, S.M., Wood, F.M., 2015c. Mortality After Burn Injury in Children: A 33-year Population-Based Study. PEDIATRICS 135, e903–e910. https://doi.org/10.1542/peds.2014-3140

Durham, R.M., Moran, J.J., Mazuski, J.E., Shapiro, M.J., Baue, A.E., Flint, L.M., 2003. Multiple Organ Failure in Trauma Patients. Journal of Trauma and Acute Care Surgery 55, 608. https://doi.org/10.1097/01.TA.0000092378.10660.D1

Edwards, N., Farookhi, R., Clarke, H.J., 2015. Identification of a β-galactosidase transgene that provides a live-cell marker of transcriptional activity in growing oocytes and embryos. Mol Hum Reprod 21, 583–593. https://doi.org/10.1093/molehr/gav020

Eggert, E., Hillig, R.C., Koehr, S., Stöckigt, D., Weiske, J., Barak, N., Mowat, J., Brumby, T., Christ, C.D., Ter Laak, A., Lang, T., Fernandez-Montalvan, A.E., Badock, V., Weinmann, H., Hartung, I.V., Barsyte-Lovejoy, D., Szewczyk, M., Kennedy, S., Li, F., Vedadi, M., Brown, P.J., Santhakumar, V., Arrowsmith, C.H., Stellfeld, T., Stresemann, C., 2016. Discovery and Characterization of a Highly Potent and Selective Aminopyrazoline-Based in Vivo Probe (BAY-598) for the Protein Lysine Methyltransferase SMYD2. J Med Chem 59, 4578–4600. https://doi.org/10.1021/acs.jmedchem.5b01890

Ellison-Hughes, G.M., 2020. First evidence that senolytics are effective at decreasing senescent cells in humans. EBioMedicine 56, 102473. https://doi.org/10.1016/j.ebiom.2019.09.053

Ellulu, M.S., Patimah, I., Khaza'ai, H., Rahmat, A., Abed, Y., 2017. Obesity and inflammation: the linking mechanism and the complications. Arch Med Sci 13, 851–863. https://doi.org/10.5114/aoms.2016.58928

Engelbrecht, M., Ndimba, R., de Kock, M., Miles, X., Nair, S., Fisher, R., du Plessis, P., Bolcaen, J., Botha, M.H., Zwanepoel, E., Sioen, S., Baeyens, A., Nieto-Camero, J., de Kock, E., Vandevoorde, C., 2021. DNA damage response of haematopoietic stem and progenitor cells to high-LET neutron irradiation. Sci Rep 11, 20854. https://doi.org/10.1038/s41598-021-00229-2

Evans, R.A., Leavy, O.C., Richardson, M., Elneima, O., McCauley, H.J.C., Shikotra, A., Singapuri, A. et al, 2022. Clinical characteristics with inflammation profiling of long COVID and association with 1-year recovery following hospitalisation in the UK: a prospective observational study. The Lancet Respiratory Medicine S2213260022001278. https://doi.org/10.1016/S2213-2600(22)00127-8

Evans, Rachael A., McAuley, Hamish, Harrison, Ewen M., Shikotra, Aarti, Singapuri, Amisha, Sereno, et al, 2021. Physical, cognitive, and mental health impacts of COVID-19 after hospitalisation (PHOSP-COVID): a UK multicentre, prospective cohort study. The Lancet Respiratory Medicine 9, 1275–1287. https://doi.org/10.1016/S2213-2600(21)00383-0

Evans, S.A., Airey, M.C., Chell, S.M., Connelly, J.B., Rigby, A.S., Tennant, A., 2003. Disability in young adults following major trauma: 5 year follow up of survivors. BMC public health 3, 8. https://doi.org/10.1186/1471-2458-3-8

Fahy, G.M., Brooke, R.T., Watson, J.P., Good, Z., Vasanawala, S.S., Maecker, H., Leipold, M.D., Lin, D.T.S., Kobor, M.S., Horvath, S., 2019. Reversal of epigenetic aging and immunosenescent trends in humans. Aging Cell 18, e13028. https://doi.org/10.1111/acel.13028

Fajgenbaum, D.C., June, C.H., 2020. Cytokine Storm. New England Journal of Medicine 383, 2255–2273. https://doi.org/10.1056/NEJMra2026131

Fedorov, O., Castex, J., Tallant, C., Owen, D.R., Martin, S., Aldeghi, M., Monteiro, O., Filippakopoulos, P., Picaud, S., Trzupek, J.D., Gerstenberger, B.S., Bountra, C., Willmann, D., Wells, C., Philpott, M., Rogers, C., Biggin, P.C., Brennan, P.E., Bunnage, M.E., Schüle, R., Günther, T., Knapp, S., Müller, S., 2015. Selective targeting of the BRG/PB1 bromodomains impairs embryonic and trophoblast stem cell maintenance. Sci Adv 1, e1500723. https://doi.org/10.1126/sciadv.1500723

Felice, B.D., Wilson, R.R., Nacca, M., 2009. Telomere shortening may be associated with human keloids. BMC medical genetics 10, 110. https://doi.org/10.1186/1471-2350-10-110

Fessler, J., Felber, A., Duftner, C., Dejaco, C., 2013. The Impact of Aging on Regulatory T-Cells. Frontiers in Immunology 4. https://doi.org/10.3389/fimmu.2013.00231

Fitzgerald, K.N., Hodges, R., Hanes, D., Stack, E., Cheishvili, D., Szyf, M., Henkel, J., Twedt, M.W., Giannopoulou, D., Herdell, J., Logan, S., Bradley, R., 2021. Potential reversal of epigenetic age using a diet and lifestyle intervention: a pilot randomized clinical trial. Aging (Albany NY) 13, 9419–9432. https://doi.org/10.18632/aging.202913

Fog, C.K., Galli, G.G., Lund, A.H., 2012. PRDM proteins: Important players in differentiation and disease. BioEssays 34, 50–60. https://doi.org/10.1002/bies.201100107

Foster, M.A., Bentley, C., Hazeldine, J., Acharjee, A., Nahman, O., Shen-Orr, S.S., Lord, J.M., Duggal, N.A., 2022. Investigating the potential of a prematurely aged immune phenotype in severely

injured patients as predictor of risk of sepsis. Immun Ageing 19, 60. https://doi.org/10.1186/s12979-022-00317-5

Foster, M.A., Taylor, A.E., Hill, N.E., Bentley, C., Bishop, J., Gilligan, L.C., Shaheen, F., Bion, J.F., Fallowfield, J.L., Woods, D.R., Bancos, I., Midwinter, M.M., Lord, J.M., Arlt, W., 2020. Mapping the Steroid Response to Major Trauma From Injury to Recovery: A Prospective Cohort Study. J Clin Endocrinol Metab 105, dgz302. https://doi.org/10.1210/clinem/dgz302

Franceschi, C., 2008. Inflammaging as a Major Characteristic of Old People: Can It Be Prevented or Cured? Nutrition Reviews 65, S173–S176. https://doi.org/10.1111/j.1753-4887.2007.tb00358.x

Franceschi, C., Bonafè, M., Valensin, S., Olivieri, F., De Luca, M., Ottaviani, E., De Benedictis, G., 2000. Inflamm-aging. An evolutionary perspective on immunosenescence. Ann N Y Acad Sci 908, 244–254. https://doi.org/10.1111/j.1749-6632.2000.tb06651.x

Franceschi, C., Campisi, J., 2014. Chronic inflammation (inflammaging) and its potential contribution to age-associated diseases. The journals of gerontology.Series A, Biological sciences and medical sciences 69 Suppl 1, 4. https://doi.org/10.1093/gerona/glu057

Franceschi, C., Capri, M., Monti, D., Giunta, S., Olivieri, F., Sevini, F., Panourgia, M.P., Invidia, L., Celani, L., Scurti, M., Cevenini, E., Castellani, G.C., Salvioli, S., 2007. Inflammaging and anti-inflammaging: a systemic perspective on aging and longevity emerged from studies in humans. Mechanisms of ageing and development 128, 92–105. https://doi.org/S0047-6374(06)00249-1

Franceschi, C., Garagnani, P., Parini, P., Giuliani, C., Santoro, A., 2018. Inflammaging: a new immune–metabolic viewpoint for age-related diseases. Nat Rev Endocrinol 14, 576–590. https://doi.org/10.1038/s41574-018-0059-4

Franceschi, C., Santoro, A., Capri, M., 2020. The complex relationship between Immunosenescence and Inflammaging: Special issue on the New Biomedical Perspectives. Semin Immunopathol 42, 517–520. https://doi.org/10.1007/s00281-020-00823-y

Fransquet, P.D., Wrigglesworth, J., Woods, R.L., Ernst, M.E., Ryan, J., 2019. The epigenetic clock as a predictor of disease and mortality risk: a systematic review and meta-analysis. Clinical Epigenetics 11, 62. https://doi.org/10.1186/s13148-019-0656-7

Franzen, J., Nüchtern, S., Tharmapalan, V., Vieri, M., Nikolić, M., Han, Y., Balfanz, P., Marx, N., Dreher, M., Brümmendorf, T.H., Dahl, E., Beier, F., Wagner, W., 2021. Epigenetic Clocks Are Not Accelerated in COVID-19 Patients. IJMS 22, 9306. https://doi.org/10.3390/ijms22179306

Frasca, D., Diaz, A., Romero, M., Blomberg, B.B., 2017. Ageing and obesity similarly impair antibody responses. Clin Exp Immunol 187, 64–70. https://doi.org/10.1111/cei.12824

Frasca, D., Diaz, A., Romero, M., Phillips, M., Mendez, N.V., Landin, A.M., Blomberg, B.B., 2012. Unique biomarkers for B-cell function predict the serum response to pandemic H1N1 influenza vaccine. International Immunology 24, 175–182. https://doi.org/10.1093/intimm/dxr123

Freund, A., Orjalo, A.V., Desprez, P.Y., Campisi, J., 2010. Inflammatory networks during cellular senescence: causes and consequences. Trends in molecular medicine 16, 238–246. https://doi.org/10.1016/j.molmed.2010.03.003

Fry, D.E., 2012. Sepsis, systemic inflammatory response, and multiple organ dysfunction: the mystery continues. Am Surg 78, 1–8. https://doi.org/10.1177/000313481207800102

Füllgrabe, J., Hajji, N., Joseph, B., 2010. Cracking the death code: apoptosis-related histone modifications. Cell Death Differ 17, 1238–1243. https://doi.org/10.1038/cdd.2010.58

Fulop, T., Dupuis, G., Baehl, S., Le Page, A., Bourgade, K., Frost, E., Witkowski, J.M., Pawelec, G., Larbi, A., Cunnane, S., 2016. From inflamm-aging to immune-paralysis: a slippery slope during aging for immune-adaptation. Biogerontology 17, 147–157. https://doi.org/10.1007/s10522-015-9615-7

Fulop, T., Larbi, A., Dupuis, G., Le Page, A., Frost, E.H., Cohen, A.A., Witkowski, J.M., Franceschi, C., 2018. Immunosenescence and Inflamm-Aging As Two Sides of the Same Coin: Friends or Foes? Front Immunol 8, 1960. https://doi.org/10.3389/fimmu.2017.01960

Fulop, T., Larbi, A., Wikby, A., Mocchegiani, E., Hirokawa, K., Pawelec, G., 2005. Dysregulation of T-Cell Function in the Elderly. Drugs Aging 22, 589–603. https://doi.org/10.2165/00002512-200522070-00005

Gallego Romero, I., Pai, A.A., Tung, J., Gilad, Y., 2014. RNA-seq: impact of RNA degradation on transcript quantification. BMC Biology 12, 42. https://doi.org/10.1186/1741-7007-12-42

Galvani, A.P., Novembre, J., 2005. The evolutionary history of the CCR5-Δ32 HIV-resistance mutation. Microbes and Infection 7, 302–309. https://doi.org/10.1016/j.micinf.2004.12.006

Gao, X., Zhang, Y., Brenner, H., 2017. Associations of Helicobacter pylori infection and chronic atrophic gastritis with accelerated epigenetic ageing in older adults. Br J Cancer 117, 1211–1214. https://doi.org/10.1038/bjc.2017.314

Garg, S.K., Delaney, C., Toubai, T., Ghosh, A., Reddy, P., Banerjee, R., Yung, R., 2014. Aging is associated with increased regulatory T-cell function. Aging Cell 13, 441–448. https://doi.org/10.1111/acel.12191

Gary, A.-S., Rochette, P.J., 2020. Apoptosis, the only cell death pathway that can be measured in human diploid dermal fibroblasts following lethal UVB irradiation. Sci Rep 10, 18946. https://doi.org/10.1038/s41598-020-75873-1

GeneCards, 2022. CAMK1D Gene - GeneCards | KCC1D Protein | KCC1D Antibody [WWW Document]. GeneCards. URL https://www.genecards.org/cgi-bin/carddisp.pl?gene=CAMK1D (accessed 11.21.22).

George, R.L., McGwin, G., Schwacha, M.G., Metzger, J., Cross, J.M., Chaudry, I.H., Rue, L.W., 2005. The Association Between Sex and Mortality Among Burn Patients as Modified by Age. Journal of Burn Care & Research 26, 416–421. https://doi.org/10.1097/01.bcr.0000176888.44949.87

Ghajar, J., 2000. Traumatic brain injury. The Lancet 356, 923–929. https://doi.org/10.1016/S0140-6736(00)02689-1

Gibson, J., Russ, T.C., Clarke, T.-K., Howard, D.M., Hillary, R.F., Evans, K.L., Walker, R.M., Bermingham, M.L., Morris, S.W., Campbell, A., Hayward, C., Murray, A.D., Porteous, D.J., Horvath, S., Lu, A.T., McIntosh, A.M., Whalley, H.C., Marioni, R.E., 2019. A meta-analysis of genome-wide association studies of epigenetic age acceleration. PLOS Genetics 15, e1008104. https://doi.org/10.1371/journal.pgen.1008104

Gindin, Y., Gaggar, A., Lok, A.S., Janssen, H.L.A., Ferrari, C., Subramanian, G.M., Jiang, Z., Masur, H., Emmanuel, B., Poonia, B., Kottilil, S., 2020. DNA Methylation and Immune Cell Markers Demonstrate Evidence of Accelerated Aging in Patients with Chronic Hepatitis B Virus or Hepatitis C Virus, with or without Human Immunodeficienct Virus Co-infection. Clin Infect Dis 73, e184–e190. https://doi.org/10.1093/cid/ciaa1371

Ginter, E., Simko, V., 2013. Women live longer than men. Bratisl Lek Listy 114, 45–49. https://doi.org/10.4149/bll_2013_011

Gong, L., Parikh, S., Rosenthal, P.J., Greenhouse, B., 2013. Biochemical and immunological mechanisms by which sickle cell trait protects against malaria. Malaria Journal 12, 317. https://doi.org/10.1186/1475-2875-12-317

González-Osuna, L., Sierra-Cristancho, A., Cafferata, E.A., Melgar-Rodríguez, S., Rojas, C., Carvajal, P., Cortez, C., Vernal, R., 2022. Senescent CD4+CD28− T Lymphocytes as a Potential Driver of Th17/Treg Imbalance and Alveolar Bone Resorption during Periodontitis. IJMS 23, 2543. https://doi.org/10.3390/ijms23052543

Goronzy, J.J., Weyand, C.M., 2019. Mechanisms underlying T cell ageing. Nat Rev Immunol 19, 573–583. https://doi.org/10.1038/s41577-019-0180-1

Gotthardt, D., Sexl, V., 2017. STATs in NK-Cells: The Good, the Bad, and the Ugly. Frontiers in Immunology 7. https://doi.org/10.3389/fimmu.2016.00694

Gounder, S.S., Abdullah, B.J.J., Radzuanb, N.E.I.B.M., Zain, F.D.B.M., Sait, N.B.M., Chua, C., Subramani, B., 2018. Effect of Aging on NK Cell Population and Their Proliferation at Ex Vivo Culture Condition. Anal Cell Pathol (Amst) 2018, 7871814. https://doi.org/10.1155/2018/7871814

Gradl, S., Steuber, H., Weiske, J., Szewczyk, M.M., Schmees, N., Siegel, S., Stoeckigt, D., Christ, C.D., Li, F., Organ, S., Abbey, M., Kennedy, S., Chau, I., Trush, V., Barsyte-Lovejoy, D., Brown, P.J., Vedadi, M., Arrowsmith, C., Husemann, M., Badock, V., Bauser, M., Haegebarth, A., Hartung, I.V., Stresemann, C., 2021. Discovery of the SMYD3 Inhibitor BAY-6035 Using Thermal Shift Assay (TSA)-Based High-Throughput Screening. SLAS DISCOVERY: Advancing the Science of Drug Discovery 26, 947–960. https://doi.org/10.1177/24725552211019409

Greenhalgh, D.G., 2017. Sepsis in the burn patient: a different problem than sepsis in the general population. Burns & Trauma 5, 23. https://doi.org/10.1186/s41038-017-0089-5

Greer, Y.E., Rubin, J.S., 2011. Casein kinase 1 delta functions at the centrosome to mediate Wnt-3a–dependent neurite outgrowth. Journal of Cell Biology 192, 993–1004. https://doi.org/10.1083/jcb.201011111

Grey, C., Baudat, F., Massy, B. de, 2018. PRDM9, a driver of the genetic map. PLOS Genetics 14, e1007479. https://doi.org/10.1371/journal.pgen.1007479

Gruver, A.L., Sempowski, G.D., 2008. Cytokines, leptin, and stress-induced thymic atrophy. Journal of Leukocyte Biology 84, 915–923. https://doi.org/10.1189/jlb.0108025

Gu, W., Liu, W., Yang, X., Zhao, X., Yuan, X., Ma, H., Tian, Y., Meng, R., 2011. Effects of intense pulsed light and ultraviolet A on metalloproteinases and extracellular matrix expression in human skin. Photomed Laser Surg 29, 97–103. https://doi.org/10.1089/pho.2010.2765

Guillory, A.N., Clayton, R.P., Herndon, D.N., Finnerty, C.C., 2016. Cardiovascular Dysfunction Following Burn Injury: What We Have Learned from Rat and Mouse Models. International Journal of Molecular Sciences 17, 53. https://doi.org/10.3390/ijms17010053

Gupte, R.P., Brooks, W.M., Vukas, R.R., Pierce, J.D., Harris, J.L., 2019. Sex Differences in Traumatic Brain Injury: What We Know and What We Should Know. Journal of Neurotrauma 36, 3063–3091. https://doi.org/10.1089/neu.2018.6171

Gürünlüoğlu, K., Demircan, M., Koç, A., Koçbıyık, A., Taşçı, A., Durmuş, K., Gürünlüoğlu, S., Gözükara Bağ, H., 2019. The Effects of Different Burn Dressings on Length of Telomere and Expression of Telomerase in Children With Thermal Burns. Journal of Burn Care & Research 40, 302–311. https://doi.org/10.1093/jbcr/irz019

Gyanwali, B., Lim, Z.X., Soh, J., Lim, C., Guan, S.P., Goh, J., Maier, A.B., Kennedy, B.K., 2022. Alpha-Ketoglutarate dietary supplementation to improve health in humans. Trends in Endocrinology & Metabolism 33, 136–146. https://doi.org/10.1016/j.tem.2021.11.003

Haas, J., Würthwein, C., Korporal-Kuhnke, M., Viehoever, A., Jarius, S., Ruck, T., Pfeuffer, S., Meuth, S.G., Wildemann, B., 2019. Alemtuzumab in Multiple Sclerosis: Short- and Long-Term Effects of Immunodepletion on the Peripheral Treg Compartment. Frontiers in Immunology 10. https://doi.org/10.3389/fimmu.2019.01204

Hampson, P., Dinsdale, R.J., Wearn, C.M., Bamford, A.L., Bishop, J.R.B., Hazeldine, J., Moiemen, N.S., Harrison, P., Lord, J.M., 2017. Neutrophil Dysfunction, Immature Granulocytes, and Cell-free DNA are Early Biomarkers of Sepsis in Burn-injured Patients: A Prospective Observational Cohort Study. Ann. Surg. 265, 1241–1249. https://doi.org/10.1097/SLA.0000000000001807

Han, S., Liu, Y., Cai, S.J., Qian, M., Ding, J., Larion, M., Gilbert, M.R., Yang, C., 2020. IDH mutation in glioma: molecular mechanisms and potential therapeutic targets. Br J Cancer 122, 1580–1589. https://doi.org/10.1038/s41416-020-0814-x

Han, X., Piao, L., Zhuang, Q., Yuan, X., Liu, Z., He, X., 2018. The role of histone lysine methyltransferase NSD3 in cancer. Onco Targets Ther 11, 3847–3852. https://doi.org/10.2147/OTT.S166006

Hannum, Gregory, Guinney, J., Zhao, L., Zhang, L., Hughes, G., Sadda, S., Klotzle, B., Bibikova, M., Fan, J.-B., Gao, Y., Deconde, R., Chen, M., Rajapakse, I., Friend, S., Ideker, T., Zhang, K., 2013. Genome-wide Methylation Profiles Reveal Quantitative Views of Human Aging Rates. Molecular Cell 49, 359–367. https://doi.org/10.1016/j.molcel.2012.10.016

Harman, D., 1991. The aging process: major risk factor for disease and death. Proc Natl Acad Sci U S A 88, 5360–5363. https://doi.org/10.1073/pnas.88.12.5360

Harrison, C., 2020. Coronavirus puts drug repurposing on the fast track. Nature Biotechnology 38, 379–381. https://doi.org/10.1038/d41587-020-00003-1

Harrison, D.E., Strong, R., Sharp, Z.D., Nelson, J.F., Astle, C.M., Flurkey, K., Nadon, N.L., Wilkinson, J.E., Frenkel, K., Carter, C.S., Pahor, M., Javors, M.A., Fernandez, E., Miller, R.A., 2009. Rapamycin fed late in life extends lifespan in genetically heterogeneous mice. Nature 460, 392–395. https://doi.org/10.1038/nature08221

Hart, D.W., Wolf, S.E., Mlcak, R., Chinkes, D.L., Ramzy, P.I., Obeng, M.K., Ferrando, A.A., Wolfe, R.R., Herndon, D.N., 2000. Persistence of muscle catabolism after severe burn. Surgery 128, 312–319. https://doi.org/10.1067/msy.2000.108059

Hayashi, M., Yanaba, K., Umezawa, Y., Yoshihara, Y., Kikuchi, S., Ishiuji, Y., Saeki, H., Nakagawa, H., 2016. IL-10-producing regulatory B cells are decreased in patients with psoriasis. Journal of Dermatological Science 81, 93–100. https://doi.org/10.1016/j.jdermsci.2015.11.003

Haycock, P.C., Heydon, E.E., Kaptoge, S., Butterworth, A.S., Thompson, A., Willeit, P., 2014. Leucocyte telomere length and risk of cardiovascular disease: systematic review and meta-analysis. BMJ 349, g4227–g4227. https://doi.org/10.1136/bmj.g4227

Haydn, T., Metzger, E., Schuele, R., Fulda, S., 2017. Concomitant epigenetic targeting of LSD1 and HDAC synergistically induces mitochondrial apoptosis in rhabdomyosarcoma cells. Cell Death Dis 8, e2879–e2879. https://doi.org/10.1038/cddis.2017.239

Hayflick, L., Moorhead, P.S., 1961. The serial cultivation of human diploid cell strains. Experimental Cell Research 25, 585–621. https://doi.org/10.1016/0014-4827(61)90192-6

Hazeldine, J., Lord, J.M., 2020. Immunesenescence: A Predisposing Risk Factor for the Development of COVID-19? Frontiers in Immunology 11. https://doi.org/10.3389/fimmu.2020.573662

Hazeldine, J., Lord, J.M., 2013. The impact of ageing on natural killer cell function and potential consequences for health in older adults. Ageing Res Rev 12, 1069–1078. https://doi.org/10.1016/j.arr.2013.04.003

Hazeldine, J., McGee, K.C., Al-Tarrah, K., Hassouna, T., Patel, K., Imran, R., Bishop, J.R.B., Bamford, A., Barnes, D., Wilson, Y., Harrison, P., Lord, J.M., Moiemen, N.S., 2021. Multicentre, longitudinal, observational cohort study to examine the relationship between neutrophil function and sepsis in adults and children with severe thermal injuries: a protocol for the Scientific Investigation of the Biological Pathways Following Thermal Injury-2 (SIFTI-2) study. BMJ Open 11, e052035. https://doi.org/10.1136/bmjopen-2021-052035

Hazeldine, J., Naumann, D.N., Toman, E., Davies, D., Bishop, J.R.B., Su, Z., Hampson, P., Dinsdale, R.J., Crombie, N., Duggal, N.A., Harrison, P., Belli, A., Lord, J.M., 2017. Prehospital immune responses and development of multiple organ dysfunction syndrome following traumatic injury: A prospective cohort study. PLoS Med 14, e1002338. https://doi.org/10.1371/journal.pmed.1002338

Hehar, H., Mychasiuk, R., 2016. The use of telomere length as a predictive biomarker for injury prognosis in juvenile rats following a concussion/mild traumatic brain injury. Neurobiology of Disease 87, 11–18. https://doi.org/10.1016/j.nbd.2015.12.007

Hewitt, G., Jurk, D., Marques, F.D.M., Correia-Melo, C., Hardy, T., Gackowska, A., Anderson, R., Taschuk, M., Mann, J., Passos, J.F., 2012. Telomeres are favoured targets of a persistent DNA damage response in ageing and stress-induced senescence. Nat Commun 3, 708. https://doi.org/10.1038/ncomms1708

Heyn, H., Li, N., Ferreira, H.J., Moran, S., Pisano, D.G., Gomez, A., Diez, J., Sanchez-Mut, J.V., Setien, F., Carmona, F.J., Puca, A.A., Sayols, S., Pujana, M.A., Serra-Musach, J., Iglesias-Platas, I., Formiga, F., Fernandez, A.F., Fraga, M.F., Heath, S.C., Valencia, A., Gut, I.G., Wang, J., Esteller, M., 2012. Distinct DNA methylomes of newborns and centenarians. Proceedings of the National Academy of Sciences 109, 10522–10527. https://doi.org/10.1073/pnas.1120658109

Hickson, L.J., Langhi Prata, L.G.P., Bobart, S.A., Evans, T.K., Giorgadze, N., Hashmi, S.K., Herrmann, S.M., Jensen, M.D., Jia, Q., Jordan, K.L., Kellogg, T.A., Khosla, S., Koerber, D.M., Lagnado, A.B., Lawson, D.K., LeBrasseur, N.K., Lerman, L.O., McDonald, K.M., McKenzie, T.J., Passos, J.F.,

Pignolo, R.J., Pirtskhalava, T., Saadiq, I.M., Schaefer, K.K., Textor, S.C., Victorelli, S.G., Volkman, T.L., Xue, A., Wentworth, M.A., Wissler Gerdes, E.O., Zhu, Y., Tchkonia, T., Kirkland, J.L., 2019. Senolytics decrease senescent cells in humans: Preliminary report from a clinical trial of Dasatinib plus Quercetin in individuals with diabetic kidney disease. EBioMedicine 47, 446–456. https://doi.org/10.1016/j.ebiom.2019.08.069

Hietbrink, F., Koenderman, L., Rijkers, G., Leenen, L., 2006. Trauma: the role of the innate immune system. World J Emerg Surg 1, 15. https://doi.org/10.1186/1749-7922-1-15

Hiroeh, U., Appleby, L., Mortensen, P.B., Dunn, G., 2001. Death by homicide, suicide, and other unnatural causes in people with mental illness: a population-based study. https://doi.org/10.1016/S0140-6736(01)07216-6

Hofer, S.J., Carmona-Gutierrez, D., Mueller, M.I., Madeo, F., 2022. The ups and downs of caloric restriction and fasting: from molecular effects to clinical application. EMBO Mol Med 14, e14418. https://doi.org/10.15252/emmm.202114418

Hofer, S.J., Davinelli, S., Bergmann, M., Scapagnini, G., Madeo, F., 2021. Caloric Restriction Mimetics in Nutrition and Clinical Trials. Front Nutr 8, 717343. https://doi.org/10.3389/fnut.2021.717343

Hoffman, B., Liebermann, D.A., 2008. Apoptotic signaling by c-MYC. Oncogene 27, 6462–6472. https://doi.org/10.1038/onc.2008.312

Hong, K.S., Ahn, J.H., Jang, J.G., Lee, J.H., Kim, H.N., Kim, D., Lee, W., 2020. GSK-LSD1, an LSD1 inhibitor, quashes SARS-CoV-2-triggered cytokine release syndrome in-vitro. Sig Transduct Target Ther 5, 1–3. https://doi.org/10.1038/s41392-020-00391-5

Honma, D., Kanno, O., Watanabe, J., Kinoshita, J., Hirasawa, M., Nosaka, E., Shiroishi, M., Takizawa, T., Yasumatsu, I., Horiuchi, T., Nakao, A., Suzuki, K., Yamasaki, T., Nakajima, K., Hayakawa, M., Yamazaki, T., Yadav, A.S., Adachi, N., 2017. Novel orally bioavailable EZH1/2 dual inhibitors with greater antitumor efficacy than an EZH2 selective inhibitor. Cancer Sci 108, 2069–2078. https://doi.org/10.1111/cas.13326

Hori, S., Sakaguchi, S., 2004. Foxp3: a critical regulator of the development and function of regulatory T cells. Microbes and Infection 6, 745–751. https://doi.org/10.1016/j.micinf.2004.02.020

Horvath, Steve, 2013. DNA methylation age of human tissues and cell types. Genome Biology 14, 3156. https://doi.org/10.1186/gb-2013-14-10-r115

Horvath, S., Erhart, W., Brosch, M., Ammerpohl, O., von Schönfels, W., Ahrens, M., Heits, N., Bell, J.T., Tsai, P.-C., Spector, T.D., Deloukas, P., Siebert, R., Sipos, B., Becker, T., Röcken, C., Schafmayer, C., Hampe, J., 2014. Obesity accelerates epigenetic aging of human liver. Proc. Natl. Acad. Sci. U.S.A. 111, 15538–15543. https://doi.org/10.1073/pnas.1412759111

Horvath, S., Garagnani, P., Bacalini, M.G., Pirazzini, C., Salvioli, S., Gentilini, D., Di Blasio, A.M., Giuliani, C., Tung, S., Vinters, H.V., Franceschi, C., 2015a. Accelerated epigenetic aging in Down syndrome. Aging Cell 14, 491–495. https://doi.org/10.1111/acel.12325

Horvath, S., Levine, A.J., 2015. HIV-1 Infection Accelerates Age According to the Epigenetic Clock. J. Infect. Dis. 212, 1563–1573. https://doi.org/10.1093/infdis/jiv277

Horvath, S., Pirazzini, C., Bacalini, M.G., Gentilini, D., Di Blasio, A.M., Delledonne, M., Mari, D., Arosio, B., Monti, D., Passarino, G., De Rango, F., D'Aquila, P., Giuliani, C., Marasco, E., Collino, S., Descombes, P., Garagnani, P., Franceschi, C., 2015b. Decreased epigenetic age of PBMCs from Italian semi-supercentenarians and their offspring. Aging (Albany NY) 7, 1159–1170.

Huang, J., Perez-Burgos, L., Placek, B.J., Sengupta, R., Richter, M., Dorsey, J.A., Kubicek, S., Opravil, S., Jenuwein, T., Berger, S.L., 2006. Repression of p53 activity by Smyd2-mediated methylation. Nature 444, 629–632. https://doi.org/10.1038/nature05287

Hukkelhoven, C.W.P.M., Steyerberg, E.W., Rampen, A.J.J., Farace, E., Habbema, J.D.F., Marshall, L.F., Murray, G.D., Maas, A.I.R., 2003. Patient age and outcome following severe traumatic brain injury: an analysis of 5600 patients. Journal of Neurosurgery 99, 666–673. https://doi.org/10.3171/jns.2003.99.4.0666

Idda, M.L., McClusky, W.G., Lodde, V., Munk, R., Abdelmohsen, K., Rossi, M., Gorospe, M., 2020. Survey of senescent cell markers with age in human tissues. Aging 12, 4052–4066. https://doi.org/10.18632/aging.102903

Igoe, N., Bayle, E.D., Tallant, C., Fedorov, O., Meier, J.C., Savitsky, P., Rogers, C., Morias, Y., Scholze, S., Boyd, H., Cunoosamy, D., Andrews, D.M., Cheasty, A., Brennan, P.E., Müller, S., Knapp, S., Fish, P.V., 2017. Design of a Chemical Probe for the Bromodomain and Plant Homeodomain Finger-Containing (BRPF) Family of Proteins. J. Med. Chem. 60, 6998–7011. https://doi.org/10.1021/acs.jmedchem.7b00611

Illumina inc., 2012. Infinium HumanMethylation450 BeadChip, [Data Sheet], Illumina inc. Pub. No. 270-2010-00. URL https://emea.illumina.com/content/dam/illumina-marketing/documents/products/datasheets/datasheet_humanmethylation450.pdf (accessed 01.01.22).

Imagawa, E., Higashimoto, K., Sakai, Y., Numakura, C., Okamoto, N., Matsunaga, S., Ryo, A., Sato, Y., Sanefuji, M., Ihara, K., Takada, Y., Nishimura, G., Saitsu, H., Mizuguchi, T., Miyatake, S., Nakashima, M., Miyake, N., Soejima, H., Matsumoto, N., 2017. Mutations in genes encoding polycomb repressive complex 2 subunits cause Weaver syndrome. Human Mutation 38, 637–648. https://doi.org/10.1002/humu.23200

Issa, J.P., 2014. Aging and epigenetic drift: a vicious cycle. The Journal of clinical investigation 124, 24–29. https://doi.org/10.1172/JCI69735

Ito, M., Wang, Q., Hao, D., Sawada, H., Huang, B., Guo, L., Daugherty, A., Li, X.-A., 2021. Ultrasound Monitoring of Thymus Involution in Septic Mice. Ultrasound in Medicine & Biology 47, 769–776. https://doi.org/10.1016/j.ultrasmedbio.2020.11.031

Jafari-Ghahfarokhi, H., Moradi-Chaleshtori, M., Liehr, T., Hashemzadeh-Chaleshtori, M., Teimori, H., Ghasemi-Dehkordi, P., 2015. Small supernumerary marker chromosomes and their correlation with specific syndromes. Adv Biomed Res 4, 140. https://doi.org/10.4103/2277-9175.161542

Jagger, A.T., Shimojima, Y., Goronzy, J.J., Weyand, C.M., 2014. T regulatory cells and the immune aging process. Gerontology 60, 130–137. https://doi.org/10.1159/000355303

Javaid, N., Choi, S., 2017. Acetylation- and Methylation-Related Epigenetic Proteins in the Context of Their Targets. Genes (Basel) 8, 196. https://doi.org/10.3390/genes8080196

Jenkins, E.C., Velinov, M.T., Ye, L., Gu, H., Li, S., Jenkins, E.C., Brooks, S.S., Pang, D., Devenny, D.A., Zigman, W.B., Schupf, N., Silverman, W.P., 2006. Telomere shortening in T lymphocytes of older individuals with Down syndrome and dementia. Neurobiology of Aging 27, 941–945. https://doi.org/10.1016/j.neurobiolaging.2005.05.021

Jeschke, M.G., Chinkes, D.L., Finnerty, C.C., Kulp, G., Suman, O.E., Norbury, W.B., Branski, L.K., Gauglitz, G.G., Mlcak, R.P., Herndon, D.N., 2008. Pathophysiologic response to severe burn injury. Annals of Surgery 248, 387–401. https://doi.org/10.1097/SLA.0b013e3181856241

Jeschke, M.G., Gauglitz, G.G., Kulp, G.A., Finnerty, C.C., Williams, F.N., Kraft, R., Suman, O.E., Mlcak, R.P., Herndon, D.N., 2011. Long-Term Persistance of the Pathophysiologic Response to Severe Burn Injury. PLoS ONE 6, e21245. https://doi.org/10.1371/journal.pone.0021245

Jeschke, M.G., van Baar, M.E., Choudhry, M.A., Chung, K.K., Gibran, N.S., Logsetty, S., 2020. Burn injury. Nat Rev Dis Primers 6, 1–25. https://doi.org/10.1038/s41572-020-0145-5

Jiang, H., Ju, Z., Rudolph, K.L., 2007. Telomere shortening and ageing. Zeitschrift fur Gerontologie und Geriatrie 40, 314–324. https://doi.org/10.1007/s00391-007-0480-0

Jiang, X., Xu, Y., Price, B.D., 2010. Acetylation of H2AX on lysine 36 plays a key role in the DNA double-strand break repair pathway. FEBS Lett 584, 2926–2930. https://doi.org/10.1016/j.febslet.2010.05.017

Johnson, A.A., Akman, K., Calimport, S.R.G., Wuttke, D., Stolzing, A., de Magalhães, J.P., 2012. The Role of DNA Methylation in Aging, Rejuvenation, and Age-Related Disease. Rejuvenation Res 15, 483–494. https://doi.org/10.1089/rej.2012.1324

Johnson, B.Z., McAlister, S., McGuire, H.M., Palanivelu, V., Stevenson, A., Richmond, P., Palmer, D.J., Metcalfe, J., Prescott, S.L., Wood, F.M., Fazekas de St Groth, B., Linden, M.D., Fear, M.W., Fear,

V.S., 2020. Pediatric Burn Survivors Have Long-Term Immune Dysfunction With Diminished Vaccine Response. Frontiers in Immunology 11. https://doi.org/10.3389/fimmu.2020.598646

Josling, G.A., Selvarajah, S.A., Petter, M., Duffy, M.F., 2012. The Role of Bromodomain Proteins in Regulating Gene Expression. Genes (Basel) 3, 320–343. https://doi.org/10.3390/genes3020320

Jovanovic, T., Vance, L.A., Cross, D., Knight, A.K., Kilaru, V., Michopoulos, V., Klengel, T., Smith, A.K., 2017. Exposure to Violence Accelerates Epigenetic Aging in Children. Sci Rep 7, 8962. https://doi.org/10.1038/s41598-017-09235-9

Jun, J.-I., Lau, L.F., 2010. Cellular senescence controls fibrosis in wound healing. Aging (Albany NY) 2, 627–631. https://doi.org/10.18632/aging.100201

Jurk, D., Wilson, C., Passos, J.F., Oakley, F., Correia-Melo, C., Greaves, L., Saretzki, G., Fox, C., Lawless, C., Anderson, R., Hewitt, G., Pender, S.L., Fullard, N., Nelson, G., Mann, J., van de Sluis, B., Mann, D.A., von Zglinicki, T., 2014. Chronic inflammation induces telomere dysfunction and accelerates ageing in mice. Nat Commun 2. https://doi.org/10.1038/ncomms5172

Justice, J.N., Nambiar, A.M., Tchkonia, T., LeBrasseur, N.K., Pascual, R., Hashmi, S.K., Prata, L., Masternak, M.M., Kritchevsky, S.B., Musi, N., Kirkland, J.L., 2019. Senolytics in idiopathic pulmonary fibrosis: Results from a first-in-human, open-label, pilot study. eBioMedicine 40, 554–563. https://doi.org/10.1016/j.ebiom.2018.12.052

Kaeser, M.D., Aslanian, A., Dong, M.-Q., Yates, J.R., Emerson, B.M., 2008. BRD7, a Novel PBAF-specific SWI/SNF Subunit, Is Required for Target Gene Activation and Repression in Embryonic Stem Cells. J Biol Chem 283, 32254–32263. https://doi.org/10.1074/jbc.M806061200

Kagoya, Y., Nakatsugawa, M., Saso, K., Guo, T., Anczurowski, M., Wang, C.-H., Butler, M.O., Arrowsmith, C.H., Hirano, N., 2018. DOT1L inhibition attenuates graft-versus-host disease by allogeneic T cells in adoptive immunotherapy models. Nat Commun 9, 1915. https://doi.org/10.1038/s41467-018-04262-0

Kananen, L., Nevalainen, T., Jylhävä, J., Marttila, S., Hervonen, A., Jylhä, M., Hurme, M., 2015. Cytomegalovirus infection accelerates epigenetic aging. Experimental Gerontology 72, 227–229. https://doi.org/10.1016/j.exger.2015.10.008

Karakelides, H., Irving, B.A., Short, K.R., O'Brien, P., Nair, K.S., 2010. Age, Obesity, and Sex Effects on Insulin Sensitivity and Skeletal Muscle Mitochondrial Function. Diabetes 59, 89–97. https://doi.org/10.2337/db09-0591

Karczewski, J., Śledzińska, E., Baturo, A., Jończyk, I., Maleszko, A., Maleszko, A., Samborski, P., Begier-Krasińska, B., Dobrowolska, A., 2018. Obesity and inflammation. European Cytokine Network 29, 83–94. https://doi.org/10.1684/ecn.2018.0415

Kargbo, R.B., 2020. SMARCA2/4 PROTAC for Targeted Protein Degradation and Cancer Therapy. ACS Med. Chem. Lett. 11, 1797–1798. https://doi.org/10.1021/acsmedchemlett.0c00347

Kari, V., Raul, S.K., Henck, J.M., Kitz, J., Kramer, F., Kosinsky, R.L., Übelmesser, N., Mansour, W.Y., Eggert, J., Spitzner, M., Najafova, Z., Bastians, H., Grade, M., Gaedcke, J., Wegwitz, F., Johnsen, S.A., 2019. The histone methyltransferase DOT1L is required for proper DNA damage response, DNA repair, and modulates chemotherapy responsiveness. Clinical Epigenetics 11, 4. https://doi.org/10.1186/s13148-018-0601-1

Kee, J., Thudium, S., Renner, D.M., Glastad, K., Palozola, K., Zhang, Z., Li, Y., Lan, Y., Cesare, J., Poleshko, A., Kiseleva, A.A., Truitt, R., Cardenas-Diaz, F.L., Zhang, X., Xie, X., Kotton, D.N., Alysandratos, K.D., Epstein, J.A., Shi, P.-Y., Yang, W., Morrisey, E., Garcia, B.A., Berger, S.L., Weiss, S.R., Korb, E., 2022. SARS-CoV-2 disrupts host epigenetic regulation via histone mimicry. Nature 610, 381–388. https://doi.org/10.1038/s41586-022-05282-z

Kerby, J.D., McGwin, G., Jr., George, R.L., Cross, J.A., Chaudry, I.H., Rue, L.W., 2006. Sex Differences in Mortality After Burn Injury: Results of Analysis of the National Burn Repository of the American Burn Association. Journal of Burn Care & Research 27, 452–456. https://doi.org/10.1097/01.BCR.0000225957.01854.EE

Kerschbaum, S., Wegrostek, C., Riegel, E., Czerny, T., 2021a. Senescence in a cell culture model for burn wounds. Experimental and Molecular Pathology 122, 104674. https://doi.org/10.1016/j.yexmp.2021.104674

Kerschbaum, S., Wegrostek, C., Riegel, E., Czerny, T., 2021b. Senescence in a cell culture model for burn wounds. Experimental and Molecular Pathology 122, 104674. https://doi.org/10.1016/j.yexmp.2021.104674

Keys, A., Fidanza, F., Karvonen, M.J., Kimura, N., Taylor, H.L., 1972. Indices of relative weight and obesity. Journal of Chronic Diseases 25, 329–343. https://doi.org/10.1016/0021-9681(72)90027-6

Khaw, K.-T., Wareham, N., Bingham, S., Welch, A., Luben, R., Day, N., 2008. Combined Impact of Health Behaviours and Mortality in Men and Women: The EPIC-Norfolk Prospective Population Study. PLoS Medicine 5, 9. https://doi.org/10.1371/journal.pmed.0050012

Kim, D., Kim, K.I., Baek, S.H., 2021. Roles of lysine-specific demethylase 1 (LSD1) in homeostasis and diseases. Journal of Biomedical Science 28, 41. https://doi.org/10.1186/s12929-021-00737-3

Kim, J.-H., Nam, C.M., Lee, D., Bang, H., Ko, J.-H., Lim, I., Kim, G.J., Koes, B.W., Lee, D.-C., 2020. Heritability of telomere length across three generations of Korean families. Pediatr Res 87, 1060–1065. https://doi.org/10.1038/s41390-019-0699-7

Kim, S., Parks, C.G., DeRoo, L.A., Chen, H., Taylor, J.A., Cawthon, R.M., Sandler, D.P., 2009. Obesity and Weight Gain in Adulthood and Telomere Length. Cancer Epidemiology, Biomarkers & Prevention 18, 816–820. https://doi.org/10.1158/1055-9965.EPI-08-0935

Kim, S.-W., Kang, H.-J., Jhon, M., Kim, J.-W., Lee, J.-Y., Walker, A.J., Agustini, B., Kim, J.-M., Berk, M., 2019. Statins and Inflammation: New Therapeutic Opportunities in Psychiatry. Frontiers in Psychiatry 10. https://doi.org/10.3389/fpsyt.2019.00103

Kim, T.Y., Kim, S.J., Choi, J.R., Lee, S.T., Kim, J., Hwang, I.S., Chung, H.G., Choi, J.H., Kim, H.W., Kim, S.H., Kang, J.I., 2017. The effect of trauma and PTSD on telomere length: An exploratory study in people exposed to combat trauma. Scientific reports 7, w. https://doi.org/10.1038/s41598-017-04682-w

Kirkland, J.L., Tchkonia, T., 2020. Senolytic drugs: from discovery to translation. J Intern Med 10.1111/joim.13141. https://doi.org/10.1111/joim.13141

Kirkland, J.L., Tchkonia, T., 2015. Clinical strategies and animal models for developing senolytic agents. Experimental Gerontology 68, 19–25. https://doi.org/10.1016/j.exger.2014.10.012

Klein, S.L., Flanagan, K.L., 2016. Sex differences in immune responses. Nat Rev Immunol 16, 626–638. https://doi.org/10.1038/nri.2016.90

Kloetzel, P.-M., Ossendorp, F., 2004. Proteasome and peptidase function in MHC-class-I-mediated antigen presentation. Current Opinion in Immunology 16, 76–81. https://doi.org/10.1016/j.coi.2003.11.004

Knaus, W.A., Draper, E.A., Wagner, D.P., Zimmerman, J.E., 1985. APACHE II: a severity of disease classification system. Crit Care Med 13, 818–829. PMID: 3928249

Koenig, S.M., Truwit, J.D., 2006. Ventilator-Associated Pneumonia: Diagnosis, Treatment, and Prevention. Clin Microbiol Rev 19, 637–657. https://doi.org/10.1128/CMR.00051-05

Koh, T.J., DiPietro, L.A., 2011. Inflammation and wound healing: The role of the macrophage. Expert Rev Mol Med 13, e23. https://doi.org/10.1017/S1462399411001943

Komarova, E.A., Gudkov, A.V., 2000. Suppression of p53: a new approach to overcome side effects of antitumor therapy. Biochemistry (Mosc) 65, 41–48. PMID: 10702639

Kondělková, K., Vokurková, D., Krejsek, J., Borská, L., Fiala, Z., Ctirad, A., 2010. Regulatory T cells (TREG) and their roles in immune system with respect to immunopathological disorders. Acta Medica (Hradec Kralove) 53, 73–77. https://doi.org/10.14712/18059694.2016.63

Kondo, Y., Miyazato, A., Okamoto, K., Tanaka, H., 2021. Impact of Sex Differences on Mortality in Patients With Sepsis After Trauma: A Nationwide Cohort Study. Frontiers in Immunology 12. https://doi.org/10.3389/fimmu.2021.678156

Kordinas, V., Ioannidis, A., Chatzipanagiotou, S., 2016. The Telomere/Telomerase System in Chronic Inflammatory Diseases. Cause or Effect? Genes 7, 10.3390/genes7090060. https://doi.org/10.3390/genes7090060

Korga, A., Ostrowska, M., Iwan, M., Herbet, M., Dudka, J., 2019. Inhibition of glycolysis disrupts cellular antioxidant defense and sensitizes HepG2 cells to doxorubicin treatment. FEBS Open Bio 9, 959–972. https://doi.org/10.1002/2211-5463.12628

Kotsantis, P., Silva, L.M., Irmscher, S., Jones, R.M., Folkes, L., Gromak, N., Petermann, E., 2016. Increased global transcription activity as a mechanism of replication stress in cancer. Nat Commun 7, 13087. https://doi.org/10.1038/ncomms13087

Krug, E.G., Sharma, G.K., Lozano, R., 2000. The global burden of injuries. Am J Public Health 90, 523–526. https://doi.org/10.2105/ajph.90.4.523

Kumar, S., Chinnusamy, V., Mohapatra, T., 2018. Epigenetics of Modified DNA Bases: 5-Methylcytosine and Beyond. Frontiers in Genetics. https://doi.org/10.3389/fgene.2018.00640

Kumari, R., Jat, P., 2021a. Mechanisms of Cellular Senescence: Cell Cycle Arrest and Senescence Associated Secretory Phenotype. Frontiers in Cell and Developmental Biology. https://doi.org/10.3389/fcell.2021.645593

Kuo, C.-L., Pilling, L.C., Atkins, J.L., Masoli, J.A., Delgado, J., Tignanelli, C., Kuchel, G.A., Melzer, D., Beckman, K.B., Levine, M.E., 2020. COVID-19 severity is predicted by earlier evidence of accelerated aging. medRxiv. https://doi.org/10.1101/2020.07.10.20147777

Lam, N.N., Hung, N.T., Duc, N.M., 2021. Prognosis value of revised Baux score among burn patients in developing country. Int J Burns Trauma 11, 197–201. PMID: 34336385

Lambden, S., Laterre, P.F., Levy, M.M., Francois, B., 2019. The SOFA score—development, utility and challenges of accurate assessment in clinical trials. Critical Care 23, 374. https://doi.org/10.1186/s13054-019-2663-7

Land, H., Parada, L.F., Weinberg, R.A., 1983. Tumorigenic conversion of primary embryo fibroblasts requires at least two cooperating oncogenes. Nature 304, 596–602. https://doi.org/10.1038/304596a0

Lane, M.A., Roth, G.S., Ingram, D.K., 2007. Caloric Restriction Mimetics, in: Tollefsbol, T.O. (Ed.), Biological Aging: Methods and Protocols, Methods in Molecular Biology™. Humana Press, Totowa, NJ, pp. 143–149. https://doi.org/10.1007/978-1-59745-361-5_11

Lang, X., Shen, L., Zhu, T., Zhao, W., Chen, Y., Zhu, C., Su, Q., Wang, C., Wang, Y., Neri, F., Jiang, H., Chen, J., 2022. Role of Age-Related Changes in DNA Methylation in the Disproportionate Susceptibility and Worse Outcomes of Sepsis in Older Adults. Frontiers in Medicine 9. https://doi.org/10.3389/fmed.2022.822847

Langie, S.A.S., Lara, J., Mathers, J.C., 2012. Early determinants of the ageing trajectory. Best Practice & Research Clinical Endocrinology & Metabolism, Early Determinants of Chronic Disease 26, 613–626. https://doi.org/10.1016/j.beem.2012.03.004

Lara, J., Cooper, R., Nissan, J., Ginty, A.T., Khaw, K.-T., Deary, I.J., Lord, J.M., Kuh, D., Mathers, J.C., 2015. A proposed panel of biomarkers of healthy ageing. BMC medicine 13, 222. https://doi.org/10.1186/s12916-015-0470-9

Latorre, E., Birar, V.C., Sheerin, A.N., Jeynes, J.C.C., Hooper, A., Dawe, H.R., Melzer, D., Cox, L.S., Faragher, R.G.A., Ostler, E.L., Harries, L.W., 2017. Small molecule modulation of splicing factor expression is associated with rescue from cellular senescence. BMC Cell Biology 18, 31. https://doi.org/10.1186/s12860-017-0147-7

Lawn, R.B., Anderson, E.L., Suderman, M., Simpkin, A.J., Gaunt, T.R., Teschendorff, A.E., Widschwendter, M., Hardy, R., Kuh, D., Relton, C.L., Howe, L.D., 2018. Psychosocial adversity and socioeconomic position during childhood and epigenetic age: analysis of two prospective cohort studies. Human Molecular Genetics 27, 1301–1308. https://doi.org/10.1093/hmg/ddy036

Lazzarini, R., Nicolai, M., Pirani, V., Mariotti, C., Di Primio, R., 2018. Effects of senescent secretory phenotype acquisition on human retinal pigment epithelial stem cells. Aging (Albany NY) 10, 3173–3184. https://doi.org/10.18632/aging.101624

Lederer, J.A., Brownstein, B.H., Lopez, M.C., MacMillan, S., Delisle, A.J., MacConmara, M.P., Choudhry, M.A., Xiao, W., Lekousi, S., Cobb, J.P., Baker, H.V., Mannick, J.A., Chaudry, I.H., 2008. Comparison of longitudinal leukocyte gene expression after burn injury or trauma-hemorrhage in mice. Physiological Genomics 32, 299–310. https://doi.org/10.1152/physiolgenomics.00086.2007

Lee, B.Y., Han, J.A., Im, J.S., Morrone, A., Johung, K., Goodwin, E.C., Kleijer, W.J., DiMaio, D., Hwang, E.S., 2006. Senescence-associated β-galactosidase is lysosomal β-galactosidase. Aging Cell 5, 187–195. https://doi.org/10.1111/j.1474-9726.2006.00199.x

Lee, D., Lee, D.-Y., Hwang, Y.-S., Seo, H.-R., Lee, S.-A., Kwon, J., 2021. The Bromodomain Inhibitor PFI-3 Sensitizes Cancer Cells to DNA Damage by Targeting SWI/SNF. Molecular Cancer Research 19, 900–912. https://doi.org/10.1158/1541-7786.MCR-20-0289

Lee, K.S., Lin, S., Copland, D.A., Dick, A.D., Liu, J., 2021. Cellular senescence in the aging retina and developments of senotherapies for age-related macular degeneration. Journal of Neuroinflammation 18, 32. https://doi.org/10.1186/s12974-021-02088-0

Lenz, A., Franklin, G.A., Cheadle, W.G., 2007. Systemic inflammation after trauma. Injury 38, 1336–1345. https://doi.org/S0020-1383(07)00418-4

Levine, M.E., Lu, A.T., Quach, A., Chen, B.H., Assimes, T.L., Bandinelli, S., Hou, L., Baccarelli, A.A., Stewart, J.D., Li, Y., Whitsel, E.A., Wilson, J.G., Reiner, A.P., Aviv, A., Lohman, K., Liu, Y., Ferrucci, L., Horvath, S., 2018. An epigenetic biomarker of aging for lifespan and healthspan. Aging (Albany NY) 10, 573–591. https://doi.org/10.18632/aging.101414

Li, D., Zhang, J., Bai, G., Chen, J., Cheng, W., Cui, N., 2020. Lymphocyte and NK Cell Counts Can Predict Sepsis-Associated Delirium in Elderly Patients. Front Aging Neurosci 12, 621298. https://doi.org/10.3389/fnagi.2020.621298

Li, M., Yao, D., Zeng, X., Kasakovski, D., Zhang, Y., Chen, S., Zha, X., Li, Y., Xu, L., 2019. Age related human T cell subset evolution and senescence. Immunity & Ageing 16, 24. https://doi.org/10.1186/s12979-019-0165-8

Li, X., Wang, J., Zhou, J., Huang, P., Li, J., 2017. The association between post-traumatic stress disorder and shorter telomere length: A systematic review and meta-analysis. Journal of Affective Disorders 218, 322–326. https://doi.org/10.1016/j.jad.2017.03.048

Li, Z., He, Y., Wang, D., Tang, J., Chen, X., 2017. Association between childhood trauma and accelerated telomere erosion in adulthood: A meta-analytic study. Journal of Psychiatric Research 93, 64–71. https://doi.org/10.1016/j.jpsychires.2017.06.002

Lian, J., Yue, Y., Yu, W., Zhang, Y., 2020. Immunosenescence: a key player in cancer development. J Hematol Oncol 13, 151. https://doi.org/10.1186/s13045-020-00986-z

Lin, X., Zhou, J., Dong, B., 2019. EFFECT OF DIFFERENT LEVELS OF EXERCISE ON TELOMERE LENGTH: A SYSTEMATIC REVIEW AND META-ANALYSIS. J Rehabil Med 6. https://doi.org/10.2340/16501977-2560

Lingsma, H.F., Bottle, A., Middleton, S., Kievit, J., Steyerberg, E.W., Marang-van de Mheen, P.J., 2018. Evaluation of hospital outcomes: the relation between length-of-stay, readmission, and mortality in a large international administrative database. BMC Health Serv Res 18, 116. https://doi.org/10.1186/s12913-018-2916-1

Liu, S., Wang, C., Green, G., Zhuo, H., Liu, K.D., Kangelaris, K.N., Gomez, A., Jauregui, A., Vessel, K., Ke, S., Hendrickson, C., Matthay, M.A., Calfee, C.S., Ware, L.B., Wolters, P.J., 2020. Peripheral blood leukocyte telomere length is associated with survival of sepsis patients. European Respiratory Journal 55. https://doi.org/10.1183/13993003.01044-2019

Liu, Y., Zhou, J., White, K.P., 2014. RNA-seq differential expression studies: more sequence or more replication? Bioinformatics 30, 301–304. https://doi.org/10.1093/bioinformatics/btt688

Liu, Z., Kuo, P.-L., Horvath, S., Crimmins, E., Ferrucci, L., Levine, M., 2018. A new aging measure captures morbidity and mortality risk across diverse subpopulations from NHANES IV: A cohort study. PLOS Medicine 15, e1002718. https://doi.org/10.1371/journal.pmed.1002718

Liu, Z., Leung, D., Thrush, K., Zhao, W., Ratliff, S., Tanaka, T., Schmitz, L.L., Smith, J.A., Ferrucci, L., Levine, M.E., 2020. Underlying features of epigenetic aging clocks in vivo and in vitro. Aging Cell 19, e13229. https://doi.org/10.1111/acel.13229

Lo Piccolo, L., Mochizuki, H., Nagai, Y., 2019. The lncRNA hsrω regulates arginine dimethylation of human FUS to cause its proteasomal degradation in Drosophila. Journal of Cell Science 132, jcs236836. https://doi.org/10.1242/jcs.236836

López-Otín, C., Blasco, M.A., Partridge, L., Serrano, M., Kroemer, G., 2023. Hallmarks of aging: An expanding universe. Cell 186, 243–278. https://doi.org/10.1016/j.cell.2022.11.001

Lopez-Otin, C., Blasco, M.A., Partridge, L., Serrano, M., Kroemer, G., 2013. The hallmarks of aging. Cell 153, 1194–1217. https://doi.org/10.1016/j.cell.2013.05.039

Lord, J.M., Midwinter, M.J., Chen, Y.-F., Belli, A., Brohi, K., Kovacs, E.J., Koenderman, L., Kubes, P., Lilford, R.J., 2014. The systemic immune response to trauma: an overview of pathophysiology and treatment. The Lancet 384, 1455–1465. https://doi.org/10.1016/S0140-6736(14)60687-5

Lorenzi, L., Tabellini, G., Vermi, W., Moratto, D., Porta, F., Notarangelo, L.D., Patrizi, O., Sozzani, S., de Saint Basile, G., Latour, S., Pace, D., Lonardi, S., Facchetti, F., Badolato, R., Parolini, S., 2013. Occurrence of nodular lymphocyte-predominant hodgkin lymphoma in hermansky-pudlak type 2 syndrome is associated to natural killer and natural killer T cell defects. PLoS One 8, e80131. https://doi.org/10.1371/journal.pone.0080131

Lu, J., Goh, S.J., Tng, P.Y.L., Deng, Y.Y., Ling, E.-A., Moochhala, S., 2009. Systemic inflammatory response following acute traumatic brain injury. Front Biosci (Landmark Ed) 14, 3795–3813. https://doi.org/10.2741/3489

Lu, Q., Longo, F.M., Zhou, H., Massa, S.M., Chen, Y.-H., 2009. Signaling Through Rho GTPase Pathway as Viable Drug Target. Curr Med Chem 16, 1355–1365. https://doi.org/10.2174/092986709787846569

Luan, Y., Ngo, L., Han, Z., Wang, X., Qu, M., Zheng, Y.G., 2015. Chapter 14 - Histone Acetyltransferases: Enzymes, Assays, and Inhibitors, in: Zheng, Y.G. (Ed.), Epigenetic Technological Applications. Academic Press, Boston, pp. 291–317. https://doi.org/10.1016/B978-0-12-801080-8.00014-4

Lucero, C.M.J., Vega, O.A., Osorio, M.M., Tapia, J.C., Antonelli, M., Stein, G.S., Van Wijnen, A.J., Galindo, M.A., 2013. The Cancer-Related Transcription Factor Runx2 Modulates Cell Proliferation in Human Osteosarcoma Cell Lines. J Cell Physiol 228, 10.1002/jcp.24218. https://doi.org/10.1002/jcp.24218

Luckheeram, R.V., Zhou, R., Verma, A.D., Xia, B., 2012. CD4 + T Cells: Differentiation and Functions. Clinical and Developmental Immunology 2012, 1–12. https://doi.org/10.1155/2012/925135

Lund, C.C., 1944. The estimation of areas of burns. Surg Gynecol Obste 79, 352–358.

Luo, C.T., Li, M.O., 2013. Transcriptional control of regulatory T cell development and function. Trends Immunol 34, 531–539. https://doi.org/10.1016/j.it.2013.08.003

Luo, M., Xu, L., Qian, Z., Sun, X., 2021. Infection-Associated Thymic Atrophy. Frontiers in Immunology 12. https://doi.org/10.3389/fimmu.2021.652538

Ma, S., Wang, C., Mao, X., Hao, Y., 2019. B Cell Dysfunction Associated With Aging and Autoimmune Diseases. Frontiers in Immunology 10. https://doi.org/10.3389/fimmu.2019.00318

Macip, S., Igarashi, M., Fang, L., Chen, A., Pan, Z.-Q., Lee, S.W., Aaronson, S.A., 2002. Inhibition of p21-mediated ROS accumulation can rescue p21-induced senescence. EMBO J 21, 2180–2188. https://doi.org/10.1093/emboj/21.9.2180

Maegawa, S., Lu, Y., Tahara, T., Lee, J.T., Madzo, J., Liang, S., Jelinek, J., Colman, R.J., Issa, J.-P.J., 2017. Caloric restriction delays age-related methylation drift. Nat Commun 8, 539. https://doi.org/10.1038/s41467-017-00607-3

Margueron, R., Li, G., Sarma, K., Blais, A., Zavadil, J., Woodcock, C.L., Dynlacht, B.D., Reinberg, D., 2008. Ezh1 and Ezh2 maintain repressive chromatin through different mechanisms. Mol Cell 32, 503–518. https://doi.org/10.1016/j.molcel.2008.11.004

Marshall, J.S., Warrington, R., Watson, W., Kim, H.L., 2018. An introduction to immunology and immunopathology. Allergy, Asthma & Clinical Immunology 14, 49. https://doi.org/10.1186/s13223-018-0278-1

Martin, G.S., Mannino, D.M., Moss, M., 2006. The effect of age on the development and outcome of adult sepsis*. Critical Care Medicine 34, 15–21. https://doi.org/10.1097/01.CCM.0000194535.82812.BA

Martin, L.F., Richardson, L.S., da Silva, M.G., Sheller-Miller, S., Menon, R., 2019. Dexamethasone induces primary amnion epithelial cell senescence through telomere-P21 associated pathway†. Biology of Reproduction 100, 1605–1616. https://doi.org/10.1093/biolre/ioz048

Martin, L.J., Koegl, M., Bader, G., Cockcroft, X.-L., Fedorov, O., Fiegen, D., Gerstberger, T., Hofmann, M.H., Hohmann, A.F., Kessler, D., Knapp, S., Knesl, P., Kornigg, S., Müller, S., Nar, H., Rogers, C., Rumpel, K., Schaaf, O., Steurer, S., Tallant, C., Vakoc, C.R., Zeeb, M., Zoephel, A., Pearson, M., Boehmelt, G., McConnell, D., 2016. Structure-Based Design of an in Vivo Active Selective BRD9 Inhibitor. J. Med. Chem. 59, 4462–4475. https://doi.org/10.1021/acs.jmedchem.5b01865

Martín, S., Pérez, A., Aldecoa, C., 2017. Sepsis and Immunosenescence in the Elderly Patient: A Review. Frontiers in Medicine 4. https://doi.org/10.3389/fmed.2017.00020

Masi, S., Salpea, K.D., Li, K., Parkar, M., Nibali, L., Donos, N., Patel, K., Taddei, S., Deanfield, J.E., D'Aiuto, F., Humphries, S.E., 2011. Oxidative stress, chronic inflammation, and telomere length in patients with periodontitis. https://doi.org/10.1016/j.freeradbiomed.2010.12.031

Mather, K.A., Jorm, A.F., Parslow, R.A., Christensen, H., 2011. Is Telomere Length a Biomarker of Aging? A Review. J Gerontol A Biol Sci Med Sci 66A, 202–213. https://doi.org/10.1093/gerona/glq180

Matthay, M.A., Zemans, R.L., Zimmerman, G.A., Arabi, Y.M., Beitler, J.R., Mercat, A., Herridge, M., Randolph, A.G., Calfee, C.S., 2019. Acute respiratory distress syndrome. Nat Rev Dis Primers 5, 1–22. https://doi.org/10.1038/s41572-019-0069-0

Mauro, C., Smith, J., Cucchi, D., Coe, D., Fu, H., Bonacina, F., Baragetti, A., Cermenati, G., Caruso, D., Mitro, N., Catapano, A.L., Ammirati, E., Longhi, M.P., Okkenhaug, K., Norata, G.D., Marelli-Berg, F.M., 2017. Obesity-Induced Metabolic Stress Leads to Biased Effector Memory CD4+ T Cell Differentiation via PI3K p110δ-Akt-Mediated Signals. Cell Metab 25, 593–609. https://doi.org/10.1016/j.cmet.2017.01.008

Mazidi, M., Penson, P., Banach, M., 2017. Association between telomere length and complete blood count in US adults. Arch Med Sci 13, 601–605. https://doi.org/10.5114/aoms.2017.67281

McElvaney, O.J., McEvoy, N.L., McElvaney, O.F., Carroll, T.P., Murphy, M.P., Dunlea, D.M., Ní Choileáin, O., Clarke, J., O'Connor, E., Hogan, G., Ryan, D., Sulaiman, I., Gunaratnam, C., Branagan, P., O'Brien, M.E., Morgan, R.K., Costello, R.W., Hurley, K., Walsh, S., de Barra, E., McNally, C., McConkey, S., Boland, F., Galvin, S., Kiernan, F., O'Rourke, J., Dwyer, R., Power, M., Geoghegan, P., Larkin, C., O'Leary, R.A., Freeman, J., Gaffney, A., Marsh, B., Curley, G.F., McElvaney, N.G., 2020. Characterization of the Inflammatory Response to Severe COVID-19 Illness. Am J Respir Crit Care Med 202, 812–821. https://doi.org/10.1164/rccm.202005-1583OC

McEwen, L.M., Jones, M.J., Lin, D.T.S., Edgar, R.D., Husquin, L.T., MacIsaac, J.L., Ramadori, K.E., Morin, A.M., Rider, C.F., Carlsten, C., Quintana-Murci, L., Horvath, S., Kobor, M.S., 2018. Systematic evaluation of DNA methylation age estimation with common preprocessing methods and the Infinium MethylationEPIC BeadChip array. Clin Epigenetics 10, 123. https://doi.org/10.1186/s13148-018-0556-2

Medvedeva, Y.A., Khamis, A.M., Kulakovskiy, I.V., Ba-Alawi, W., Bhuyan, M.S.I., Kawaji, H., Lassmann, T., Harbers, M., Forrest, A.R., Bajic, V.B., 2014. Effects of cytosine methylation on transcription factor binding sites. BMC Genomics 15, 119. https://doi.org/10.1186/1471-2164-15-119

Mehrabani, S., Bagherniya, M., Askari, G., Read, M.I., Sahebkar, A., 2020. The effect of fasting or calorie restriction on mitophagy induction: a literature review. J Cachexia Sarcopenia Muscle 11, 1447–1458. https://doi.org/10.1002/jcsm.12611

Mehta, D., Bruenig, D., Lawford, B., Harvey, W., Carrillo-Roa, T., Morris, C.P., Jovanovic, T., Young, R.M., Binder, E.B., Voisey, J., 2018. Accelerated DNA methylation aging and increased resilience in veterans: The biological cost for soldiering on. Neurobiol Stress 8, 112–119. https://doi.org/10.1016/j.ynstr.2018.04.001

Meira, L.B., Bugni, J.M., Green, S.L., Lee, C.W., Pang, B., Borenshtein, D., Rickman, B.H., Rogers, A.B., Moroski-Erkul, C.A., McFaline, J.L., Schauer, D.B., Dedon, P.C., Fox, J.G., Samson, L.D., 2008. DNA damage induced by chronic inflammation contributes to colon carcinogenesis in mice. The Journal of clinical investigation 118, 2516–2525. https://doi.org/10.1172/JCI35073

Melnik, S., Werth, N., Boeuf, S., Hahn, E.-M., Gotterbarm, T., Anton, M., Richter, W., 2019. Impact of c-MYC expression on proliferation, differentiation, and risk of neoplastic transformation of human mesenchymal stromal cells. Stem Cell Res Ther 10, 73. https://doi.org/10.1186/s13287-019-1187-z

Michael, D.B., Byers, D.M., Irwin, L.N., 2005. Gene expression following traumatic brain injury in humans: analysis by microarray. Journal of Clinical Neuroscience 12, 284–290. https://doi.org/10.1016/j.jocn.2004.11.003

Michael, S., Auld, D., Klumpp, C., Jadhav, A., Zheng, W., Thorne, N., Austin, C.P., Inglese, J., Simeonov, A., 2008. A Robotic Platform for Quantitative High-Throughput Screening. Assay Drug Dev Technol 6, 637–657. https://doi.org/10.1089/adt.2008.150

Mijit, M., Caracciolo, V., Melillo, A., Amicarelli, F., Giordano, A., 2020. Role of p53 in the Regulation of Cellular Senescence. Biomolecules 10, 420. https://doi.org/10.3390/biom10030420

Milner, J.J., Beck, M.A., 2012. Micronutrients, immunology and inflammation The impact of obesity on the immune response to infection. Proc Nutr Soc 71, 298–306. https://doi.org/10.1017/S0029665112000158

Min, K.-J., Lee, C.-K., Park, H.-N., 2012. The lifespan of Korean eunuchs. Current Biology 22, R792–R793. https://doi.org/10.1016/j.cub.2012.06.036

Misawa, T., Tanaka, Y., Okada, R., Takahashi, A., 2020. Biology of extracellular vesicles secreted from senescent cells as senescence-associated secretory phenotype factors. Geriatrics & Gerontology International 20, 539–546. https://doi.org/10.1111/ggi.13928

Mishima, Y., Miyagi, S., Saraya, A., Negishi, M., Endoh, M., Endo, T.A., Toyoda, T., Shinga, J., Katsumoto, T., Chiba, T., Yamaguchi, N., Kitabayashi, I., Koseki, H., Iwama, A., 2011. The Hbo1-Brd1/Brpf2 complex is responsible for global acetylation of H3K14 and required for fetal liver erythropoiesis. Blood 118, 2443–2453. https://doi.org/10.1182/blood-2011-01-331892

Misumi, I., Starmer, J., Uchimura, T., Beck, M.A., Magnuson, T., Whitmire, J.K., 2019. Obesity Expands a Distinct Population of T Cells in Adipose Tissue and Increases Vulnerability to Infection. Cell Reports 27, 514-524.e5. https://doi.org/10.1016/j.celrep.2019.03.030

Mitsdoerffer, M., Lee, Y., Jäger, A., Kim, H.-J., Korn, T., Kolls, J.K., Cantor, H., Bettelli, E., Kuchroo, V.K., 2010. Proinflammatory T helper type 17 cells are effective B-cell helpers. Proceedings of the National Academy of Sciences 107, 14292–14297. https://doi.org/10.1073/pnas.1009234107

Molenaar, R.J., Radivoyevitch, T., Maciejewski, J.P., van Noorden, C.J.F., Bleeker, F.E., 2014. The driver and passenger effects of isocitrate dehydrogenase 1 and 2 mutations in oncogenesis and survival prolongation. Biochimica et Biophysica Acta (BBA) - Reviews on Cancer 1846, 326–341. https://doi.org/10.1016/j.bbcan.2014.05.004

Monroe, D.M., Goldstein, R.L., Teylan, M.A., Hart, J.E., DeVivo, I., Orr, E.H., Garshick, E., 2019. Clinical associations with telomere length in chronic spinal cord injury. Spinal Cord 57, 1084–1093. https://doi.org/10.1038/s41393-019-0336-7

Monstrey, S., Hoeksema, H., Verbelen, J., Pirayesh, A., Blondeel, P., 2008. Assessment of burn depth and burn wound healing potential. Burns 34, 761–769. https://doi.org/10.1016/j.burns.2008.01.009

Moore, L.D., Le, T., Fan, G., 2013. DNA Methylation and Its Basic Function. Neuropsychopharmacol 38, 23–38. https://doi.org/10.1038/npp.2012.112

Moreira, A., Alari-Pahissa, E., Munteis, E., Vera, A., Zabalza, A., Llop, M., Villarrubia, N., Costa-García, M., Álvarez-Lafuente, R., Villar, L.M., López-Botet, M., Martínez-Rodríguez, J.E., 2019. Adaptive Features of Natural Killer Cells in Multiple Sclerosis. Frontiers in Immunology 10. https://doi.org/10.3389/fimmu.2019.02403

Morley, J.E., Argiles, J.M., Evans, W.J., Bhasin, S., Cella, D., Deutz, N.E.P., Doehner, W., Fearon, K.C.H., Ferrucci, L., Hellerstein, M.K., Kalantar-Zadeh, K., Lochs, H., MacDonald, N., Mulligan, K., Muscaritoli, M., Ponikowski, P., Posthauer, M.E., Fanelli, F.R., Schambelan, M., Schols, A.M.W.J., Schuster, M.W., Anker, S.D., 2010. Nutritional Recommendations for the Management of Sarcopenia. J Am Med Dir Assoc 11, 391–396. https://doi.org/10.1016/j.jamda.2010.04.014

Moskalev, A.A., Shaposhnikov, M.V., Plyusnina, E.N., Zhavoronkov, A., Budovsky, A., Yanai, H., Fraifeld, V.E., 2013. The role of DNA damage and repair in aging through the prism of Koch-like criteria. Ageing Research Reviews 12, 661–684. https://doi.org/10.1016/j.arr.2012.02.001

Mouchiroud, L., Molin, L., Dalliere, N., Solari, F., 2010. Life span extension by resveratrol, rapamycin, and metformin: The promise of dietary restriction mimetics for an healthy aging. Biofactors 36, 377–382. https://doi.org /10.1002/biof.127

Müezzinler, A., Zaineddin, A.K., Brenner, H., 2013. A systematic review of leukocyte telomere length and age in adults. Ageing Research Reviews 12, 509–519. https://doi.org/10.1016/j.arr.2013.01.003

Mulder, P.P.G., Vlig, M., Boekema, B.K.H.L., Stoop, M.M., Pijpe, A., van Zuijlen, P.P.M., de Jong, E., van Cranenbroek, B., Joosten, I., Koenen, H.J.P.M., Ulrich, M.M.W., 2021. Persistent Systemic Inflammation in Patients With Severe Burn Injury Is Accompanied by Influx of Immature Neutrophils and Shifts in T Cell Subsets and Cytokine Profiles. Front Immunol 11, 621222. https://doi.org/10.3389/fimmu.2020.621222

Mulder, P.P.G., Vlig, M., Fasse, E., Stoop, M.M., Pijpe, A., van Zuijlen, P.P.M., Joosten, I., Boekema, B.K.H.L., Koenen, H.J.P.M., 2022. Burn-injured skin is marked by a prolonged local acute inflammatory response of innate immune cells and pro-inflammatory cytokines. Frontiers in Immunology 13. https://doi.org/10.3389/fimmu.2022.1034420

Müller-Heck, R.M., Bösken, B., Michiels, I., Dudda, M., Jäger, M., Flohé, S.B., 2021. Major Surgical Trauma Impairs the Function of Natural Killer Cells but Does Not Affect Monocyte Cytokine Synthesis. Life (Basel) 12, 13. https://doi.org/10.3390/life12010013

Muraleedharan, V., Marsh, H., Kapoor, D., Channer, K.S., Jones, T.H., 2013. Testosterone deficiency is associated with increased risk of mortality and testosterone replacement improves survival in men with type 2 diabetes. European Journal of Endocrinology 169, 725–733. https://doi.org/10.1530/EJE-13-0321

Murari, A., Singh, K.N., 2019. Lund and Browder chart—modified versus original: a comparative study. Acute Crit Care 34, 276–281. https://doi.org/10.4266/acc.2019.00647

Murray, C.K., Hoffmaster, R.M., Schmit, D.R., Hospenthal, D.R., Ward, J.A., Cancio, L.C., Wolf, S.E., 2007. Evaluation of White Blood Cell Count, Neutrophil Percentage, and Elevated Temperature as Predictors of Bloodstream Infection in Burn Patients. Archives of Surgery 142, 639–642. https://doi.org/10.1001/archsurg.142.7.639

Murray, M.A., Chotirmall, S.H., 2015. The Impact of Immunosenescence on Pulmonary Disease. Mediators of Inflammation 2015, e692546. https://doi.org/10.1155/2015/692546

Muss, H.B., Smitherman, A., Wood, W.A., Nyrop, K., Tuchman, S., Randhawa, P.K., Entwistle, A.R., Mitin, N., Shachar, S.S., 2020. p16 a biomarker of aging and tolerance for cancer therapy. Transl Cancer Res TCR 9, 5732–5742. https://doi.org/10.21037/tcr.2020.03.39

Nakajima, H., Watanabe, N., Shibata, F., Kitamura, T., Ikeda, Y., Handa, M., 2006. N-terminal Region of CCAAT/Enhancer-binding Protein ϵ Is Critical for Cell Cycle Arrest, Apoptosis, and Functional

Maturation during Myeloid Differentiation *. Journal of Biological Chemistry 281, 14494–14502. https://doi.org/10.1074/jbc.M600575200

Nakatsuka, T., Tateishi, K., Kato, H., Fujiwara, H., Yamamoto, K., Kudo, Y., Nakagawa, H., Tanaka, Y., Ijichi, H., Ikenoue, T., Ishizawa, T., Hasegawa, K., Tachibana, M., Shinkai, Y., Koike, K., 2021. Inhibition of histone methyltransferase G9a attenuates liver cancer initiation by sensitizing DNA-damaged hepatocytes to p53-induced apoptosis. Cell Death Dis 12, 1–13. https://doi.org/10.1038/s41419-020-03381-1

Nakayama, K., Szewczyk, M.M., dela Sena, C., Wu, H., Dong, A., Zeng, H., Li, F., de Freitas, R.F., Eram, M.S., Schapira, M., Baba, Y., Kunitomo, M., Cary, D.R., Tawada, M., Ohashi, A., Imaeda, Y., Saikatendu, K.S., Grimshaw, C.E., Vedadi, M., Arrowsmith, C.H., Barsyte-Lovejoy, D., Kiba, A., Tomita, D., Brown, P.J., 2018. TP-064, a potent and selective small molecule inhibitor of PRMT4 for multiple myeloma. Oncotarget 9, 18480–18493. https://doi.org/10.18632/oncotarget.24883

Namas, R., Ghuma, A., Hermus, L., Zamora, R., Okonkwo, D., Billiar, T., Vodovotz, Y., 2009. The Acute Inflammatory Response in Trauma / Hemorrhage and Traumatic Brain Injury: Current State and Emerging Prospects. Libyan Journal of Medicine 4, 136–148. https://doi.org/10.4176/090325

Napolitano, L.M., 2001. Testosterone administration in male burn patients: The good, the bad, and the ugly. Critical Care Medicine 29, 2032–2033. https://doi.org/10.1097/00003246-200110000-00036

NCBI - Gene, 2022a. KCTD11 potassium channel tetramerization domain containing 11 [Homo sapiens (human)] - Gene - NCBI [WWW Document]. URL https://www.ncbi.nlm.nih.gov/gene/147040#summary (accessed 11.18.22).

NCBI - Gene, 2022b. PCDHGA4 protocadherin gamma subfamily A, 4 [Homo sapiens (human)] - Gene - NCBI [WWW Document]. URL https://www.ncbi.nlm.nih.gov/gene/56111#summary (accessed 11.18.22).

NCBI - Gene, 2022c. KPNA2 karyopherin subunit alpha 2 [Homo sapiens (human)] - Gene - NCBI [WWW Document]. URL https://www.ncbi.nlm.nih.gov/gene/3838#summary (accessed 11.18.22).

NCBI - Gene, 2022d. ANKRD11 ankyrin repeat domain containing 11 [Homo sapiens (human)] - Gene - NCBI [WWW Document]. URL https://www.ncbi.nlm.nih.gov/gene/29123#summary (accessed 11.18.22).

NCBI - Gene, 2022e. DAZAP1 DAZ associated protein 1 [Homo sapiens (human)] - Gene - NCBI [WWW Document]. URL https://www.ncbi.nlm.nih.gov/gene/26528#summary (accessed 11.18.22).

NCBI - Gene, 2022f. TAF4 TATA-box binding protein associated factor 4 [Homo sapiens (human)] - Gene - NCBI [WWW Document]. URL https://www.ncbi.nlm.nih.gov/gene/6874#summary (accessed 11.18.22).

NCBI - Gene, 2022g. TMEM123 transmembrane protein 123 [Homo sapiens (human)] - Gene - NCBI [WWW Document]. URL https://www.ncbi.nlm.nih.gov/gene?Db=gene&Cmd=ShowDetailView&TermToSearch=114908 (accessed 11.18.22).

NCBI - Gene, 2022h. SLC25A20 solute carrier family 25 member 20 [Homo sapiens (human)] - Gene - NCBI [WWW Document]. URL https://www.ncbi.nlm.nih.gov/gene/788#summary (accessed 11.18.22).

NCBI - Gene, 2022i. RERGL RERG like [Homo sapiens (human)] - Gene - NCBI [WWW Document]. URL https://www.ncbi.nlm.nih.gov/gene/79785#summary (accessed 11.18.22).

NCBI - Gene, 2022j. ANO10 anoctamin 10 [Homo sapiens (human)] - Gene - NCBI [WWW Document]. URL https://www.ncbi.nlm.nih.gov/gene/55129 (accessed 11.18.22).

NCBI - Gene, 2022k. FNDC3B fibronectin type III domain containing 3B [Homo sapiens (human)] - Gene - NCBI [WWW Document]. URL https://www.ncbi.nlm.nih.gov/gene/64778#bibliography (accessed 11.21.22).

NCBI - Gene, 2022l. HDLBP high density lipoprotein binding protein [Homo sapiens (human)] - Gene - NCBI [WWW Document]. URL https://www.ncbi.nlm.nih.gov/gene/3069 (accessed 11.21.22).

NCBI - Gene, 2022m. P4HB Gene - GeneCards | PDIA1 Protein | PDIA1 Antibody [WWW Document]. URL https://www.genecards.org/cgi-bin/carddisp.pl?gene=P4HB#pathways_interactions (accessed 11.21.22).

NCBI - Gene, 2022n. MT1M metallothionein 1M [Homo sapiens (human)] - Gene - NCBI [WWW Document]. URL https://www.ncbi.nlm.nih.gov/gene?Db=gene&Cmd=DetailsSearch&Term=4499 (accessed 3.2.23).

NCBI - Gene, 2022o. LRRTM1 leucine rich repeat transmembrane neuronal 1 [Homo sapiens (human)] - Gene - NCBI [WWW Document]. URL https://www.ncbi.nlm.nih.gov/gene/347730 (accessed 3.2.23).

NCBI - Gene, 2022p. EFNA2 ephrin A2 [Homo sapiens (human)] - Gene - NCBI [WWW Document]. URL https://www.ncbi.nlm.nih.gov/gene/1943 (accessed 3.2.23).

NCBI - Gene, 2022q. GCSAML germinal center associated signaling and motility like [Homo sapiens (human)] - Gene - NCBI [WWW Document]. URL https://www.ncbi.nlm.nih.gov/gene/148823 (accessed 3.2.23).

NCBI - Gene, 2022r. FREM3 FRAS1 related extracellular matrix 3 [Homo sapiens (human)] - Gene - NCBI [WWW Document]. URL https://www.ncbi.nlm.nih.gov/gene/166752 (accessed 3.2.23).

NCBI - Gene, 2021. OR52P1P olfactory receptor family 52 subfamily P member 1, pseudogene [Equus caballus (horse)] - Gene - NCBI [WWW Document]. URL https://www.ncbi.nlm.nih.gov/gene/100069592 (accessed 3.2.23).

Nelson, G., Kucheryavenko, O., Wordsworth, J., von Zglinicki, T., 2018. The senescent bystander effect is caused by ROS-activated NF-κB signalling. Mech Ageing Dev 170, 30–36. https://doi.org/10.1016/j.mad.2017.08.005

Neurohr, G.E., Terry, R.L., Lengefeld, J., Bonney, M., Brittingham, G.P., Moretto, F., Miettinen, T.P., Vaites, L.P., Soares, L.M., Paulo, J.A., Harper, J.W., Buratowski, S., Manalis, S., van Werven, F.J., Holt, L.J., Amon, A., 2019. Excessive Cell Growth Causes Cytoplasm Dilution And Contributes to Senescence. Cell 176, 1083-1097.e18. https://doi.org/10.1016/j.cell.2019.01.018

Nevalainen, T., Kananen, L., Marttila, S., Jylhävä, J., Mononen, N., Kähönen, M., Raitakari, O.T., Hervonen, A., Jylhä, M., Lehtimäki, T., Hurme, M., 2017. Obesity accelerates epigenetic aging in middle-aged but not in elderly individuals. Clin Epigenet 9, 20. https://doi.org/10.1186/s13148-016-0301-7

Newgard, C.B., Sharpless, N.E., 2013. Coming of age: molecular drivers of aging and therapeutic opportunities. J Clin Invest 123, 946–950. https://doi.org/10.1172/JCI68833

Ng, T.P., Camous, X., Nyunt, M.S.Z., Vasudev, A., Tan, C.T.Y., Feng, L., Fulop, T., Yap, K.B., Larbi, A., 2015. Markers of T-cell senescence and physical frailty: insights from Singapore Longitudinal Ageing Studies. npj Aging Mech Dis 1, 15005. https://doi.org/10.1038/npjamd.2015.5

Nguyen, L.N., Nguyen, T.G., 2009. Characteristics and outcomes of multiple organ dysfunction syndrome among severe-burn patients. Burns 35, 937–941. https://doi.org/10.1016/j.burns.2009.04.015

Njajou, O.T., Hsueh, W.-C., Blackburn, E.H., Newman, A.B., Wu, S.-H., Li, R., Simonsick, E.M., Harris, T.M., Cummings, S.R., Cawthon, R.M., for the Health ABC study, 2009. Association Between Telomere Length, Specific Causes of Death, and Years of Healthy Life in Health, Aging, and Body Composition, a Population-Based Cohort Study. The Journals of Gerontology: Series A 64A, 860–864. https://doi.org/10.1093/gerona/glp061

Novelle, M.G., Ali, A., Diéguez, C., Bernier, M., de Cabo, R., 2016. Metformin: A Hopeful Promise in Aging Research. Cold Spring Harb Perspect Med 6, a025932. https://doi.org/10.1101/cshperspect.a025932

O'Donovan, A., Epel, E., Lin, J., Wolkowitz, O., Cohen, B., Maguen, S., Metzler, T., Lenoci, M., Blackburn, E., Neylan, T.C., 2011. Childhood Trauma Associated with Short Leukocyte Telomere Length in Posttraumatic Stress Disorder. Biological Psychiatry 70, 465–471. https://doi.org/10.1016/j.biopsych.2011.01.035

Ohlsson, C., Nethander, M., Kindmark, A., Ljunggren, Ö., Lorentzon, M., Rosengren, B.E., Karlsson, M.K., Mellström, D., Vandenput, L., 2017. Low Serum DHEAS Predicts Increased Fracture Risk in Older Men: The MrOS Sweden Study. J Bone Miner Res 32, 1607–1614. https://doi.org/10.1002/jbmr.3123

Oliaro, J., Van Ham, V., Sacirbegovic, F., Pasam, A., Bomzon, Z., Pham, K., Ludford-Menting, M.J., Waterhouse, N.J., Bots, M., Hawkins, E.D., Watt, S.V., Cluse, L.A., Clarke, C.J.P., Izon, D.J., Chang, J.T., Thompson, N., Gu, M., Johnstone, R.W., Smyth, M.J., Humbert, P.O., Reiner, S.L., Russell, S.M., 2010. Asymmetric Cell Division of T Cells Upon Antigen Presentation Utilizes Multiple Conserved Mechanisms. J Immunol 185, 367–375. https://doi.org/10.4049/jimmunol.0903627

Palmer, A.K., Tchkonia, T., Kirkland, J.L., 2022. Targeting cellular senescence in metabolic disease. Mol Metab 66, 101601. https://doi.org/10.1016/j.molmet.2022.101601

Palmer, C., 2007. Major Trauma and the Injury Severity Score - Where Should We Set the Bar? Annu Proc Assoc Adv Automot Med 51, 13–29. PMID: 18184482

Palmer, D.B., 2013. The Effect of Age on Thymic Function. Front Immunol 4, 316. https://doi.org/10.3389/fimmu.2013.00316

Pan, W.-R., Suami, H., Taylor, G.I., 2008. Senile Changes in Human Lymph Nodes. Lymphatic Research and Biology 6, 77–83. https://doi.org/10.1089/lrb.2007.1023

Pánico, P., Ostrosky-Wegman, P., Salazar, A.M., 2022. The potential role of COVID-19 in the induction of DNA damage. Mutation Research/Reviews in Mutation Research 789, 108411. https://doi.org/10.1016/j.mrrev.2022.108411

Papaconstantinou, J., 2019. The Role of Signaling Pathways of Inflammation and Oxidative Stress in Development of Senescence and Aging Phenotypes in Cardiovascular Disease. Cells 8, 1383. https://doi.org/10.3390/cells8111383

Papadopoulos, D., Siempis, T., Theodorakou, E., Tsoulfas, G., 2013. Hepatic Ischemia and Reperfusion Injury and Trauma: Current Concepts. Arch Trauma Res 2, 63–70. https://doi.org/10.5812/atr.12501

Parihar, A., Parihar, M.S., Milner, S., Bhat, S., 2008. Oxidative stress and anti-oxidative mobilization in burn injury. Burns 34, 6–17. https://doi.org/10.1016/j.burns.2007.04.009

Park, D.S., Fishman, G.I., 2011. The cardiac conduction system. Circulation 123, 904–915. https://doi.org/10.1161/CIRCULATIONAHA.110.942284

Park, S.G., Lee, D., Seo, H.-R., Lee, S.-A., Kwon, J., 2020. Cytotoxic activity of bromodomain inhibitor NVS-CECR2-1 on human cancer cells. Sci Rep 10, 16330. https://doi.org/10.1038/s41598-020-73500-7

Parry, S.M., Puthucheary, Z.A., 2015. The impact of extended bed rest on the musculoskeletal system in the critical care environment. Extrem Physiol Med 4. https://doi.org/10.1186/s13728-015-0036-7

Passos, J.F., Saretzki, G., Ahmed, S., Nelson, G., Richter, T., Peters, H., Wappler, I., Birket, M.J., Harold, G., Schaeuble, K., Birch-Machin, M.A., Kirkwood, T.B.L., Zglinicki, T. von, 2007. Mitochondrial Dysfunction Accounts for the Stochastic Heterogeneity in Telomere-Dependent Senescence. PLOS Biology 5, e110. https://doi.org/10.1371/journal.pbio.0050110

Patenaude, J., D'Elia, M., Hamelin, C., Garrel, D., Bernier, J., 2005. Burn injury induces a change in T cell homeostasis affecting preferentially CD4+ T cells. Journal of Leukocyte Biology 77, 141–150. https://doi.org/10.1189/jlb.0703314

Pavlicek, D., Krebs, J., Capossela, S., Bertolo, A., Engelhardt, B., Pannek, J., Stoyanov, J., 2017. Immunosenescence in persons with spinal cord injury in relation to urinary tract infections -a cross-sectional study-. Immun Ageing 14, 22. https://doi.org/10.1186/s12979-017-0103-6

Pawelec, G., 2019. Is There a Positive Side to T Cell Exhaustion? Front Immunol 10, 111. https://doi.org/10.3389/fimmu.2019.00111

Pereira, B.I., Devine, O.P., Vukmanovic-Stejic, M., Chambers, E.S., Subramanian, P., Patel, N., Virasami, A., Sebire, N.J., Kinsler, V., Valdovinos, A., LeSaux, C.J., Passos, J.F., Antoniou, A., Rustin, M.H.A., Campisi, J., Akbar, A.N., 2019. Senescent cells evade immune clearance via HLA-E-mediated NK and CD8+ T cell inhibition. Nat Commun 10, 2387. https://doi.org/10.1038/s41467-019-10335-5

Petr, M.A., Tulika, T., Carmona-Marin, L.M., Scheibye-Knudsen, M., 2020. Protecting the Aging Genome. Trends in Cell Biology 30, 117–132. https://doi.org/10.1016/j.tcb.2019.12.001

Pham, T.N., Kramer, C.B., Wang, J., Rivara, F.P., Heimbach, D.M., Gibran, N.S., Klein, M.B., 2009. Epidemiology and Outcomes of Older Adults With Burn Injury: An Analysis of the National Burn Repository. Journal of Burn Care & Research 30, 30–36. https://doi.org/10.1097/BCR.0b013e3181921efc

Phillips, A.C., Carroll, D., Gale, C.R., Lord, J.M., Arlt, W., Batty, G.D., 2010. Cortisol, DHEA sulphate, their ratio, and all-cause and cause-specific mortality in the Vietnam Experience Study. European journal of endocrinology 163, 285–292. https://doi.org/10.1530/EJE-10-0299

Phillips, C.M., Dillon, C.B., Perry, I.J., 2017. Does replacing sedentary behaviour with light or moderate to vigorous physical activity modulate inflammatory status in adults? Int J Behav Nutr Phys Act 14, 138. https://doi.org/10.1186/s12966-017-0594-8

Pido-Lopez, J., Imami, N., Aspinall, R., 2001. Both age and gender affect thymic output: more recent thymic migrants in females than males as they age. Clinical and Experimental Immunology 125, 409–413. https://doi.org/10.1046/j.1365-2249.2001.01640.x

Pinheiro da Silva, F., Machado, M.C.C., 2017. Septic Shock and the Aging Process: A Molecular Comparison. Frontiers in Immunology 8. https://doi.org/10.3389/fimmu.2017.01389

Pinti, M., De Biasi, S., Gibellini, L., Lo Tartaro, D., De Gaetano, A., Mattioli, M., Fidanza, L., Nasi, M., Cossarizza, A., 2021. Chapter 7 - Aging of immune system, in: Caruso, C., Candore, G. (Eds.), Human Aging. Academic Press, pp. 113–128. https://doi.org/10.1016/B978-0-12-822569-1.00008-1

Pires-daSilva, A., Sommer, R.J., 2003. The evolution of signalling pathways in animal development. Nat Rev Genet 4, 39–49. https://doi.org/10.1038/nrg977

Polho, G.B., De-Paula, V.J., Cardillo, G., dos Santos, B., Kerr, D.S., 2015. Leukocyte telomere length in patients with schizophrenia: A meta-analysis. Schizophrenia Research 165, 195–200. https://doi.org/10.1016/j.schres.2015.04.025

Pollock, R.D., Carter, S., Velloso, C.P., Duggal, N.A., Lord, J.M., Lazarus, N.R., Harridge, S.D.R., 2015. An investigation into the relationship between age and physiological function in highly active older adults. J Physiol 593, 657–680. https://doi.org/10.1113/jphysiol.2014.282863

Pospelova, T.V., Demidenko, Z.N., Bukreeva, E.I., Pospelov, V.A., Gudkov, A.V., Blagosklonny, M.V., 2009. Pseudo-DNA damage response in senescent cells. Cell Cycle 8, 4112–4118. https://doi.org/10.4161/cc.8.24.10215

Prather, A.A., Epel, E.S., Portela Parra, E., Coccia, M., Puterman, E., Aiello, A.E., Dhabhar, F.S., 2018. Associations between chronic caregiving stress and T cell markers implicated in immunosenescence. Brain, Behavior, and Immunity 73, 546–549. https://doi.org/10.1016/j.bbi.2018.06.019

Princiotta, M.F., Finzi, D., Qian, S.-B., Gibbs, J., Schuchmann, S., Buttgereit, F., Bennink, J.R., Yewdell, J.W., 2003. Quantitating Protein Synthesis, Degradation, and Endogenous Antigen Processing. Immunity 18, 343–354. https://doi.org/10.1016/S1074-7613(03)00051-7

Przemska-Kosicka, A., Childs, C.E., Maidens, C., Dong, H., Todd, S., Gosney, M.A., Tuohy, K.M., Yaqoob, P., 2018. Age-Related Changes in the Natural Killer Cell Response to Seasonal Influenza Vaccination Are Not Influenced by a Synbiotic: a Randomised Controlled Trial. Frontiers in Immunology 9. https://doi.org/10.3389/fimmu.2018.00591

PubChem, 2023. ELAVL2 - ELAV like RNA binding protein 2 (human) [WWW Document]. PubChem. URL https://pubchem.ncbi.nlm.nih.gov/gene/ELAVL2/human (accessed 3.2.23).

PubChem, 2022a. NMBR - neuromedin B receptor (human) [WWW Document]. PubChem. URL www.ncbi.nlm.nih.gov/gene/4829#summary (accessed 11.18.22).

PubChem, 2022b. ITGB2 - integrin subunit beta 2 (human) [WWW Document]. PubChem. URL https://pubchem.ncbi.nlm.nih.gov/gene/ITGB2/human (accessed 11.18.22).

PubChem, 2022c. LIPC - lipase C, hepatic type (human) [WWW Document]. PubChem. URL https://pubchem.ncbi.nlm.nih.gov/gene/LIPC/human (accessed 11.18.22).

PubChem, 2022d. AIM2 - absent in melanoma 2 (human) [WWW Document]. PubChem. URL https://pubchem.ncbi.nlm.nih.gov/gene/AIM2/human (accessed 11.18.22).

PubChem, 2022e. BAZ1B - bromodomain adjacent to zinc finger domain 1B (human) [WWW Document]. PubChem. URL https://pubchem.ncbi.nlm.nih.gov/gene/BAZ1B/human (accessed 11.21.22).

PubChem, 2022f. CRTAP - cartilage associated protein (human) [WWW Document]. PubChem. URL https://pubchem.ncbi.nlm.nih.gov/gene/CRTAP/human (accessed 11.21.22).

PubChem, 2022g. PML - PML nuclear body scaffold (human) [WWW Document]. PubChem. URL https://pubchem.ncbi.nlm.nih.gov/gene/PML/human (accessed 11.21.22).

PubChem, 2022h. ADRA1B - adrenoceptor alpha 1B (human) [WWW Document]. PubChem. URL https://pubchem.ncbi.nlm.nih.gov/gene/ADRA1B/human (accessed 3.2.23).

PubChem, 2022i. PDE11A - phosphodiesterase 11A (human) [WWW Document]. PubChem. URL https://pubchem.ncbi.nlm.nih.gov/gene/PDE11A/human (accessed 3.2.23).

Public Health England, 2016. Chapter 1: life expectancy and healthy life expectancy [WWW Document]. GOV.UK. URL https://www.gov.uk/government/publications/health-profile-for-england/chapter-1-life-expectancy-and-healthy-life-expectancy (accessed 4.23.18).

Purves, D., Williams, S.M., 2001. Neuroscience. 2nd edition. Sinauer Associates 2001. ISBN-10: 0-87893-742-0

Qin, L., Jing, X., Qiu, Z., Cao, W., Jiao, Y., Routy, J.-P., Li, T., 2016. Aging of immune system: Immune signature from peripheral blood lymphocyte subsets in 1068 healthy adults. Aging (Albany NY) 8, 848–859. https://doi.org/10.18632/aging.100894

Rallidis, L.S., Vikelis, M., Panagiotakos, D.B., Rizos, I., Zolindaki, M.G., Kaliva, K., Kremastinos, D.T., 2006. Inflammatory markers and in-hospital mortality in acute ischaemic stroke. Atherosclerosis 189, 193–197. https://doi.org/10.1016/j.atherosclerosis.2005.11.032

Randall, S.M., Fear, M.W., Wood, F.M., Rea, S., Boyd, J.H., Duke, J.M., 2015. Long-term musculoskeletal morbidity after adult burn injury: a population-based cohort study. BMJ Open 5, e009395. https://doi.org/10.1136/bmjopen-2015-009395

Rani, M., Schwacha, M.G., 2011. Aging and the Pathogenic Response to Burn. Aging Dis 3, 171–180. PMID: 22724078

Raskov, H., Orhan, A., Christensen, J.P., Gögenur, I., 2021. Cytotoxic CD8+ T cells in cancer and cancer immunotherapy. Br J Cancer 124, 359–367. https://doi.org/10.1038/s41416-020-01048-4

Raveendran, A.V., Jayadevan, R., Sashidharan, S., 2021. Long COVID: An overview. Diabetes & Metabolic Syndrome: Clinical Research & Reviews 15, 869–875. https://doi.org/10.1016/j.dsx.2021.04.007

Rayess, H., Wang, M.B., Srivatsan, E.S., 2012. Cellular senescence and tumor suppressor gene p16. Int J Cancer 130, 1715–1725. https://doi.org/10.1002/ijc.27316

Rees, D.C., Williams, T.N., Gladwin, M.T., 2010. Sickle-cell disease. The Lancet 376, 2018–2031. https://doi.org/10.1016/S0140-6736(10)61029-X

Rettew, J.A., Huet-Hudson, Y.M., Marriott, I., 2008. Testosterone reduces macrophage expression in the mouse of toll-like receptor 4, a trigger for inflammation and innate immunity. Biol Reprod 78, 432–437. https://doi.org/10.1095/biolreprod.107.063545

Rieger, A.M., Nelson, K.L., Konowalchuk, J.D., Barreda, D.R., 2011. Modified Annexin V/Propidium Iodide Apoptosis Assay For Accurate Assessment of Cell Death. J Vis Exp 2597. https://doi.org/10.3791/2597

Ritzel, R.M., Doran, S.J., Barrett, J.P., Henry, R.J., Ma, E.L., Faden, A.I., Loane, D.J., 2018. Chronic Alterations in Systemic Immune Function after Traumatic Brain Injury. Journal of Neurotrauma 35, 1419–1436. https://doi.org/10.1089/neu.2017.5399

Rizvi, S., Raza, S., Mahdi, F., 2014. Telomere length variations in aging and age-related diseases. Curr. Aging Sci 7, 161–167. https://doi.org/10.2174/1874609808666150122153151

Robbins, P.D., Jurk, D., Khosla, S., Kirkland, J.L., LeBrasseur, N.K., Miller, J.D., Passos, J.F., Pignolo, R.J., Tchkonia, T., Niedernhofer, L.J., 2021. Senolytic Drugs: Reducing Senescent Cell Viability to Extend Health Span. Annu Rev Pharmacol Toxicol 61, 779–803. https://doi.org/10.1146/annurev-pharmtox-050120-105018

Roberts, A.L., Koenen, K.C., Chen, Q., Gilsanz, P., Mason, S.M., Prescott, J., Ratanatharathorn, A., Rimm, E.B., Sumner, J.A., Winning, A., De Vivo, I., Kubzansky, L.D., 2017. Posttraumatic stress disorder and accelerated aging: PTSD and leukocyte telomere length in a sample of civilian women. Depression and Anxiety 34, 391–400. https://doi.org/10.1002/da.22620

Robinson, O., Chadeau Hyam, M., Karaman, I., Climaco Pinto, R., Ala-Korpela, M., Handakas, E., Fiorito, G., Gao, H., Heard, A., Jarvelin, M.-R., Lewis, M., Pazoki, R., Polidoro, S., Tzoulaki, I., Wielscher, M., Elliott, P., Vineis, P., 2020. Determinants of accelerated metabolomic and epigenetic aging in a UK cohort. Aging Cell 19, e13149. https://doi.org/10.1111/acel.13149

Rochon, P.A., Katz, J.N., Morrow, L.A., McGlinchey-Berroth, R., Ahlquist, M.M., Sarkarati, M., Minaker, K.L., 1996. Comorbid Illness Is Associated with Survival and Length of Hospital Stay in Patients with Chronic Disability: A Prospective Comparison of Three Comorbidity Indices. Medical Care 34, 1093–1101. https://doi.org/10.1097/00005650-199611000-00004

Rodier, F., Coppé, J.-P., Patil, C.K., Hoeijmakers, W.A.M., Muñoz, D.P., Raza, S.R., Freund, A., Campeau, E., Davalos, A.R., Campisi, J., 2009. Persistent DNA damage signaling triggers senescence-associated inflammatory cytokine secretion. Nat Cell Biol 11, 973–979. https://doi.org/10.1038/ncb1909

Rodriguez, I.J., Lalinde Ruiz, N., Llano León, M., Martínez Enríquez, L., Montilla Velásquez, M. del P., Ortiz Aguirre, J.P., Rodríguez Bohórquez, O.M., Velandia Vargas, E.A., Hernández, E.D., Parra López, C.A., 2021. Immunosenescence Study of T Cells: A Systematic Review. Frontiers in Immunology 11. https://doi.org/10.3389/fimmu.2020.604591

Roh, J.S., Sohn, D.H., 2018. Damage-Associated Molecular Patterns in Inflammatory Diseases. Immune Netw 18, e27. https://doi.org/10.4110/in.2018.18.e27

Rosa, B.A., Ahmed, M., Singh, D.K., Choreño-Parra, J.A., Cole, J., Jiménez-Álvarez, L.A., Rodríguez-Reyna, T.S., Singh, B., Gonzalez, O., Carrion, R., Schlesinger, L.S., Martin, J., Zúñiga, J., Mitreva, M., Kaushal, D., Khader, S.A., 2021. IFN signaling and neutrophil degranulation transcriptional signatures are induced during SARS-CoV-2 infection. Commun Biol 4, 1–14. https://doi.org/10.1038/s42003-021-01829-4

Rosa, S.G.V., Santos, W.C., 2020. Clinical trials on drug repositioning for COVID-19 treatment. Rev Panam Salud Publica 44, e40. https://doi.org/10.26633/RPSP.2020.40

Roubenoff, R., 2003. Catabolism of aging: is it an inflammatory process? Curr Opin Clin Nutr Metab Care 6, 295–299. https://doi.org/10.1097/01.mco.0000068965.34812.62

Ruchko, M., Gorodnya, O., LeDoux, S.P., Alexeyev, M.F., Al-Mehdi, A.-B., Gillespie, M.N., 2005. Mitochondrial DNA damage triggers mitochondrial dysfunction and apoptosis in oxidant-challenged lung endothelial cells. American Journal of Physiology-Lung Cellular and Molecular Physiology 288, L530–L535. https://doi.org/10.1152/ajplung.00255.2004

Ryan, A., Wallace, E., O'Hara, P., Smith, S.M., 2015. Multimorbidity and functional decline in community-dwelling adults: a systematic review. Health Qual Life Outcomes 13. https://doi.org/10.1186/s12955-015-0355-9

Sagiv, A., Krizhanovsky, V., 2013. Immunosurveillance of senescent cells: the bright side of the senescence program. Biogerontology 14, 617–628. https://doi.org/10.1007/s10522-013-9473-0

SAKTHIVADIVEL, V., BOHRA, G.K., MAITHILIKARPAGASELVI, N., KHICHAR, S., MEENA, M., PALANISAMY, N., GAUR, A., GARG, M.K., 2021. Association of Inflammatory Markers with COVID-19 Outcome among Hospitalized Patients: Experience from a Tertiary Healthcare Center in Western India. Maedica (Bucur) 16, 620–627. https://doi.org/10.26574/maedica.2021.16.4.620

Saleh, T., Tyutynuk-Massey, L., Cudjoe, E.K., Idowu, M.O., Landry, J.W., Gewirtz, D.A., 2018. Non-Cell Autonomous Effects of the Senescence-Associated Secretory Phenotype in Cancer Therapy. Front Oncol 8, 164. https://doi.org/10.3389/fonc.2018.00164

Salvestrini, V., Sell, C., Lorenzini, A., 2019. Obesity May Accelerate the Aging Process. Front Endocrinol (Lausanne) 10, 266. https://doi.org/10.3389/fendo.2019.00266

Sanchis-Gomar, F., Lavie, C.J., Mehra, M.R., Henry, B.M., Lippi, G., 2020. Obesity and Outcomes in COVID-19: When an Epidemic and Pandemic Collide. Mayo Clinic Proceedings 95, 1445–1453. https://doi.org/10.1016/j.mayocp.2020.05.006

Sanders, J.L., Newman, A.B., 2013. Telomere Length in Epidemiology: A Biomarker of Aging, Age-Related Disease, Both, or Neither? Epidemiol Rev 35, 112–131. https://doi.org/10.1093/epirev/mxs008

Santoso, A., Pranata, R., Wibowo, A., Al-Farabi, M.J., Huang, I., Antariksa, B., 2021. Cardiac injury is associated with mortality and critically ill pneumonia in COVID-19: A meta-analysis. The American Journal of Emergency Medicine 44, 352–357. https://doi.org/10.1016/j.ajem.2020.04.052

Sapey, E., Greenwood, H., Walton, G., Mann, E., Love, A., Aaronson, N., Insall, R.H., Stockley, R.A., Lord, J.M., 2014. Phosphoinositide 3-kinase inhibition restores neutrophil accuracy in the elderly: toward targeted treatments for immunosenescence. Blood 123, 239–248. https://doi.org/10.1182/blood-2013-08-519520

Sawadogo, W., Tsegaye, M., Gizaw, A., Adera, T., 2022. Overweight and obesity as risk factors for COVID-19-associated hospitalisations and death: systematic review and meta-analysis. BMJ Nutrition, Prevention & Health e000375. https://doi.org/10.1136/bmjnph-2021-000375

Sayed, N., Huang, Y., Nguyen, K., Krejciova-Rajaniemi, Z., Grawe, A.P., Gao, T., Tibshirani, R., Hastie, T., Alpert, A., Cui, L., Kuznetsova, T., Rosenberg-Hasson, Y., Ostan, R., Monti, D., Lehallier, B., Shen-Orr, S.S., Maecker, H.T., Dekker, C.L., Wyss-Coray, T., Franceschi, C., Jojic, V., Haddad, F., Montoya, J.G., Wu, J.C., Davis, M.M., Furman, D., 2021. An inflammatory aging clock (iAge) based on deep learning tracks multimorbidity, immunosenescence, frailty and cardiovascular aging. Nat Aging 1, 598–615. https://doi.org/10.1038/s43587-021-00082-y

Schafer, M.J., White, T.A., Evans, G., Tonne, J.M., Verzosa, G.C., Stout, M.B., Mazula, D.L., Palmer, A.K., Baker, D.J., Jensen, M.D., Torbenson, M.S., Miller, J.D., Ikeda, Y., Tchkonia, T., Deursen, J.M. van, Kirkland, J.L., LeBrasseur, N.K., 2016. Exercise Prevents Diet-induced Cellular Senescence in Adipose Tissue. Diabetes db15029. https://doi.org/10.2337/db15-0291

Scheetz, L.J., 2005. Relationship of age, injury severity, injury type, comorbid conditions, level of care, and survival among older motor vehicle trauma patients. Research in Nursing & Health 28, 198–209. https://doi.org/10.1002/nur.20075

Schetz, M., De Jong, A., Deane, A.M., Druml, W., Hemelaar, P., Pelosi, P., Pickkers, P., Reintam-Blaser, A., Roberts, J., Sakr, Y., Jaber, S., 2019. Obesity in the critically ill: a narrative review. Intensive Care Med 45, 757–769. https://doi.org/10.1007/s00134-019-05594-1

Schindelin, J., Arganda-Carreras, I., Frise, E., Kaynig, V., Longair, M., Pietzsch, T., Preibisch, S., Rueden, C., Saalfeld, S., Schmid, B., Tinevez, J.-Y., White, D.J., Hartenstein, V., Eliceiri, K., Tomancak, P., Cardona, A., 2012. Fiji: an open-source platform for biological-image analysis. Nat Methods 9, 676–682. https://doi.org/10.1038/nmeth.2019

Schneider, C.V., Schneider, K.M., Teumer, A., Rudolph, K.L., Hartmann, D., Rader, D.J., Strnad, P., 2022. Association of Telomere Length With Risk of Disease and Mortality. JAMA Internal Medicine 182, 291–300. https://doi.org/10.1001/jamainternmed.2021.7804

Schroeder, A., Mueller, O., Stocker, S., Salowsky, R., Leiber, M., Gassmann, M., Lightfoot, S., Menzel, W., Granzow, M., Ragg, T., 2006. The RIN: an RNA integrity number for assigning integrity values to RNA measurements. BMC Molecular Biology 7, 3. https://doi.org/10.1186/1471-2199-7-3

Sehl, M.E., Henry, J.E., Storniolo, A.M., Ganz, P.A., Horvath, S., 2017. DNA methylation age is elevated in breast tissue of healthy women. Breast cancer research and treatment 164, 209–219. https://doi.org/10.1007/s10549-017-4218-4

Dimensions.ai, 2022. Search term: “Senolytic” in Publications [WWW Document]. Dimensions.ai. URL https://app.dimensions.ai/analytics/publication/overview/timeline?search_mode=content&search_text=senolytic&search_type=kws&search_field=full_search (accessed 3.2.22).

Setareh, M., Alavi, N.M., Atoof, F., 2021. Severity of illness affecting the length of stay and outcomes in patients admitted to intensive care units, Iran, 2019. J Educ Health Promot 10, 142. https://doi.org/10.4103/jehp.jehp_780_20

Shammas, M.A., 2011. Telomeres, lifestyle, cancer, and aging: Current Opinion in Clinical Nutrition and Metabolic Care 14, 28–34. https://doi.org/10.1097/MCO.0b013e32834121b1

Shaw, A.C., Goldstein, D.R., Montgomery, R.R., 2013. Age-dependent dysregulation of innate immunity. Nat Rev Immunol 13, 875–887. https://doi.org/10.1038/nri3547

Shaw, A.C., Joshi, S., Greenwood, H., Panda, A., Lord, J.M., 2010. Aging of the Innate Immune System. Curr Opin Immunol 22, 507–513. https://doi.org/10.1016/j.coi.2010.05.003

Shiels, P.G., 2010. Improving Precision in Investigating Aging: Why Telomeres Can Cause Problems. The Journals of Gerontology: Series A 65A, 789–791. https://doi.org/10.1093/gerona/glq095

Shirakawa, K., Sano, M., 2021. T Cell Immunosenescence in Aging, Obesity, and Cardiovascular Disease. Cells 10, 2435. https://doi.org/10.3390/cells10092435

Shive, C.L., Freeman, M.L., Younes, S.-A., Kowal, C.M., Canaday, D.H., Rodriguez, B., Lederman, M.M., Anthony, D.D., 2021. Markers of T Cell Exhaustion and Senescence and Their Relationship to Plasma TGF-β Levels in Treated HIV+ Immune Non-responders. Frontiers in Immunology 12. https://doi.org/10.3389/fimmu.2021.638010

Shrestha, A., Kim, N., Lee, S.-J., Jeon, Y.H., Song, J.-J., An, H., Cho, S.J., Kadayat, T.M., Chin, J., 2021. Targeting the Nuclear Receptor-Binding SET Domain Family of Histone Lysine Methyltransferases for Cancer Therapy: Recent Progress and Perspectives. J. Med. Chem. 64, 14913–14929. https://doi.org/10.1021/acs.jmedchem.1c01116

Silva, L., Garcia, L., Oliveira, B., Tanita, M., Festti, J., Cardoso, L., Lavado, L., Grion, C., 2016. Acute respiratory distress syndrome in burn patients: incidence and risk factor analysis. Ann Burns Fire Disasters 29, 178–182. PMID: 28149245

Şimşek, T., Şimşek, H.U., Cantürk, N.Z., 2014. Response to trauma and metabolic changes: posttraumatic metabolism. Ulus Cerrahi Derg 30, 153–159. https://doi.org/10.5152/UCD.2014.2653

Soeroto, A.Y., Soetedjo, N.N., Purwiga, A., Santoso, P., Kulsum, I.D., Suryadinata, H., Ferdian, F., 2020. Effect of increased BMI and obesity on the outcome of COVID-19 adult patients: A systematic review and meta-analysis. Diabetes & Metabolic Syndrome: Clinical Research & Reviews 14, 1897–1904. https://doi.org/10.1016/j.dsx.2020.09.029

Sommer, N., Noack, S., Hecker, A., Hackstein, H., Bein, G., Weissmann, N., Seeger, W., Mayer, K., Hecker, M., 2020. Decreased Thymic Output Contributes to Immune Defects in Septic Patients. J Clin Med 9, 2695. https://doi.org/10.3390/jcm9092695

Sommershof, A., Aichinger, H., Engler, H., Adenauer, H., Catani, C., Boneberg, E.-M., Elbert, T., Groettrup, M., Kolassa, I.-T., 2009. Substantial reduction of naïve and regulatory T cells following traumatic stress. Brain, Behavior, and Immunity 23, 1117–1124. https://doi.org/10.1016/j.bbi.2009.07.003

Soto-Gamez, A., Demaria, M., 2017. Therapeutic interventions for aging: the case of cellular senescence. Drug discovery today 22, 786–795. https://doi.org/S1359-6446(17)30017-X

Spiegel, R., Saada, A., Halvardson, J., Soiferman, D., Shaag, A., Edvardson, S., Horovitz, Y., Khayat, M., Shalev, S.A., Feuk, L., Elpeleg, O., 2014. Deleterious mutation in FDX1L gene is associated with a novel mitochondrial muscle myopathy. Eur J Hum Genet 22, 902–906. https://doi.org/10.1038/ejhg.2013.269

Spitzer, J.A., 1999. Gender differences in some host defense mechanisms. Lupus 8, 380–383. https://doi.org/10.1177/096120339900800510

Stafford, J.M., Lee, C.-H., Voigt, P., Descostes, N., Saldaña-Meyer, R., Yu, J.-R., Leroy, G., Oksuz, O., Chapman, J.R., Suarez, F., Modrek, A.S., Bayin, N.S., Placantonakis, D.G., Karajannis, M.A., Snuderl, M., Ueberheide, B., Reinberg, D., 2018. Multiple modes of PRC2 inhibition elicit global chromatin alterations in H3K27M pediatric glioma. Sci Adv 4, eaau5935. https://doi.org/10.1126/sciadv.aau5935

Starke, K.R., Reissig, D., Petereit-Haack, G., Schmauder, S., Nienhaus, A., Seidler, A., 2021. The isolated effect of age on the risk of COVID-19 severe outcomes: a systematic review with meta-analysis. BMJ Global Health 6, e006434. https://doi.org/10.1136/bmjgh-2021-006434

Steves, C.J., Spector, T.D., Jackson, S.H.D., 2012. Ageing, genes, environment and epigenetics: what twin studies tell us now, and in the future. Age and Ageing 41, 581–586. https://doi.org/10.1093/ageing/afs097

Sturm, R., Xanthopoulos, L., Heftrig, D., Oppermann, E., Vrdoljak, T., Dunay, I.R., Marzi, I., Relja, B., 2020. Regulatory T Cells Modulate CD4 Proliferation after Severe Trauma via IL-10. J Clin Med 9, 1052. https://doi.org/10.3390/jcm9041052

Sudhesh Dev, S., Zainal Abidin, S.A., Farghadani, R., Othman, I., Naidu, R., 2021. Receptor Tyrosine Kinases and Their Signaling Pathways as Therapeutic Targets of Curcumin in Cancer. Frontiers in Pharmacology 12. https://doi.org/10.3389/fphar.2021.772510

Sullivan, J., Mirbahai, L., Lord, J.M., 2018. Major trauma and acceleration of the ageing process. Ageing Research Reviews 48, 32–39. https://doi.org/10.1016/j.arr.2018.10.001

Summer, G.J., Puntillo, K.A., Miaskowski, C., Green, P.G., Levine, J.D., 2007. Burn Injury Pain: The Continuing Challenge. The Journal of Pain 8, 533–548. https://doi.org/10.1016/j.jpain.2007.02.426

Surova, O., Zhivotovsky, B., 2013. Various modes of cell death induced by DNA damage. Oncogene 32, 3789–3797. https://doi.org/10.1038/onc.2012.556

Suzuki, M.M., Bird, A., 2008. DNA methylation landscapes: provocative insights from epigenomics. Nature Reviews Genetics 9, 465–476. https://doi.org/10.1038/nrg2341

Szymański, P., Markowicz, M., Mikiciuk-Olasik, E., 2011. Adaptation of High-Throughput Screening in Drug Discovery—Toxicological Screening Tests. Int J Mol Sci 13, 427–452. https://doi.org/10.3390/ijms13010427

Takahashi, T., Ellingson, M.K., Wong, P., Israelow, B., Lucas, C., Klein, J., Silva, J., Mao, T., Oh, J.E., Tokuyama, M., Lu, P., Venkataraman, A., Park, A., Liu, F., Meir, A., Sun, J., Wang, E.Y., Casanovas-Massana, A., Wyllie, A.L., Vogels, C.B.F., Earnest, R., Lapidus, S., Ott, I.M., Moore, A.J., Shaw, A., Fournier, J.B., Odio, C.D., Farhadian, S., Dela Cruz, C., Grubaugh, N.D., Schulz, W.L., Ring, A.M., Ko, A.I., Omer, S.B., Iwasaki, A., 2020. Sex differences in immune responses that underlie COVID-19 disease outcomes. Nature 588, 315–320. https://doi.org/10.1038/s41586-020-2700-3

Talens, R.P., Christensen, K., Putter, H., Willemsen, G., Christiansen, L., Kremer, D., Suchiman, H.E.D., Slagboom, P.E., Boomsma, D.I., Heijmans, B.T., 2012. Epigenetic variation during the adult lifespan: cross-sectional and longitudinal data on monozygotic twin pairs. Aging Cell 11, 694–703. https://doi.org/10.1111/j.1474-9726.2012.00835.x

Tarazona, R., Solana, R., Ouyang, Q., Pawelec, G., 2002. Basic biology and clinical impact of immunosenescence. Experimental Gerontology, ImAginE: 2nd Conference on Basic Biology and Clinical Impact of Immunosenescence 37, 183–189. https://doi.org/10.1016/S0531-5565(01)00182-6

Tchkonia, T., Zhu, Y., van Deursen, J., Campisi, J., Kirkland, J.L., 2013. Cellular senescence and the senescent secretory phenotype: therapeutic opportunities. J Clin Invest 123, 966–972. https://doi.org/10.1172/JCI64098

Teissier, T., Boulanger, E., Cox, L.S., 2022. Interconnections between Inflammageing and Immunosenescence during Ageing. Cells 11, 359. https://doi.org/10.3390/cells11030359

Teschendorff, A.E., West, J., Beck, S., 2013. Age-associated epigenetic drift: implications, and a case of epigenetic thrift? Hum Mol Genet 22, R7–R15. https://doi.org/10.1093/hmg/ddt375

Tiwari, V.K., 2012. Burn wound: How it differs from other wounds? Indian J Plast Surg 45, 364–373. https://doi.org/10.4103/0970-0358.101319

Tokutomi, T., Miyagi, T., Ogawa, T., Ono, J., Kawamata, T., Sakamoto, T., Shigemori, M., Nakamura, N., 2008. Age-Associated Increases in Poor Outcomes after Traumatic Brain Injury: A Report from the Japan Neurotrauma Data Bank. Journal of Neurotrauma 25, 1407–1414. https://doi.org/10.1089/neu.2008.0577

Turvey, S.E., Broide, D.H., 2010. Innate immunity. Journal of Allergy and Clinical Immunology, 2010 Primer on Allergic and Immunologic Diseases 125, S24–S32. https://doi.org/10.1016/j.jaci.2009.07.016

Ullah, M., Pelletier, N., Xiao, L., Zhao, S.P., Wang, K., Degerny, C., Tahmasebi, S., Cayrou, C., Doyon, Y., Goh, S.-L., Champagne, N., Côté, J., Yang, X.-J., 2008. Molecular Architecture of Quartet MOZ/MORF Histone Acetyltransferase Complexes. Mol Cell Biol 28, 6828–6843. https://doi.org/10.1128/MCB.01297-08

UniProt, 2022a. ZEB2 - Zinc finger E-box-binding homeobox 2 - Homo sapiens (Human) | UniProtKB | UniProt [WWW Document]. URL https://www.uniprot.org/uniprotkb/O60315/entry (accessed 11.18.22).

UniProt, 2022b. SNTA1 - Alpha-1-syntrophin - Homo sapiens (Human) | UniProtKB | UniProt [WWW Document]. URL https://www.uniprot.org/uniprotkb/Q13424/entry#function (accessed 11.18.22).

United Nations, Department of Economic and Social Affairs, Population Division, 2020. World population ageing 2020 Highlights: living arrangements of older persons. ISBN: 978-92-1-148347-5

van der Veeken, J., Gonzalez, A.J., Cho, H., Arvey, A., Leslie, C.S., Rudensky, A.Y., 2016. Memory of inflammation in regulatory T cells. Cell 166, 977–990. https://doi.org/10.1016/j.cell.2016.07.006

Vangamudi, B., Paul, T.A., Shah, P.K., Kost-Alimova, M., Nottebaum, L., Shi, X., Zhan, Y., Leo, E., Mahadeshwar, H.S., Protopopov, A., Futreal, A., Tieu, T.N., Peoples, M., Heffernan, T.P., Marszalek, J.R., Toniatti, C., Petrocchi, A., Verhelle, D., Owen, D.R., Draetta, G., Jones, P., Palmer, W.S., Sharma, S., Andersen, J.N., 2015. The SMARCA2/4 ATPase Domain Surpasses the Bromodomain as a Drug Target in SWI/SNF-Mutant Cancers: Insights from cDNA Rescue and PFI-3 Inhibitor Studies. Cancer Research 75, 3865–3878. https://doi.org/10.1158/0008-5472.CAN-14-3798

Velarde, M.C., Demaria, M., 2016. Targeting Senescent Cells: Possible Implications for Delaying Skin Aging: A Mini-Review. GER 62, 513–518. https://doi.org/10.1159/000444877

Verhoeven, J.E., Yang, R., Wolkowitz, O.M., Bersani, F.S., Lindqvist, D., Mellon, S.H., Yehuda, R., Flory, J.D., Lin, J., Abu-Amara, D., Makotkine, I., Marmar, C., Jett, M., Hammamieh, R., 2018. Epigenetic Age in Male Combat-Exposed War Veterans: Associations with Posttraumatic Stress Disorder Status. Mol Neuropsychiatry 4, 90–99. https://doi.org/10.1159/000491431

Verlinden, I., Güiza, F., Derese, I., Wouters, P.J., Joosten, K., Verbruggen, S.C., Van den Berghe, G., Vanhorebeek, I., 2020. Time course of altered DNA methylation evoked by critical illness and by early administration of parenteral nutrition in the paediatric ICU. Clin Epigenetics 12, 155. https://doi.org/10.1186/s13148-020-00947-w

Villanueva, R.A.M., Chen, Z.J., 2019. ggplot2: Elegant Graphics for Data Analysis (2nd ed.), Measurement: Interdisciplinary Research and Perspectives, 17:3, 160-167, DOI: 10.1080/15366367.2019.1565254

Vlaming, H., McLean, C.M., Korthout, T., Alemdehy, M.F., Hendriks, S., Lancini, C., Palit, S., Klarenbeek, S., Kwesi-Maliepaard, E.M., Molenaar, T.M., Hoekman, L., Schmidlin, T.T., Altelaar, A.F.M., Welsem, T. van, Dannenberg, J.-H., Jacobs, H., Leeuwen, F. van, 2019. Evolutionarily-conserved chromatin crosstalk generates a DOT1L-dose dependency in thymic lymphoma caused by loss of HDAC1. https://doi.org/10.1101/509976

Wallis, C.J.D., Lo, K., Lee, Y., Krakowsky, Y., Garbens, A., Satkunasivam, R., Herschorn, S., Kodama, R.T., Cheung, P., Narod, S.A., Nam, R.K., 2016. Survival and cardiovascular events in men treated with testosterone replacement therapy: an intention-to-treat observational cohort study. The Lancet Diabetes & Endocrinology 4, 498–506. https://doi.org/10.1016/S2213-8587(16)00112-1

Walters, H.E., Deneka-Hannemann, S., Cox, L.S., 2016. Reversal of phenotypes of cellular senescence by pan-mTOR inhibition. Aging (Albany NY) 8, 231–244. https://doi.org/10.18632/aging.100872

Wang, Q., Zhan, Y., Pedersen, N.L., Fang, F., Hägg, S., 2018. Telomere Length and All-Cause Mortality: A Meta-analysis. Ageing Research Reviews 48, 11–20. https://doi.org/10.1016/j.arr.2018.09.002

Weinstein, Y., Ran, S., Segal, S., 1984. Sex-associated differences in the regulation of immune responses controlled by the MHC of the mouse. J Immunol 132, 656–661. PMID: 6228595

Weir, C.B., Jan, A., 2021. BMI Classification Percentile And Cut Off Points. StatPearls Publishing, Treasure Island (FL). PMID: 31082114

Weisell, R.C., 2002. Body mass index as an indicator of obesity: Body mass index as an indicator of obesity. Asia Pacific Journal of Clinical Nutrition 11, S681–S684. https://doi.org/10.1046/j.1440-6047.11.s8.5.x

WHO, 2017. WHO health statistics 2017: monitoring health for the SDGs. ISBN 978-92-4-156548-6

WHO, 2011. World Report on Disability 350. ISBN: 9789241564182

WHO, 2010. Injuries and violence, the facts. (World Health Organisation). ISBN 978 92 4 159937 5

Wijaya, R.S., Read, S.A., Schibeci, S., Eslam, M., Azardaryany, M.K., El-Khobar, K., van der Poorten, D., Lin, R., Yuen, L., Lam, V., George, J., Douglas, M.W., Ahlenstiel, G., 2019. KLRG1+ natural killer cells exert a novel antifibrotic function in chronic hepatitis B. Journal of Hepatology 71, 252–264. https://doi.org/10.1016/j.jhep.2019.03.012

Williams, Felicia N, Herndon, D.N., Hawkins, H.K., Lee, J.O., Cox, R.A., Kulp, G.A., Finnerty, C.C., Chinkes, D.L., Jeschke, M.G., 2009. The leading causes of death after burn injury in a single pediatric burn center. Crit Care 13, R183. https://doi.org/10.1186/cc8170

Williams, F. N., Herndon, D.N., Jeschke, M.G., 2009. The hypermetabolic response to burn injury and interventions to modify this response. Clinics in plastic surgery 36, 583–596. https://doi.org/10.1016/j.cps.2009.05.001

Williams, F.N., Herndon, D.N., Suman, O.E., Lee, J.O., Norbury, W.B., Branski, L.K., Mlcak, R.P., Jeschke, M.G., 2011. CHANGES IN CARDIAC PHYSIOLOGY AFTER SEVERE BURN INJURY. J Burn Care Res 32, 269–274. https://doi.org/10.1097/BCR.0b013e31820aafcf

Wissler Gerdes, E.O., Zhu, Y., Tchkonia, T., Kirkland, J.L., 2020. Discovery, development, and future application of senolytics: theories and predictions. The FEBS Journal 287, 2418–2427. https://doi.org/10.1111/febs.15264

Wolf, E. J., Logue, M.W., Stoop, T.B., Schichman, S.A., Stone, A., Sadeh, N., Hayes, J.P., Miller, M.W., 2017. Accelerated DNA Methylation Age: Associations with PTSD and Mortality. Psychosomatic medicine. https://doi.org/10.1097/PSY.0000000000000506

Wolf, E J., Maniates, H., Nugent, N., Maihofer, A.X., Armstrong, D., Ratanatharathorn, A., Ashley-Koch, A.E., Garrett, M., Kimbrel, N.A., Lori, A., 2017. Traumatic Stress and Accelerated DNA Methylation Age: A Meta-Analysis. Psychoneuroendocrinology. https://doi.org/10.1016/j.psyneuen.2017.12.007

Wright, D.K., O'Brien, T.J., Mychasiuk, R., Shultz, S.R., 2018. Telomere length and advanced diffusion MRI as biomarkers for repetitive mild traumatic brain injury in adolescent rats. NeuroImage: Clinical 18, 315–324. https://doi.org/10.1016/j.nicl.2018.01.033

Xiao, W., Mindrinos, M.N., Seok, J., Cuschieri, J., Cuenca, A.G., Gao, H., Hayden, D.L., Hennessy, L., Moore, E.E., Minei, J.P., 2011. A genomic storm in critically injured humans. Journal of Experimental Medicine 208, 2581–2590. https://doi.org/10.1084/jem.20111354

Xiu, F., Jeschke, M.G., 2013. Perturbed mononuclear phagocyte system in severely burned and septic patients. Shock 40, 81–88. https://doi.org/10.1097/SHK.0b013e318299f774

Xu, M., Pirtskhalava, T., Farr, J.N., Weigand, B.M., Palmer, A.K., Weivoda, M.M., Inman, C.L., Ogrodnik, M.B., Hachfeld, C.M., Fraser, D.G., Onken, J.L., Johnson, K.O., Verzosa, G.C., Langhi, L.G.P., Weigl, M., Giorgadze, N., LeBrasseur, N.K., Miller, J.D., Jurk, D., Singh, R.J., Allison, D.B., Ejima, K., Hubbard, G.B., Ikeno, Y., Cubro, H., Garovic, V.D., Hou, X., Weroha, S., Robbins, P.D., Niedernhofer, L.J., Khosla, S., Tchkonia, T., Kirkland, J.L., 2018. Senolytics Improve Physical Function and Increase Lifespan in Old Age. Nat Med 24, 1246–1256. https://doi.org/10.1038/s41591-018-0092-9

Xu, W., Larbi, A., 2017. Markers of T Cell Senescence in Humans. International Journal of Molecular Sciences 18, 1742. https://doi.org/10.3390/ijms18081742

Yamakawa, K., Tajima, G., Keegan, J.W., Nakahori, Y., Guo, F., Seshadri, A.J., Cahill, L.A., Lederer, J.A., 2021. Trauma induces expansion and activation of a memory-like Treg population. J Leukoc Biol 109, 645–656. https://doi.org/10.1002/JLB.4A0520-122R

Yan, J., Greer, J.M., Hull, R., O'Sullivan, J.D., Henderson, R.D., Read, S.J., McCombe, P.A., 2010. The effect of ageing on human lymphocyte subsets: comparison of males and females. Immunity & Ageing 7, 4. https://doi.org/10.1186/1742-4933-7-4

Yan, K., Rousseau, J., Littlejohn, R.O., Kiss, C., Lehman, A., Rosenfeld, J.A., Stumpel, C.T.R., Stegmann, A.P.A., Robak, L., Scaglia, F., Nguyen, T.T.M., Fu, H., Ajeawung, N.F., Camurri, M.V., Li, L., Gardham, A., Panis, B., Almannai, M., Sacoto, M.J.G., Baskin, B., Ruivenkamp, C., Xia, F., Bi, W., DDD Study, CAUSES Study, Cho, M.T., Potjer, T.P., Santen, G.W.E., Parker, M.J., Canham, N., McKinnon, M., Potocki, L., MacKenzie, J.J., Roeder, E.R., Campeau, P.M., Yang, X.-J., 2017. Mutations in the Chromatin Regulator Gene BRPF1 Cause Syndromic Intellectual Disability and Deficient Histone Acetylation. Am J Hum Genet 100, 91–104. https://doi.org/10.1016/j.ajhg.2016.11.011

Yang, H., Youm, Y.-H., Vandanmagsar, B., Rood, J., Kumar, K.G., Butler, A.A., Dixit, V.D., 2009. Obesity accelerates thymic aging. Blood 114, 3803–3812. https://doi.org/10.1182/blood-2009-03-213595

Yang, X., Han, H., De Carvalho, D.D., Lay, F.D., Jones, P.A., Liang, G., 2014. Gene Body Methylation can alter Gene Expression and is a Therapeutic Target in Cancer. Cancer Cell 26, 577–590. https://doi.org/10.1016/j.ccr.2014.07.028

Yi, H.-S., Kim, S.Y., Kim, J.T., Lee, Y.-S., Moon, J.S., Kim, M., Kang, Y.E., Joung, K.H., Lee, J.H., Kim, H.J., Chun, K., Shong, M., Ku, B.J., 2019. T-cell senescence contributes to abnormal glucose homeostasis in humans and mice. Cell Death Dis 10, 249. https://doi.org/10.1038/s41419-019-1494-4

Yi, X., Jiang, X.-J., Fang, Z.-M., 2019. Histone methyltransferase SMYD2: ubiquitous regulator of disease. Clinical Epigenetics 11, 112. https://doi.org/10.1186/s13148-019-0711-4

Ying, K., Liu, H., Tarkhov, A.E., Lu, A.T., Horvath, S., Kutalik, Z., Shen, X., Gladyshev, V.N., 2022. Causal Epigenetic Age Uncouples Damage and Adaptation (preprint). Genetics. https://doi.org/10.1101/2022.10.07.511382

Yousefzadeh, M.J., Flores, R.R., Zhu, Y., Schmiechen, Z.C., Brooks, R.W., Trussoni, C.E., Cui, Y., Angelini, L., Lee, K.-A., McGowan, S.J., Burrack, A.L., Wang, D., Dong, Q., Lu, A., Sano, T., O'Kelly, R.D., McGuckian, C.A., Kato, J.I., Bank, M.P., Wade, E.A., Pillai, S.P.S., Klug, J., Ladiges, W.C., Burd, C.E., Lewis, S.E., LaRusso, N.F., Vo, N.V., Wang, Y., Kelley, E.E., Huard, J., Stromnes, I.M., Robbins, P.D., Niedernhofer, L.J., 2021a. An aged immune system drives senescence and ageing of solid organs. Nature 594, 100–105. https://doi.org/10.1038/s41586-021-03547-7

Yousefzadeh, M.J., Zhu, Y., McGowan, S.J., Angelini, L., Fuhrmann-Stroissnigg, H., Xu, M., Ling, Y.Y., Melos, K.I., Pirtskhalava, T., Inman, C.L., McGuckian, C., Wade, E.A., Kato, J.I., Grassi, D., Wentworth, M., Burd, C.E., Arriaga, E.A., Ladiges, W.L., Tchkonia, T., Kirkland, J.L., Robbins, P.D., Niedernhofer, L.J., 2018. Fisetin is a senotherapeutic that extends health and lifespan. EBioMedicine 36, 18. https://doi.org/10.1016/j.ebiom.2018.09.015

Zatterale, F., Longo, M., Naderi, J., Raciti, G.A., Desiderio, A., Miele, C., Beguinot, F., 2020. Chronic Adipose Tissue Inflammation Linking Obesity to Insulin Resistance and Type 2 Diabetes. Frontiers in Physiology 10.

Zdanov, S., Remacle, J., Toussaint, O., 2006. Establishment of H2O2-Induced Premature Senescence in Human Fibroblasts Concomitant with Increased Cellular Production of H2O2. Annals of the New York Academy of Sciences 1067, 210–216. https://doi.org/10.1196/annals.1354.025

Zglinicki, T. von, Serra, V., Lorenz, M., Saretzki, G., Lenzen-Groβimlighaus, R., Geβner, R., Risch, A., Steinhagen-Thiessen, E., 2000. Short Telomeres in Patients with Vascular Dementia: An Indicator of Low Antioxidative Capacity and a Possible Risk Factor? Laboratory Investigation 80, 1739–1747. https://doi.org/10.1038/labinvest.3780184

Zhang, J., Rane, G., Dai, X., Shanmugam, M.K., Arfuso, F., Samy, R.P., Lai, M.K.P., Kappei, D., Kumar, A.P., Sethi, G., 2016. Ageing and the telomere connection: An intimate relationship with inflammation. Ageing Research Reviews 25, 55–69. https://doi.org/10.1016/j.arr.2015.11.006

Zhang, Q., Raoof, M., Chen, Y., Sumi, Y., Sursal, T., Junger, W., Brohi, K., Itagaki, K., Hauser, C.J., 2010. Circulating mitochondrial DAMPs cause inflammatory responses to injury. Nature 464, 104. https://doi.org/10.1038/nature08780

Zhao, N., Ang, M.-K., Yin, X.-Y., Patel, M.R., Fritchie, K., Thorne, L., Muldrew, K.L., Hayward, M.C., Sun, W., Wilkerson, M.D., Chera, B.S., Hackman, T., Zanation, A.M., Grilley-Olson, J.E., Couch, M.E., Shockley, W.W., Weissler, M.C., Shores, C.G., Funkhouser, W.K., Olshan, A.F., Hayes, D.N., 2012. Different cellular p16INK4a localisation may signal different survival outcomes in head and neck cancer. Br J Cancer 107, 482–490. https://doi.org/10.1038/bjc.2012.264

Zhu, W.G., Lakshmanan, R.R., Beal, M.D., Otterson, G.A., 2001. DNA methyltransferase inhibition enhances apoptosis induced by histone deacetylase inhibitors. Cancer Res 61, 1327–1333. PMID: 11245429

Zhu, Y., Doornebal, E.J., Pirtskhalava, T., Giorgadze, N., Wentworth, M., Fuhrmann-Stroissnigg, H., Niedernhofer, L.J., Robbins, P.D., Tchkonia, T., Kirkland, J.L., 2017. New agents that target senescent cells: the flavone, fisetin, and the BCL-XL inhibitors, A1331852 and A1155463. Aging 9, 955–963. https://doi.org/10.18632/aging.101202

Zhu, Y., Tchkonia, T., Pirtskhalava, T., Gower, A.C., Ding, H., Giorgadze, N., Palmer, A.K., Ikeno, Y., Hubbard, G.B., Lenburg, M., O'Hara, S.P., LaRusso, N.F., Miller, J.D., Roos, C.M., Verzosa, G.C., LeBrasseur, N.K., Wren, J.D., Farr, J.N., Khosla, S., Stout, M.B., McGowan, S.J., Fuhrmann-Stroissnigg, H., Gurkar, A.U., Zhao, J., Colangelo, D., Dorronsoro, A., Ling, Y.Y., Barghouthy, A.S., Navarro, D.C., Sano, T., Robbins, P.D., Niedernhofer, L.J., Kirkland, J.L., 2015. The Achilles' heel of senescent cells: from transcriptome to senolytic drugs. Aging Cell 14, 644–658. https://doi.org/10.1111/acel.12344

Zribi, B., Uziel, O., Lahav, M., Mesilati Stahy, R., Singer, P., 2019. Telomere Length Changes during Critical Illness: A Prospective, Observational Study. Genes 10, 761. https://doi.org/10.3390/genes10100761